Design and Synthesis of Indoleamine 2,3-Dioxygenase 1 Inhibitors

A dissertation submitted to the
Indian Institute of Technology Guwahati
as Partial fulfilment for the Degree of
Doctor of Philosophy in Chemistry

Submitted by
Saurav Paul

Department of Chemistry
Indian Institute of Technology Guwahati
Guwahati 781039, Assam, India

Dedicated

To

My Parents and Family

Contents

INDIAN INSTITUTE OF TECHNOLOGY GUWAHATI

Department of Chemistry

STATEMENT

I do hereby declare that the matter embodied in this thesis is the result of investigations carried out by me in the Department of Chemistry, Indian Institute of Technology Guwahati, India, under the supervision of associate professor Dr. Debasis Manna. This thesis has been submitted by me to the Department of Chemistry, Indian Institute of Technology Guwahati, for the award of the degree of Doctor of Philosophy.

In keeping with the general practice of reporting scientific observations, due acknowledgements have been made wherever the work described is based on the findings of other investigators.

Date **Saurav Paul**

IIT Guwahati

INDIAN INSTITUTE OF TECHNOLOGY GUWAHATI

Department of Chemistry

CERTIFICATE

This is to certify that Saurav Paul (Roll No. 126122015) has been working under my supervision since July, 2012 as a regular registered Ph. D. student. I am forwarding his thesis entitled **"Design and Synthesis of Indoleamine 2,3-dioxygenase 1 Inhibitors"** being submitted for the Ph.D. (Science) degree of this Institute. I certify that this work is an authentic record of the results obtained from the research work and he has fulfilled all the requirements according to the rules of this Institute regarding the investigations embodied in his thesis and this work has not been submitted elsewhere for a degree.

Date
IIT Guwahati

Dr. Debasis Manna
IIT Guwahati (Thesis Supervisor)
Department of Chemistry
IIT Guwahati

Acknowledgements

It would have not been possible to write this doctoral thesis without the help and support of the kind people around me, to only some of whom it is possible to give particular mention here.

First and foremost, I would like to convey my heartfelt thanks to my thesis supervisor Dr. Debasis Manna for his precious suggestion, incisive guidance and decisive insights during the entire course of my Ph.D. research. His true scientific spirit has helped me a lot during my research work. I am also thankful to him for giving me freedom and support both professionally and personally during my struggle and hard times throughout the tenure of my research work. I find myself privileged to have worked under his kind guidance. My sincere everlasting gratitude goes towards him.

I would like to acknowledge my sincere gratitude to all my doctoral committee members, Prof. Gopal Das, Dr. Debapratim Das and Dr. Vishal Trivedi for their insightful advices and valuable suggestions. My honest regards to all the faculty members of the Department of Chemistry for their motivation and encouragements. I am also grateful to Dr. Vishal Trivedi (Department of BSBE, IIT Guwahati) for his collaborative support in carrying out the in vivo cellular studies during my research work.

I wish to acknowledge my sincere gratitude to the IIT Guwahati for the financial support and facilities that were made available to me. I also thankful to the Central Instrument Facility (CIF), IIT Guwahati for providing the instrument facility and to all the official staff members of the Department of Chemistry for their generous help and support.

I would like to thank all my former group members Dr. Narsimha Mamidi, Dr. Sukhamoy Gorai, Dr. Rituparna Borah and my labmates namely Dipjyoti Talukdar, Subhankar Panda, Ashalata Roy, Abhishek Saha, Nirmalya Pradhan, Nasim Akhtar, Oindrilla Biswas, Subhasis Dey, Shilbhadra Chatterjee and Dr. Sreeparna Das for their continuous help and support in carrying out my research work and providing an enthusiastic environment that motivated me to work effectively. I extend my sincere thanks especially to Ashalata Roy for her collaborative effort in carrying out the enzyme expression and the biological studies as well as to Subhankar Panda and Nirmalya Pradhan for their contribution during my entire research work.

I also take this opportunity to thank all my Ph.D. batchmates (July, 2012), the other research scholars in the Chemistry Department and all my IITG friends, who have shared their thoughts and views with me. I am very much thankful to most of my batchmates for their supportive nature and frequent help in many aspects.

Most importantly, my Ph.D. endeavours would not have been completed without the endless love, unending support, tolerance and blessing from my family members. I wish to express my sincere gratitude to my parents, my brother and guardian for their trust and support throughout the period of my stay here. They are the main soul and inspiration for each and every step that I have achieved in my life.

And finally I express my humble gratitude and prayers to the Almighty God for guiding me through and blessing me with the necessary patience and strength to carry out my work and responsibilities so far.

Saurav Paul

List of Abbreviations

5-HT	5-hydroxytryptamine
AcOH	Acetic acid
AIDS	Acquired immunodeficiency syndrome
CSF	Cerebral spinal fluid
D-1-MT	1-methyl-*D*-tryptophan
DCM	Dichloromethane
DMF	Dimethyl formamide
DMEM/F12	Dulbecco Modified Eagle Medium: Nutrient mixture F-12
DMSO	Dimethylsulfoxide
DNA	Deoxyribonucleic acid
EDC.HCl	1-ethyl-3-(3-dimethylaminopropyl)carbodiimide hydrochloride
ESI	Electrospray ionisation
Et_3N	Triethylamine
EtOAc	Ethyl acetate
EtOH	Ethanol
h	Hour
HeLa	Henrietta Lacks
HEPES	4-(2-hydroxyethyl)-1-piperazineethanesulfonic acid
hIDO	Human Indoleamine 2,3-dioxygenase
HIV	Human immunodeficiency virus
HOBt	1-Hydroxybenzotriazole
HRMS	High resolution mass spectrometry
HTS	High throughput screening
HuIFN-γ	Human interferon gamma
IDO1	Indoleamine 2,3-dioxygenase 1
IFN-γ	Interferon gamma
IR	Infrared
K_2CO_3	Potassium carbonate
kDa	kilodalton
KPB	Potassium Phosphate Buffer
Kyn	Kynurenine
L-1-MT	1-methyl-*L*-tryptophan

L-Trp	*L*-tryptophan
m/z	Mass to charge ratio
MeOH	Methanol
mL	Milliliter
mM	Millimolar
mp	Melting point
MVD	MoleGro. virtual docking
MTT	3-(4,5-dimethylthiazol-2-yl)-2,5-diphenyltetrazolium bromide
Na_2CO_3	Sodium carbonate
Na_2SO_4	Sodium sulphate
NAD^+	Nicotineamide adenine dinucleotide
NADPH	Nicotinamide adenine dinucleotide phosphate
$NaHCO_3$	Sodium hydrogen carbonate
NaOH	Sodium hydroxide
NFK	*N*-formylkynurenine
NH_4Cl	Ammonium chloride
nm	Nanometer
nM	Nanomolar
NMR	Nuclear magnetic resonance
ORF	Open reading frame
PBS	Phosphate buffer saline
PDB	Protein data bank
Pd-C	Palladium on activated charcoal
*p*DMAB	4-dimethylaminobenzaldehyde
ppm	Parts per million
PTSA	*p*-Toluenesulfonic acid
r.t.	Room temperature
RNA	Ribonucleic acid
SAR	Structure activity relationship
SDS	Sodium dodecyl sulphate
TDO	Tryptophan 2,3-dioxygenase
THF	Tetrahydrofuran
TLC	Thin layer chromatography

TMS	Trimethylsilane
UV	Ultra violet
μM	Micromolar

Amino Acid	3-letter symbol	1-Letter symbol	Amino Acid	3-letter symbol	1-Letter symbol
Alanine	Ala	A	Methionine	Met	M
Arginine	Arg	R	Phenylalanine	Phe	F
Aspargine	Asn	N	Proline	Pro	P
Aspartic acid	Asp	D	Pyrrolysine	Pyl	O
Cysteine	Cys	C	Selenocystein	Sec	U
Glutamic acid	Glu	E	Serine	Ser	S
Glutamine	Gln	Q	Threonine	Thr	T
Glycine	Gly	G	Tryptophan	Trp	W
Histidine	His	H	Tyrosine	Tyr	Y
Isoleucine	Ile	I	Valine	Val	V
Leucine	Leu	L			

Abbreviations for intensities of ^{1}H-NMR signals			
s	singlet	m	multiplet
d	doublet	brs	broad signal
dd	doublet of doublet	Hz	Hertz
t	Triplet	MHz	Mega-Hertz

Compounds and inhibitor constants parameters

EC_{50}	The concentration of an compound which causes 50% of a maximal effect
IC_{50}	The concentration of an inhibitor which causes 50% inhibition
K_i	Inhibitor dissociation constant

Abstract

The contents of this thesis entitled **"*Design and Synthesis of Indoleamine 2,3-Dioxygenase 1 Inhibitors*"** have been divided into four chapters based on the results of experimental work carried out during the research period. The introductory chapter (**Chapter 1**) of the thesis describes the various physiological function of the heme-protein, indoleamine 2,3-dioxygenase 1 (IDO1). This chapter also describes the importance of IDO1as a key therapeutic target for the treatment of diseases (like cancer, Alzheimer etc.) which are associated with the *L*-tryptophan (*L*-Trp) metabolism through the kynurenine pathways. Moreover, it explains the several consequences of over expression of IDO1 enzyme in tumor cell which results in the uncontrolled metabolism of *L*-Trp not only to escape the immune responses but also enhances its immune tolerance capability. Thus this chapter provide an insight regarding the immunosuppressive and immunomodulatory role of the over-expressed IDO1 enzyme thereby justify the importance of the design of inhibitor molecules for IDO1 enzyme. **Chapter 2** demonstrates the synthesis of a series of nitrobenzofurazan derivatives of *N*′-hydroxybenzimidamides and their IDO1 inhibitory activity studies against purified enzyme and under cellular environment. This chapter also reports the enzyme kinetic study and the molecular docking analysis for understanding the mode of inhibition and binding, respectively. IDO1 selectivity of the synthesized compounds with respect to the tryptophan 2,3-dioxygenase (TDO) enzyme is also described in this chapter. **Chapter 3** describes the synthesis of a series of 3-substituted oxindoles and their IDO1 inhibitory activity studies against purified enzyme and under cellular environment. These 3-substituted oxindoles based derivatives were synthesized with an aim to develop mechanism-based IDO1 inhibitors with the ability to mimic the epoxide intermediate. Selected compounds showed low-micromolar level of IDO1 inhibitory activities, negligible cytotoxicity and better selectivity toward the IDO1 enzyme. **Chapter 4** demonstrates the synthesis of a series of C3-substituted 1*H*-indazoles and their IDO1 inhibitory activity studies against purified enzyme and under cellular environment. Moderate selectivity of these potent compounds for IDO1 over TDO enzyme also suggests that these heterocyclic compounds are attractive molecules for immunotherapeutic applications.

L-Trp is one of the least abundant of all the essential amino acids and it undergoes catabolism through a tightly controlled manner in the human body. *L*-Trp is not only

involved in protein synthesis but also utilized in various physiological processes through the generation of biologically active products such as the neurotransmitter serotonin (5-hydroxytryptamine), the neurohormone melatonin and its kynurenine metabolites. These essential amino acids consists of two metabolic pathways namely methoxyindoles and kynurenine pathways. The second one being the major pathway since, around 95% of the *L*-Trp is metabolized by this route, results in the conversion of *L*-Trp to kynurenine (Figure1).

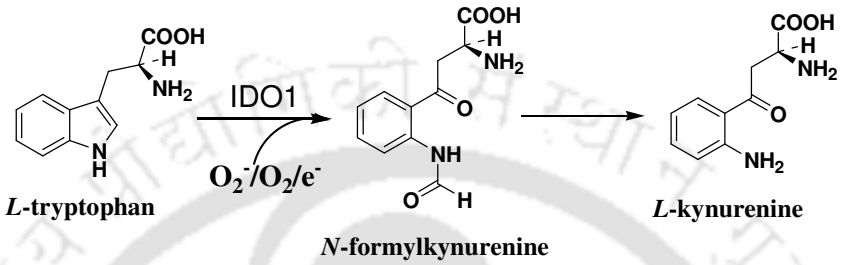

Figure 1. The first step of the kynurenine pathway. IDO1 enzyme cleaves the C2-C3 double bond of the *L*-Trp to form *N*-formylkynurenine which spontaneously forms *L*-kynurenine via enzymatic cleavage.

IDO1 catalyses the initial and rate limiting step of the kynurenine pathway. It is observed that *L*-Trp and its metabolites have a lot of biological significance and it is also essential for the T-lymphocyte proliferation. Due to the over-expression of IDO1, the cellular *L*-Trp level is lowered and the downstream metabolites of the kynurenine pathway is accumulated which exerts a local immunosuppressive effect on T-lymphocytes. Depletion of *L*-Trp is also related to several biological disorders like Alzheimer's disease, age related cataracts and cancer.[3] It is also observed that many tumor cells constitutively express IDO1 and this over-expression is further associated with its enhanced capability to suppress a potentially effective immune system. Clinical studies suggest that this phenomenon is further related with poor survival rate in different types of cancer patient.[4]

This immunomodulatory role of IDO1 has led to the hypothesis that its inhibition might results in the restoration of normal immune response and thereby enhances the efficacy of cancer treatment. Hence the therapeutic potential underlying the IDO1 inhibition has led to the development and design of various IDO1 inhibitors that can be used efficiently as an adjuvant chemotherapeutic agent. This concomitant administration of the IDO1 inhibitors along with chemotherapy can simultaneously enhance the chance of the patient survival.

The basic objective of chapter 2 is the optimization of hydroxyamidine scaffold-based IDO1 inhibitors relying on our rational drug design approach. In this chapter, a series of nitrobenzofurazan derivatives of *N′*-hydroxybenzimidamides (**1**) moiety were synthesized and their IDO1 inhibitory activity against purified enzyme and under cellular conditions were investigated. Interestingly, several hydroxyamidine based compounds proved to be potent inhibitors of IDO1 enzyme with inhibitory potency in the nanomolar range. Selected compounds also showed strong IDO1 enzyme inhibitory activity in MDA-MB-231 cells with no/negligible amount of toxicity. Additional screening against TDO enzyme showed their stronger selectivity for IDO1 enzyme.

The compounds **1(a-n)** were synthesized in two steps under mild conditions. First, condensation of hydroxylamine with corresponding benzonitrile under basic condition produced substituted *N′*-hydroxybenzimidamide with good yields. Further treatment of these hydroxyamidines with 4-chloro-7-nitrobenzofurazan (NBD-Cl) in the presence of $NaHCO_3$ under ethanolic solution produced the target compounds **1(a-n)** with moderate to good yields.

The *N′*-hydroxybenzimidamide compounds, **1(a-n)** displayed strong hIDO1 inhibitory activities with IC_{50} values ranging from 63 to 268 nM. The IC_{50} value of the reported potent compound 4-amino-*N*-(3-chloro-4-fluorophenyl)-*N′*-hydroxy-1,2,5-oxadiazole-3-carboxymidimade under the experimental conditions was 91 nM, which is in accordance with the reported values. For further confirmation of their efficacies, IDO1 activity assay was also performed by HPLC analysis and the calculated IC_{50} values are also in nanomolar range. The therapeutic potential of the synthesized hydroxyamidines was investigated under the *in vitro* cellular environment using MDA-MB-231 breast cancer cell line. The tested compounds showed EC_{50} values ranging from 66 to 242 nM. The mode of IDO1 inhibition by the potent hydroxyamidines was determined using Line weaver-Burk equation. The kinetic plots suggested both competitive as well as uncompetitive modes of inhibition under the similar experimental conditions. The probable mode of interaction of the potent compounds with the IDO1 enzyme (PDB code: 2DOT) was investigated by molecular docking studies and it was observed that both hydrogen bonding and hydrophobic interactions play important roles in stronger binding of the compounds to the active site of IDO1 enzyme. Counter-screening against TDO enzyme showed that the potent compounds have 100 to 1700-fold stronger selectivity for IDO1 enzyme over TDO enzyme. HPLC-based TDO activity assay also showed that

these potent compounds have preferential selectivity for IDO1 over TDO enzyme inhibitions.

In chapter 3, Trp and indole-based IDO1 inhibitors were developed that can block the enzyme-dependent oxidative cleavage reaction of the pyrrole ring and construct mechanism-based effective IDO1 inhibitors. Comprehensive mechanistic studies of IDO1 induced *L*-Trp catabolism revealed that the addition of ferrous heme-iron coordinated molecular oxygen to the C2-C3 double bond of the pyrrole ring is the prerequisite for the IDO1 supported oxidation of *L*-Trp. These studies also proposed the formation of epoxide intermediate state during the transformation of *L*-Trp to *N*-formylkynurenine by IDO1 enzyme. We hypothesized that the presence of carbonyl group at the C2-position of the pyrrole ring of *L*-Trp could perturb further radical addition of Fe (III)-superoxide intermediate. Consequently, oxindole derivatives can hinder the IDO1 enzyme-dependent oxidative cleavage reaction of the pyrrole ring of *L*-Trp. Hence, based on this hypothesis, we synthesized oxindole-based derivatives that can mimic the epoxide intermediate state of *L*-Trp and can be used as potent inhibitor of IDO1 enzyme.

3-Substituted oxindole derivatives **2** and **3** were synthesized from *L*-Trp and tryptamine, respectively by treating with the oxidizing mixture of DMSO/HCl in AcOH solution. To explore the role of C3-substitution of the oxindole moiety at inhibiting the IDO1 enzyme activity, we also synthesized hydrazone (**12**-**17**), phenylimino (**18**-**20**) and alkene-oxindole (**21** and **22**) derivatives of isatin. C3-substituted 3-hydroxy-3-alkyl derivatives of isatin and 5-chloroisatin were synthesized according to the reported procedure to explore the role of substitution in the oxindole ring on IDO1 enzyme activity. Condensation of 5-chloroisatin with acetone yielded 3-hydroxy-3-alkyl compound **27** in the presence of K_2CO_3. Dehydration of compound **27** in the presence of concentrated HCl and catalytic amount of AcOH in ethanol yielded compound **23.** Condensation of 5-chloroisatin with acetylacetone in the presence of K_2CO_3 yielded both alkene and 3-hydroxy-3-alkyl derivatives **24** and **28** respectively.

The result showed moderate inhibitory activity of 3-substituted oxindole derivative against purified IDO1 enzyme. The optimization directed to the identification of potent compound **7**, 1**3**, **24** and **26** with IC_{50} value of 0.19 to 0.63 µM. The inhibitory potency of the compounds was also quantified by HPLC based method. The calculated EC_{50} values of the compounds obtained after performing cellular study in MDA-MB-231 cells are within 0.33-1.26 µM range. The mode of IDO1 inhibition by the potent oxindole derivatives was determined using Line weaver-Burk equation. The kinetic plots suggested

both competitive as well as uncompetitive modes of inhibition under the similar experimental conditions. The probable mode of interaction with the IDO1 enzyme (PDB code: 2DOT) was determined using molecular docking study and it suggested that the oxindole moiety is mimicking the intermediate state for the *L*-Trp oxidation. Screening against purified TDO enzyme revealed that these oxindoles were considerably inactive ($IC_{50} \geq 20$ μM) against TDO enzyme exhibiting 18 to 210 fold of selectivity.

The chapter 4 describes the synthesis of a series of C3-substituted 1*H*-indazoles and their IDO1 inhibitory activity studies against purified enzyme and under cellular conditions. Although, recent molecular docking analyses and pharmacophore models identified 1*H*-indazole scaffold as a novel class of IDO1 inhibitor but no indazole derivatives displayed low-micromolar activities. In-depth structural investigation, molecular docking analyses and reported experimental evidences revealed that these 4- and 6-substituted 1*H*-indazole may not be suitable for proper binding to the active site of IDO1 enzyme. Hence, in an attempt to find potent IDO1 inhibitors, we synthesized 3-and 5-substituted 1*H*-indazoles and examined their IDO1 enzyme inhibition potential.

A series of 3(*N*′-aryl) carboxamide derivatives of 1*H*-indazoles were synthesized from 1*H*-indazole-3-carboxylic acid. Coupling of 1*H*-indazole-3-carboxylic acid with substituted arylamine in the presence of HOBt and EDC.HCl in DMF solvent yielded the target compounds **29(a-f)** and **30**. Similarly, compound **30** was synthesized using 2-aminopyrimidine under the similar reaction conditions. *N*′-Aryl-1*H*-indazole-3-carbohydrazide derivatives **31(a-e**) were also synthesized under the similar experimental conditions using 1*H*-indazole-3-carboxylic acid and arylhydrazines.

The result showed the IDO1 inhibitory efficiency of the 1*H*-indazoles in low micromolar range. Among the tested compounds, **29c** showed moderate IDO1 inhibition potency with IC_{50} value of 8.5 μM. Compounds **31a** and **31d** exhibited stronger IDO1 inhibitory activities with the IC_{50} value of 0.72 and 0.77 μM respectively. For additional validation of their inhibition efficiencies HPLC based IDO1 enzyme activities were also performed. The compounds under the cellular environments showed inhibitory activities (EC_{50}) in low micromolar range. Enzyme kinetic studies in the presence of the compounds showed both uncompetitive and mixed inhibition modes. Molecular docking analysis of the potent compounds with the IDO1 enzyme (PDB code: 4PK5) revealed that hydrogen bonding, hydrophobic interactions and pi-stacking play important roles in stronger binding of these compounds. TDO activity studies showed 5 to 25 fold selectivity of these 1*H*-indazoles for IDO1 enzyme.

IDO1 plays a key role in tryptophan catabolism via the kynurenine pathway in the immune system. Over-expression of IDO1 is associated with poor prognosis of patients for a wide range of malignancies. Hence, IDO1 is a validated target for the treatment of diseases that are associated with immune suppression, including cancer. So far a variety of IDO1 inhibitors have been reported. Most of them have moderate IDO1 inhibitory potency. Hence, there is a demand for design and synthesis of novel molecules, which can actively inhibit the IDO1 with high potency as well as with selective specificity as compared to that of the other heme-containing enzymes.

In this regard, we synthesized a series of nitrobenzofurazan derivatives of *N'*-hydroxyamidines, 3-substituted oxindoles and C3-substituted 1*H*-indazoles as a new class of IDO1 enzyme inhibitors. Activity measurements and molecular modelling studies of the compounds suggest that the presence of hydroxyamidine and nitrobenzofurazan moieties and suitable substitution in the benzene ring of the compounds play a critical role in their stronger IDO1 enzyme inhibitory properties. Activity measurements showed that suitable substitution and restricted rotation around C3-position of the oxindole ring were effective in improving the IDO1 enzyme inhibitory efficacies. The presence of 1*H*-indazole ring and suitably substituted carbohydrazide moiety at the C3 position of the parent scaffold plays a key role for their strong *in vitro* inhibitory activities. Overall, our findings suggest that structural simplicity, low cytotoxicity and inactivity for TDO enzyme makes them quite attractive and potential drug target for further investigation of IDO1 function and immunotherapeutic applications.

CHAPTER 1

Introduction

1. Physiological role of enzymes

Enzymes are biocatalysts that occur ubiquitously in almost all living organisms. These bio-macromolecules play a vital role in carrying out numerous biochemical reactions by catalyzing them under mild-physiological conditions with large turnover number and high degree of specificity. Based upon the types of reactions they catalyze, enzymes are broadly classified into six major categories as follows:

(a) Oxidoreductases: participates in the regulation of oxidation and reduction reaction

(b) Transferases: regulates transfer of a group from one molecule to another

(c) Hydrolases: hydrolysis of various functional groups

(d) Lyases: catalyzes the reactions involved in the cleavages of a bond by non-oxidative and non-hydrolytic procedure

(e) Isomereases: takes part in the interconversion of all types of isomer

(f) Ligases: regulates the formation of a bond between two molecules

Structurally enzymes are large protein molecules and most of them consist of group(s) of metal ion(s), which play a key role in their overall activity. Any perturbation to these metal ions renders the enzyme inactive towards a particular reaction. These enzymes are termed as metalloenzymes and this chapter provides an introduction regarding the function and activity of one such metalloenzyme of the dioxygenases class of enzymes namely indoleamine 2,3-dioxygenases1 (IDO1) with heme as the prosthetic group.

1.1. Role of metal ion in biological oxidation

Oxygen is not only the third most abundant element in the universe, but also one of the major constituent of the vital structural molecules in the living organisms such as carbohydrate, fats and proteins. Almost all living organisms utilize oxygen by respiration that involves cleavage of dioxygen through an energetically favorable process. Under typical conditions, oxygen molecule is unreactive due to its triplet ground state electronic configuration. All stable organic compounds are in singlet state with all of their electrons paired in comparison with that of oxygen ground state, which hinders the spontaneous reaction between the two species due to the high-energy requirement.[1] Transition metal

ion such as iron, copper and others are present as the cofactor in various metalloenzymes that plays a crucial role in carrying out various biological oxidation processes. Several metalloenzymes assists in overcoming the high kinetic energy barrier inherent to the reaction of triplet oxygen.

These transition metal ions in the metalloprotein in their appropriate oxidation states readily reacts with triplet oxygen forming a dioxygen adduct that easily participates in reaction pathways resulting in the oxidation reactions involving the incorporation of the oxygen atom into the desired organic substrate.[2] Apart from the first row transition metals, most of them have various shells of electrons that favors spin transition and the presence of unpaired electrons in most of them enables to actively participate in the reaction involving the transport, activation and reduction of dioxygen in the biological system. Moreover, they also have several excited state configuration with unpaired electrons that have the energy in the close proximity to the ground state energy of the dioxygen, that enhances the possibility of spin transition within the system.[3] The dioxygen activation by these transition metal ion containing 3d-orbital electrons occurs by three methods.[4] Firstly, the presence of the 3d-orbital with unpaired electrons in transition metals facilitates the overlap of the unpaired electrons in the dioxygen π^* orbitals during the addition of dioxygen to the transition metal ion. This further facilitates the reaction of the transition metal-dioxygen with a singlet organic molecule.[5] Secondly, the transition metals present in the metalloenzyme exhibits two consecutive oxidation states (e.g. Fe^{II} / Fe^{III}, Cu^{I} / Cu^{II} etc.) and hence are capable of carrying out single oxygen transfer to the bound dioxygen, thereby enabling the triplet oxygen ground state to accept a single electron to form superoxide. This can again participate into various 1-electron or 2-electron transfer reactions.[6] Finally, various proposals refers to the possibility of reaction of dioxygen via radical mechanism in some non-heme dioxygenases, in which a bound intermediate that forms a substrate radical can attack dioxygen to form a stable radical.[4,7]

1.2. Role of heme-protein in the biological system

Iron protoporphyrin-IX is also known as heme. It is an iron containing macrocyclic compound found to be present in several proteins of both prokaryotes and eukaryotes. Structurally it has a tetra-pyrrole structure connected by methane bridges at positions α, β, γ and δ resulting in a square planar structure with eight side chains; four methyl positions (i.e., position 1, 3, 5 and 8, respectively), two vinyl position (i.e., position 2, 4) and two

propionates at position 6 and 7, respectively. The central metal ion (Fe^{III}) of the porphyrin-IX has six co-ordination sites with the fifth and sixth axial bonds termed as the proximal and distal co-ordination sites, respectively. In majority of cases the proximal ligand is histidine. Furthermore, the oxidation state of iron also varies and range from ferrous (Fe^{II}) to ferric (Fe^{III}) and to ferryl (Fe^{IV}) in some cases such as peroxidises and cytochrome - P450.[8,9]

The biological function of the heme-protein is primarily determined by the sequence of the amino acids forming the polypeptide chains, as well as by the distal and proximal ligands to the heme group that can control its ability for oxidation and reduction of the iron. In general, heme-proteins take part in many biological functions in eukaryotes such as transport and storage of oxygen, catalysis and active membrane transport as well as electron transport pathways.

1.3. Oxygenases

The primary biological function of oxygenases in aerobic life forms is the incorporation of oxygen in the dietary nutrients such as amino acids leading to the generation of various biologically active compounds.[10] Depending on the number of oxygen atoms of the dioxygen molecule incorporated into the substrate, the oxygenases are classified into two categories, monoxygenase and dioxygenase.[9] IDO1 and tryptophan 2,3-dixygenases (TDO) are such types of heme-containing dioxygenase enzymes, which incorporate two atoms of oxygen to the substrate.[11,12]

Monoxygenase: $XH + O_2^* + 2e^- + 2H^+ \rightarrow X(O^*)H + H_2O$

Dioxygenases: $XH + O_2^* \rightarrow X(O_2^*)H$

1.4. Reactions catalyzed by the IDO1 and TDO enzymes

IDO1 and TDO are heme-containing enzymes that catalyze the highly specific irreversible pyrrole ring cleavage of the *L*-tryptophan (*L*-Trp). Metabolism of *L*-Trp to nicotinamide adenine dinucleotide (NAD^+) through the formation of *N*-formylkynurenine is known as kynurenine pathway. The first rate-limiting step of the kynurenine pathway is catalyzed by IDO1/TDO enzyme leading to the formation of *N*-formylkynurenine through the simultaneous cleavage of the C2-C3 bond of the *L*-Trp and the incorporation of the oxygen molecule in the substrate molecule (Figure 1.1). In 1975, Hirata and coworkers demonstrated that the molecular oxygen was directly incorporated into the *L*-Trp to form *N*-formylkynurenine. They performed heavy oxygen isotope ($^{18}O_2$) labeling experiment to

experimentally support that IDO1/TDO enzyme catalyzes the oxidation reaction of *L*-Trp using oxygen.[13]

Although, both IDO1 and TDO enzyme are involved in the oxidative cleavage of *L*-Trp to *N*-formylkynurenine, yet there are certain essential differences between both the enzymes. While, IDO1 enzyme is ubiquitously distributed in the extra-hepatic tissues,[14] TDO is found to be primarily identified in the liver and placenta.[15,16] In healthy human body, IDO1 enzyme is primarily found to be concentrated in the lungs, small intestine and placenta along with a moderate amount in the spleen and stomach.[17] IDO1 is a monomeric protein with one heme-prosthetic group. On the other hand, TDO is a tetrameric protein having one heme-unit per subunits.[18] Moreover, they also vary in their substrate specificity.

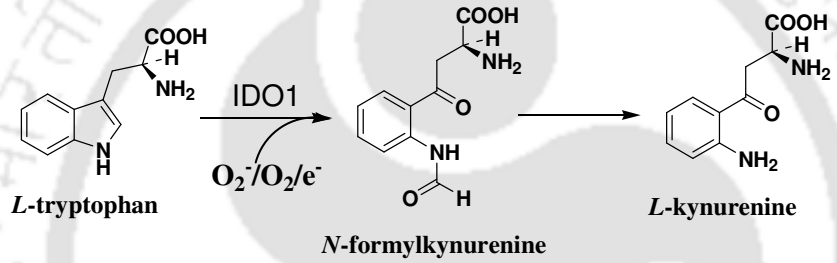

Figure 1.1. The first step of the kynurenine pathway. IDO1 cleaves the 2,3-double bond of the *L*-Trp to form *N*-formylkynurenine which spontaneously forms *L*-kynurenine via enzymatic cleavage.

TDO enzyme contains an additional activating-site apart from the substrate binding-site, that can be occupied both by its natural substrate *L*-Trp as well as by its various other analogues even though they do not compete for the binding to the substrate site. However, *L*-Trp is the solitary substrate for the active site of TDO.[18] Whereas, IDO1 exhibits broad range of specificity compared to TDO and considers both *D*- and *L*-Trp as well as other metabolites like tryptamine, 5-hydroxytryptophan and others as substrate(s).[14]

1.5. Metabolism of *L*-Trp

L-Trp is one of the essential amino acid and it is structurally unique with an indole nucleus in the side chain. It comprises approximately 1% of the overall amino acid content of the protein in the human body. It is an essential amino acid, hence there is no in-built mechanism for its synthesis in human body and it is obtained exclusively from

external dietary sources. Apart from the protein synthesis, various biochemical pathways catabolize 99% of the dietary intake of *L*-Trp. However, in healthy human body the balance of *L*-Trp is properly maintained between the process of tryptophan catabolism and protein synthesis.[19] The metabolism of *L*-Trp first produces tryptamine, which is the decarboxylated product of *L*-Trp. It acts as neurotransmitter with a variety of neural functions including pain response and dose dependent constriction of the smooth muscle.[20] The conversion of *L*-Trp to serotonin and kynurenine through two different enzymatic cascade pathways produces a variety of metabolites that have both physiological and pharmacological significances (Figure1.2).

A large amount of extensive research work has been carried out in the serotonin pathway that converts *L*-Trp into several bioactive metabolites like serotonin, melatonin and niacin. Serotonin (5-hydroxytryptamine) is an aminergic neurotransmitter that is primarily localized in the gut and regulates the intestinal movements.[22] It is also an important neurotransmitter in the central nervous system and controls numerous functions including regulation of mood, sleep as well as memory and learning. Moreover, it also plays a crucial role in several clinical conditions such as migraines, schizophrenia, depression and others.[23,24] In the first step of the serotonin pathway 5-hydroxytryptophan is produced due to the hydroxylation of *L*-Trp at the 5-position. It is then further decarboxylated to 5-hydroxytryptamine by vitamin B6 dependent enzyme aromatic *L*-amino acid decarboxylases.[21] Another neuro-hormone namely melatonin plays an important role in lightening skin pigmentation as well as maintaining the cicardian rhythms of various biological functions (Figure1.2). Moreover, it is a strong antioxidant and is crucial for the protection of nuclear and mitochondrial DNA.[25,26] Similarly, niacin (Vitamin B3) is involved in the production of steroid hormone and DNA repair. Its dysregulation causes a deficiency disease called pellagra.[27] The *L*-Trp is also catabolized to niacin through kynurenine pathway.

1.6. The kynurenine pathway

The kynurenine pathway is the major catabolic pathway for *L*-Trp and this pathway catabolizes approximately 90% of the *L*-Trp to nicotinamide dinucleotide (NAD^+) in the mammalian peripheral tissues.[18,28] The NAD^+ acts as an electron carrier in the catabolic reaction viz. glycolysis.[24] The first rate-limiting step of the kynurenine pathway involves the incorporation of molecular oxygen or superoxide anion for the oxidative cleavage of the C2-C3 double bond of the *L*-Trp indole ring. Both IDO1 [1.13.1.12] and TDO

[1.13.11.17] enzymes catalyzes this step and the resultant product *N*-formylkynurenine (NFK) is then hydrolyzed to form kynurenine by a formidases enzyme.[18,24,29]

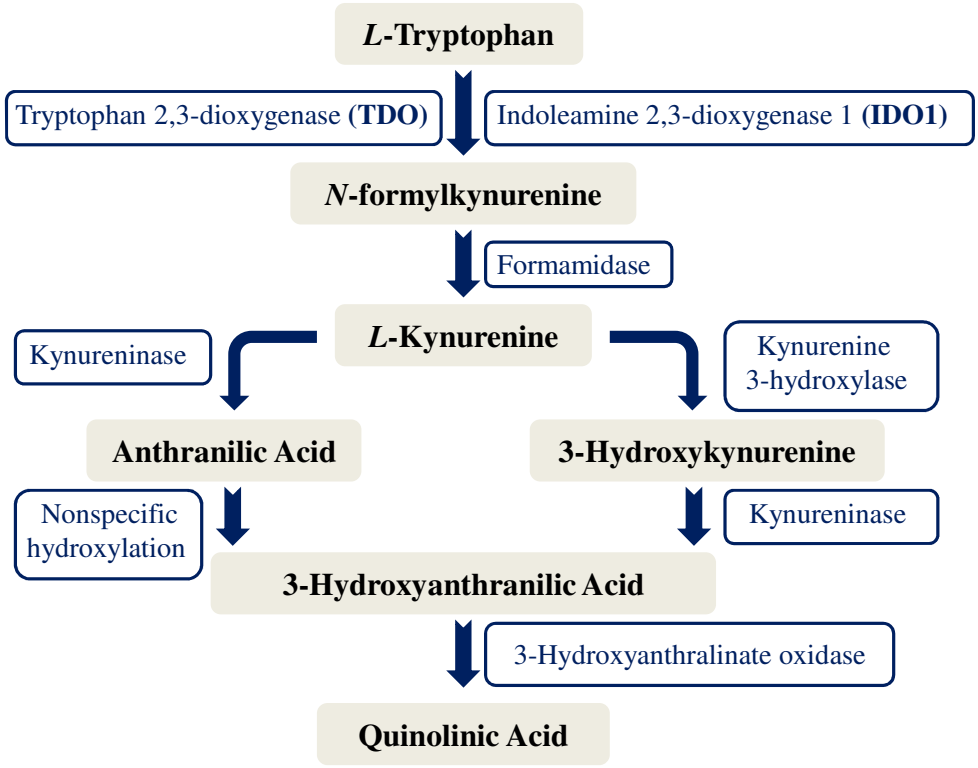

Figure1.2. Metabolism of *L*-Trp via the kynurenine pathway.

The key intermediate kynurenine which is formed from the *L*-Trp metabolism is responsible for the formation of other bioactive metabolites though other three basic pathways. Firstly it produces 3-hydroxykynuenine via oxidation of the aromatic ring by kynurenine 3-hydroxylases [EC. 1.14.13.9] which is further converted to 3-hydroxyanthranillic acid through cleavage by kynureniase [EC. 3.7.13]. This subsequently converts to quinolinic acid by 3-hydroxyanthranilate oxidase [EC. 1.13.11.16]. Finally, it converts to nicotinic acid mononucleotide by the enzyme QPRTase [EC. 2.4.2.19], which is the precursor for the NAD pathway. However, 3-hydroxykynurenine can also lead to the formation of xanthurenic acid by kynurenine aminotransferases.[18,30] Secondly, kynurenine undergoes cleavage to form anthranilic acid, which is catalyzed by kynureninase [EC. 3.7.13].[18] The third step results in the formation of 2-aminobenzoyl pyruvate, which is a transamination product of kynurenine that is catalyzed by the enzyme kynurenine aminotransferases [EC. 2.6.17]. The kynurenine is converted to kynurenic acid by subsequent dehydration.[18]

These metabolites generated along the pathway from the degradation of *L*-Trp, performs a variety of significant biophysical roles. High level of the neurotoxic metabolite quinolinic acid (quinolate) and kynurenine in cerebrospinal fluid (CSF) may be responsible for various neurological disorders e.g. ischemic brain injury, multiple sclerosis, cerebral malaria as well as AIDS related dementia.[31-34] It has also been observed that there has been an increase in the concentration of these metabolites along with the severity neurological dysfunction or injury involving wide range of inflammatory condition. On the other hand, 3-hydroxyanthranilic acid and 3-hydroxykynurenine acts as UV filters that binds to the lens protein of the eye and its high concentration have been related to the formation of cataract in the eyes resulting in the impaired vision of the patient.[34] Moreover, kynurenine pathway metabolites play an immunomodulatory role and are involved in immunosuppressive pathways leading to the suppression of T-cell proliferation. This apoptosis of the T-cells causes a detrimental side effect to the active function of the immune system as a whole.[35,36]

1.7. IDO1 enzyme

1.7.1. Isolation of IDO1 enzyme

Initially IDO1 enzyme was first isolated and purified from rabbit intestine[14] in 1978, based upon a protocol developed by Yamamoto and Hayaishi.[37] This purification protocol yielded around 11% of 500 fold purified rabbit intestinal IDO1 providing 171 μM kynurenine/h/mg enzyme activity with *L*-Trp and was used for further studies.[10] Later on, it was isolated and purified from human placenta following a protocol similar to that was developed for the rabbit intestinal IDO1 isolation. Isolation of IDO1 from human placenta provided 0.9% of a 10,000 fold purified enzyme with a specific activity of 157 μM kynurenine/h/mg protein with *L*-Trp as the natural substrate.[10,38]

1.7.2. Identification of the primary structure of IDO1 enzyme

Two research groups namely Tone et al.[39] and Dai et al.[40] first concurrently reported the primary sequence of the human IDO1 in 1989. The Tone et al. group isolated the cDNA clone from a λgt library, which was prepared from poly(A)$^+$ RNA of interferon gamma (IFN-γ) treated HeLa cells with a monoclonal antibody to human IDO1.Whereas, the Dai et al. group used poly(A)$^+$ RNA from HuIFN-γ infected human fibroblast to isolate cDNA of IDO1. The cDNA of human IDO1 consists of an open reading frame (ORF) with 1209

nucleotides that encoded a protein of 403 amino acids and having a molecular weight of 45.324 kDa.

The murine IDO1 gene was isolated from mouse rectal cancer cell using human IDO1 cDNA as a probe. The murine IDO1 had an ORF of 1221 nucleotides that encodes a protein of 407 amino acids with a molecular weight of 45.639 kDa. The IDO1 from mouse exhibits 61% homology to human IDO1 and the residues 101-184 were highly homologous the residues 96-181 of the human IDO1 with 89% identity.[41] The gene obtained from the rat IDO1 has 91% and 75% identity with that of mouse IDO1 and human IDO1, respectively.[42] Although, IDO1 is a heme-protein but shares very little homology with other heme-proteins such as hemoglobin, myoglobin or cytochrome-P450. TDO, the other hemeprotein also responsible for *L*-Trp metabolism through kynurenine shares only 10% amino acid sequence identity.

1.7.3. IDO1 and its catalytic properties

IDO1 is a monomeric protein having protoheme-IX as the sole prosthetic group.[14,43] The ultraviolet (UV)-visible spectrum of IDO1 have an absorbance maxima at 405 nm in the Soret region, along with bands at 500 nm and 632 nm at pH 6.0, which is a prominent characteristic of a high-spin ferric (Fe^{3+}) hemeprotein.[44] The heme-iron is in its reduced ferrous (Fe^{2+}) state in the active form of the enzyme. IDO1 is prone to autoxidation, therefore a reducing agent is necessary to uphold its activity. IDO1 reduction under in vivo conditions is maintained by cytochrome-b_5 and cytochrome-P450 reductases with NADPH. The purified IDO1 is also inactive with iron at ferric (Fe^{3+}) state and requires methylene blue and ascorbic acid for its activity *in vitro*.[37] Various superoxide (O_2^{*}) generating enzymes such as glutathione reductase and xanthine oxidase can also be used instead of ascorbic acid. However, methylene blue that is assumed to act as an electron carrier has not been replaced with any other natural co-factors, metals or dyes apart from toluidine blue.[10]

IDO1 is found to be an unique heme-containing oxygenase and it utilizes both univalent reduced molecular oxygen (superoxide) and molecular oxygen for the initiation and propagation of the catalytic cycle during the steady state.[10,45] Several observations validate the role of superoxide in the catalytic requirement of IDO1.[10,43,46] Firstly, the superoxide anion can independently support the IDO1 activity and presence of any superoxide scavenger such as superoxide dismutase, significantly reduces its activity by removing the available superoxide anions (O_2^{*}). Secondly, the incorporation of ^{18}O into

the reaction products occurs following the addition of $^{18}O_2^*$. Thirdly, the inhibition of superoxide dismutase by diethyldithiocarbamate results in the enhancement of the intracellular IDO1 activity. Moreover, the native, ferric (Fe^{3+}) form of IDO1 binds with the superoxide anion to form the oxygenated enzyme ($Fe^{3+}O_2^-$) and this reacts with the substrate to form the product.

1.7.4. Ternary complex of IDO1 with oxygen and *L*-Trp and reaction mechanism

The formation of ternary complex was identified first in 1970 from the experiments performed with IDO1[47] and it was concluded that the active form of the enzyme contains iron in the ferrous form, whereas the ferric form was found to be inactive.[47] The ternary complex formation plays a crucial role in the progression of reaction of IDO1 as it results in the activation of oxygen and facilitates the otherwise spin forbidden reaction to proceed. It was proposed that the presence of a reducing agent is necessary for the activation of the ferric form to active ferrous form. However, within the biological system electron carrier proteins like cytochrome-b_5 serve this purpose by donating electrons to the ferric form.[38,48] One of the proposals also suggests the role of superoxide in the activation of the ferric form of the enzyme IDO1.[49]

Hence, it can be concluded that the formation of the ternary complex initiates the reaction mechanism with the substrate and dioxygen bound to the ferrous form of the enzyme. The initial proposed mechanism states that the deprotonation of the indole-N1 through an active site base, which might initiates the nucleophilic attack by the electron rich C3-position on the distal oxygen atom resulting the formation of a 3-indolenylperoxy-Fe^{2+} intermediate. Although it is proposed that the iron bound oxygen plays the catalytic role since various experimental evidence shows that the catalytic activity is retained even though the His55 residue is replaced with alanine, which is the only basic residue present.[50] Subsequently, the conversion of the intermediate via two routes namely 'Dioxetane or Criegee' results in the formation of the product *N*-formylkynurenine (Figure1.3). Although, the 'Criegee' mechanism is well discussed in the literature of non-heme iron, but neither of the 'Criegee or Dioxetene' mechanism has any experimental evidence. Moreover, computational work such as density functional theory provided the only information related to this mechanism and recent findings does not supports either of the mechanism owing to its high activation barrier for the formation of the neutral indole intermediate.

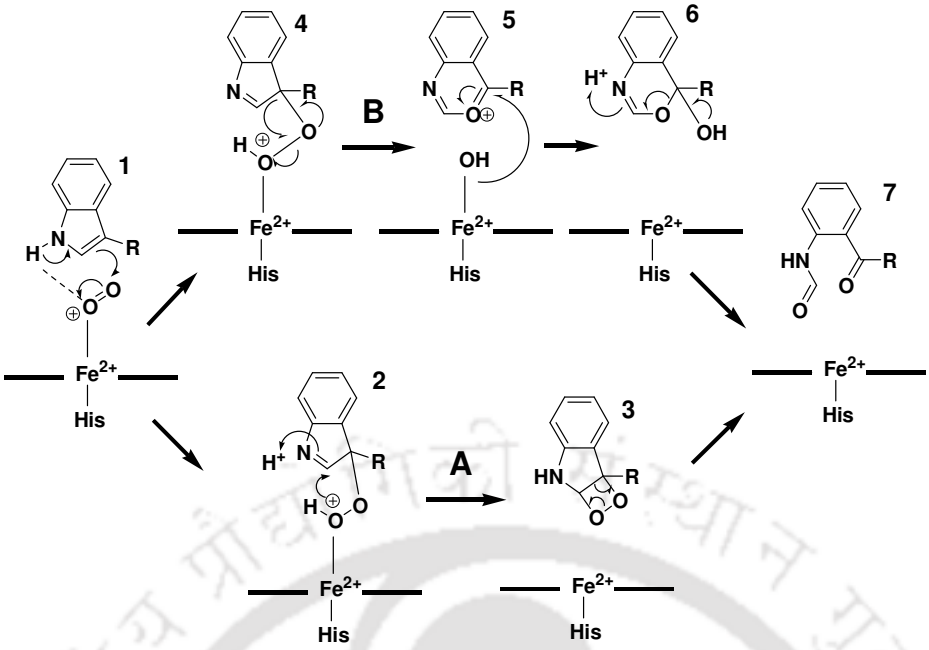

Figure 1.3. Formation of the initial ternary complex (**1**) through binding of substrate tryptophan and oxygen with the ferrous heme-protein followed by the formation of peroxyindole intermediate (**2** and **4**) that undergoes rearrangement to form the final product *N*-formylkynurenine via two proposed mechanism namely Criegee **(B)** and Dioxetane **(A)** respectively.

A recent proposal suggests a new mechanism, which involves a ferryl intermediate, in which the oxygen molecules is added through a two-step mechanism.[51,52] It involves the initial addition of one oxygen molecule that spontaneously converts to the ferryl intermediate resulting in homolytic O-O bond cleavage in which the second oxygen molecule is incorporated to form the product. Recent theoretical studies suggest the formation of epoxide as the first oxidation step (Figure 1.4).[53]

One of the key points that contradict the usual requirement for the heme-mediated catalysis in the scheme involving the Crigee and Dioxitene mechanism, is the absence of the formal change in the oxidation state in the turnover step. But various reports indicate the formation of a ferryl heme species involved in the turnover step of the dioxygenase. Yeh and co-workers,[54] first reported this phenomenon by using resonance Raman method that indicated the presence of a characteristic stretching frequency of ferryl heme ($\nu_{Fe=O}$) (compound A) observed during the turnover in hIDO1.

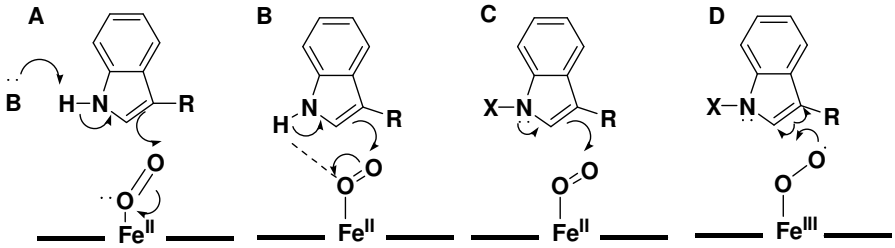

Figure 1.4. Different proposed reaction mechanism for Heme dioxygenases.[52] (**A**) the base-catalysed abstraction mechanism, (**B**) alternative to the base-catalysed mechanism, using abstraction of protons by the bound oxygen, (**C**) electrophilic addition and (**D**) radical addition.

Moreover, when independently observed, similar stretching frequency has also been found in IDO1 enzyme.[55,56] This suggests a stepwise insertion of oxygen into the substrate accompanied by the oxidation leading to the formation of ferryl heme (Figure 1.5), to be the preferred route in contrary to the simultaneous incorporation of both the oxygen atom as depicted in Figure 1.3.

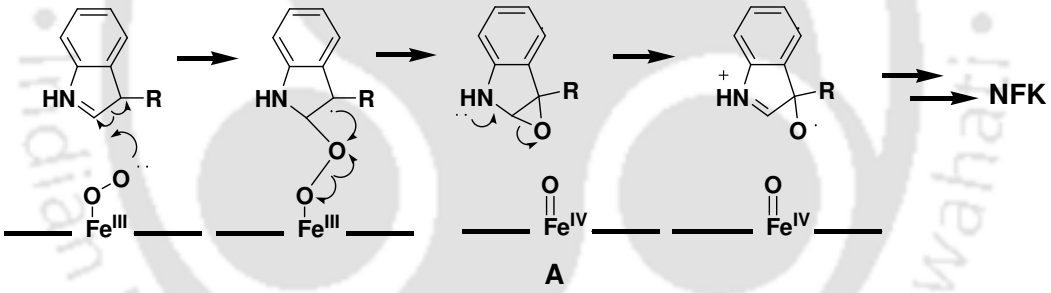

Figure 1.5. Formation of the *N*-formylkynurenine (NFK) via radical addition leading to the formation of a ferryl heme species (**A**) and a proposed epoxide species respectively.[52]

There are various evidences available in the literature that supports the possibility of the epoxide mechanism. Certain features of the mechanism proposed in figure 1.5, exhibits similarity with that of few related enzymes such as cytochrome-P450s, in which the formation of epoxide intermediate is already well established. Moreover there are also reports that suggests the homolytic cleavage of the bound endoperoxide O-O bond as well as the formation of the ferryl heme resulting to the isomerisation of the endoperoxides mediated by the heme enzymes prostacylin synthase and thromboxane synthase.[57] Similarly, non heme iron enzymes e.g. tyrosine hydroxylase also exhibits the formation of Fe^{IV}=O species resulting from ferrous iron and oxygen.[58]

Although there is no experimental proof related to the final step of the mechanism i.e. the formation of NFK from the proposed intermediates, yet from a chemistry point of view it can concluded that the epoxide intermediate would easily undergo a favorable C2-O bond cleavage assisted by the adjacent nitrogen lone pair. This justifies the first step that involves the ring opening through the C2-C3 bond cleavage as shown in the figure 1.5. Moreover, literature also suggests that epoxide ring preferably undergoes such ring opening which is observed in case of the chemical epoxidation of tryptophan by peracids.[59] Various recent computational studies also supports the ring opening of the proposed epoxide intermediate, with the probable assistance by the protonated amine group of the substrate.[53] Although the corresponding steps involved in the detailed mechanism of conversion of epoxide to NFK have been proposed but the validity of these final steps are yet to be verified by experimental evidences.

1.7.5. Crystal structure and active site of IDO1 enzyme

Heme-containing proteins are one of the most widely studied metalloproteins. IDO1 is one of the members of such heme-containing proteins. In general, the heme-unit is electronically neutral but in the presence of the iron in its oxidized-ferric form (Fe^{3+}) renders an overall positive charge to the hemin structure. Apart from the four coordinated-site of the porphyrin ring, other groups/amino acid residues from the protein also take part in binding to the remaining coordination site(s) of iron, to satisfy the coordination requirement of the heme-proteins. Few common coordinating functional groups are the imidazole nitrogen of histidine, the phenoxide group of tyrosine, the sulfur of the methionine and cysteine and the carboxylate group of aspartic acid and glutamic acid.

Currently there are quite a few co-crystal structures of IDO1 in complexation with different ligands. The first reported crystal structure of IDO1is a complex between the ferric IDO1 along with either the inhibitor 4-phenylimidazole or cyanide (2DOT).[60,61] The complex was crystallized in dimeric-form with a disulfide bridge between the cysteine 308 residues on each monomer. Structurally it is a monomeric protein with two domains. The major domain consists of the active site or the catalytic pocket along with a small domain and consists of both α-helices and β-strands. The major domain is primarily composed of 15 α-helices, in which the endogenous proximal ligand namely histidine 346 is provided by one such helix. The small domain is comprised of nine α-helices and two

β-sheets and they are connected by a loop of 17 residues that also contributes to the part of the catalytic pocket cavity along with the distal side (Figure 1.6).

The crystal structure of the IDO1 reveals that there is an abundance of hydrophobic residues in the active and some of these residues play an important role in the substrate binding. The amino acid residues like R231, F226, F163, S167, H364 are involved in the binding of *L*-Trp which is observed from the overlaid crystal structure of IDO1 (2DOT). This detail regarding the active site residues have resulted in the advancement of knowledge regarding the substrate protein interaction within the active site. It is observed that the dioxygenase can also undergo a conformational change and the arginine active site residue is capable of forming electrostatic interactions with the carboxylate group of the *L*-Trp through interchange in absence of substrate.

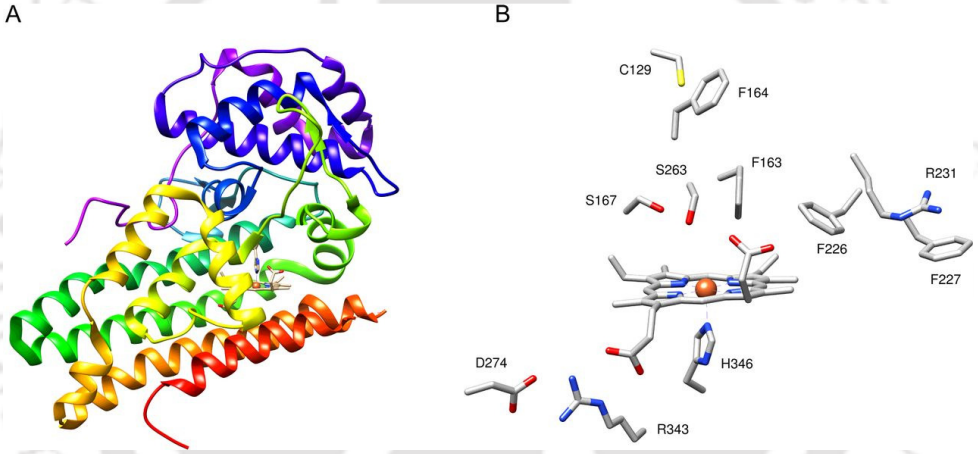

Figure 1.6. (A) Overall crystal structure of human IDO1,[33] showing α-helices, β-sheets and the loop region. (B) Active site of human IDO1[33] along with the residues and the heme (orange) as the prosthetic group.

1.8. Role of IDO1enzyme in various diseases

It has been observed that any deregulation of the kynurenine pathway largely contributes to the elevation of IDO1 activity as well as the generation and accumulation of various downstream harmful neurotoxic metabolites. Moreover uncontrolled metabolism of the *L*-Trp due to the over expression of IDO1 induced by cytokines like interferon gamma (IFN-γ) assists the tumor cells to escape from the immune responses resulting in its growth and propagation.[62,63] Various studies have shown that many tumors develops the capacity to effectively suppress a potentially active immune response by hijacking the various signaling pathways through which the immune system identifies and eliminates

any potential tumor cell within the body. In general, it is observed that in healthy condition IDO1 has a low activity within the human body and have insignificant physiological effects.[64] However, an increasing evidence of clinical data shows that there has been an increase in the level of IDO1 in the primary tumor cell lines obtained from patients and this suggest IDO1 assists in cancer progression and metastasis.[65,66] Cancer cells over expresses IDO1which not only reduces the *L*-Trp concentration in the cellular microenvironment but also results in the generation of several catabolites leading to the dysfunction of the immune system. Hence the reduction in the local concentration of *L*-Trp and uninhibited formation of the metabolites along the kynurenine pathway such as excitotoxin, quinolinic acid, *N*-methyl-*D*-aspartate receptor antagonist, kynurenic acid and nicotinamide adenine dinucleotide (NAD) assists the IDO1 enzyme to suppress the local immune response. This occurs due to the inhibition of the T-cell proliferation in the G1-phase of the cell cycle since its division is typically sensitive to the local *L*-Trp concentration and lower concentration of *L*-Trp in the microenvironment results in the recruitment of the local regulatory T-cells thereby suppressing the T-lymphocyte proliferation. Thus, IDO1 generate a tolerogenic state in the tumor cell and its lymph nodes by modulating the immune system and rendering it tolerant toward them. Moreover, studies have shown that this over expression of IDO1 enzyme is related with the poor prognosis in different cancers including ovarian and pancreatic.[62,67,68] Recent reports also suggests that various neurodegenerative disorders, HIV-1 encephalitis, cerebral malaria, Huntington diseases, age related cataract etc. are also associated with the up regulation of IDO1 activity.[69,70] Hence, IDO1 has emerged to be a promising molecular target for the development of new therapeutic agents that can be used for the treatment of neurological disorder, cancer and various other diseases, which are characterized by pathological *L*-Trp metabolism.

1.9. IDO1 enzyme as therapeutic target

Modern medical science has developed various methods and approaches towards the diagnosis and treatment of various diseases. Targeting the functions of the enzymes present in the living organisms and to use it as a tool for the treatment of various diseases by proper understanding of the structure and function is of such influential approach, which is recently developed. IDO1 plays a vital physiological role in the human body by precisely controlling and regulating the levels of *L*-Trp, which is one of the essential amino acid obtained primarily through dietary intake.

Recent studies showed that inhibition of IDO1 enzyme activity with small molecules successfully restrain the abnormal growth of tumors and showed complemented effect with chemotherapeutic and radio-therapeutic treatment of malignant tumors.[71,72] TDO enzyme is highly selective and preferably binds to *L*-Trp. Whereas, the active site of IDO1 enzyme is amenable to small molecules and thus IDO1 has emerged as an attractive target in the cancer immunotherapy. Presently, two IDO1 inhibitors, INCB024360 and NLG919 are under clinical trials for the treatment of cancer and other diseases.[73] Another inhibitor of the kynurenine pathway namely *D*-1-MT is also under clinical trial but its mechanism of action is still doubtful since reports suggest that although it inhibits kynurenine production at high concentration but is inefficient in restoring the IDO1 induce arrest of the T-cell proliferation. It is observed that compared to other antitumor agent that have cytotoxic and other antiangiogenic effect, IDO1 inhibitors possesses an appealing ability of modulating immunity. Moreover, the treatment of diseases e.g. cerebral malaria, AIDS dementia complex, Alzheimer's disease etc. requires selective drug delivery to the brain and this may be obtained by the development of a pro-drug form of the inhibitor with an ability of crossing the blood brain barrier thereby transforming into the active inhibitor. Similarly, in case of age-related cataract, there is a scope of development of eye drops that promote localized use of IDO1 inhibitors and hence increasing its selectivity. Several studies have demonstrated encouraging results that increases the potential value of IDO1 inhibitors to be used in the cancer treatment. Hence, the development of small molecule-based IDO1 inhibitors is essential to satisfactorily address the cancer immunotherapeutic opportunity as well as several other diseases related to the deregulations of *L*-Trp metabolism.

1.10. Inhibitors of IDO1 enzyme

Ever since the discovery IDO1 as an attractive target for the cancer immunotherapy, there has been an intense ongoing study in both academics as well as in the pharmaceuticals for the development of potent inhibitors of IDO1. Various novel IDO1 inhibitors have so far been developed including a few potent ones that have entered into the clinical trials. The discovery of the crystal structure of IDO1 in 2006 have provided a scope for the structure based in-silico design of IDO1 inhibitors.[60] Another two new X-ray structures of IDO1 complexed with larger ligands have been recently available with PDB accession code of 4PK5 and 4PK6, respectively.[74] Different IDO1 inhibitors which were designed initially were of moderate micromolar level activity and many of which were the analogues of its

natural substrate *L*-Trp[9,75-77] or other established heme-binder such as 4PI[78] and norharman.[9,78-80] Recently numerous novel IDO1 inhibitor scaffolds were discovered within the past decade through various methods such as natural product screening, structure based drug design as well as by high-throughput screening (HTS), which is for the majority of the cases.

Most of the earlier known IDO1 inhibitors were basically derivatives of Trp and indole moiety[75-77] with 2,5-dihydro-*L*-phenylaniline being the oldest (Figure 1.7A).[9] One of such most widely used is the 1-methyl-*L*-tryptophan (*L*-1-MT)[75] which have a moderate range of activity (K_i = 19-53 μM). Another indole derivative namely 5-((1H-indol-3-yl)methyl)-3-methyl-2-thioxoimidazolin-4-one under the name MTH-Trp (Figure 1.7C)[66] was also reported as IDO1 inhibitor with a K_i value of 12 μM. This compound also acted as necroptosis inhibitor with a cellular IC_{50} = 0.5 μM[81] and was widely used by the name necrostatin-1. Hence, due to its dual role of this compound there was a necessity of compounds with more selectivity in order to study the two pathways separately. Recently various Trp derivatives were developed having micromolar range of IDO1 inhibitory activity that includes 1-methyl tryptophantirapazamine,[82] keto-indoles obtained from virtual screen,[83] tryptoline[84] as well as tryptamine derivatives.[85] Until date no Trp analogue was obtained having submicromolar activities which may be because Trp itself exhibits only a moderate affinity towards IDO1 (K_d = 290-320 μM).[60,86] Hence, a better approach towards the development of inhibitors would be accomplished by designing of molecules capable of mimicking the transition state of the enzymatic reaction by taking into account the iron bound dioxygen ternary complex.

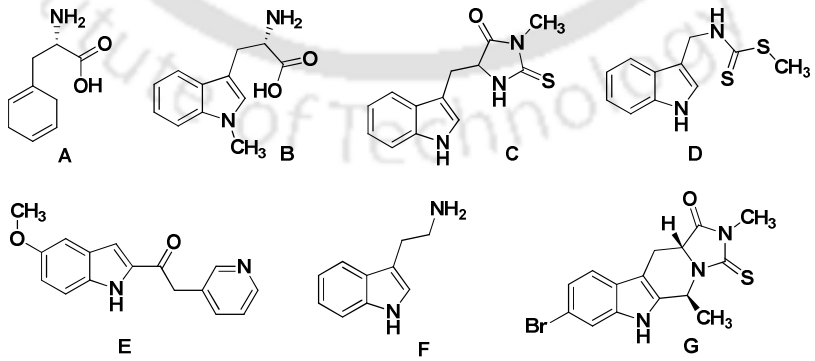

Figure 1.7. Tryptophan and indole analogs. (A) 2,5-dihydro-*L*-phenylalanine,[9] (B) 1-methyl-*L*-tryptophan (*L*-1-MT),[75] (C) MTH-Trp or necrostatin-1,[66] (D) brassinin,[105](E) keto-indole derivative,[83] (F) tryptamine,[85] (G) tryptoline derivative.[84]

Another class of compound developed that displayed high inhibitory activity of IDO1 were the inhibitor scaffolds having quinone/iminoquinone motifs (Figure 1.8).[87-91] The inhibitory activity of menadione and other related quinine compounds towards IDO1 was already reported in the patent literature in 2006.[91] Quinone exhibits its inhibition property through various ways, that includes specific interaction with the enzyme active sites or through the redox-cycling the reducing co-factors[92] as well as by the chemical reactivity towards nucleophillic amino acids side chains.[88,93,94] The mouse melanoma model study data for menadione also showed reduced tumor volume as well as IDO1 mediated efficacy.[88] Although the mode of action of the structurally highly diverse quinone compounds is, yet to be solved still various experimental results obtained from the promiscuous compounds reveals that it lacks the potential to be a suitable base structure for the development of highly selective IDO1 inhibitors.

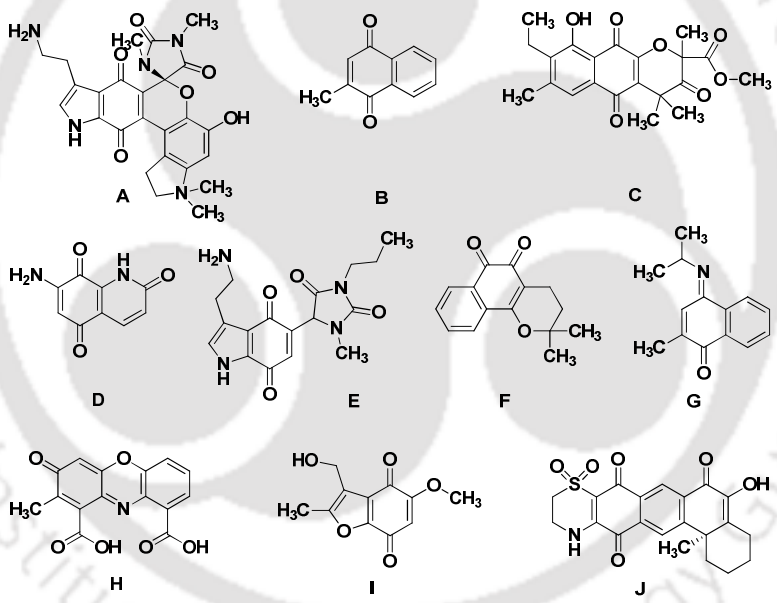

Figure 1.8. Inhibition scaffold with quinone or iminoquinone function. (A) exiguamine A,[89] (B) menadione,[88] (C) annulin B,[91] (D) NSC111041 from the National Cancer Institute, (E) indolequinone,[89] (F) β-lapachone,[91] (G) 4-iminonapthalene-1-one derivative,[87] (H) cinnabarinic acid, (I) benzofuranquinone,[87] (J) xestosaprol-O analog.[90]

Various reports in the literature also suggest different natural products that show inhibitory activity towards IDO1 (Figure 1.9). Norharman or β-carboline derivatives[66,77,78-80] were the first reported natural product inhibitors with moderate inhibitory activity. Similarly, benzomalvin E,[95] halicloic acids A and B,[96] and thielavin[95]

derivatives are some of the other reported natural product inhibitors of IDO1. On the other hand, tryptanthrin derivatives and phytochemical galanal exhibited both *in vivo* and *in vitro* inhibitory activity but there is no availability of cell viability data for the later.[97]

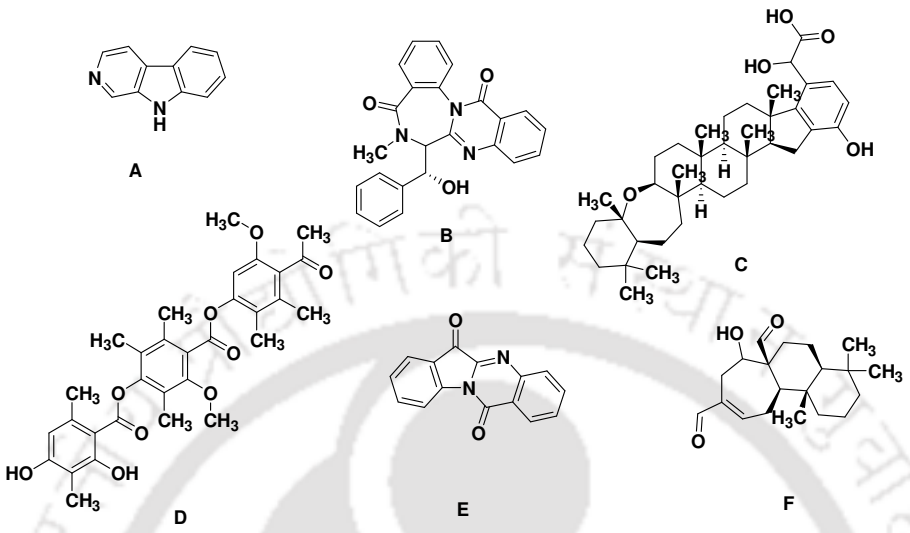

Figure 1.9. Few natural product inhibitors. (A) Norharman/β-carboline,[77] (B) Benzomalvin E,[95] (C) halicloic acid A,[96] (D) thielavin F,[95] (E) tryptanthrin,[97] (F) galanal.[97]

Although majority of the inhibitors scaffolds for IDO1 contains at least two aromatic rings, different scaffolds with a single aromatic ring were also reported (Figure 1.10). Patented in 2009, o-benzyl hydroxylamine and derivatives[98] were reported to show unimicromolar range activity both in enzymatic and cellular studies.

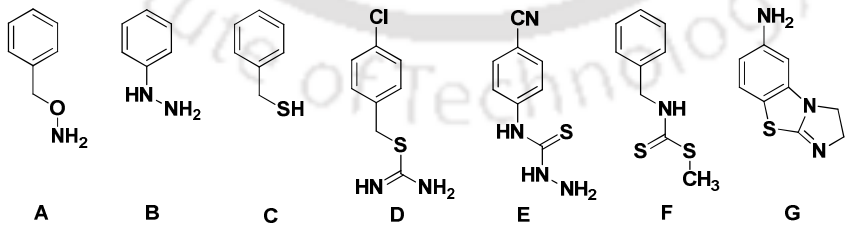

Figure 1.10. Inhibitors with single aromatic ring. (A) O-benzylhydroxylamine, (B) phenylhydrazine, (C) benzyl mercaptan, (D) S-benzylthiourea derivative,[103] (E) thiosemicarbazide,[104] (F) dithiocarbamate derivative,[105] (G) AC12308, Maybridge Screening Collection.[106]

Other IDO1 inhibitors namely phenylhydrazine, (Figure 1.10) discovered by fragment screening also reported inhibitory potency both in *in vivo* as well as *in vitro* studies[99] but in its selectivity for IDO1 over other heme-proteins and reversibility is yet to be investigated. Structurally modified compounds of 2-(3*H*)-benzo-thiazolethione scaffold, provided a series of *N*-phenylthiosemicarbazides also exhibited good inhibitory property towards IDO1 with the most potent compound with an enzymatic IC_{50} value of 1.2 μM.

Similarly, 4-phenylimidazole (4PI), another heme-binding compound was described earlier as an IDO1 inhibitor[78] was highlighted due to its co-crystallization with IDO1 in 2006 (Figure 1.11). Various other derivatives of 4PI were designed by a structural based approach, which showed up to 10-fold greater potency than the parent compound.[100] Moreover different fungi-static drugs of the imidazole type such as miconazole (Figure 1.11) and econazole (Figure 1.11) were also found to be active against IDO1 in different independent screens, whereas similar 1,2,4-triazole drugs like fluconazole were devoid of any activity.[101,102]

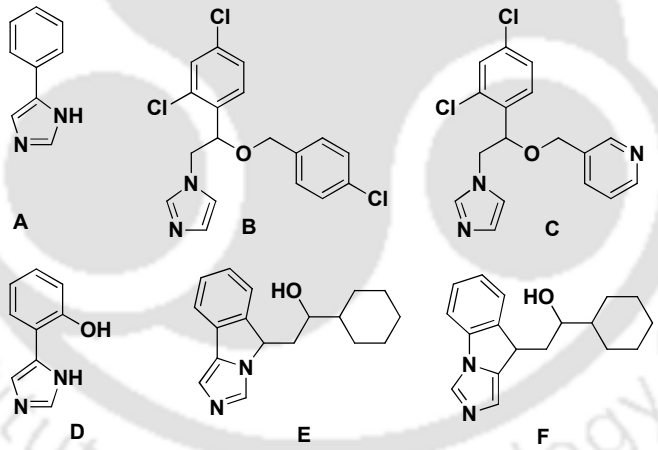

Figure 1.11. Inhibitors with imidazole scaffold. (A) 4-phenylimidazole (4PI), (B) econazole, (C) derivative of fungi-static imidazoles,[101] (D) 4PI derivative,[100] (E) fused imidazole,[122] (F) fused imidazole.[123]

Overall studies suggests the phenylimidazole scaffold to be a potential target that provides scope for the development of various other IDO1 inhibitors since its binding mode with the active sites have already been revealed through X-ray crystallography. Since 4PI and the other fungi-static imidazole are known to be potential inhibitors of various other heme-containing enzymes, therefore it can be assumed that the specificity

for IDO1 can be achieved through optimization of molecules targeting the B pocket of the active sites.

Another heterocyclic compound namely 4-aryl-1,2,3-triazoles was identified by pharmacophore modeling in 2010.[87] The parent compound displayed an enzymatic IC_{50} value of 60 μM, although the rationally designed triazole (MMG-0358) exhibited activity in nanomolar range in both enzymatic and cellular assays (Figure 1.12). It also showed low cytotoxicity along with a high selectivity for IDO1 over TDO.[107] Overall, the 1,2,3-triazole scaffold provided an interesting option for the imidazole scaffold due to its comparatively higher specificity with respect to other proteins.

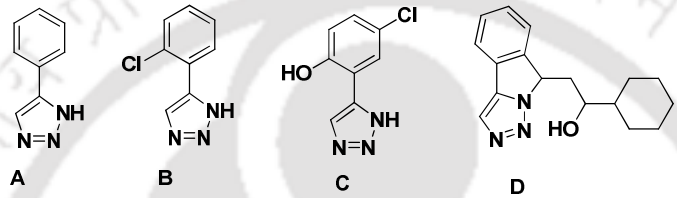

Figure 1.12. Inhibitors with 1,2,3-triazole scaffold. (A) 4-pheny-1,2,3-triazole (B) 4-(2-chloro-phenyl)-1,2,3-triazole,[124] (C) 4-(2-hydroxy-5-chloro-phenyl)-1,2,3-triazole, (compound**3**)[107] (D) fused triazole.[123]

One of the findings of the Incyte's corporate is *N*-hydroxyamidines, which is potent, competitive and reversible inhibitor of IDO1.[108] The compound (Z)-4-amino-*N*-(3-chloro-4-fluorophenyl)-*N'*-hydroxy-1,2,5-oxadiazole-3-carboximidamide (**5l**, Figure 1.13B) with the highest potency of this series showed an IC_{50} value of 67 and 19 nM, in both enzymatic and cellular assay respectively.[108] Modeling studies of it revealed that the oxygen of the hydroxyamidines preferably binds with the iron of the heme-group and forms hydrogen bond with the aniline nitrogen, whereas the phenyl ring was oriented inside the pocket A producing a tight fit. Moreover, the amino substituent on the furazan ring facilitates in the formation of a hydrogen bond with the propanoic acid group of the heme-ring.[108] Another potent compound epacadostat, (CAS No. 1204669-58-8) which is a result of further optimization of the *N*-hydroxyamidine series with an extension to the B pocket of the active site, also showed inhibitory activity towards IDO1 with an IC_{50} value of 72 nM and 7.1 nM in both enzymatic as well as cellular studies respectively.[109-111]

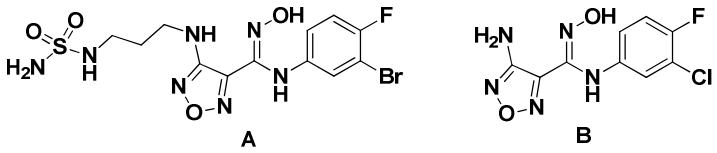

Figure 1.13. *N*-Hydroxyamidine inhibitors from Incyte (A) epacadostat,[109] (B) 4-amino-*N*-(3-chloro-4-fluorophenyl)-*N'*-hydroxy-1,2,5-oxadiazole-3-carboxymidimade (compound **4**).[108]

Similarly, various other scaffolds were also reported in the past few years that showed potential to be a promising candidate for IDO1 inhibitor (Figure 1.14). NCI diversity set reported in 2006 a selenic anti-inflammatory antioxidant namely ebselen,[112] that inhibits IDO1 through its interaction with several of its cysteine residues.[113] Candesartan cilexetil, which is a pro-drug, also displayed inhibitory potency toward IDO1 with an enzymatic IC_{50} value of 12 μM.[114] Moreover a range of benzene sulfonyl hydrazides were also tested in both *in vivo* and *in vitro* assays which showed IC_{50} value within the nanomolar range.[115] Another compound (Figure 1.14E) was reported by Amgen with an IC_{50} value of 3 μM[116] which was later co-crystallized with IDO1 and utilized for the rational compound optimization leading to the discovery of imidazothiazole derivatives that occupied both the pocket A and pocket B.[74] An additional urea linker provided an enzymatic inhibition within the nanomolar range with a reported IC_{50} value of 77 nM for the most potent compound (Figure 1.14G). A pharma company named Curadev also reported aminonitriles as potential IDO1 inhibitors (Figure 1.14C)[117] although most of them failed to meet the criteria for the pain filter as phenolic Mannich bases and Lily MedChem filter due to presence of its cyanomethylamine functionality. On the other hand, the compounds of 2-aminophenyl urea scaffold and similar inhibitors showed extensive inhibitory activity towards IDO1 with a lower nanomolar to picomolar cellular IC_{50} values as described by Bristol-Myers Squibb.[118-121]

Until date, these were the most potent compounds reported so far although sufficient studies are yet to be carried out regarding their specificity and mode of action. Moreover, the three-dimensional structure also seemed to interact with the surrounding protein residues apart from its interaction with the IDO1 active sites.

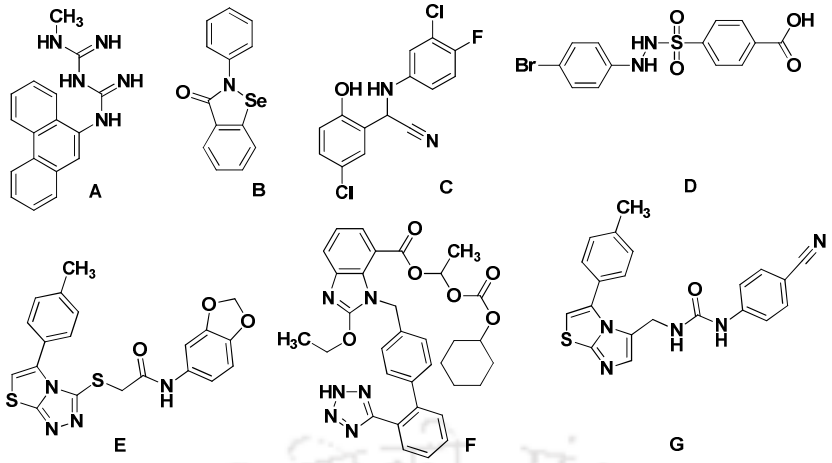

Figure 1.14. Few other reported inhibitors (A) NSC401366 from the NCI Diversity set,[112] (B) ebselen,[113] (C) aminonitrile derivative,[117] (D) benzenesulfonyl hydrazide,[115] (E) *N*-Benzo[1,3]dioxol-5-yl-2-(5-p-tolyl-thiazolo[2,3-c][1,2,4]triazol-3-ylsulfanyl)-acetamide(compound **2**),[116](F) candesartan cilexitel,[114] (G) imidazothiazole.[74]

Another study reported by Su-Ying Wu and co-workers[125] explores the inhibitory potencies of different imidazoleisoindole derivatives (Figure 1.15) towards IDO1 and highlighted the important hydrogen bond network involved which plays a crucial role in the interaction and thus provided a better insight towards the overall designing of IDO1 inhibitors. Moreover the crystal structure of one such potent inhibitor (compound C), which is a NLG919 analogue[125] was also solved at 2.2 Å resolution. It was clearly revealed from the density map that the compound C was covalently bonded with the co-ordination site of the heme iron through the imidazole nitrogen, which can be correlated with the Sorret peak shift from 403-413 nm in the UV-visible spectra. Extensive hydrophobic interaction of Try126, Cys126, Val130, Phe163, Phe164, Gly262, Ala264 as well as the porphyrin ring was observed along with the imidazole isoindole core located deep inside pocket A.

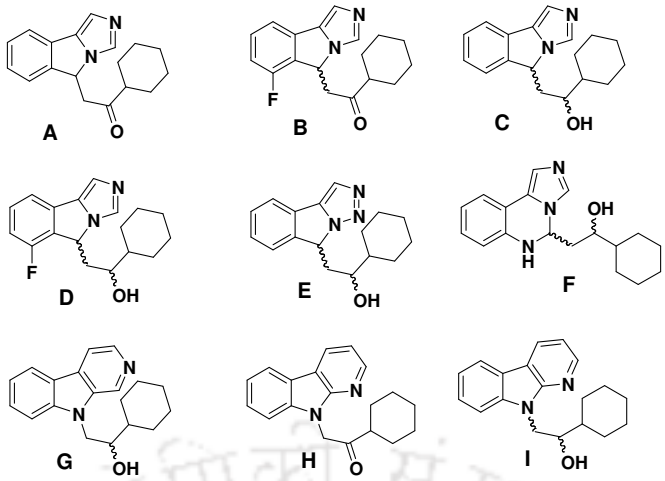

Figure 1.15. Reported inhibitors of imidazoleisoindole derivatives. (A) 1-Cyclohexyl-2-(5*H*-imidazo[5,1-a]isoindol-5-yl)-ethanone (compound **22**),[125] (B) 1-Cyclohexyl-2-(6-fluoro-5*H*-imidazo[5,1-a]isoindol-5-yl)-ethanone (compound **23**),[125] (C) 1-Cyclohexyl-2-(5*H*-imidazo[5,1-a]isoindol-5-yl)-ethanol (compound **24**),[125] (D) 1-Cyclohexyl-2-(6-fluoro-5*H*-imidazo[5,1-a]isoindol-5-yl)-ethanol (compound **25**),[125] (E) 1-Cyclohexyl-2-(8*H*-[1,2,3]triazolo[5,1-a]isoindol-8-yl)-ethanol (compound **26**),[125] (F) 1-Cyclohexyl-2-(5,6-dihydroimidazo[1,5-c]quinazolin-5-yl)-ethanol (compound **15**),[125] (G) 2-β-Carbolin-9-yl-1-cyclohexylethanol (compound **18**),[125] (H) 1-Cyclohexyl-2-pyrido[2,3-b]indol-9-ylethanone (compound **20**),[125] (I) 1-Cyclohexyl-2-pyrido[2,3-b]indol-9-ylethanol (compound **21**).[125]

Similar hydrophobic interaction was also observed for the 1-cyclohexylethanol moiety which was extended to pocket B, along with Phe226, Ile354 and Leu384. One of the distinct features is the presence of dual intermolecular hydrogen bond network between the compound **24** and IDO1 in which it binds to the 7-propanoic acid of the heme and the main chain -NH group of Ala264 alongside with an intramolecular hydrogen bond between the isoindole nitrogen and the hydroxyl group.

Similarly S.Qian et al. also developed different 1*H*-pyrazolo [3,4-d]pyrimidins and 1*H*-indazole scaffolds containing compounds and reported their structure and activity relationship regarding their inhibitory potencies towards IDO1.[126] From the study, it was evident that the 6-position bromine atom substituted derivative of the compound B (Figure 1.16) series showed better inhibitory activity as that of their unsubstituted counterparts. Hence it can be concluded that the halogen atom at the 6-position plays a key role for the enhancement of the inhibitory activity due to its hydrophobic interaction with the hydrophobic residues of the pocket A. Moreover among the two series of 1*H*-

indazole derivatives i.e., 4-amino-1*H*-indazole and 4-oxo-1*H*-indazole which are primarily differentiated by the presence of nitrogen (-NH) and oxygen (-O) atom at the 4-position linker site respectively, the former set of compounds were found to be more potent towards inhibition of IDO1. This indicated that the alternation of the bond angle between –NH and –O at the 4-position linker site plays an important role by affecting the interaction between the compounds and the enzymes. Another key feature is the presence of hydroxyl group or polar carboxyl group at the *para*-position of benzene ring which enhanced the inhibitory potency of the compound B.

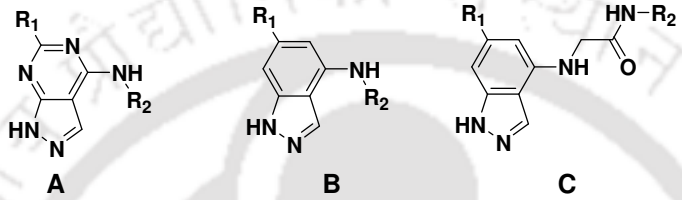

Figure 1.16. Reported inhibitors of 1*H*-pyrazolo[3,4-d]pyrimidins (**A**) and 1*H*-indazoles (**B** and **C**).[126]

Thus, varieties of chemical series of IDO1 inhibitors have been reported until date but most of the scaffolds have never been further used after their initial studies have been carried out. Different inconsistent results or unconfirmed activity and /or specificity in the subsequent studies are one of the major factors for such cases. Hence, there is a demand for the design and synthesis of novel molecules, which can actively, inhibits the IDO1 with high potency as well as with selective specificity as compared to that of the other heme-containing enzymes.

1.11. Conclusion

A large number of inhibitors of IDO1 are reported having moderate inhibitory potencies and there is scope for the development of compound having stronger inhibitory activity. The present approach for the development of inhibitors for IDO1 is based upon a ligand based methodology which involves the screening of the potential inhibitor compounds against the purified IDO1 thereby calculating the inhibitory constants along with structural related information using various computer aided molecular techniques. This process not only facilitates the development of a pharmacophore but also provides a rational ligand-based drug design approach. Hence, an improved recombinant IDO1protein would provide a better understanding towards the 3-dimensional structure of

IDO1 and help in enhanced interpretation of the structure based inhibitor design, which is one of the most powerful methods of drug design.

1.12. Aim of the work

1. Discovery and development of potent inhibitors with activity more than those of the prevailing inhibitors i.e., preferably at nanomolar range.
2. To gain a better insight regarding the role of the various structural moieties and their importance in binding with the active sites to facilitate the design and synthesis of potential inhibitors that can efficiently inhibit the activity of the target protein (IDO1).
3. Study of enzyme kinetics to determine the mode of inhibition viz. competitive, mixed competitive etc.

References

(1) Emsley, J. Nature's building blocks: an A-Z guide to the elements. *Oxford University Press, Oxford* **2001**.

(2) Valentine, J. S. Active oxygen in biochemistry. *Blackie Academic & Professional, London* **1995**.

(3) Jensen, K. P.; Ryde, U. How O_2 binds to heme: reasons for rapid binding and spin inversion. *J. Biol. Chem*. **2004**, *279*, 14561-14569.

(4) Bugg, T. D. H. Dioxygenase enzymes: catalytic mechanisms and model chemistry. *Tetrahedron* **2003**, *59*, 7075-7101.

(5) Jones, R. D.; Summerville, D. A.; Basolo, F. Synthetic Oxygen Carriers Related to Biological Systems. *Chem. Rev*. **1979**, *79*,139-179.

(6) Lee-Ruff, E. The Organic Chemistry of Superoxide. *Chem. Soc. Rev*. **1977**, *6*, 195-214.

(7) Que, L. Jr.; Ho, R. Y. Dioxygen Activation by Enzymes with Mononuclear Non-Heme Iron Active Sites. *Chem. Rev*. **1996**, *96*, 2607-2624.

(8) English, A. M.; Tsaprailis, G. Catalytic and structure-function relationships in heme peroxidases. *Adv. Inorg. Chem.* **1995**, *43*, 79-125.

(9) Sono, M.; Roach, M. P.; Coulter, E. D.; Dawson, J. H. Heme-Containing Oxygenases. *Chem. Rev*.**1996**, *96*, 2841-2888.

(10) Hayaishi, O.; Yoshida, R. Indoleamine 2,3-dioxygenase: Properties and functions of a superoxide utilising enzyme. *Prog. Inorg. Chem*. **1990**, *38*, 75-95.

(11) Mason, H. S.; Fowelks, W. K.; Peterson, E. Oxygen transfer and electron transport by the phenolase complex. *J. Am. Chem. Soc.* **1955**, *77*, 2914-2915.

(12) Hayaishi, O.; Hirata, F.; Ohnishi, T.; Henry, J. P.; Rosenthal, I.; Katoh, A. Indoleamine 2,3-dioxygenase: incorporation of $^{18}O_2^{--}$ and $^{18}O_2$ into the reaction products. *J. Biol. Chem.* **1977**, *252*, 3548-3550.

(13) Stone, T. W. Neuropharmacology of quinolinic and kynurenic acids. *Pharmacol. Rev*. **1993**, *45*, 309-379.

(14) Shimizu, T.; Nomiyama, S.; Hirata, F.; Hayaishi, O. Indoleamine 2,3-dioxygenase; purification and some properties. *J. Biol. Chem.* **1978**, *253*, 4700-4706.

(15) Taylor, M. W.; Feng, G. S. Relationship between interferon-γ, Indoleamine 2,3-dioxygenase and tryptophan catabolism. *FASEB J.* **1991**, *5*, 2516-2522.

(16) Suzuki, S.; Tone, S.; Takikawa, O.; Kubo, T.; Kohno, I.; Minatogawa, Y. Expression of Indoleamine 2,3-dioxygenase and tryptophan 2,3-dioxygenase in early concepti. *Biochem. J.* **2001**, *355*, 425-429.

(17) Yamazaki, F.; Kuroiwa, T.; Takikawa, O.; Kido, R. Human indolylamine2,3-dioxygenase. Its tissue distribution and characterisation of the placental enzyme. *J. Biochem.* **1985**, *230*, 635-638.

(18) Botting, N. P. Chemistry and neurochemistry of the kynurenine pathway of tryptophan metabolism. *Chem. Soc. Rev.* **1995**, *24*, 401-412.

(19) Peters, J. C. Tryptophan nutrition and metabolism: an overview. *Adv. Exp. Med. Biol.* **1991**, *294*, 345-358.

(20) Shrocksnadel, H.; Baier-Bitterlich, G.; Dapunt, O.; Wachter, H.; Fuchs, D. Decreased plasma tryptopan in pregnancy. *Obstet. Gynecol.* **1996**, *88*, 47-50.

(21) Wolf, H. Studies on tryptophan metabolism in man: The effect of hormones and vitamin B6 on urinary excretion of metabolites of the kynurenine pathway. *Scand. J. Clin. Lab. Invest.* **1974**, *136*, 1-86.

(22) Berger, M.; Gray, J. A.; Roth, B. L. The expanded biology of serotonin. *Annu. Rev. Med*. **2009**, *60*, 355-366.

(23) Mathews, C. K.; van Hold, K. E. Biochemistry. *The Benjamin/Cummings Publishing Company, California* **1990**.

(24) Bender, D. A. Amino acid metabolism. *2nd Ed., John Wiley and Sons, Great Britain* **1985**.

(25) Caniato, R.; Filippini, R.; Piovan, A.; Puricelli, L.; Borsarini, A.; Cappelletti, E. M. Melatonin in plants. *Adv. Exp. Med. Biol*. **2003**, *527*, 593-597.

(26) Hardeland, R. Antioxidative protection by melatonin: multiplicity of mechanisms from radical detoxification to radical avoidance. *Endocrine* **2005**, *27*, 119-130.

(27) Lehninger, A. L.; Nelson, D. L.; Cox, M. M. Lehninger principles of biochemistry. *3rd ed. / David L. Nelson, Michael M. Cox.ed., Worth Publishers, New York* **2000**.

(28) Stone, T. W.; Connick, J. H. Quinolinic acid and other kynurenines in the central nervous system. *Neuroscience* **1985**, *15*, 597-617.

(29) Mehler, A. H.; Knox, W. E. The conversion of tryptophan to kynurenine in liver. II. The enzymatic hydrolysis of formylkynurenine. *J. Biol. Chem.***1950**, *187*, 431-438.

(30) Hayaishi, O. My life with tryptophan—never a dull moment. *Protein Sci.* **1993**, *2*, 472-475.

(31) Ohashi, H.; Saito, K.; Fujii, H.; Wada, H.; Furuta, N.; Takemura, M.; Maeda, S.; Seishima, M. Changes in quinolinic acid production and its related enzymes following D-galactosamine and lipopolysaccharide-induced hepatic injury. *Arch. Biochem. Biophys*. **2004**, *428*, 154-159.

(32) Saito, K.; Fujigaki, S.; Heyes, M. P.; Shibata, K.; Takemura, M.; Fujii, H.; Wada, H.; Noma, A.; Seishima, M. Mechanism of increases in L-kynurenine and quinolinic acid in renal insufficiency. *Am. J. Physiol. Renal. Physiol*. **2000**, *279*, F565-F572.

(33) Yeung, A. W. S.; Terentis, A. C.; King, N. J. C.; Thomas, S. R. Role of Indoleamine 2,3-dioxygenase in health and diseases. *Clin. Sci.* **2015**, *129*, 601-672.

(34) Aquilina, J. A.; Carver, J. A.; Truscott, R. J. Oxidation products of 3-hydroxykynurenine bind to lens proteins: relevance for nuclear cataract. *Exp. Eye Res*. **1997**, *64*, 727-735.

(35) Grohmann, U.; Fallarino, F.; Puccetti, P. Tolerance, DCs and tryptophan: much ado about IDO. *Trends Immunol*. **2003**, *24*, 242-248.

(36) Munn, D. H.; Mellor, A. L. Indoleamine 2,3-dioxygenase and tumor-induced tolerance. *J. Clin. Invest*. **2007**, *117*, 1147-1154.

(37) Yamamoto, S.; Hayaishi, O. Tryptophan pyrrolase of rabbit intestine: D- and L-tryotophan-cleaving enzyme or enzymes. *J. Biol. Chem.* **1967**, *242*, 5260-5266.

(38) Takikawa, O.; Kuroiwa, T.; Yamazaki, F.; Kido, R. Mechanism of interferon-γ action; characterisation of Indoleamine 2,3-dioxygenase in cultured human cells induced by interferon-γ and evaluations of the enzyme-mediated tryptophan degradation an its anticellular activity. *J. Biol. Chem.* **1988**, *263*, 2041-2048.

(39) Tone, S.; Takikawa, O.; Habara-Ohkubo, A.; Kadoya, A.; Yoshida, R.; Kido, R. Primary structure of human Indoleamine 2,3-dioxygenase deduced from the nucleotide sequence of its cDNA. *Nucleic Acids Res.* **1989**, *18*, 367.

(40) Dai, W.; Gupta, S. L. Molecular cloning, sequencing and expression of human interferon-γ-inducible Indoleamine 2,3-dioxygenase cDNA. *Biochem. Biophys. Res. Commun.* **1990**, *168*, 1-8.

(41) Habara-Ohkubo, A.; Takikawa, O.; Yoshida, R. Cloning and expression of a cDNA encoding mouse Indoleamine 2,3-dioxygenase. *Gene* **1991**, *105*, 221-227.

(42) Pan, T.; Lin, C.; Chen, C.; Lin, Y.; Gojo, S.; Lee, T.; Wang, Y.; Lord, R.; Lai, C.; Tsu, L.; Tseng, H.; Wu, M.; Iwashita, Y.; Kitano, S.; Chiang, K.; Hashimoto, T.; Sugioka, A.; Goto, S. Identification of the Indoleamine 2,3-dioxygenase nucleotide sequence in a rat liver transplant model. *Transpl. Immunol.* **2000**, *8*, 189-194.

(43) Hirata, F.; Hayaishi, O. Studies on Indoleamine 2,3-dioxygenase 1. Superoxide anion as substrate. *J. Biol. Chem.* **1975**, *250*, 5960-5966.

(44) Sono, M.; Taniguchi, T.; Watanabe, Y.; Hayaishi, O. Indoleamine 2,3-dioxygenase. Equilibrium studies of the tryptophan binding to the ferric, ferrous and co-bound enzymes. *J. Biol. Chem.* **1980**, *255*, 1339-1345.

(45) Yoshida, R.; Hayaishi, O. Induction of pulmonary Indoleamine 2,3-dioxygenase by intraperitoneal injection of bacterial lipopolysaccharide. *Proc. Natl. Acad. Sci. U.S.A.* **1978**, *75*, 3998-4000.

(46) Ohnishi, T.; Hirata, F.; Hayaishi, O. Indoleamine 2,3-dioxygenase: Potassium superoxide as substrate. *J. Biol. Chem.* **1977**, *252*, 4643-4647.

(47) Ishimura, Y.; Nozaki, M.; Hayaishi, O. The oxygenated form of L-tryptophan 2,3-dioxygenase as reaction intermediate. *J. Biol. Chem*. **1970**, *245*, 3593-3602.

(48) Maghzal, G. J.; Thomas, S. R.; Hunt, N. H.; Stocker, R. Cytochrome b_5, not superoxide anion radical, is a major reductant of indoleamine 2,3-dioxygenase in human cells. *J. Biol. Chem*. **2008**, *283*, 12014-12025.

(49) Taniguchi, T.; Hirata, F.; Hayaishi, O. Intracellular utilization of superoxide anion by indoleamine 2,3-dioxygenase of rabbit enterocytes. *J. Biol. Chem*. **1977**, *252*, 2774-2776.

(50) Forouhar, F.; Anderson, J. L. R.; Mowat, C. G.; Vorobiev, S. M.; Hussain, A.; Abashidze, M.; Bruckmann, C.; Thackray, S. J.; Seetharaman, J.; Tucker, T.; Xiao, R.; Ma, Li-C.; Zhao, L.; Acton, T. B.; Montelione, G. T.; Chapman, S. K.; Tong, L. Molecular insights into substrate recognition and catalysis by tryptophan 2,3-dioxygenase. *Proc. Natl. Acad. Sci. U.S.A*. **2007**, *104*, 473-478.

(51) Lu, C.; Lin, Y.; Yeh, S. R. Inhibitory substrate binding site of human indoleamine 2,3-dioxygenase. *J. Am. Chem. Soc*. **2009**, *131*, 12866-12867.

(52) Eflimov, I.; Basran. J.; Thackray. S. J.; Handa. S.; Mowat. C. G.; Raven. E. L. Structure and Reaction Mechenism in the Heme Dioxygenases. *Biochemistry* **2011**, *50*, 2717-2724.

(53) Chung, L. W.; Li, X.; Sugimoto, H.; Shiro, Y.; Morokuma, K. ONIOM study on a missing piece in our understanding of heme chemistry: Bacterial tryptophan 2,3-dioxygenase with dual oxidants. *J. Am. Chem. Soc*. **2010**, *132*, 11993-12005.

(54) Lewis-Ballester, A.; Batabyal, D.; Egawa, T.; Lu, C.; Lin, Y.; Marti, M. A.; Capece, L.; Estrin, D. A.; Yeh, S. R. Evidence for a ferryl intermediate in a heme-based dioxygenase. *Proc. Natl. Acad. Sci. U.S.A*. **2009**, *106*, 17371-17376.

(55) Yanagisawa, S.; Yotsuya, K.; Hashiwaki, Y.; Horitani, M.; Sugimoto, H.; Shiro, Y.; Appelman, E. H.; Ogura, T. Identification of the Fe-O_2 and the Fe=O heme species for Indoleamine 2,3-dioxygenase during catalytic turnover. *Chem. Lett*. **2010**, *39*, 36-37.

(56) Yanagisawa, S.; Horitani, M.; Sugimoto, H.; Shiro, Y.; Okada, N.; Ogura, T. Resonance Raman study on theoxygenated and the ferryl-oxo species of indoleamine 2,3-dioxygenase during catalytic turnover. *Faraday Discuss*. **2011**, *148*, 239-247.

(57) Yamane, T.; Makino, K.; Umezawa, N.; Kato, N.; Higuchi, T. Extreme rate acceleration by axial thiolate coordination on the isomerization of endoperoxide catalyzed by iron porphyrin. *Angew. Chem. Int. Ed*. **2008**, *47*, 6438-6440.

(58) Eser, B. E.; Barr, E. W.; Frantom, P. A.; Saleh, L.; Bollinger, J. M. Jr.; Krebs, C.; Fitzpatrick, P. F. Direct spectroscopic evidence for a high-spin Fe(IV) intermediate in tyrosine hydroxylase. *J. Am. Chem. Soc.* **2007**, *129*, 11334-11335.

(59) Savige, W. E. New oxidation products of tryptophan. *Aust. J. Chem*. **1975**, *28*, 2275-2287.

(60) Sugimoto, H.; Oda, S.; Otsuki, T.; Hino, T.; Yoshida, T.; Shiro, Y. Crystal structure of human indoleamine 2,3-dioxygenase: catalytic mechanism of O_2 incorporation by a heme-containing dioxygenase. *Proc. Natl. Acad. Sci. U.S.A*. **2006**, *103*, 2611-2616.

(61) Sono, M. Enzyme kinetic and spectroscopic studies of inhibitor and effector interactions with indoleamine 2,3-dioxygenase 2. Evidence for the existence of another binding site in the enzyme for indole derivative effectors. *Biochemistry* **1989**, *28*, 5400-5407.

(62) Rohrig, U. F.; Majjigapu, S. R.; Vogel, P.; Zoete, V.; Michielin, O. Challenges in the discovery of indoleamine 2,3-Dioxygenase 1 (IDO1) inhibitors. *J. Med. Chem*. **2015**, *58*, 9421-9437.

(63) Yamamoto, S.; Hayaishi, O. Tryptophan pyrrolase of rabbit intestine. *D*- and *L*-tryptophan-cleaving enzyme or enzymes. *J. Biol. Chem*. **1967**, *242*, 5260-5266.

(64) Dang, Y.; Dale, W. E.; Brown, O. R. Comparative effects of oxygen on Indoleamine 2,3-dioxygenase and tryptophan 2,3-dioxygenase of the kynurenine pathway. *Free Radical Biol. Med.* **2000**, *28*, 615-624.

(65) Hou, D. Y.; Muller, A. J.; Sharma, M. D.; DuHadaway, J.; Banerjee, T.; Johnson, M.; Mellor, A. L.; Prendergast, G. C.; Munn, D. H. Inhibition of indoleamine 2,3-dioxygenase in dendritic cells by stereoisomers of 1-methyl-tryptophan correlates with antitumor responses. *Cancer Res*. **2007**, *67*, 792-801.

(66) Muller, A. J.; DuHadaway, J. B.; Donover, P. S.; Sutanto-Ward, E.; Prendergast, G. C. Inhibition of indoleamine 2,3-dioxygenase, an immunoregulatory target of the cancer suppression gene Bin1, potentiates cancer chemotherapy. *Nat. Med*. **2005**, *11*, 312-319.

(67) Takikawa, O.; Yoshida, R.; Kido, R.; Hayaishi, O. Tryptophan degradation in mice initiated by indoleamine 2,3-Dioxygenase. *J. Biol. Chem*. **1986**, *261*, 3648-3653.

(68) Platten, M.; Wick, W.; Van den Eynde, B. J. Tryptophan catabolism in cancer: beyond IDO and tryptophan depletion. *Cancer Res*. **2012**, *72*, 5435-5440.

(69) Sanni, L. A.; Thomas, S. R.; Tattam, B. N.; Moore, D. E.; Chaudhri, G.; Stocker, R.; Hunt, N. H. Dramatic changes in oxidative tryptophan metabolism along the kynurenine pathway in experimental cerebral and noncerebral malaria. *Am. J. Pathol.* **1998**, *152*, 611-619.

(70) Sardar, A. M.; Reynolds, G. P. Frontal cortex Indoleamine-2,3-dioxygenase activity is increased in HIV-1-associated dementia. *Neurosci. Lett.* **1995**, *187*, 9-12.

(71) Uyttenhove, C.; Pilotte, L.; Theate, I.; Stroobant, V.; Colau, D.; Parmentier, N.; Boon, T.; Van den Eynde, B. J.; Evidence for a tumoral immune resistance mechanism based on tryptophan degradation by indoleamine 2,3-dioxygenase. *Nat. Med*. **2003**, *9*, 1269-1274.

(72) Okamoto, A.; Nikaido, T.; Ochiai, K.; Takakura, S.; Saito, M.; Aoki, Y.; Ishii, N.; Yanaihara, N.; Yamada, K.; Takikawa, O.; Kawaguchi, R.; Isonishi, S.; Tanaka, T.; Urashima, M. Indoleamine 2,3-dioxygenase serves as a marker of poor prognosis in gene expression profiles of serous ovarian cancer cells. *Clin. Cancer Res*. **2005**, *11*, 6030-6039.

(73) Malachowski, W. P.; Winters, M.; DuHadaway, J. B.; Ariel Lewis-Ballester, A.; Badira, S.; Wai, J.; Rahman, M.; Sheikh, E.; LaLonde, J. M.; Yeh, S. R.; Prendergast, G. C.; Muller, A. J. O-alkylhydroxylamines as rationally-designed mechanism-based inhibitors of indoleamine 2,3-dioxygenase-1. *Eur. J. Med. Chem*. **2016**, *108*, 564-576.

(74) Tojo, S.; Kohno, T.; Tanaka, T.; Kamioka, S.; Ota, Y.; Ishii, T.; Kamimoto, K.; Asano, S.; Isobe, Y. Crystal structures and structure activity relationships of imidazothiazole derivatives as IDO1 inhibitors. *ACS Med. Chem. Lett*. **2014**, *5*, 1119-1123.

(75) Cady, S. G.; Sono, M. 1-Methyl-DL-tryptophan, beta-(3-benzofuranyl)-D L-alanine (the oxygen analog of tryptophan), and beta-[3-benzo(b)thienyl]-DL-alanine (the sulfur analog of tryptophan) are competitive inhibitors for indoleamine 2,3-dioxygenase. *Arch. Biochem. Biophys*. **1991**, *291*, 326-333.

(76) Peterson, A. C.; Migawa, M. T.; Martin, M. J.; Hamaker, L. K.; Czerwinski, K. M.; Zhang, W.; Arend, R. A.; Fisette, P. L.; Okazi, Y.; Will, J. A.; Brown, R. R.; Cook, J. M. Evaluation of functionalized tryptophan derivatives and related compounds as competitive inhibitors of indoleamine 2,3-dioxygenase. *Med. Chem. Res*. **1994**, *3*, 531-544.

(77) Saito, K.; Chen, C. Y.; Masana, M.; Crowley, J. S.; Markey, S. P.; Heyes, M. P. 4-Chloro-3-hydroxyanthranilate, 6-chlorotryptophan and norharmane attenuate quinolinic acid formation by interferon gamma-stimulated monocytes (THP-1 cells). *Biochem. J*. **1993**, *291*, 11-14.

(78) Sono, M.; Cady, S. G. Enzyme kinetic and spectroscopic studies of inhibitor and effector interactions with indoleamine 2,3-dioxygenase. 1. Norharman and 4-phenylimidazole binding to the enzyme as inhibitors and heme ligands. *Biochemistry* **1989**, *28*, 5392-5399.

(79) Eguchi, N.; Watanabe, Y.; Kawanishi, K.; Hashimoto, Y.; Hayaishi, O. Inhibition of indoleamine 2,3-dioxygenase and tryptophan 2,3-dioxygenase by beta-carboline and indole derivatives. *Arch. Biochem. Biophys*. **1984**, *232*, 602-609.

(80) Peterson, A. C.; Loggia, A. J. L.; Hamaker, L. K.; Arend, R. A.; Fisette, P. L.; Okazi, Y.; Will, J. A.; Brown, R. R.; Cook, J. M. Evaluation of substituted β-carbolines as noncompetitive Indoleamine 2,3-dioxygenase inhibitors. *Med. Chem. Res*. **1993**, *3*, 473-482.

(81) Degterev, A.; Huang, Z.; Boyce, M.; Li, Y.; Jagtap, P.; Mizushima, N.; Cuny, G. D.; Mitchison, T. J.; Moskowitz, M. A.; Yuan, J. Chemical inhibitor of nonapoptotic cell death with therapeutic potential for ischemic brain injury. *Nat. Chem. Biol*. **2005**, *1*, 112-119.

(82) Nakashima, H.; Uto, Y.; Nakata, E.; Nagasawa, H.; Ikkyu, K.; Hiraoka, N.; Nakashima, K.; Sasaki, Y.; Sugimoto, H.; Shiro, Y.; Hashimoto, T.; Okamoto, Y.; Asakawa, Y.; Hori, H. Synthesis and biological activity of 1-methyl-tryptophan-tirapazamine hybrids as hypoxia-targeting indoleamine 2,3-dioxygenase inhibitors. *Bioorg. Med. Chem*. **2008**, *16*, 8661-8669.

(83) Dolusic, E.; Larrieu, P.; Blanc, S.; Sapunaric, F.; Pouyez, J.; Moineaux, L.; Colette, D.; Stroobant, V.; Pilotte, L.; Colau, D.; Ferain, T.; Fraser, G.; Galleni, M.; Frere, J.-M.; Masereel, B.; Van den Eynde, B.; Wouters, J.; Frédérick, R. Indol-2-yl ethanones as novel indoleamine 2,3-dioxygenase (IDO) inhibitors. *Bioorg. Med. Chem*. **2011**, *19*, 1550-1561.

(84) Tanaka, M.; Li, X.; Hikawa, H.; Suzuki, T.; Tsutsumi, K.; Sato, M.; Takikawa, O.; Suzuki, H.; Yokoyama, Y. Synthesis and biological evaluation of novel tryptoline derivatives as indoleamine 2,3-dioxygenase (IDO) inhibitors. *Bioorg. Med. Chem.* **2013**, *21*, 1159-1165.

(85) CavalheiroTourino, M.; de Oliveira, E. M.; Belle, L. P.; Knebel, F. H.; Albuquerque, R. C.; Dorr, F. A.; Okada, S. S.; Migliorini, S.; Soares, I. S.; Campa, A. Tryptamine and dimethyltryptamine inhibit indoleamine 2,3 dioxygenase and increase the tumor-reactive effect of peripheral blood mononuclear cells. *Cell Biochem. Funct.* **2013**, *31*, 361-364.

(86) Chauhan, N.; Basran, J.; Rafice, S. A.; Efimov, I.; Millett, E. S.; Mowat, C. G.; Moody, P. C. E.; Handa, S.; Raven, E. L. How is the distal pocket of a heme-protein optimized for binding of tryptophan? *FEBS J.* **2012**, *279*, 4501-4509.

(87) Rohrig, U. F.; Awad, L.; Grosdidier, A.; Larrieu, P.; Stroobant, V.; Colau, D.; Cerundolo, V.; Simpson, A. J. G.; Vogel, P.; Van den Eynde, B. J.; Zoete, V.; Michielin, O. Rational design of Indoleamine 2,3-dioxygenase inhibitors. *J. Med. Chem.* **2010**, *53*, 1172-1189.

(88) Kumar, S.; Malachowski, W.; DuHadaway, J.; Lalonde, J.; Carroll, P.; Jaller, D.; Metz, R.; Prendergast, G.; Muller, A. Indoleamine 2,3-dioxygenase is the anticancer target for a novel series of potent naphthoquinone-based inhibitors. *J. Med. Chem.* **2008**, *51*, 1706-1718.

(89) Carr, G.; Chung, M. K. W.; Mauk, A. G.; Andersen, R. J. Synthesis of indoleamine 2,3-dioxygenase inhibitory analogues of the sponge alkaloid exiguamine A. *J. Med. Chem.* **2008**, *51*, 2634-2637.

(90) Centko, R. M.; Steino, A.; Rosell, F. I.; Patrick, B. O.; de Voogd, N.; Mauk, A. G.; Andersen, R. J. Indoleamine 2,3-dioxygenase inhibitors isolated from the sponge Xestospongiavansoesti: structure elucidation, analogue synthesis, and biological activity. *Org. Lett.* **2014**, *16*, 6480-6483.

(91) Andersen, R.; Pereira, A.; Huang, X.-H.; Mauk, G.; Vottero, E.; Roberge, M.; Balgi, A. Indoleamine 2,3-dioxygenase (IDO) inhibitors. Patent WO2006/005185, 2006.

(92) Pearson, J. T.; Siu, S.; Meininger, D. P.; Wienkers, L. C.; Rock, D. A. In vitro modulation of cytochrome P450 reductase supported indoleamine 2,3-dioxygenase activity by allosteric effectors cytochrome b(5) and methylene blue. *Biochemistry* **2010**, *49*, 2647-2656.

(93) Huth, J. R.; Mendoza, R.; Olejniczak, E. T.; Johnson, R. W.; Cothron, D. A.; Liu, Y.; Lerner, C. G.; Chen, J.; Hajduk, P. J. ALARM NMR: a rapid and robust experimental

method to detect reactive false positives in biochemical screens. *J. Am. Chem. Soc*. **2005**, *127*, 217-224.

(94) McCallum, M. M.; Nandhikonda, P.; Temmer, J. J.; Eyermann, C.; Simeonov, A.; Jadhav, A.; Yasgar, A.; Maloney, D.; Arnold, A. L. High-throughput identification of promiscuous inhibitors from screening libraries with the use of a thiol-containing fluorescent probe. *J. Biomol.Screen.* **2013**, *18*, 705-713.

(95) Jang, J. P.; Jang, J. H.; Soung, N. K.; Kim, H. M.; Jeong, S. J.; Asami, Y.; Shin, K. S.; Kim, M. R.; Oh, H.; Kim, B. Y.; Ahn, J. S. Benzomalvin E, an indoleamine 2,3-dioxygenase inhibitor isolated from Penicillium sp. FN070315. *J. Antibiot*. **2012**, *65*, 215-217.

(96) Williams, D. E.; Steino, A.; de Voogd, N. J.; Mauk, A. G.; Andersen, R. J. Halicloic acids A and B isolated from the marine sponge Haliclona sp. collected in the Philippines inhibit Indoleamine 2,3-dioxygenase. *J. Nat. Prod*. **2012**, *75*, 1451-1458.

(97) Yamamoto, R.; Yamamoto, Y.; Imai, S.; Fukutomi, R.; Ozawa, Y.; Abe, M.; Matuo, Y.; Saito, K. Effects of various phytochemicals on indoleamine 2,3-dioxygenase 1 activity: galanal is a novel, competitive inhibitor of the enzyme. *PLoS One* **2014**, *9*, e88789.

(98) Mautino, M.; Jaipuri, F.; Marcinowicz-Flick, A.; Kesharwani, T.; Waldo, J. IDO inhibitors. Patent WO2009/073620, 2009.

(99) Fung, S. P. S.; Wang, H.; Tomek, P.; Squire, C. J.; Flanagan, J. U.; Palmer, B. D.; Bridewell, D. J.; Tijono, S. M.; Jamie, J. F.; Ching, L. M. Discovery and characterisation of hydrazines as inhibitors of the immune suppressive enzyme, indoleamine 2,3-dioxygenase 1 (IDO1). *Bioorg. Med. Chem*. **2013**, *21*, 7595-7603.

(100) Kumar, S.; Jaller, D.; Patel, B.; LaLonde, J. M.; DuHadaway, J. B.; Malachowski, W. P.; Prendergast, G. C.; Muller, A. J. Structure based development of phenylimidazole-derived inhibitors of Indoleamine 2,3-dioxygenase. *J. Med. Chem*. **2008**, *51*, 4968-4977.

(101) Rohrig, U. F.; Majjigapu, S. R.; Chambon, M.; Bron, S.; Pilotte, L.; Colau, D.; Turcatti, B. J.; Van den Eynde, G.; Vogel, P.; Zoete, V.; Michielin, O. Detailed analysis and follow-up studies of a high throughput screening for indoleamine 2,3-dioxygenase 1 (IDO1) inhibitors. *Eur. J. Med. Chem*. **2014**, *84*, 284-301.

(102) Bakmiwewa, S. M.; Fatokun, A.; Tran, A.; Payne, R. J.; Hunt, N. H.; Ball, H. J. Identification of selective inhibitors of indoleamine 2,3- dioxygenase 2. *Bioorg. Med. Chem. Lett*. **2012**, *22*, 7641-7646.

(103) Matsuno, K.; Takai, K.; Isaka, Y.; Unno, Y.; Sato, M.; Takikawa, O.; Asai, A. S-benzylisothiourea derivatives as smallmolecule inhibitors of indoleamine-2,3-dioxygenase. *Bioorg. Med. Chem. Lett*. **2010**, *20*, 5126-5129.

(104) Serra, S.; Moineaux, L.; Vancraeynest, C.; Masereel, B.; Wouters, J.; Pochet, L.; Frédérick, R. Thiosemicarbazide, a fragment with promising indolamine-2,3-dioxygenase (IDO) inhibition properties. *Eur. J. Med. Chem*. **2014**, *82*, 96-105

(105) Gaspari, P.; Banerjee, T.; Malachowski, W. P.; Muller, A. J.; Prendergast, G. C.; Bennett, J.; DuHadaway, S.; Donovan, A. M. Structure-activity study of brassinin derivatives as indoleamine 2,3- dioxygenase inhibitors. *J. Med. Chem*. **2006**, *49*, 684-692.

(106) Smith, J. R.; Evans, K. J.; Wright, A.; Willows, R. D.; Jamie, J. F.; Griffith, R. Novel indoleamine 2,3-dioxygenase-1 inhibitors from a multistep in silico screen. *Bioorg. Med. Chem*. **2012**, *20*, 1354-1363.

(107) Rohrig, U. F.; Majjigapu, S. R.; Grosdidier, A.; Bron, S.; Stroobant, V.; Pilotte, L.; Colau, D.; Vogel, P.; Van den Eynde, B. J.; Zoete, V.; Michielin, O. Rational design of 4-aryl-1,2,3-triazoles for indoleamine 2,3-dioxygenase 1 inhibition. *J. Med. Chem*. **2012**, *55*, 5270-5290.

(108) Yue, E. W.; Douty, B.; Wayland, B.; Bower, M.; Liu, X.; Leffet, L.; Wang, Q.; Bowman, K. J.; Hansbury, M. J.; Liu, C.; Wei, M.; Li, Y.; Wynn, R.; Burn, T. C.; Koblish, H. K.; Fridman, J. S.; Metcalf, B.; Scherle, P. A.; Combs, A. P. Discovery of potent competitive inhibitors of indoleamine 2,3-dioxygenase with in vivo pharmacodynamic activity and efficacy in a mouse melanoma model. *J. Med. Chem*. **2009**, *52*, 7364-7367.

(109) Combs, A.; Yue, E.; Sparks, R.; Zhu, W.; Zhou, J.; Lin, Q.; Weng, L.; Yue, T.; Liu, P. 1,2,5-Oxadiazoles as inhibitors of indoleamine 2,3-dioxygenase. Patent WO2010/005958, 2010.

(110) Liu, X.; Shin, N.; Koblish, H. K.; Yang, G.; Wang, Q.; Wang, K.; Leffet, L.; Hansbury, M. J.; Thomas, B.; Rupar, M.; Waeltz, P.; Bowman, K. J.; Polam, P.; Sparks, R. B.; Yue, E. W.; Li, Y.; Wynn, R.; Fridman, J. S.; Burn, T. C.; Combs, A. P.; Newton, R. C.; Scherle, P. A. Selective inhibition of IDO1 effectively regulates mediators of antitumor immunity. *Blood* **2010**, *115*, 3520-3530.

(111) Koblish, H. K.; Hansbury, M. J.; Bowman, K. J.; Yang, G.; Neilan, C. L.; Haley, P. J.; Burn, T. C.; Waeltz, P.; Sparks, R. B.; Yue, E. W.; Combs, A. P.; Scherle, P. A.; Vaddi, K.; Fridman, J. S. Hydroxyamidine inhibitors of indoleamine-2,3-dioxygenase

potently suppress systemic tryptophan catabolism and the growth of IDO expressing tumors. *Mol. Cancer Ther*. **2010**, *9*, 489-498.

(112) Vottero, E.; Balgi, A.; Woods, K.; Tugendreich, S.; Melese, T.; Andersen, R. J.; Mauk, A. G.; Roberge, M. Inhibitors of human indoleamine 2,3-dioxygenase identified with a target-based screen in yeast. *Biotechnol. J*. **2006**, *1*, 282-288.

(113) Terentis, A. C.; Freewan, M.; Sempértegui Plaza, T. S.; Raftery, M. J.; Stocker, R.; Thomas, S. R. The selenazal drug ebselen potently inhibits indoleamine 2,3-dioxygenase by targeting enzyme cysteine residues. *Biochemistry* **2010**, *49*, 591-600.

(114) Matsuno, K.; Yamazaki, H.; Isaka, Y.; Takai, K.; Unno, Y.; Ogo, N.; Ishikawa, Y.; Fujii, S.; Takikawa, O.; Asai, A. Novel candesartan derivatives as indoleamine 2,3-dioxygenase inhibitors. *Med. Chem. Commun*. **2012**, *3*, 475-479.

(115) Cheng, M. F.; Hung, M. S.; Song, J. S.; Lin, S. Y.; Liao, F. Y.; Wu, M. H.; Hsiao, W.; Hsieh, C. L.; Wu, J. S.; Chao, Y. S.; Shih, C.; Wu, S. Y.; Ueng, S. H. Discovery and structure-activity relationships of phenyl benzenesulfonylhydrazides as novel indoleamine 2,3-dioxygenase inhibitors. *Bioorg. Med. Chem. Lett*. **2014**, *24*, 3403-3406.

(116) Meininger, D.; Zalameda, L.; Liu, Y.; Stepan, L. P.; Borges, L.; McCarter, J. D.; Sutherland, C. L. Purification and kinetic characterization of human indoleamine 2,3-dioxygenases 1 and 2 (IDO1 and IDO2) and discovery of selective IDO1 inhibitors. *Biochim. Biophys. Acta* **2011**, *1814*, 1947-1954.

(117) Banerjee, M.; Middya, S.; Shrivastava, R.; Raina, S.; Surya, A.; Yadav, V. K.; Kapoor, K. K. Aminonitriles as kynurenine pathway inhibitors. Patent WO2014/141110, 2014.

(118) Balog, J.; Huang, A.; Chen, B.; Chen, L.; Shan, W. IDO inhibitors.Patent WO2014/150646, 2014.

(119) Balog, J.; Huang, A.; Chen, B.; Chen, L.; Seitz, S.; Hart, A.; Markwalder, J. Inhibitors of indoleamine 2,3-dioxygenase (IDO). Patent WO2014/150677, 2014.

(120) Markwalder, J.; Seitz, S.; Balog, J.; Huang, A.; Mandal, S.; Williams, D.; Hart, A.; Inghrim, J. IDO inhibitors. Patent WO2015/ 002918, 2015.

(121) Markwalder, J.; Balog, J.; Huang, A.; Seitz, S. IDO inhibitors.Patent WO2015/006520, 2015.

(122) Mautino, M.; Kumar, S.; Waldo, J.; Jaipuri, F.; Kesharwani, T. Fused imidazole derivatives useful as IDO inhibitors. Patent WO2012/142237, 2012.

(123) Kumar, S.; Waldo, J.; Jaipuri, F.; Mautino, M. Tricyclic compounds as inhibitors of immunosuppression mediated by tryptophan metabolization. Patent WO2014/159248, 2014.

(124) Huang, Q.; Zheng, M.; Yang, S.; Kuang, C.; Yu, C.; Yang, Q. Structure-activity relationship and enzyme kinetic studies on 4-aryl- 1H-1,2,3-triazoles as indoleamine 2,3-dioxygenase (IDO) inhibitors. *Eur. J. Med. Chem.* **2011**, *46*, 5680-5687.

(125) Peng, Y. H.; Ueng, S. H.; Tseng, C. T.; Hung, M. S.; Song, J. S.; Wu, J. S.; Liao, F. Y.; Fan, Y. S.; Wu, M. H.; Hsiao, W. C.; Hsueh, C. C.; Lin, S. Y.; Cheng, C. Y.; Tu, C. H.; Lee, L. C.; Cheng, M. F.; Shia, K. S.; Shih, C.; Wu, S. Y. Important Hydrogen Bond Networks in Indoleamine 2,3-Dioxygenase 1 (IDO1) Inhibitor Design Revealed by Crystal Structures of Imidazoleisoindole Derivatives with IDO1. *J. Med. Chem.* **2016**, *59*, 282-293.

(126) Qian, S.; He, T.; Wang, W.; He, Y.; Zhang, M.; Yang, L.; Li, G.; Wang, Z. Discovery and preliminary structure–activity relationship of 1H-indazoles with promising indoleamine-2,3-dioxygenase 1 (IDO1) inhibition properties. *Bioorg. Med. Chem.* **2016**, *24*, 6194-6205.

CHAPTER 2

N′-hydroxyamidines Based Nitrobenzofurazan Derivatives as Potent Inhibitors of IDO1

Tryptophan metabolism through the kynurenine pathway is considered as a crucial mechanism in immune tolerance. Indoleamine 2,3-dioxygenase 1 (IDO1) plays a key role in tryptophan catabolism in the immune system and it is also considered as an important therapeutic target for the treatment of cancer and other diseases that are linked with kynurenine pathway. In this chapter, a series of nitrobenzofurazan derivatives of *N′*-hydroxybenzimidamides were synthesized and their inhibitory activities against human IDO1 enzyme were tested using *in vitro* and cellular enzyme activity assay.

Highlights

- Synthesis of nitrobenzofurazan derivatives of *N′*-hydroxybenzimidamides as IDO1 inhibitors.
- Inhibitory activities were demonstrated by spectroscopic and HPLC-based methods.
- Stronger inhibition with halogen substituted *N′*-hydroxyamidine derivatives.
- Higher selectivity for IDO1 enzyme over TDO enzyme.
- Nanomolar level of IDO1 inhibition potency with low toxicity in cells.

2.1. Background and focus of the present work

Cancer immunotherapy by targeting IDO1 and tryptophan 2,3-dioxygenase (TDO) enzymes is considered as an exciting approach for drug development.[1,2] Both these enzymes catalyze the initial and rate limiting step in the catabolism of *L*-Trp to *N*-formylkynurenine by oxidative cleavage of the pyrrole ring through kynurenine pathway.[3,4] Uncontrolled metabolism of *L*-Trp abets tumor cells to escape from the immune responses.[1,4] Reduction in local concentrations of *L*-Trp and uninhibited formation of kynurenine and other metabolites, including neurotransmitters serotonin and melatonin, excitotoxin quinolinic acid, *N*-methyl-*D*-aspartate receptor antagonist kynurenic acid, and the production of nicotinamide adenine dinucleotide (NAD) assists IDO1 enzyme to suppress the local immune response by hindering the proliferation of T-lymphocyte in the G1-phase of the cell cycle.[1,2,5,6] Cytokines like interferon-γ are primarily responsible for the over-expression of IDO1 enzyme in the macrophages, epithelial and dendritic cells.[7] The over-expression of IDO1 enzyme is interconnected with poor prognosis in different cancers, including, ovarian and pancreatic.[1,3,8] However, recently it is reported that endothelial IDO1 expression in kidney tumors is associated with a better prognosis.[9,10] Cellular IDO1 activities are also related with neurodegenerative disorder HIV-1 encephalitis and age related cataract.[1,11-14]

Recent studies demonstrated that inhibition of IDO1 activity with small molecules successfully restrain the abnormal growth of tumors and also showed complemented effect with chemotherapeutic and radiotherapeutic treatment of malignant tumors.[6,15] TDO enzyme is highly selective and preferably binds to *L*-Trp. Whereas, the active site of IDO1 enzyme is amenable to small molecules. Moreover, TDO enzyme is mainly expressed in the liver and catabolizes more than 90% of the *L*-Trp. This catabolism of *L*-Trp in the liver by the TDO enzyme systematically regulates *L*-Trp balance in response to dietary intake. Hence, IDO1 has emerged as an attractive target in cancer immunotherapy. Presently, two IDO1 inhibitors, INCB024360 and NLG919 are under clinical trials for the treatment of cancer and other diseases.[16] Even though *D*-1-MT is under clinical trial as kynurenine pathway inhibitor but its mechanism of action is not certain. Although, it is reported that *D*-1-MT inhibit the kynurenine production at high concentrations but it does not effectively restore IDO-induced arrest of T-cell proliferation.[1,16-19] Therefore, developments of small molecule-based IDO1 inhibitors are essential to satisfactorily address this cancer immunotherapeutic opportunity.

Incyte Corporation identified *N′*-hydroxyamidines as reversible and potent inhibitors of IDO1 enzyme. One of the most potent compounds, 4-amino-*N*-(3-chloro-4-fluorophenyl)-*N′*-hydroxy-1,2,5-oxadiazole-3-carboxymidimade (**5l**) showed IC_{50} values of 67 nM and 19 nM for *in vitro* and cellular enzyme activity assay, respectively.[20] This potent compound lowered blood plasma level of kynurenine and restricted tumor growth in a mouse model. *N′*-hydroxyamidine moiety containing compound INCB024360 is currently under clinical trial for the treatment of several types of cancer and other diseases.[1,16] Compound CBR703 with *N′*-hydroxyamidine moiety notably alter the activity of RNA polymerase from bacteria.[21] *N′*-hydroxyamidines can be also used as pro-drugs of amidines, which is an important tool in drug discovery.[5] Therefore, hydroxyamidine-based compounds show several biological activities and found to be a useful drug scaffold. So far there are no other reports on the modifications of hydroxyamidine scaffold for the improvement of IC_{50} values (for IDO1 enzyme inhibitory activity) of the compounds like 4-amino-*N*-(3-chloro-4-fluorophenyl)-*N′*-hydroxy-1,2,5-oxadiazole-3-carboxymidimade (**5l**).[20]

In this chapter we investigated IDO1 enzyme inhibitory activity by a series of *N′*-hydroxyamidine moiety containing nitrobenzofurazan derivatives. Interestingly, the resulting compounds proved to be potent inhibitors of IDO1 enzyme with inhibitory potency in the nanomolar range under *in vitro* conditions. Selected compounds also showed strong IDO1 enzyme inhibitory activity in MDA-MB-231 cells and almost no/negligible amount of toxicity at the cellular level. Additional counter screening against TDO enzyme showed their selectivity for IDO1 enzyme.

2.2. Origin of Design

High-throughput screening (HTS) by Incyte Corporation led to the discovery of hydroxyamidine-based potent, competitive inhibitors of IDO1 enzyme.[1,20] Hydroxyamidine containing compound INCB024360 in combination with pembrolizumab is now in phase-I/II clinical trials for the treatment of several types of cancers.[1] As already mentioned, the hydroxyamidine-based potent compound, namely 4-amino-*N*-(3-chloro-4-fluorophenyl)-*N′*-hydroxy-1,2,5-oxadiazole-3-carboxymidimade (**5l**) showed enzymatic and cellular IC_{50} values of 67 nM and 19 nM (in Hela cell), respectively and inhibit melanoma growth in a mouse model.[20] A thorough structure-activity-relationship (SAR) studies revealed that the oxygen atom of these hydroxyamidines interact with the heme-iron and play a decisive role in inhibiting IDO1

activity. Model structure also proposed that the substitute phenyl ring of compound INCB024360 or **5l** placed itself in the hydrophobic "pocket-A", whereas the furazan ring interacts with the 7-propionate of the heme-group of IDO1 enzyme.[1,20] Detailed mechanistic studies suggested that addition of ferrous heme iron coordinated molecular oxygen across the C2-C3 double bond is the prerequisite for the IDO1 promoted oxidative cleavage of *L*-Trp in extrahepatic tissues. These studies also proposed the formation of alkylperoxy transition/intermediate state or dioxetane intermediate state during the transformation of *L*-Trp to *N*-formylkynurenine by IDO1 enzyme.[1,16]

In our attempt to synthesize compounds containing hydroxyamidine scaffold with better inhibitory potencies and to mimic the alkylperoxy transition/intermediate state, we developed a series of nitrobenzofurazan derivatives of substituted *N*′-hydroxybenzimidamides where one oxygen atom of the peroxo-moiety is substituted with a nitrogen atom (Figure 2.1). We hypothesized that substituted hydroxybenzimidamides would be placed inside the hydrophobic "pocket A" and interact with heme iron and can act as a mimic of the alkylperoxy transition/intermediate state for the transformation of *L*-Trp to *N*-formylkynurenine by IDO1 enzyme. Whereas, the benzofurazan moiety may interact with the 7-propionate of the heme group.

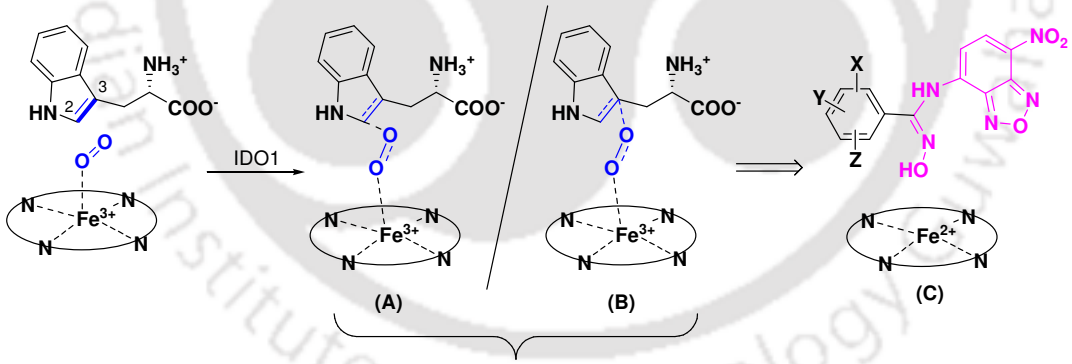

Figure 2.1. Proposed alkylperoxy transition/intermediate state of IDO1 (A and B) and its mimic (C).

2.3. Synthesis

The desired compounds were synthesized in two steps under mild conditions. First, condensation of hydroxylamine with corresponding benzonitrile under basic condition produced substituted *N*′-hydroxybenzimidamide with good yields.[22,23] Further treatment of these hydroxyamidines with 4-chloro-7-nitrobenzofurazan (NBD-Cl) in the presence of

$NaHCO_3$ under ethanolic solution produced the target compounds **1(a-n)** with moderate to good yields (Scheme 2.1).[24]

The inhibitory potencies of the synthesized nitrobenzofurazan derivatives towards the human IDO1 enzyme were initially evaluated by performing enzyme activity assay using purified human IDO1 enzyme. The IC_{50} values were calculated by measuring the change in absorbance values of the product produced from kynurenine and *p*-dimethylaminobenzaldehyde (*p*DMAB) at 480 nm in acidic medium.[25-27]

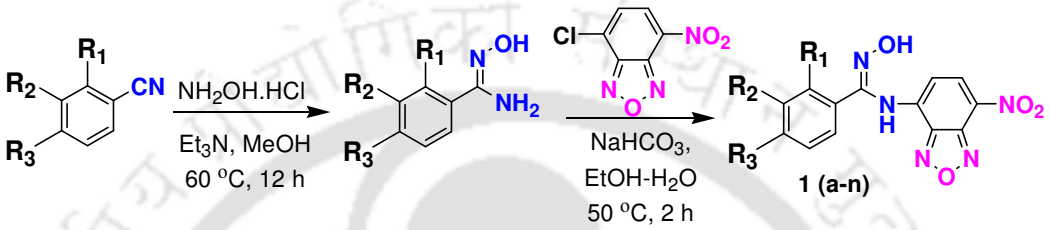

Scheme 2.1. Synthesis of nitrobenzofurazan derivatives of *N′*-hydroxybenzimidamides.

The effect of substitutions on the aryl ring was investigated for potential interactions with the hydrophobic residues positioned within the "pocket-A", by incorporating methyl or halogen substitutions. Several research groups had successfully exploited these hydrophobic interactions in the optimization of the IDO1 inhibition efficacies.[1,26,28-30] Table 2.1 shows the IC_{50} values of nitrobenzofurazan derivatives of the substituted *N′*-hydroxybenzimidamides **1(a-n)** respectively. The IC_{50} value of the reported potent compound **5l** under the experimental conditions was 91 nM, which is in accordance with the reported values.[20]

The *N′*-hydroxybenzimidamide compounds, **1(a-n)** displayed strong hIDO1 inhibitory activities with IC_{50} values ranging from 63 nM to 268 nM (Table 2.1). The SAR studies demonstrated that halogen substituted phenyl derivative **1b, 1d**, **1f**, **1j** and **1n** have stronger IDO1 enzyme inhibition capabilities than the other synthesized *N′*-hydroxybenzimidamides. Among these tested *N′*-hydroxybenzimidamides derivatives, ortho-fluoro **1b** showed stronger hIDO1 inhibitory activity (IC_{50} = 63 nM) than original benzimidamide lead **1a**. A substantial preference for the fluoro-substitution at the ortho- (**1b**) meta- (**1f**) and para- (**1j**) positions of the phenyl ring was also observed from IDO1 enzyme inhibition studies.

Table 2.1. Inhibitory activity of the nitrobenzofurazan derivatives of *N′*-hydroxybenzimidamides against purified human IDO1 enzyme.

Compound	IDO1 inhibition IC_{50} (nM)[a]	Ligand efficiency (LE) = 1.4 × pIC_{50}/HAC[b]
1a; $R_1 = R_2 = R_3 = H$	268 ± 23	0.418
1b; $R_1 = F$, $R_2 = R_3 = H$	63 ± 3	0.438
1c; $R_1 = Cl$, $R_2 = R_3 = H$	135 ± 17	0.418
1d; $R_1 = Br$, $R_2 = R_3 = H$	80 ± 6	0.431
1e; $R_1 = H$, $R_2 = CH_3$, $R_3 = H$	163 ± 8	0.413
1f; $R_1 = H$, $R_2 = F$, $R_3 = H$	75 ± 5	0.433
1g; $R_1 = H$, $R_2 = Cl$, $R_3 = H$	184 ± 6	0.410
1h; $R_1 = H$, $R_2 = Br$, $R_3 = H$	105 ± 3	0.425
1i; $R_1 = R_2 = H$, $R_3 = CH_3$	204 ± 11	0.407
1j; $R_1 = R_2 = H$, $R_3 = F$	100 ± 9	0.426
1k; $R_1 = R_2 = H$, $R_3 = Cl$	113 ± 7	0.423
1l; $R_1 = R_2 = H$, $R_3 = Br$	117 ± 1	0.422
1m; $R_1 = H$, $R_2 = Cl$, $R_3 = F$	158 ± 26	0.397
1n; $R_1 = H$, $R_2 = Br$, $R_3 = F$	92 ± 1	0.411
4-amino-*N*-(3-chloro-4-fluorophenyl)-*N′*-hydroxy-1,2,5-oxadiazole-3-carboxymidimade[c] (derivative of *N′*-hydroxyamidine)	91 ± 2	0.547

[a]IC_{50} values are the mean of five independent assays.

[b]HAC = heavy atom count.

[c]Reported compound.

Various other substitutions showed moderate inhibition potencies but with IC_{50} values still in the nanomolar range. Further optimizations revealed that di-halogen (3-Br, 4-F) substituted compound, **1n** showed stronger IDO1 inhibition potency. However, other di-substituted compound, **1m** failed to show stronger inhibition efficiency. All of these IDO1 inhibition studies were performed by spectrophotometric technique. For further confirmation of their efficacies, IDO1 activity assay was also performed by HPLC analysis. The amount of kynurenine generated due to the catabolism of *L*-Trp, was directly quantified by HPLC analysis.[28] A standard curve generated from pure kynurenine under similar experimental conditions was used to calculate the inhibitory activity of the compounds. The calculated concentrations of the compounds required to inhibit the kynurenine production from the *L*-Trp were in the nanomolar range (Table 2.2) and in accordance with the measured IC_{50} values calculated using the *p*DMAB-method. The IC_{50} values of compounds **1b**, **1d** and **1j** (as measured by HPLC method) are within 56-64 nM

which is lower than the reported potent compound **5l**, under the similar experimental conditions.[20]

Table 2.2. HPLC based IDO1 inhibition assay of the selected compounds.

Compound	IDO1 inhibition (IC_{50} nM)[a]
5l[b]	67 ± 5
1b	56 ± 6
1d	64 ± 6
1f	84 ± 8
1j	60 ± 4
1n	106 ± 9

[a]IC_{50} values calculated by HPLC method (are the mean of three independent assays).

[b]Reported compound.

Our study revealed that most of the compounds displayed stronger hIDO1 inhibitory activities. The common characteristic of these compounds is that, all of them possess nitrobenzofurazan and *N′*-hydroxyamidine moieties, which emerge to be critical for their stronger hIDO1 inhibitory activity. Separate inhibition activity studies with 4-chloro-7-nitrobenzofurazan and a derivative of *N′*-hydroxyamidine showed very weak or no inhibition of IDO1 enzyme activity under the similar experimental conditions. This implies the importance of both nitrobenzofurazan and *N′*-hydroxybenzimidamides moiety for stronger inhibition of hIDO1 activity. ESI-MS spectral analyses of the selected potent compounds in water, 100 mM phosphate buffer at pH 6.5 and enzymatic assay solution revealed that these compounds are also stable under the experimental conditions.

2.4. Cellular IDO1 inhibitory activities of hydroxyamidine derivatives

For the investigation of the therapeutic potential of these hydroxyamidines in inhibiting the IDO1 activity under the *in vitro* cellular environment, we used MDA-MB-231 breast cancer cell line. It is well demonstrated that MDA-MB-231 cells express mRNA of native human IDO1 enzyme and interferon gamma (IFN-γ) considerably induce the IDO1 enzyme expression level in MDA-MB-231 cells.[31] In this regard, MDA-MB-231 cells were first treated with human IFN-γ (20 ng/mL) for 48 h and then cells were grown in the presence of tested compounds (20 nM, 50 nM, 100 nM and 500 nM) and *L*-Trp (150 μM).

The IDO1 activity was determined by measuring the formation of *L*-kynurenine using the *p*DMAB-method (Table 2.3).[27, 28, 31]

Table 2.3. IDO1 enzyme inhibitory activity of the selected compounds in MDA-MB-231 cells.

Compounds	IDO1 inhibition in MDA-MB-231 cell[a] IC_{50} (nM)[b]
1b	131 ± 17
1d	66 ± 8
1f	242 ± 15
1j	125 ± 17
1n	107 ± 12
5l[c]	59 ± 4

[a]IDO1 protein expression in MDA-MB-231 cells was induced by human IFN-γ (20 ng/mL).
[b]IC_{50} values are the mean of three independent assays.
[c]Reported compound.

The calculated cellular IC_{50} values of most of the tested compounds are in accordance with our *in vitro* enzyme assay data. Control compound **5l** showed IC_{50} values of 59 nM (Table 2.3) under the similar experimental conditions.[20] The deviation in IC_{50} values of the compounds between the enzymatic assay against purified IDO1 and cellular assays could be due to the methylene blue-ascorbate regeneration system which maintains IDO1 in active state (Fe^{2+}) or environmental effect on the assay system. In general, a good correlation between these assays confirmed that these tested hydroxyamidine analogues are potent inhibitors of IDO1 enzyme. MTT assay of the compounds (concentrations of IC_{50} and 2 × IC_{50} values from the enzymatic assay) in MDA-MB-231 cells also demonstrated no/negligible level of toxicity of the compounds under the tested conditions (Figure 2.2 and 2.3).

2.5. Mode of IDO1 enzyme inhibition by the potent hydroxyamidines

The enzyme kinetics of selected compounds was performed and their mode of IDO1 inhibition was calculated from the plot of [S]/V against inhibitor concentrations. The results showed that compounds **1b** and **1n** had competitive modes of IDO1 enzyme inhibition whereas compounds **1d, 1f** and **1j** followed uncompetitive modes of IDO1

enzyme inhibition under the similar experimental conditions (Figure 2.4). [S] and V represent the substrate concentration and initial rate of the reaction, respectively.[32]

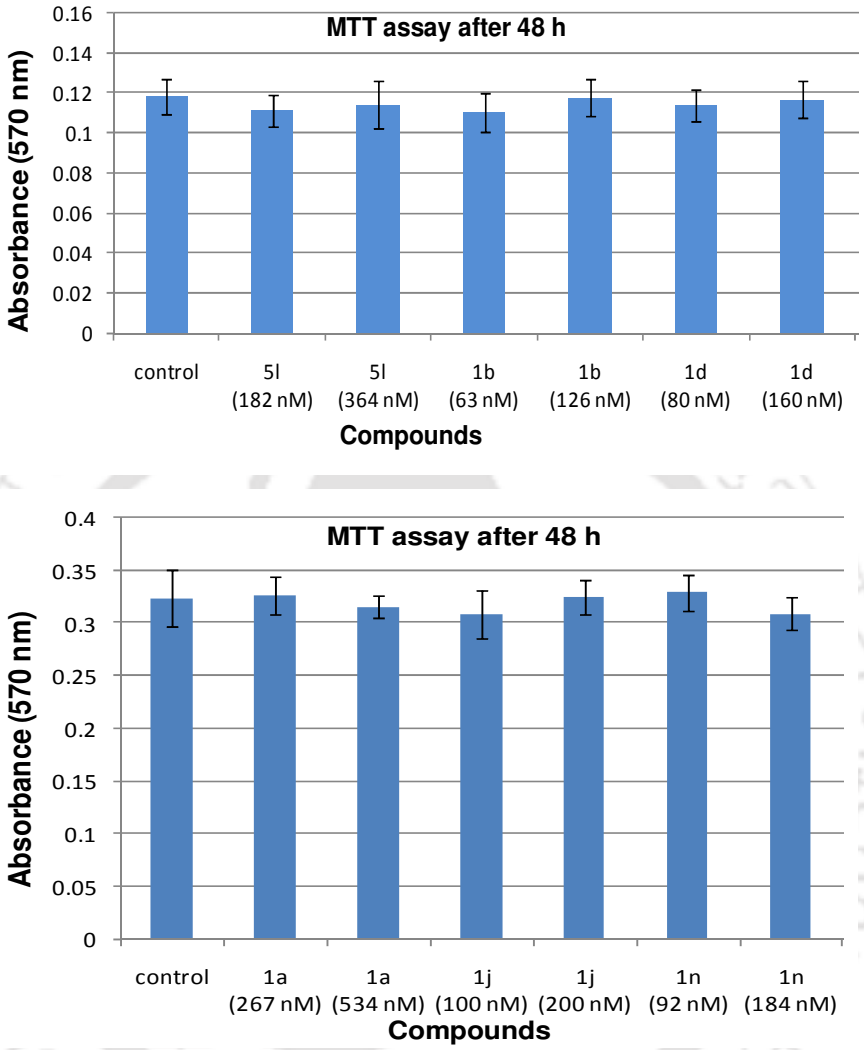

Figure 2.2. Effect of the selected hydroxyamidines (**5l**, **1a, 1b, 1d, 1j** and **1n**) on the viability of MDA-MB-231 cells. MDA-MB-231 cells were treated with the indicated concentrations of the compounds for 48 h. Cell viability was determined by the MTT assay. Absorbance of different amount of formazan were plotted against the mentioned concentrations of the compounds. Data are averages with standard deviation (error bars) from three independent experiments. Mentioned concentrations of the compounds are the IC_{50} and 2 × IC_{50} values of the compounds obtained from *in vitro* IDO1 enzyme activity assay.

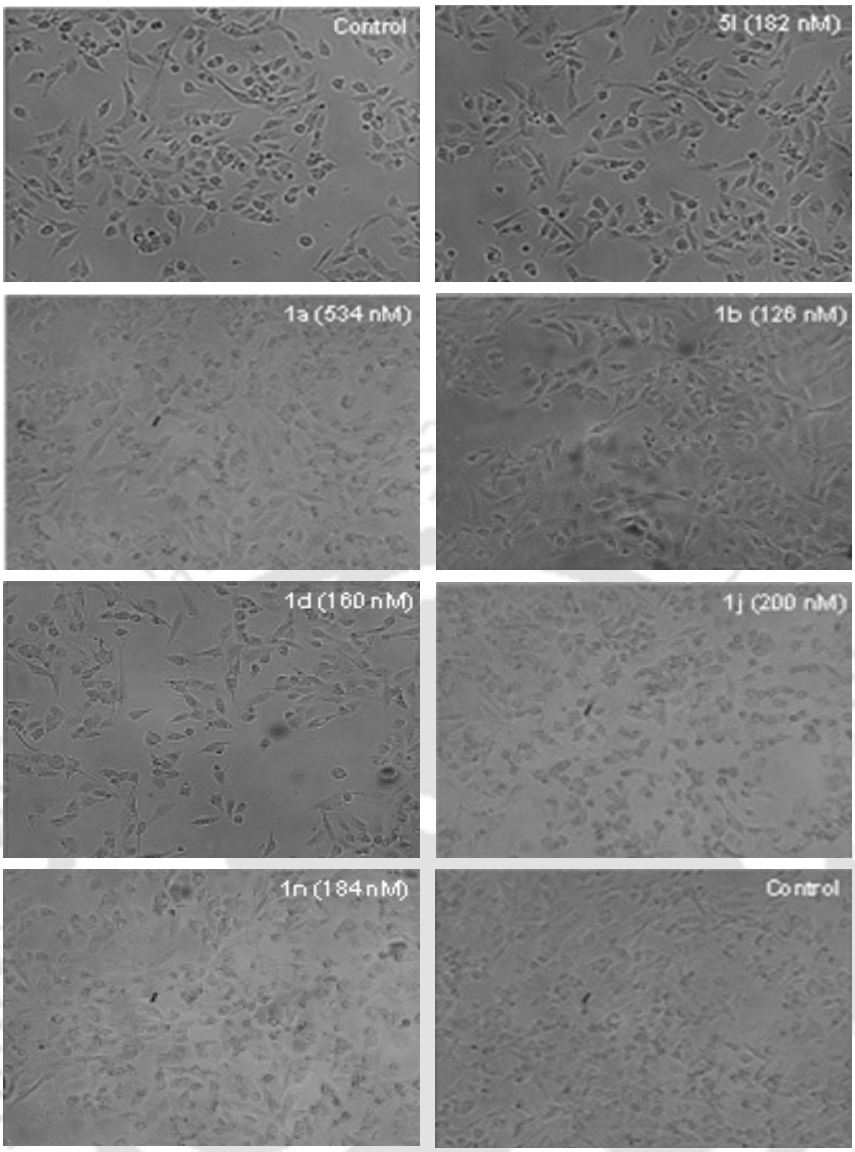

Figure 2.3. Effect of selected hydroxyamidines (**5l, 1a, 1b, 1d, 1j** and **1n**) on the morphological changes of MDA-MB-231 cells. MDA-MB-231 cells were treated with the indicated concentrations of the compounds for 48 h and morphological changes were observed using cytell imaging system. Images were collected at 10X magnification. Images are representative of three independent experiments. Mentioned concentrations of the compounds are the 2 × IC_{50} values of the compounds obtained from *in vitro* IDO1 enzyme activity assay.

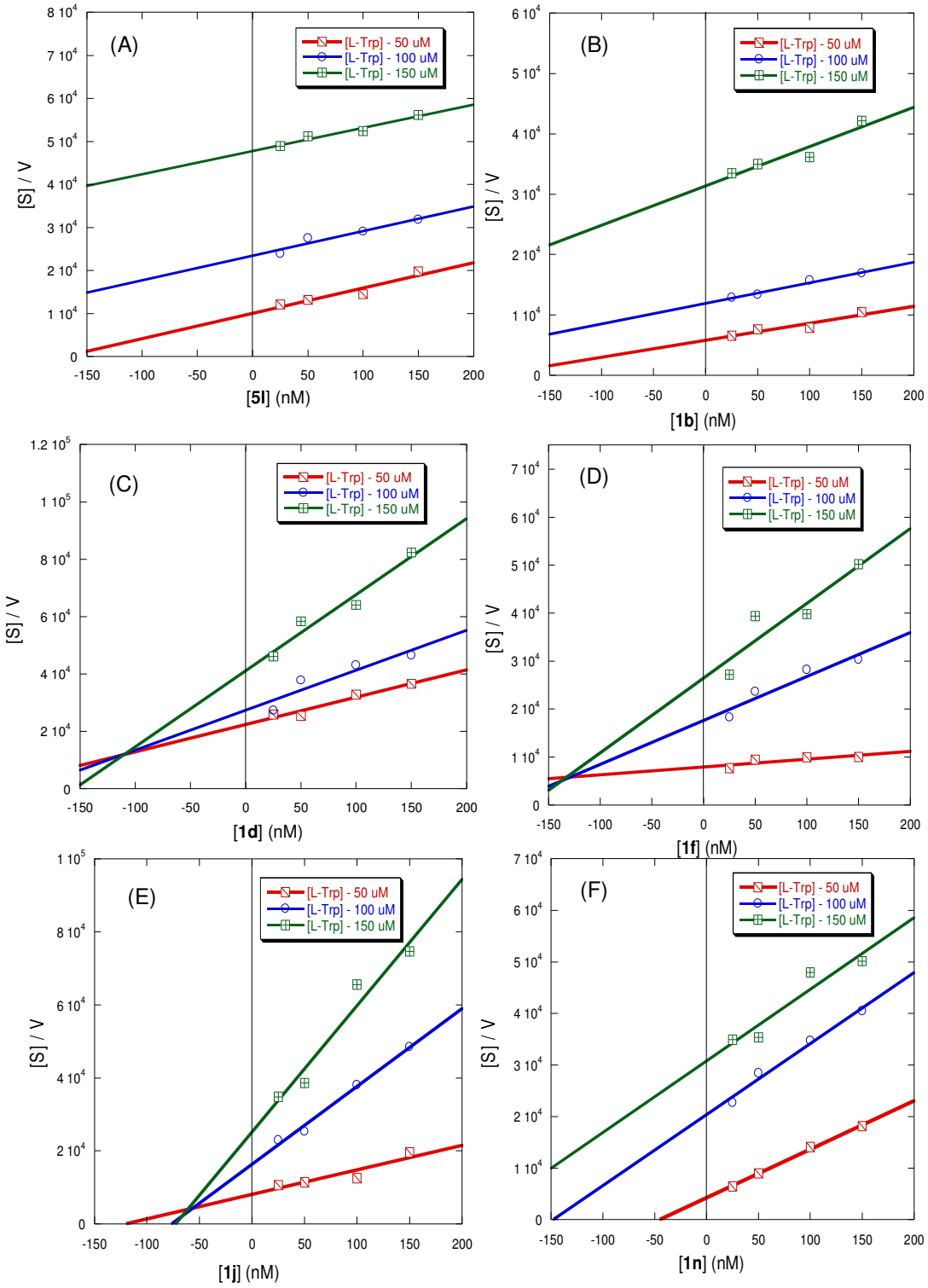

Figure 2.4. Determination of mode of inhibition of the potent compounds. Plot of [S]/V against concentrations of compounds **5l** (A), **1b** (B), **1d** (C), **1f** (D), **1j** (E) **1n** (F) and Concentration of *L*-Trp was varied from 50 µM to 150 µM. The concentrations of compounds were varied from 25 nM to 150 nM.

It is important to mention that IDO1 is an oxido-reductase enzyme and binding of O_2 to the heme-group is required for the transformation of *L*-Trp to *N*-formylkynurenine. The results showed that the tested compounds followed competitive or uncompetitive modes of enzyme inhibition with respect to *L*-Trp. However, these compounds may also follow different mode of inhibition with respect to O_2 under the similar experimental conditions. Hence, additional enzyme kinetics measurement with respect to O_2 is required for detailed understanding, which is beyond the scope of the current study. Compound **5l** is a known competitive inhibitor of hIDO1 enzyme which is in accordance with our experimental results.[20]

2.6. Probable mode of interaction of the potent compounds with IDO1 enzyme

With confirmation that potent hydroxyamidines strongly inhibit IDO1 enzyme activity, we performed molecular docking studies to investigate the probable mode of interaction of the potent compounds with the IDO1 enzyme (PDB code: 2DOT). The docked structures demonstrate that the substituted phenyl ring of the *N*′-hydroxybenzimidamide moieties of the compounds are placed in 'pocket-A' of the IDO1 enzyme (Figure 2.5).

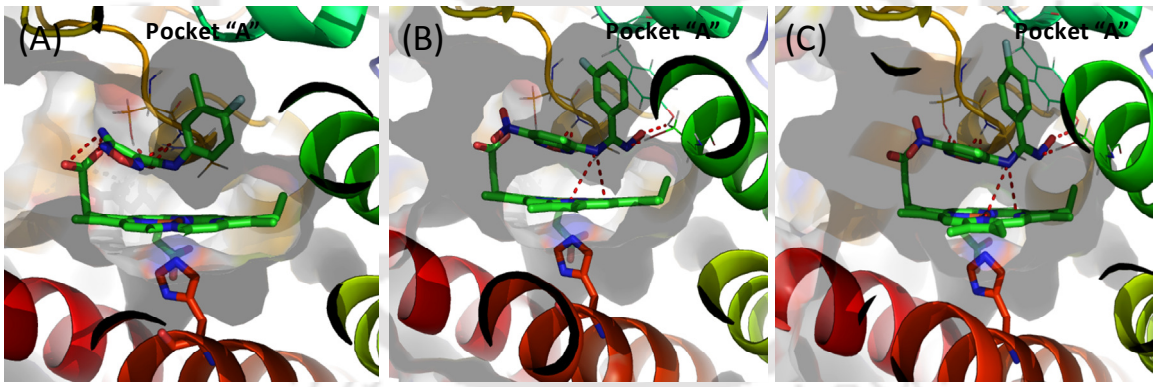

Figure 2.5. Predicted mode of interaction of the compounds, **5l** (A), **1f** (B), and **1j,** (C) with the active site of the human IDO1 enzyme (2DOT). The modelled structures were generated using MoleGro Virtual Docker (MVD), version 6.0. The oxygen and nitrogen atoms are shown in red and blue, respectively. Residues involved in interactions through hydrogen bond formation are shown using dashed lines (red).

The furazan moiety interact with Ser263, Ala264 residues, NH-group interacts with the pyrrole ring of the heme-group and *N*′-hydroxy group interacts with Ser167,

Tyr126 residues through hydrogen bonding. Hydrophobic amino acids like Phe163, Phe164, Tyr126 and others present in 'pocket-A' could be also involved in hydrophobic interaction with the substituted benzene groups. Therefore, both hydrogen bonding and hydrophobic interactions play important roles in stronger binding of the compounds to the active site of IDO1 enzyme. This suggests that volume and electronic properties of the substituent in the benzene ring are significant for stronger binding to the IDO1 enzyme.

2.7. Inhibitory activities of hydroxyamidines against purified TDO enzyme

Strong IDO1 inhibition proficiency and very good ligand efficiency (LE > 0.4) of the compounds prompted us to determine their selectivity for IDO1 over TDO enzyme. It is well documented that TDO enzyme is primarily responsible for the catabolism of *L*-Trp in liver and maintaining its level through kynurenine pathway. Counter-screening against TDO enzyme showed that the potent compounds were appreciably inactive ($IC_{50} \geq 20$ μM) against TDO enzyme (Table 2.4). Tested compounds showed 100 to 1700-fold stronger IDO1 inhibition in comparison with TDO enzyme, demonstrating their selectivity for IDO1 enzyme.

Table 2.4. Inhibitory activity of the selected compounds against purified human IDO1 and TDO enzymes.

Compound	Mode of hIDO1 Inhibition	hIDO1 inhibition (IC_{50} (nM))[a]	hTDO inhibition (IC_{50} (μM))[a]	Selectivity ratio[b]
1b	competitive	63 ± 3	110 ± 13	1746
1d	uncompetitive	80 ± 6	25 ± 3	312
1f	uncompetitive	75 ± 5	45 ± 5	600
1h	NM[c]	105 ± 3	20 ± 1	190
1j	uncompetitive	100 ± 9	21 ± 1	210
1k	NM[c]	113 ± 7	40 ± 2	354
1l	NM[c]	117 ± 1	50 ± 7	427
1n	competitive	92 ± 1	47 ± 1	511
5l[d]	competitive	91 ± 2	24 ± 1	263

[a]IC_{50} values are the mean of three independent assays against purified enzymes.

[b]Selectivity ratio is calculated as (IC_{50} value of TDO)/(IC_{50} value of IDO1).

[c]NM = not measured.

[d]Reported compound.

HPLC-based TDO activity assay also showed that these potent compounds have preferential selectivity for IDO1 over TDO enzyme inhibitions (Table 2.5).

Table 2.5. HPLC based IDO1 and TDO inhibition assay of the selected compounds.

Compound	IDO1 inhibition (IC_{50} nM)[a]	TDO inhibition (IC_{50} μM)[a]
5l[b]	67 ± 5	11 ± 2
1b	56 ± 6	116 ± 9
1d	64 ± 6	14 ± 1
1f	84 ± 8	22 ± 2
1j	60 ± 4	8 ± 2
1n	106 ± 9	22 ± 2

[a]IC_{50} values calculated by HPLC method (are the mean of three independent assays).

[b]Reported compound.

Overall it was observed that suitable substitutions in the benzene ring of the compounds lead to the identification of the potent compounds with nanomolar (< 100 nM) IDO1 enzyme inhibitory activities under *in vitro* conditions. The potency of the selected compounds under cellular environment (IC_{50} = 50-242 nM) and no/ negligible level of toxicity at the cellular level reveal the therapeutic potential of the nitrobenzofurazan derivatives of *N′*-hydroxyamidines. Measured IC_{50} values and molecular modeling studies of the compounds suggest that the presence of hydroxyamidine and nitrobenzofurazan moieties and suitable substitution in the benzene ring of the compounds play a critical role in their stronger IDO1 enzyme inhibitory properties. Until now, only few hydroxyamidine based compounds have been reported with such stronger IDO1 enzyme inhibition properties.[20] The inhibition modes of the tested compounds were determined to be both either competitive or uncompetitive. The potent hydroxyamidine analogues also showed 100 to 1700-fold stronger IDO1 enzyme inhibitory activities in comparison with TDO enzyme, which catabolizes *L*-Trp through the same mechanistic pathway. The low cytotoxicity and inactivity for TDO enzyme support further development of nitrobenzofurazan derivatives of hydroxyamidines.

2.8. Conclusion

In conclusion, we have designed and synthesized a new series of nitrobenzofurazan derivatives of the *N′*-hydroxybenzimidamides as a new class of IDO1 enzyme inhibitors.

Most of the tested compounds showed strong inhibitory activities against purified IDO1 enzyme. The presence of both *N′*-hydroxyamidine and nitrobenzofurazan moieties in the compounds core structure could be the driving force for their strong inhibitory activities. Halogen substitutions in the aryl ring were successful in improving the potency. IDO1 inhibition assay in the interferon gamma (IFN-γ) induced MDA-MB-231 cells showed that the nitrobenzofurazan derivatives of hydroxyamidines have minimal toxicity and stronger potencies. These hydroxyamidine derivatives also exhibited stronger selectivity for IDO1 enzyme over TDO enzyme. These compounds also could be considered as good molecular probes on the basis of their ligand efficiency values. Overall, our findings suggest that these nitrobenzofurazan derivatives of the *N′*-hydroxyamidines can be a useful structural class of compounds for cancer and other human diseases.

2.9. Experimental section

2.9.1. Instrumentation and Characterisation

All reagents were purchased from different commercial sources and used directly without further purification. Column chromatography was performed using 60-120 mesh silica gel. Reactions were monitored by thin-layer chromatography (TLC) on silica gel 60 F254 (0.25 mm). ^{1}H NMR and ^{13}C NMR were recorded at 400 MHz and 100 MHz respectively, with Varian AS400 spectrometer and 600 MHz and 151 MHz respectively, with Brucker spectrometer, using TMS as an internal standard with $CDCl_3$ and DMSO-d_6. The coupling constant (*J* values) and chemical shifts (δ_{ppm}) were described in Hertz (Hz) and parts per million (ppm) respectively. Multiplicities are described as follows: s (singlet), d (doublet), t (triplet), m (multiplet) and br (broadened). High resolution mass spectra (HRMS) were recorded at Agilent Q-TOF mass spectrometer with Z-spray source using built-in software for analysis of the recorded data.

2.9.2. General procedure for the synthesis of substituted hydroxyamidines

To a stirring solution of substituted benzonitrile (1 mmol) in anhydrous methanol (20 mL) under N_2 atmosphere was added hydroxylamine hydrochloride (1.2 mmol). Triethylamine (2.5 mmol) was added under continuous stirring condition and the mixture was then heated under reflux condition for overnight at 60 °C and continued until complete consumption of the starting material (monitored by TLC).[22,23] The excess solvent was then removed under reduced pressure and the obtained residue was washed successively with water and brine, and extracted with ethylacetate (3 × 10 mL). The organic layer was

dried over anhydrous Na_2SO_4 and concentrated under reduced pressure. This reaction mixture was purified using silica gel column chromatography with a gradient solvent system of 10-20% ethylacetate to hexane to obtain the desired product with an average yield of 70-80%.

2.9.3. General procedure for the synthesis of 2-substituted *N′*-hydroxy *N*- (7 nitro benzoxadiazole) imidamide

Sodium bicarbonate (3.5 mmol) was added to a stirring solution of 2-substituted *N′*-hydroxyimidamide (1.1 mmol) in 20 ml of EtOH/H_2O (9:1) and the solution was stirred for 10 min at room temperature. To this mixture an ethanolic solution of 4-chloro 7-nitrobenzofurazan (1 mmol) was added drop wise under continuous stirring condition and the resulting solution was stirred at 50 °C for another 2-4 h.[24] After completion of the reaction (monitored by TLC) the excess solvent was removed under reduced pressure and the pH adjusted to 1.5 using 1N HCl solution. Then aqueous layer was extracted with dichloromethane (3 × 20 ml) and the organic layer was dried over anhydrous Na_2SO_4 and concentrated under reduced pressure. The reaction mixture was further purified using silica gel column chromatography using 20-30% ethylacetate to hexane gradient solvent system to afford the desired pure product with 60-90% yield.

2.9.4. Purification of the compounds by HPLC analysis

All compounds were further purified by analytical-HPLC analyses (with a purity level ≥ 94-95%) and used for enzymatic assay, cellular activity assay, MTT assay, morphological analysis and others. The compounds were purified using Varian star # 1 HPLC system with a Hypersil GOLD aQ C18 analytical column (Thermo Scientific) at a flow rate of 1 mL/min. All the compounds (~1 mg) were dissolved in MeOH (1 mL) for HPLC analyses. All the compounds have a strong absorption peak at 465 nm. In this regard, HPLC analyses were performed using a UV-detector at 465 nm. During each injection 20 µL of the compound solution was used and fractions were collected. This step was repeated for more than 10-times to get sufficient amount of the pure compounds. A total run time was 10 min. All the collected fractions for each compound were dried under reduced pressure and verified by HRMS analyses. The mobile phase for HPLC measurements was 60% MeOH & 40% H_2O (isocratic mode).

2.9.5. IDO1 and TDO inhibition assay by spectrometric method

Both, IDO1 and TDO inhibition assays were performed according to the earlier reported procedures.[25,27-29] The solubility of the compounds in water was either moderate or poor. Hence, stock solution of the compounds were prepared by first dissolving in DMSO and then diluted with buffer. In the assay system the minimum and maximum amount of DMSO were 0.02% and 2%, respectively. The standard reaction mixture (500 µL) contained potassium phosphate buffer (100 mM, pH 6.5 for IDO1 enzyme and 100 mM, pH 8.0 for TDO enzyme), sodium ascorbate (20 mM), methylene blue (10 µM), catalase (240 nM, from bovine liver), *L*-Trp (100 µM), purified enzyme (41 nM for IDO1 and 20 nM for TDO), DMSO (0.05%, v/v), triton-X 100 (0.01%, v/v) and inhibitors. First, the assay was performed using the inhibitors at different concentrations of 50 nM to 1 µM (for IDO1) and 100 nM to 10 µM (for TDO) then repeated five times at a particular concentration. The reaction was quenched using 100 µL of 30% (w/v) trichloroacetic acid. The amount of kynurenine formation was quantified using 2% (w/v) p-dimethylaminobenzaldehyde (*p*DMAB) in acetic acid. The absorbance of the reaction mixture was recorded by at 480 nm. A standard curve was also prepared with pure kynurenine (from Sigma) under similar experimental conditions.[28] The IC_{50} values were calculated using this standard curve. All these experiments were repeated for three times for each compound.

2.9.6. IDO1 and TDO inhibition assay by HPLC analysis

The enzymatic reaction was carried out (100 µL) in 100 mM potassium phosphate buffer at pH 6.5 using sodium-ascorbate (20 mM), catalase (240 nM), methylene blue (10 µM), purified enzyme (41 nM for IDO1 and 20 nM for TDO), *L*-Trp (150 µM), DMSO (0.05%, v/v) and triton-X 100 (0.01%, v/v). Inhibitor concentrations used for this assay were 50 nM to 100 nM for IDO1 and 10 µM for TDO. The reaction mixture was incubated at 37 °C in dark for 1 h and then quenched by addition of 30% (w/v) trichloroacetic acid (20 µL). The reaction mixture was further incubated at 50 °C for 30 min and then centrifuged at 10,000 rpm for 10 min. A 20 µL of supernatant from each reaction mixture was used for HPLC analyses. The mobile phase for HPLC measurements was 50% sodium citrate buffer (40 mM, pH 2.25) and 50% methanol with 400 µM SDS. The rate of flow through the Ascentis® Express C18, 2.7 µm HPLC columns was 0.5 mL/min, and kynurenine was detected at a wavelength of 365 nm.[28] A similar HPLC analyses were performed using

pure kynurenine and a standard curve was prepared. The IC_{50} values of the compounds were calculated from this standard curve.

2.9.7. Determination of inhibition modes

The mode of IDO1 enzyme inhibition by the selected compounds was measured according to the reported method.[32] The IDO1 activity assay was performed with 50 μM, 100 μM and 150 μM of *L*-Trp and 25 nM, 50 nM, 100 nM and 150 nM of inhibitors. The amount of generated *N*-formylkynurenine was monitored at different time interval by UV-Vis spectroscopy. The mode of inhibition was determined from the plot of [S]/V against inhibitor concentration [I]. Where, [S] and V represent *L*-Trp concentration and initial rate of enzyme catalysis, respectively.[32]

2.9.8. In-silico molecular docking analysis

Molecular docking studies to understand the probable mode of interaction of the compounds with hIDO1 enzyme (PDB code: 2DOT) was performed using MoleGro Virtual Docker version 6.0 (Molegro ApS, Aarhus, Denmark).[29,30] To generate apo-protein, the ligands were removed from the co-crystal structures and then were processed by energy minimization. The energy minimized three-dimensional structure of the ligands was prepared by using the GlycoBioChem PRODRG2 server (http://davapc1.bioch.dundee.ac.uk/prodrg/). The occupied position of the ligand PIM (in the crystal structure) was used as the centre of docking site (radius: 12 Å; and center: x = 64.3, y = 54.5, z = 19.3). Other parameters were set default during docking analyses. In each docking run, two hundred docked structures were generated for individual ligands. Energetically favoured docked conformations were evaluated on the basis of the moledock and re-rank scores. The docking poses were exported and examined using PyMOL software (The PyMol Molecular Graphics System, Version 1.0r1, Schrödinger, LLC).

2.9.9. Cellular activity assay

For the *in vitro* cellular activity assay, MDA-MB-231 breast cancer cells were selected. The cells were treated with human interferon gamma (IFN-γ) (20 ng/mL) in DMEM/F12 complete media for 48 h to allow the over expression of IDO1 enzyme in the cells. After that, the compounds (20 nM to 500 nM) were incubated for a period of 4 h and 150 μM of *L*-Trp was incubated for further 5 h. Cells stimulated with IFN-γ alone served as

negative control while cells stimulated with 150 µM *L*-Trp served as positive control. Then, the cells were washed with sterile cell-culture grade PBS and were trypsinized followed by centrifugation at 1000 rpm. The cell pellet was re-dissolved in sterile PBS and centrifuged at 1000 rpm. Then the pellet was lysed in 10 mM HEPES buffer by passing through a sterile syringe. The lysate was used for standard IDO1 assay as mentioned earlier and the IC_{50} values were determined for each compounds.[3,26,28]

2.9.10. MTT assay and morphological analysis

The dye MTT (3-(4,5-dimethylthiazol-2-yl)-2,5-diphenyltetrazolium bromide) was used to measure cell viability analysis. For this experiment 10,000 cells were seeded in 0.2 mL DMEM/F12 complete medium in 96 well plates and cell culture grade PBS was used to wash the cells after 12 h incubation.[35] After that, the compounds, at a concentration of IC_{50} and 2 × IC_{50}, respectively were incubated into the incomplete medium for 48 h. Only the cells treated with incomplete medium were considered as 100% viable. Then the cells were washed with PBS and taken for morphological analysis using cytell imaging system (GE Healthcare). After imaging, 100 µL of MTT (0.5 mg/mL in PBS) was added into the each well and incubated for 4 h at 37 ºC with 5% CO_2. Then the MTT solution was removed and the formazan crystals were dissolved in 100 µL cell culture grade DMSO. The absorbance was determined using spectrophotomter (Spectromax M2) at 570 nm and 660 nm (to subtract scattering effects of crystals).

2.10. Sprectroscopic Characterization of the Synthesized Compounds

(Z)-*N′*-hydroxy-*N*-(7-nitrobenzo[c][1,2,5]oxadiazol-4-yl)benzimidamide (1a): As yellow solid (85% yield; mp: 201-203 °C); ^{1}H NMR (600 MHz, $CDCl_3$ + DMSO-d_6) δ_{ppm} 8.50 (d, 1H, *J* = 12 Hz), 7.70 (d, 1H, *J* = 12 Hz), 7.46-7.36 (m, 5H), 6.12 (br s, 1H);^{13}C NMR (151 MHz, $CDCl_3$ + DMSO-d_6) δ_{ppm} 157.7, 154.3, 144.1, 144.0, 134.9, 131.5, 130.6, 129.2, 128.9, 126.9, 106.7; HRMS (ESI) calcd. for $C_{13}H_9N_5O_4$ $[M + H]^+$ 300.0727, found 300.0725.

(Z)-2-fluoro-*N′*-hydroxy-*N*-(7-nitrobenzo[c][1,2,5]oxadiazol-4-yl)benzimidamide (1b): As yellow solid (60% yield; mp: 134-135 °C); ^{1}H NMR (400 MHz, DMSO-d_6) δ_{ppm} 8.55 (d, 1H, *J* = 8.8 Hz), 7.64-7.62 (m, 1H), 7.47-7.45 (m, 1H), 7.37 (d, 1H, *J* = 8.4 Hz), 7.23-7.13 (m, 2H), 6.74 (br, s, 1H); ^{13}C NMR (151 MHz, $CDCl_3$+DMSO-d_6) δ_{ppm} 160.7,

154.2, 153.5, 143.2, 143.1, 134.6, 131.8, 129.7, 128.0, 123.6, 115.7, 115.4, 106.1; HRMS (ESI) calcd. for $C_{13}H_8FN_5O_4$ $[M + H]^+$ 318.0633, found 318.0635.

(Z)-2-chloro-*N′*-hydroxy-*N*-(7-nitrobenzo[c][1,2,5]oxadiazol-4-yl)benzimidamide

(1c): As yellow solid (70% yield; mp: 178-180 °C); ^{1}H NMR (600 MHz, $CDCl_3$ + DMSO-d_6) δ_{ppm} 8.45 (d, 1H, J = 12 Hz), 7.48-7.46 (m, 1H), 7.40-7.35 (m, 2H), 7.32-7.27 (m, 2H), 6.24 (br s, 1H); ^{13}C NMR (151 MHz, $CDCl_3$ + DMSO-d_6) δ_{ppm} 161.3, 158.5, 148.0, 147.9, 139.5, 139.3, 136.9, 135.6, 134.8, 134.7, 132.8, 131.0, 110.9; HRMS (ESI) calcd. for $C_{13}H_8ClN_5O_4$ $[M + H]^+$ 334.0338, found 334.0340.

(Z)-2-bromo-*N′*-hydroxy-*N*-(7-nitrobenzo[c][1,2,5]oxadiazol-4-yl)benzimidamide

(1d): As brown solid (60% yield; mp: 162-164 °C); ^{1}H NMR (400 MHz, $CDCl_3$ + DMSO-d_6) δ_{ppm} 8.50 (d, 1H, J = 8.4 Hz), 7.61 (d, 1H, J = 7.6 Hz), 7.49-7.42 (m, 1H), 7.37-7.29 (m, 3H), 6.53 (br, s, 1H); ^{13}C NMR (151 MHz, $CDCl_3$ + DMSO-d_6) δ_{ppm} 157.8, 154.0, 143.7, 143.5, 134.9, 133.0, 132.2, 131.4, 130.8, 128.5, 127.2, 121.7, 106.5; HRMS (ESI) calcd. for $C_{13}H_8BrN_5O_4$ $[M + H]^+$ 377.9832, found 377.9835.

(Z)-*N′*-hydroxy-3-methyl-*N*-(7-nitrobenzo[c][1,2,5]oxadiazol-4-yl)benzimidamide

(1e): As yellow solid (75% yield; mp: 203-205 °C); ^{1}H NMR (400 MHz, $CDCl_3$ + DMSO-d_6) δ_{ppm} 8.38-8.35 (m, 1H), 7.58-7.56 (m, 1H),7.30-7.21 (m, 4H), 6.18 (br, s, 1H), 2.29 (s, 3H); ^{13}C NMR (151 MHz, $CDCl_3$ + DMSO-d_6) δ_{ppm} 157.8, 154.6, 144.2, 135.1, 132.3, 131.3, 130.6, 128.7, 126.9, 106.7, 22.8; HRMS (ESI) calcd. for $C_{14}H_{11}N_5O_4$ $[M + H]^+$ 314.0884, found 314.0880.

(Z)-3-fluoro-*N′*-hydroxy-*N*-(7-nitrobenzo[c][1,2,5]oxadiazol-4-yl)benzimidamide

(1f): As yellow solid (75% yield; mp: 167-169 °C); ^{1}H NMR (600 MHz, $CDCl_3$ + DMSO-d_6) δ_{ppm} 8.54-8.51 (m, 1H), 7.75-7.72 (m, 1H), 7.47-7.39 (m, 3H), 7.35-7.34 (m, 1H), 6.23 (br, s, 1H); ^{13}C NMR (151 MHz, $CDCl_3$ + DMSO-d_6) δ_{ppm} 157.7, 154.3, 143.9, 143.7, 135.0, 131.1, 130.5, 128.8, 128.6, 126.8, 106.5; HRMS (ESI) calcd. for $C_{13}H_8FN_5O_4$ $[M + H]^+$ 318.0633, found 318.0635.

(Z)-3-chloro-*N′*-hydroxy-*N*-(7-nitrobenzo[c][1,2,5]oxadiazol-4-yl)benzimidamide

(1g): As yellow solid (77% yield; mp: 210-212 °C);^{1}H NMR (400 MHz, $CDCl_3$ + DMSO-d_6) δ_{ppm} 8.64 (d, 1H, J = 8.8 Hz), 7.87 (s, 1H), 7.77 (d, 1H, J = 7.6 Hz), 7.53-7.51

(m, 2H), 7.47-7.43 (m, 1H), 6.72 (br, s, 1H); ^{13}C NMR (100 MHz, $CDCl_3$ + DMSO-d_6) δ_{ppm} 156.2, 153.8, 143.6, 143.4, 134.8, 133.9, 132.0, 130.6, 129.5, 128.5, 126.7, 124.8, 106.3; HRMS (ESI) calcd. for $C_{13}H_8ClN_5O_4$ $[M + H]^+$ 334.0338, found 334.0340.

(Z)-3-bromo-*N′*-hydroxy-*N*-(7-nitrobenzo[c][1,2,5]oxadiazol-4-yl)benzimidamide (1h): As yellow solid (78% yield; mp: 189-191 °C); ^{1}H NMR (400 MHz, $CDCl_3$ + DMSO-d_6) δ_{ppm} 8.53-8.49 (m, 1H), 7.90-7.87 (m, 1H), 7.69-7.65 (m, 1H), 7.56-7.52(m, 1H),7.42-7.40 (m, 1H), 7.29-7.24 (m, 1H), 6.40 (br, s, 1H); ^{13}C NMR (151 MHz, $CDCl_3$ + DMSO-d_6) δ_{ppm} 156.3, 154.0, 134.8, 133.9, 132.5, 130.1, 129.8, 125.5, 106.5; HRMS (ESI) calcd. for $C_{13}H_8BrN_5O_4$ $[M + H]^+$ 377.9832, found 377.9828.

(Z)-*N′*-hydroxy-4-methyl-*N*-(7-nitrobenzo[c][1,2,5]oxadiazol-4-yl)benzimidamide (1i): As yellow semi solid (70% yield); ^{1}H NMR (600 MHz, $CDCl_3$ + DMSO-d_6) δ_{ppm} 8.65 (d, 1H, J = 12 Hz), 7.71 (d, 2H, J = 12 Hz), 7.57 (d, 1H, J = 12 Hz), 7.37 (d, 2H, J = 12 Hz), 1.31 (s, 3H); ^{13}C NMR (151 MHz, $CDCl_3$ + DMSO-d_6) δ_{ppm} 157.5, 154.2, 143.8, 143.6, 140.7, 135.8, 128.8, 128.1, 127.5, 126.6, 106.7, 21.0; HRMS (ESI) calcd. for $C_{14}H_{11}N_5O_4$ $[M + H]^+$ 314.0884, found 314.0882.

(Z)-4-fluoro-*N′*-hydroxy-*N*-(7-nitrobenzo[c][1,2,5]oxadiazol-4-yl)benzimidamide (1j): As yellow solid (70% yield; mp: 191-193 °C); ^{1}H NMR (600 MHz, $CDCl_3$) δ_{ppm} 8.58 (d, 1H, J = 8.4 Hz), 7.79-7.76 (m, 2H),7.49 (d, 1H, J = 8.4 Hz), 7.22-7.19 (m, 2H), 5.49 (br, s, 1H);^{13}C NMR (151 MHz, $CDCl_3$) δ_{ppm} 156.5, 154.1, 144.0, 134.8, 129.1, 129.0, 116.6, 116.5, 106.9; HRMS (ESI) calcd. for $C_{13}H_8FN_5O_4$ $[M + H]^+$ 318.0633, found 318.0635.

(Z)-4-chloro-*N′*-hydroxy-*N*-(7-nitrobenzo[c][1,2,5]oxadiazol-4-yl)benzimidamide (1k): As orange solid (50% yield; mp: 200-202 °C); ^{1}H NMR (600 MHz, $CDCl_3$ + MeOD-d_4 + DMSO-d_6) δ_{ppm} 8.56 -8.54 (m, 1H), 7.74-7.72 (m, 2H), 7.44-7.41 (m, 1H), 7.38-7.36 (m, 2H), 6.68 (br, s, 1H); ^{13}C NMR (151 MHz, $CDCl_3$ + MeOD-d_4 + DMSO-d_6) δ_{ppm} 156.8, 154.2, 144.0, 143.8, 136.8, 135.3, 129.1, 128.7, 128.3, 106.7; HRMS (ESI) calcd. for $C_{13}H_8ClN_5O_4$ $[M + H]^+$ 334.0338, found 334.0338.

(Z)-4-bromo-*N′*-hydroxy-*N*-(7-nitrobenzo[c][1,2,5]oxadiazol-4-yl)benzimidamide (1l): As orange solid (65% yield; mp: 213-215 °C); ^{1}H NMR (400 MHz, $CDCl_3$ +

DMSO-d_6) δ_{ppm} 8.61-8.59 (m, 1H), 7.73-7.71 (m, 2H), 7.56-7.54 (m, 2H), 7.44-7.42 (m, 1H), 6.98 (br, s, 1H); ^{13}C NMR (100 MHz, $CDCl_3$ + DMSO-d_6) δ_{ppm} 156.6, 154.0, 143.7, 143.5, 135.4, 131.3, 129.5, 128.5, 128.3, 124.7, 106.6; HRMS (ESI) calcd. for $C_{13}H_8BrN_5O_4$ $[M + H]^+$ 379.9813, found 379.9848.

(Z)-3-chloro-4-fluoro-*N′*-hydroxy-*N*-(7-nitrobenzo[c][1,2,5]oxadiazol-4-yl)benzimidamide (1m): As yellow solid (50% yield; mp: 251-253 °C); ^{1}H NMR (600 MHz, MeOD-d_4) δ_{ppm} 8.43 (d, 2H, J = 8 Hz), 7.42 (s, 1H), 6.08 (d, 2H, J = 8 Hz); ^{13}C NMR (151 MHz, MeOD-d_4 + DMSO-d_6) δ_{ppm} 148.5, 146.5, 139.3, 114.7, 112.1; HRMS (ESI) calcd. for $C_{13}H_7ClFN_5O_4$ $[M + H]^+$ 351.0171 found 351.0168.

(Z)-3-bromo-4-fluoro-*N′*-hydroxy-*N*-(7-nitrobenzo[c][1,2,5]oxadiazol-4-yl)benzimidamide (1n): As brown solid (60%; yield; mp: 112-113 °C); ^{1}H NMR (600 MHz, $CDCl_3$ + DMSO-d_6) δ_{ppm} 8.55 (d, 1H, J = 12 Hz), 8.03-8.01 (m, 1H), 7.95 (s, 1H), 7.75-7.71 (m, 1H), 7.44 (d, 1H, J = 12 Hz), 7.21-7.17 (m, 1H), 6.20 (br s, 1H); ^{13}C NMR (100 MHz, MeOD-d_4 + $CDCl_3$ + DMSO-d_6) δ_{ppm} 160.9, 159.2, 155.5, 153.7, 143.5, 143.4, 134.9, 131.7, 128.4, 127.9, 116.2, 116.0, 106.3; HRMS (ESI) calcd. for $C_{13}H_7BrFN_5O_4$ $[M + H]^+$ 397.9719, found 397.9752.

References

(1) Rohrig, U. F.; Majjigapu, S. R.; Vogel, P.; Zoete, V.; Michielin, O. Challenges in the Discovery of Indoleamine 2,3-Dioxygenase 1 (IDO1) Inhibitors. *J. Med. Chem.* **2015**, *58*, 9421-9437.

(2) Kershaw, M. H.; Westwood, J. A.; Slaney, C. Y.; Darcy, P. K. Clinical application of genetically modified T cells in cancer therapy. *Clin. Transl. Oncol.* **2014**, *3,* e16.

(3) Takikawa, O.; Yoshida, R.; Kido, R.; Hayaishi, O. Tryptophan Degradation in Mice Initiated by Indoleamine 2,3-Dioxygenase. *J. Biol. Chem.* **1986**, *261,* 3648-3653.

(4) Yamamoto, S.; Hayaishi, O. Tryptophan pyrrolase of rabbit intestine. *D*- and *L*-tryptophan-cleaving enzyme or enzymes. *J. Biol. Chem.* **1967**, *242,* 5260-5266.

(5) Clement, B. Reduction of N-hydroxylated compounds: amidoximes (*N*-hydroxyamidines) as pro-drugs of amidines. *Drug Metab. Rev.* **2002**, *34*, 565-579.

(6) Uyttenhove, C.; Pilotte, L.; Theate, I.; Stroobant, V.; Colau, D.; Parmentier, N.; Boon, T.; Van den Eynde, B. J. Evidence for a tumoral immune resistance mechanism based on tryptophan degradation by indoleamine 2,3-dioxygenase. *Nat. Med.* **2003**, *9*, 1269-1274.

(7) Croitoru-Lamoury, J.; Lamoury, F. M.; Caristo, M.; Suzuki, K.; Walker, D.; Takikawa, O.; Taylor, R.; Brew, B. J. Interferon-gamma regulates the proliferation and differentiation of mesenchymal stem cells via activation of indoleamine 2,3 dioxygenase (IDO). *PLoS One* **2011**, *6*, e14698.

(8) Platten, M.; Wick, W.; Van den Eynde, B. J. Tryptophan catabolism in cancer: beyond IDO and tryptophan depletion. *Cancer Res.* **2012**, *72*, 5435-5440.

(9) van Baren, N.; Van den Eynde, B. J. Tryptophan-degrading enzymes in tumoral immune resistance. *Front. Immunol*. **2015**, *6*, 34.

(10) Riesenberg, R.; Weiler, C.; Spring, O.; Eder, M.; Buchner, A.; Popp, T.; Castro, M.; Kammerer, R.; Takikawa, O.; Hatz, R. A.; Stief, C. G.; Hofstetter, A.; Zimmermann, W. Expression of indoleamine 2,3-dioxygenase in tumor endothelial cells correlates with long-term survival of patients with renal cell carcinoma. *Clin. Cancer Res.* **2007**, *13*, 6993-7002.

(11) Heyes, M. P.; Saito, K.; Crowley, J. S.; Davis, L. E.; Demitrack, M. A.; Der, M.; Dilling, L. A.; Elia, J.; Kruesi, M. J.; Lackner, A.; et al. Quinolinic acid and kynurenine pathway metabolism in inflammatory and non-inflammatory neurological disease. *Brain* **1992**, *115*, 1249-1273.

(12) Wichers, M. C.; Maes, M. The role of indoleamine 2,3-dioxygenase (IDO) in the pathophysiology of interferon-alpha-induced depression. *J. Psychiatry Neurosci.* **2004**, *29*, 11-17.

(13) Vazquez, S.; Parker, N. R.; Sheil, M.; Truscott, R. J. Protein-bound kynurenine decreases with the progression of age-related nuclear cataract. *Invest. Ophthalmol. Vis. Sci.* **2004**, *45*, 879-883.

(14) Sardar, A. M.; Reynolds, G. P. Frontal cortex indoleamine 2,3-dioxygenase activity is increased in HIV-1-associated dementia. *Neurosci. Lett.* **1995**, *187*, 9-12.

(15) Okamoto, A.; Nikaido, T.; Ochiai, K.; Takakura, S.; Saito, M.; Aoki, Y.; Ishii, N.; Yanaihara, N.; Yamada, K.; Takikawa, O.; Kawaguchi, R.; Isonishi, S.; Tanaka, T.; Urashima, M. Indoleamine 2,3-dioxygenase serves as a marker of poor prognosis in gene expression profiles of serous ovarian cancer cells. *Clin. Cancer Res.* **2005**, *11*, 6030-6039.

(16) Malachowski, W .P.; Winters, M.; DuHadaway, J. B.; Lewis-Ballestere, A.; Badir, S.; Wai, J.; Rahman, M.; Sheikh, E.; LaLonde, J. M.; Yeh, S. R.; Prendergast, G. C.; Muller, A. J. O-alkylhydroxylamines as rationally-designed mechanism-based inhibitors of indoleamine 2,3-dioxygenase 1. *Eur. J. Med. Chem.* **2016**, *108*, 564-576.

(17) Pasceri, R.; Siegel, D.; Ross, D.; Moody, C .J. Aminophenoxazinones as Inhibitors of Indoleamine 2,3-Dioxygenase (IDO). Synthesis of Exfoliazone and Chandrananimycin A. *J. Med. Chem.* **2013**, *56*, 3310-3317.

(18) Vacchelli, E.; Aranda, F.; Eggermont, A.; Sautes-Fridman, C.; Tartour, E.; Kennedy, E. P.; Platten, M.; Zitvogel, L.; Kroemer, G.; Galluzzi, L. Trial watch: IDO inhibitors in cancer therapy. *Oncoimmunology* **2014**, *3*, e957994.

(19) Qian, F.; Villella, J.; Wallace, P. K.; Mhawech-Fauceglia, P.; Tario, J. D.; Andrews, C.; Matsuzaki, J.; Valmori, D.; Ayyoub, M.; Frederick, P .J.; Beck, A.; Liao, J. Q.; Cheney, R.; Moysich, K.; Lele, S.; Shrikant, P.; Old, L. J.; Odunsi, K. Efficacy of Levo-1-Methyl Tryptophan and Dextro-1-Methyl Tryptophan in Reversing Indoleamine-2,3-Dioxygenase-Mediated Arrest of T-Cell Proliferation in Human Epithelial Ovarian Cancer. *Cancer Res.* **2009**, *69*, 5498-5504.

(20) Yue, E. W.; Douty, B.; Wayland, B.; Bower, M.; Liu, X. D.; Leffet, L.; Wang, Q.; Bowman, K. J.; Hansbury, M. J.; Liu, C. N.; Wei, M.; Li, Y. L.; Wynn, R.; Burn, T. C.; Koblish, H. K.; Fridman, J. S.; Metcalf, B.; Scherle, P. A.; Combs, A. P. Discovery of Potent Competitive Inhibitors of Indoleamine 2,3-Dioxygenase with in Vivo Pharmacodynamic Activity and Efficacy in a Mouse Melanoma Model. *J. Med. Chem.* **2009**, *52*, 7364-7367.

(21) Malinen, A. M.; Nandy Mazumdar, M.; Turtola, M.; Malmi, H.; Grocholski, T.; Artsimovitch, I.; Belogurov, G. A. CBR antimicrobials alter coupling between the bridge helix and the beta subunit in RNA polymerase. *Nat. Comm.* **2014**, *5*, 3408-3416.

(22) Wang, Y. J.; Rong, J.; Zhang, B.; Hu, L. M.; Wang, X. L.; Zeng, C. C. Design and synthesis of N-methylpyrimidone derivatives as HIV-1 integrase inhibitors. *Bioorg. Med. Chem.* **2015**, *23*, 735-741.

(23) Cai, J.; Wei, H. T.; Hong, K. H.; Wu, X. Q.; Cao, M.; Zong, X.; Li, L. S.; Sun, C. L.; Chen, J. Q.; Ji, M. Discovery and preliminary evaluation of 2-aminobenzamide and hydroxamate derivatives containing 1,2,4-oxadiazole moiety as potent histone deacetylase inhibitors. *Eur. J. Med. Chem.* **2015**, *96*, 1-13.

(24) Zhuang, Y. D.; Chiang, P. Y.; Wang, C. W.; Tan, K. T. Environment-Sensitive Fluorescent Turn-On Probes Targeting Hydrophobic Ligand-Binding Domains for Selective Protein Detection. *Angew. Chem. Int. Ed.* **2013**, *52*, 8124-8128.

(25) Takikawa, O.; Kuroiwa, T.; Yamazaki, F.; Kido, R. Mechanism of Interferon-Gamma Action - Characterization of Indoleamine 2,3-Dioxygenase in Cultured Human-Cells Induced by Interferon-Gamma and Evaluation of the Enzyme-Mediated Tryptophan Degradation in Its Anticellular Activity. *J. Biol. Chem.* **1988**, *263*, 2041-2048.

(26) Rohrig, U. F.; Awad, L.; Grosdidier, A.; Larrieu, P.; Stroobant, V.; Colau, D.; Cerundolo, V.; Simpson, A. J. G.; Vogel, P.; Van den Eynde, B. J.; Zoete, V.; Michielin, O. Rational Design of Indoleamine 2,3-Dioxygenase Inhibitors. *J. Med. Chem.* **2010**, *53*, 1172-1189.

(27) Austin, C. J. D.; Mizdrak, J.; Matin, A.; Sirijovski, N.; Kosim-Satyaputra, P.; Willows, R. D.; Roberts, T. H.; Truscott, R. J. W.; Polekhina, G.; Parker, M. W.; Jamie, J. F. Optimised expression and purification of recombinant human indoleamine 2,3-dioxygenase. *Protein Express. Purif.* **2004**, *37*, 392-398.

(28) Rohrig, U. F.; Majjigapu, S. R.; Grosdidier, A.; Bron, S.; Stroobant, V.; Pilotte, L.; Colau, D.; Vogel, P.; Van den Eynde, B. J.; Zoete, V.; Michielin, O. Rational Design of 4-Aryl-1,2,3-Triazoles for Indoleamine 2,3-Dioxygenase 1 Inhibition. *J. Med. Chem.* **2012**, *55*, 5270-5290.

(29) Wu, J. S.; Lin, S. Y.; Liao, F. Y.; Hsiao, W. C.; Lee, L. C.; Peng, Y. H.; Hsieh, C. L.; Wu, M. H.; Song, J. S.; Yueh, A.; Chen, C. H.; Yeh, S. H.; Liu, C. Y.; Lin, S. Y.; Yeh, T. K.; Hsu, J. T. A.; Shih, C.; Ueng, S. H.; Hung, M. S.; Wu, S. Y. Identification of Substituted Naphthotriazolediones as Novel Tryptophan 2,3-Dioxygenase (TDO)

Inhibitors through Structure-Based Virtual Screening. *J. Med. Chem*. **2015**, *58*, 7807-7819.

(30) Yu, L. F.; Li, Y. Y.; Su, M. B.; Zhang, M.; Zhang, W.; Zhang, L.N.; Pang, T.; Zhang, R. T.; Liu, B.; Li, J. Y.; Li, J.; Nan, F. J. Development of Novel Alkene Oxindole Derivatives As Orally Efficacious AMP-Activated Protein Kinase Activators. *Acs Med. Chem. Lett*. **2013**, *4*, 475-480.

(31) Travers, M. T.; Gow, I. F.; Barber, M. C.; Thomson, J.; Shennan, D. B. Indoleamine 2,3-dioxygenase activity and L-tryptophan transport in human breast cancer cells. *Biochim. Biophys. Acta.* **2004**, *1661*, 106-112.

(32) Yang, S. S.; Li, X. S.; Hu, F. F.; Li, Y. L.; Yang, Y. Y.; Yan, J. K.; Kuang, C. X.; Yang, Q.; Discovery of Tryptanthrin Derivatives as Potent Inhibitors of Indoleamine 2,3-Dioxygenase with Therapeutic Activity in Lewis Lung Cancer (LLC) Tumor-Bearing Mice. *J. Med. Chem*. **2013**, *56*, 8321-8331.

(33) Tojo, S.; Kohno, T.; Tanaka, T.; Kamioka, S.; Ota, Y.; Ishii, T. ; Kamimoto, K.; Asano, S.; Isobe, Y. Crystal Structures and Structure Activity Relationships of Imidazothiazole Derivatives as IDO1 Inhibitors. *Acs Med. Chem. Lett.* **2014**, *5*, 1119-1123.

(34) Mamidi, N.; Borah, R.; Sinha, N.; Jana, C.; Manna, D. Effects of ortho substituent groups of protocatechualdehyde derivatives on binding to the C1 domain of novel protein kinase C. *J. Phys. Chem. B* **2012**, *116*, 10684-10692.

(35) Kumar, P.; Gorai, S.; Santra, M. K.; Mondal, B.; Manna, D. DNA binding, nuclease activity and cytotoxicity studies of Cu(II) complexes of tridentate ligands. *Dalton Transac.* **2012**, *41*, 7573-7581.

2.11. NMR Spectra of the Synthesised Compounds

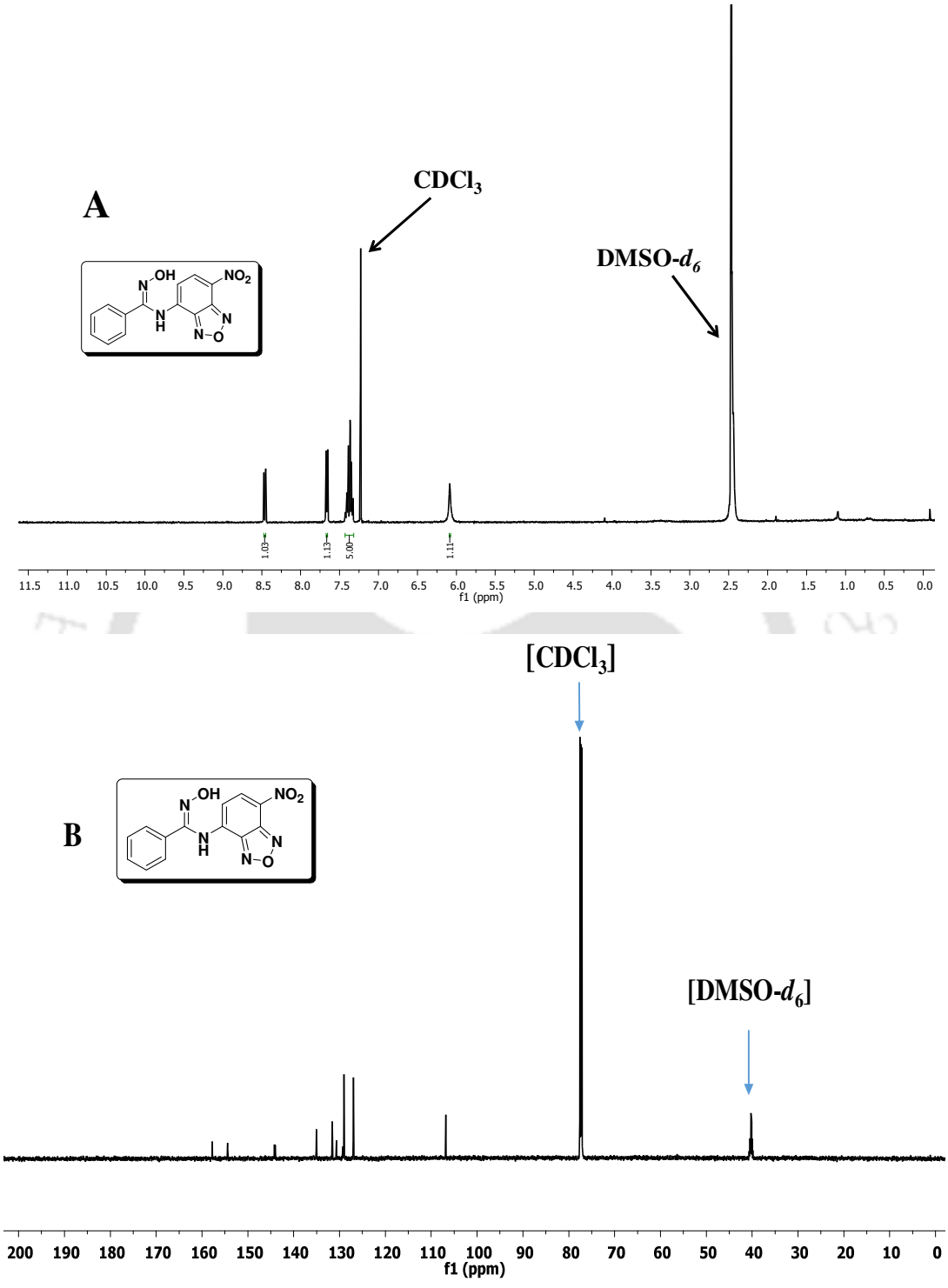

Figure 2.11.1. ^{1}H (**A**) NMR and ^{13}C (**B**) NMR of (Z)-N'-hydroxy-N-(7-nitrobenzo[c][1,2,5]oxadiazol-4-yl)benzimidamide (**1a**).

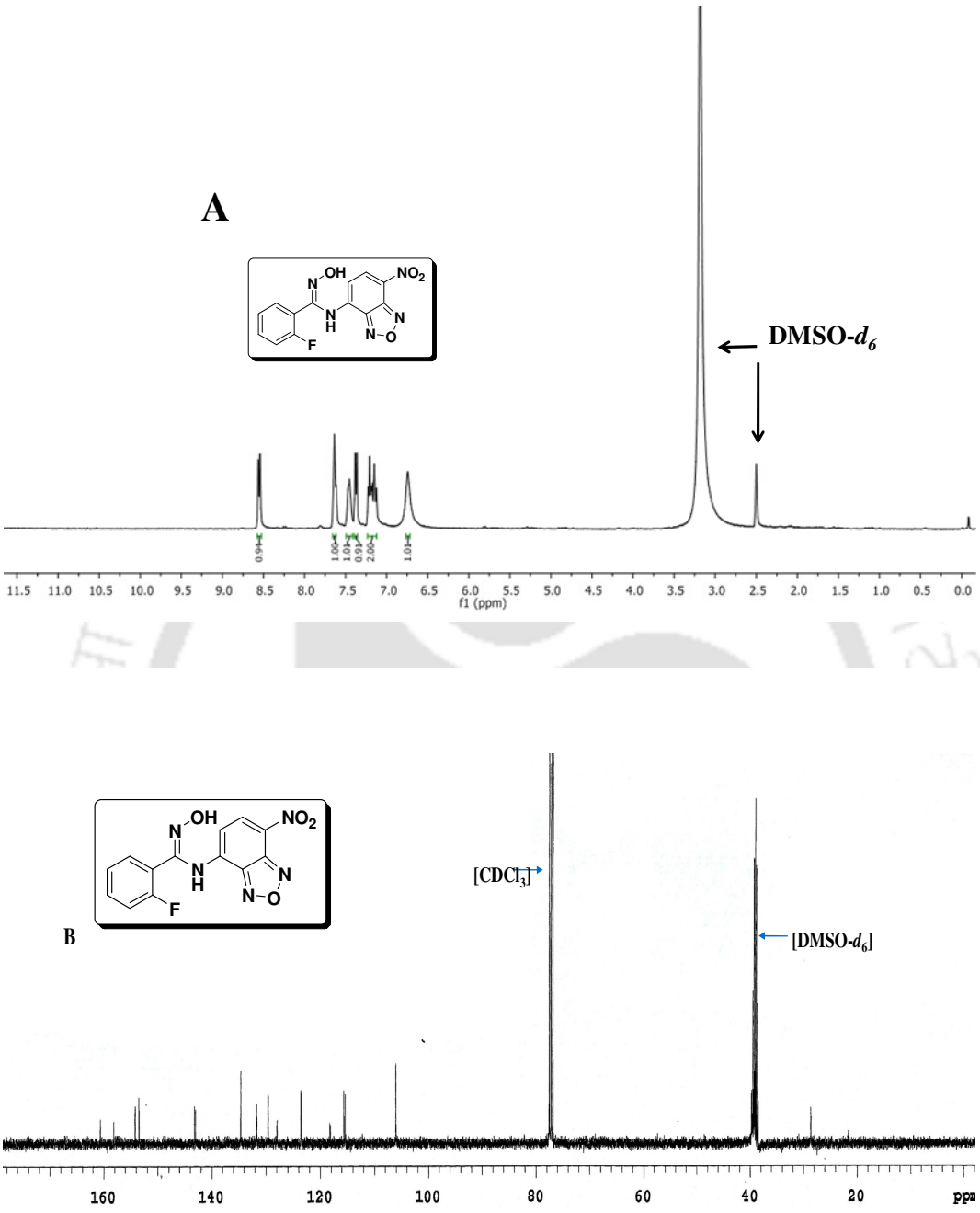

Figure 2.11.2. ^{1}H (**A**) NMR and ^{13}C (**B**) NMR of (Z)-2-fluoro-N'-hydroxy-N-(7-nitrobenzo[c][1,2,5]oxadiazol-4-yl)benzimidamide (**1b**).

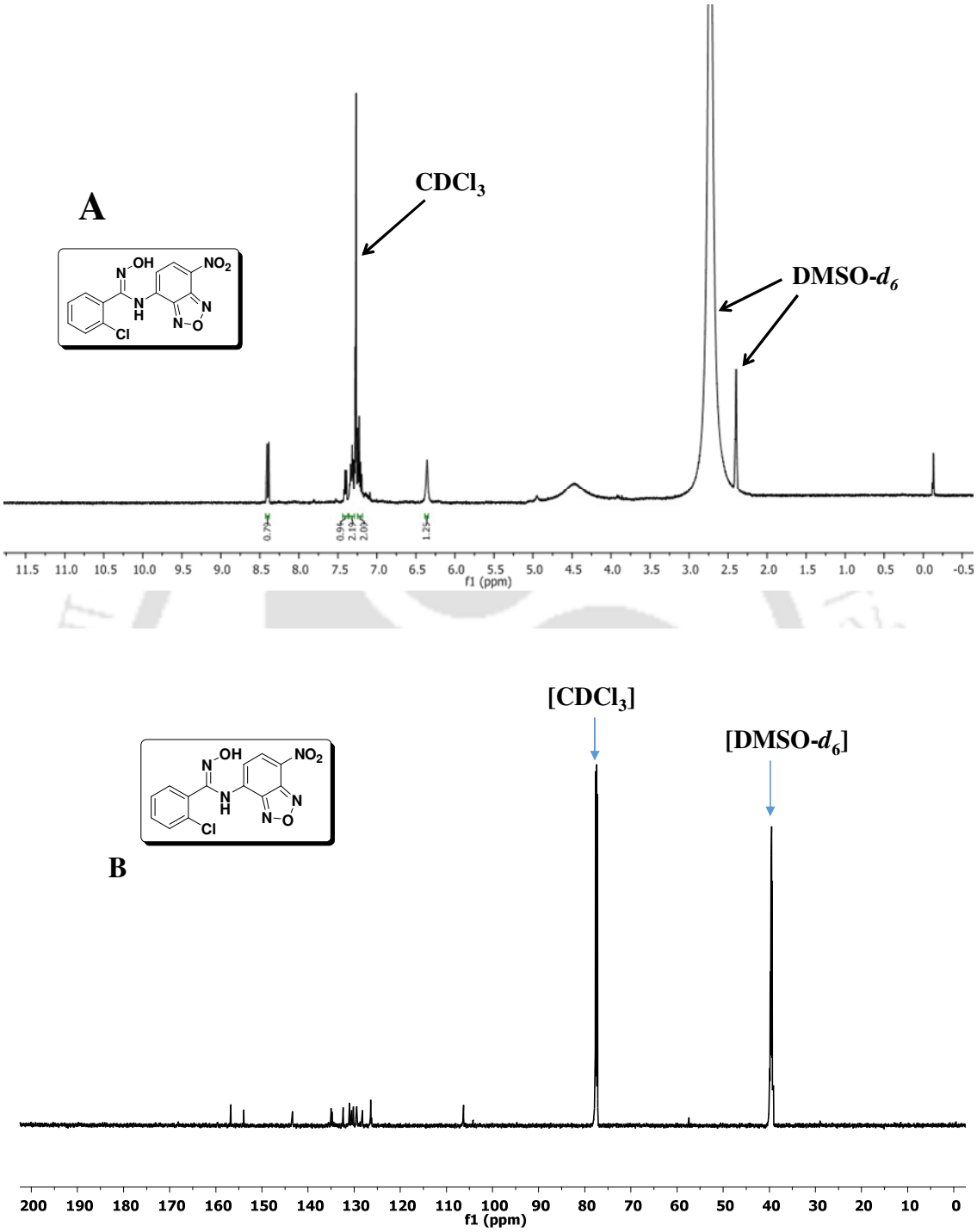

Figure 2.11.3. ^{1}H (**A**) NMR and ^{13}C (**B**) NMR of (Z)-2-chloro-N'-hydroxy-N-(7-nitrobenzo[c][1,2,5]oxadiazol-4-yl)benzimidamide (**1c**).

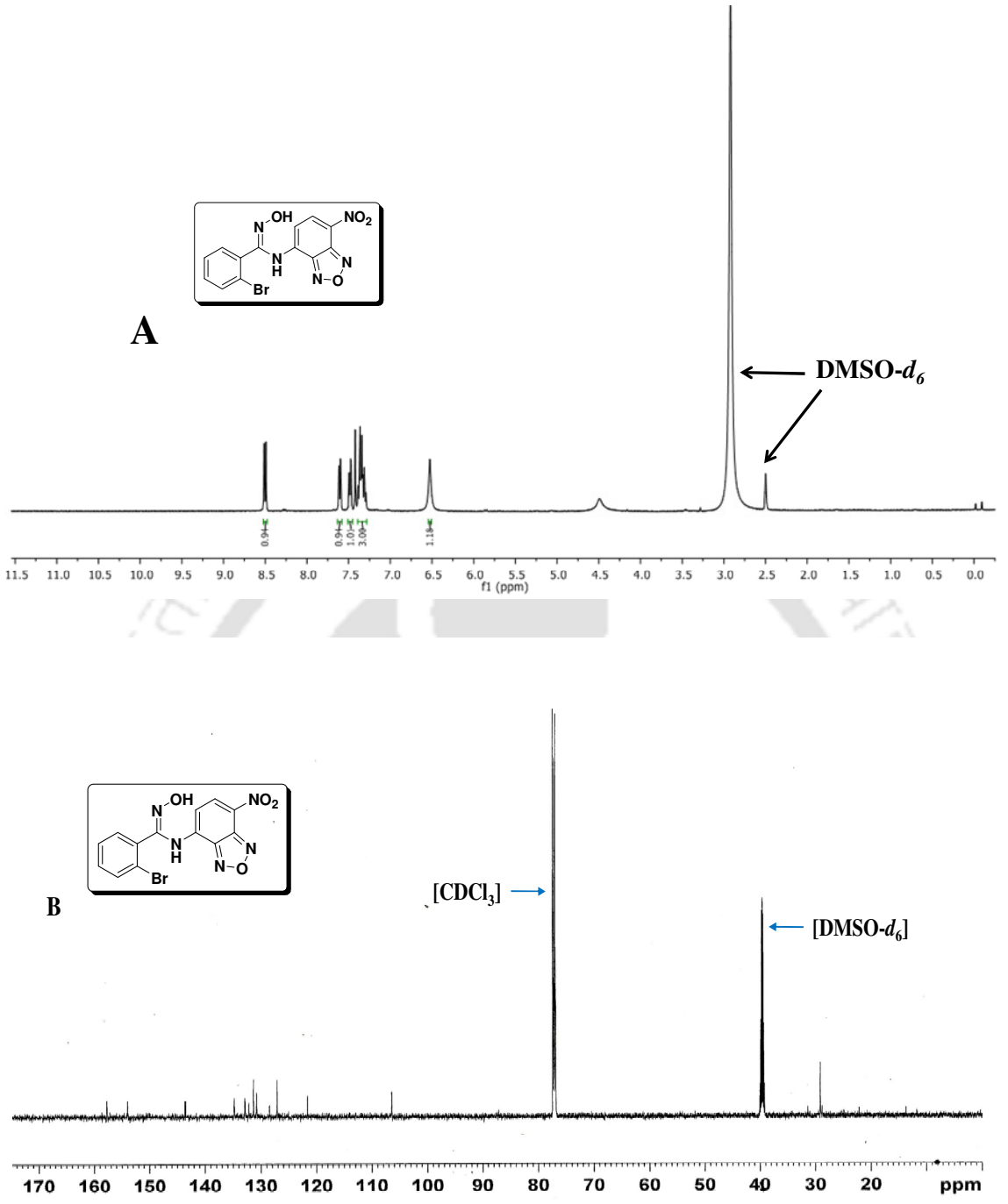

Figure 2.11.4. ^{1}H (**A**) NMR and ^{13}C (**B**) NMR of (Z)-2-bromo-N'-hydroxy-N-(7-nitrobenzo[c][1,2,5]oxadiazol-4-yl)benzimidamide (**1d**).

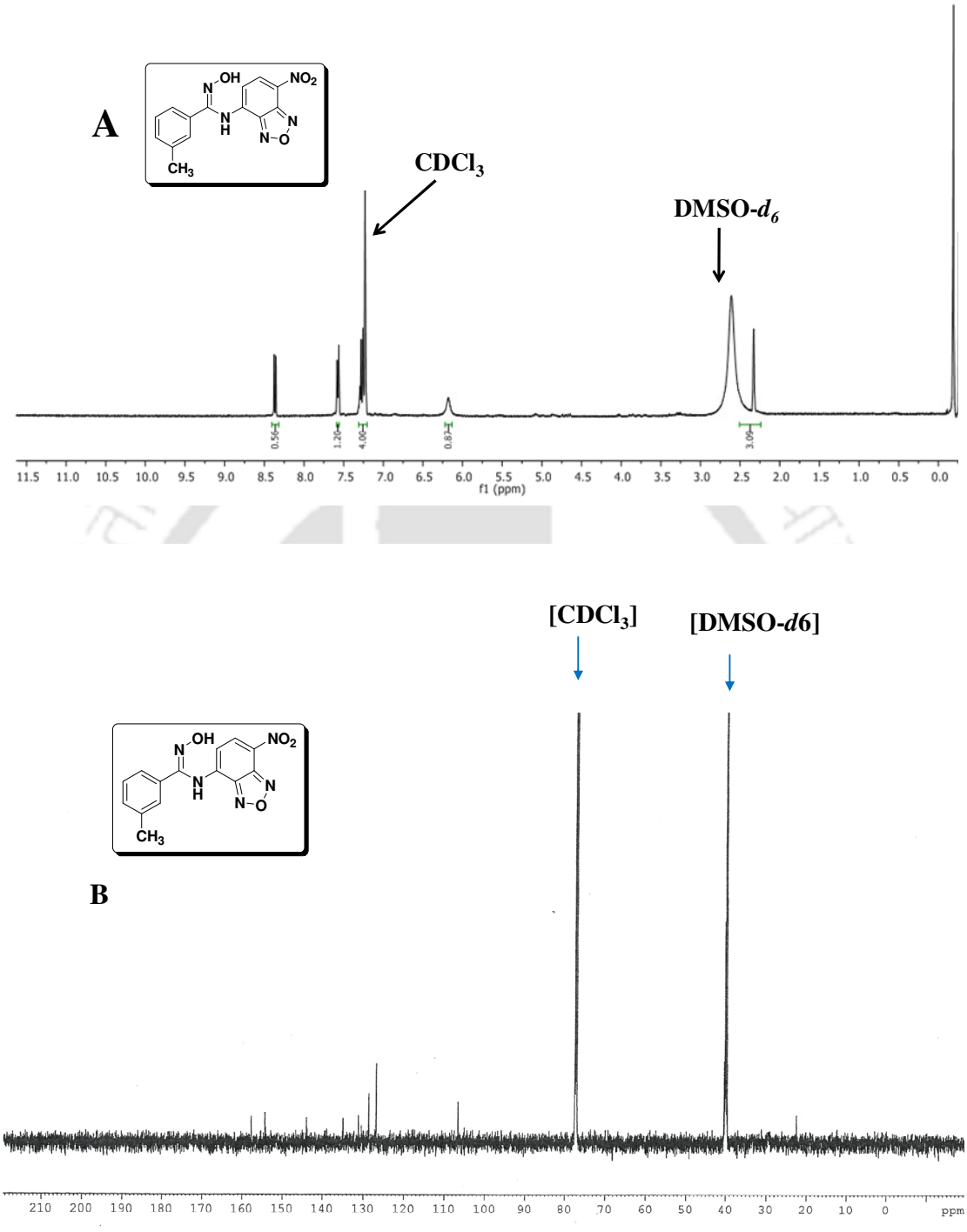

Figure 2.11.5. ^{1}H (**A**) NMR and ^{13}C (**B**) NMR of (Z)-N'-hydroxy-3-methyl-N-(7-nitrobenzo[c][1,2,5]oxadiazol-4-yl)benzimidamide (**1e**).

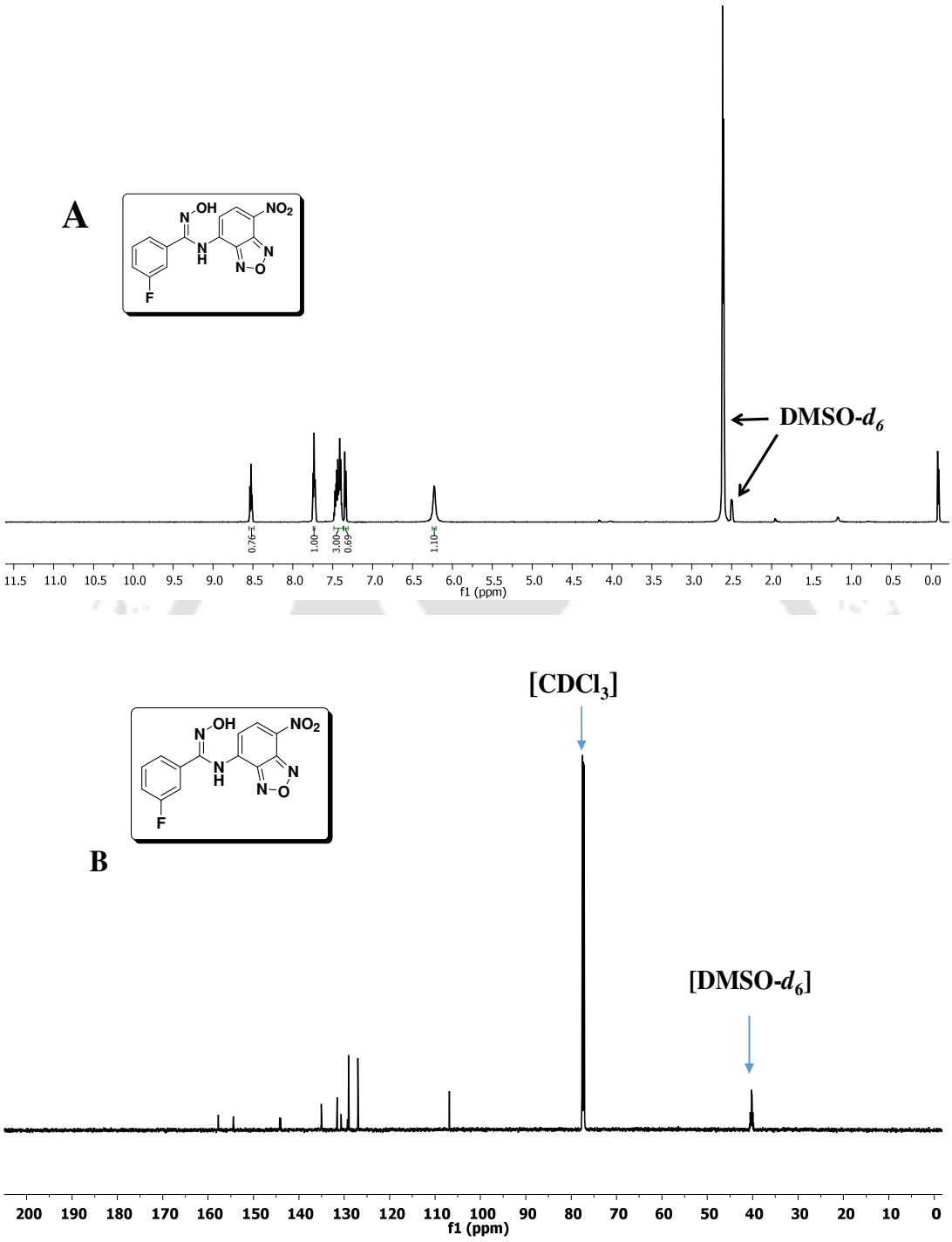

Figure 2.11.6. ^{1}H (**A**) NMR and ^{13}C (**B**) NMR of (Z)-3-fluoro-N'-hydroxy-N-(7-nitrobenzo[c][1,2,5]oxadiazol-4-yl)benzimidamide (**1f**).

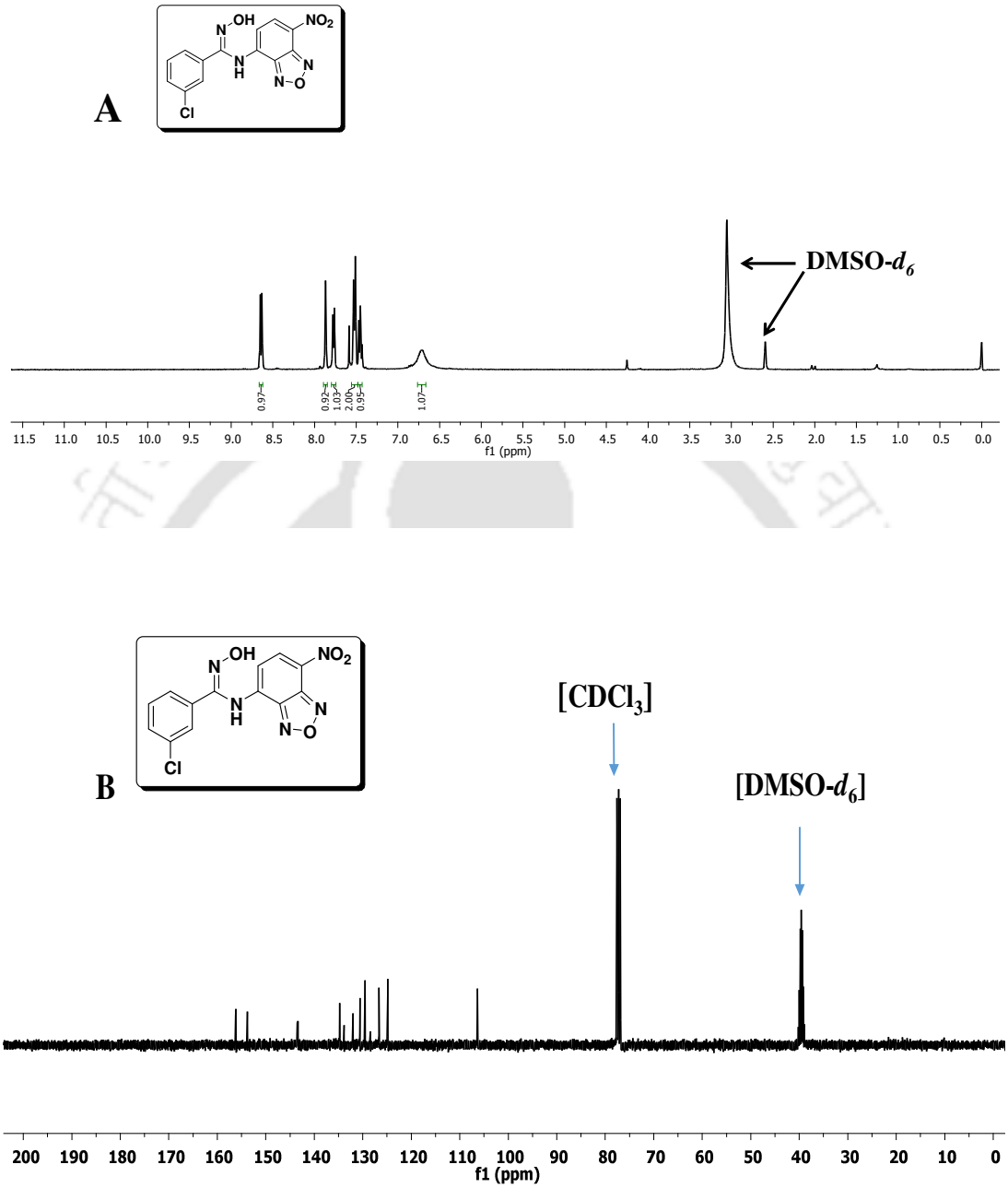

Figure 2.11.7. ^{1}H (**A**) NMR and ^{13}C (**B**) NMR of (Z)-3-chloro-N'-hydroxy-N-(7-nitrobenzo[c][1,2,5]oxadiazol-4-yl)benzimidamide (**1g**).

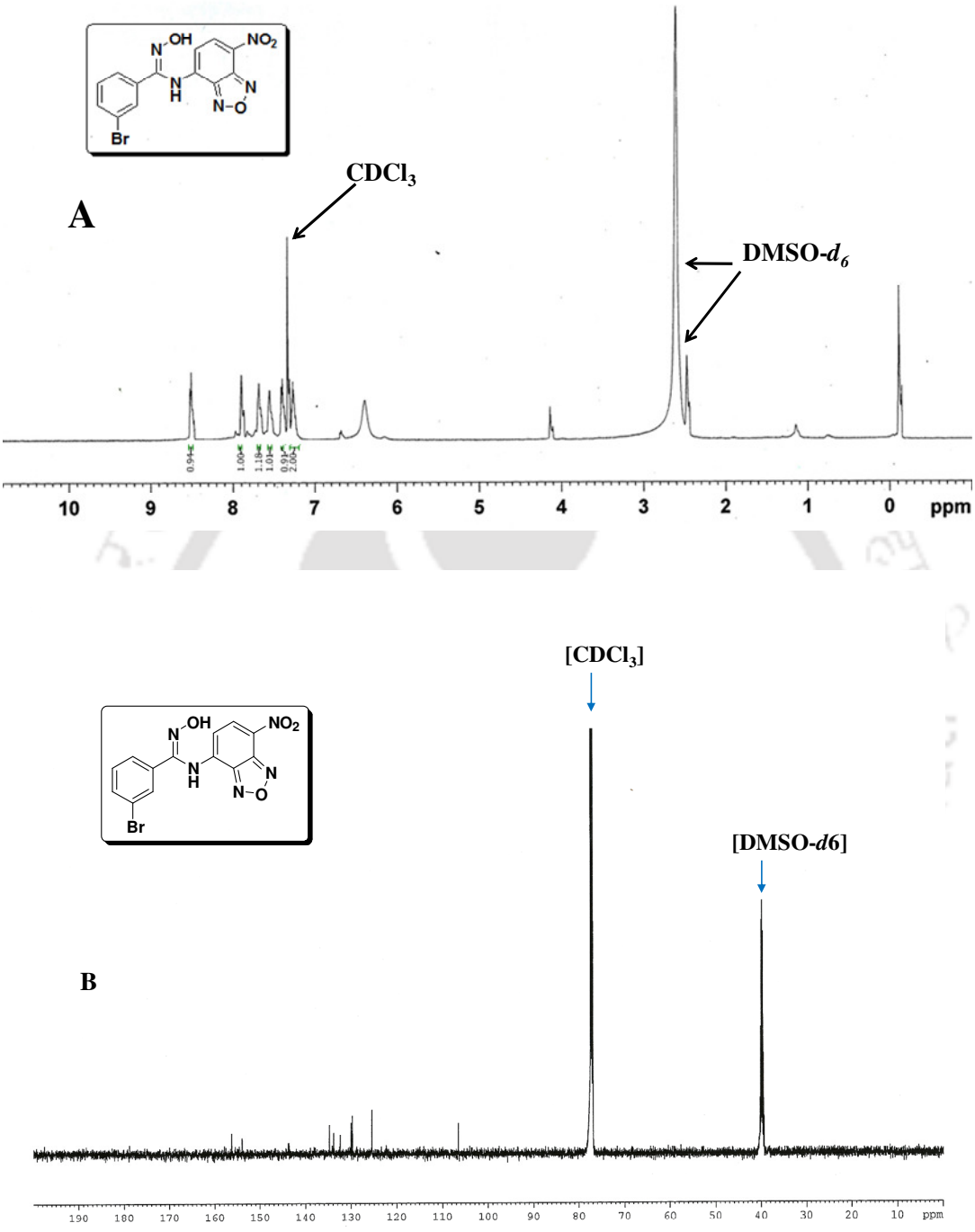

Figure 2.11.8. ^{1}H (**A**) NMR and ^{13}C (**B**) NMR of (Z)-3-bromo-N'-hydroxy-N-(7-nitrobenzo[c][1,2,5]oxadiazol-4-yl)benzimidamide (**1h**).

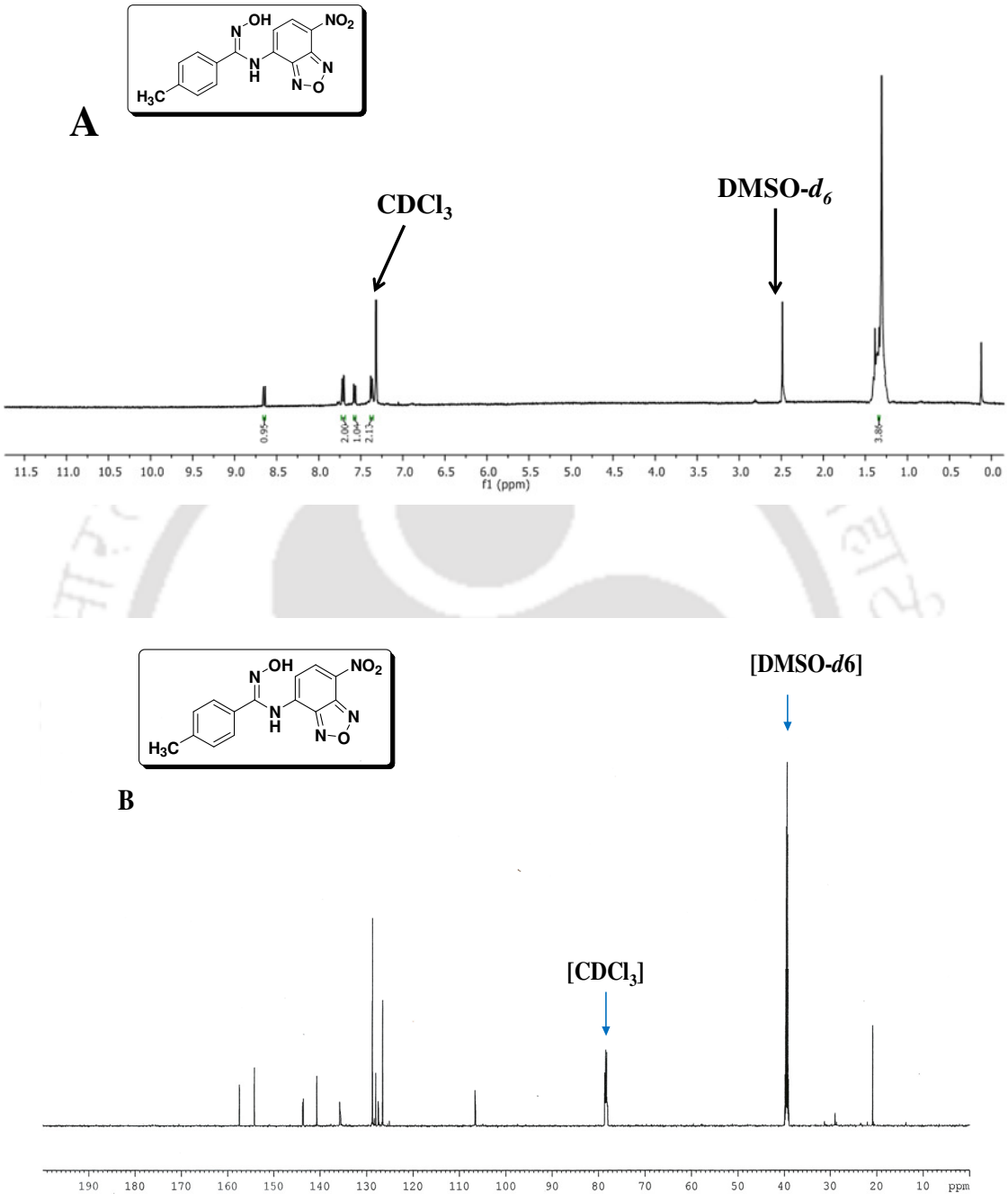

Figure 2.11.9. ^{1}H (**A**) NMR and ^{13}C (**B**) NMR of (Z)-N'-hydroxy-4-methyl-N-(7-nitrobenzo[c][1,2,5]oxadiazol-4-yl)benzimidamide (**1i**).

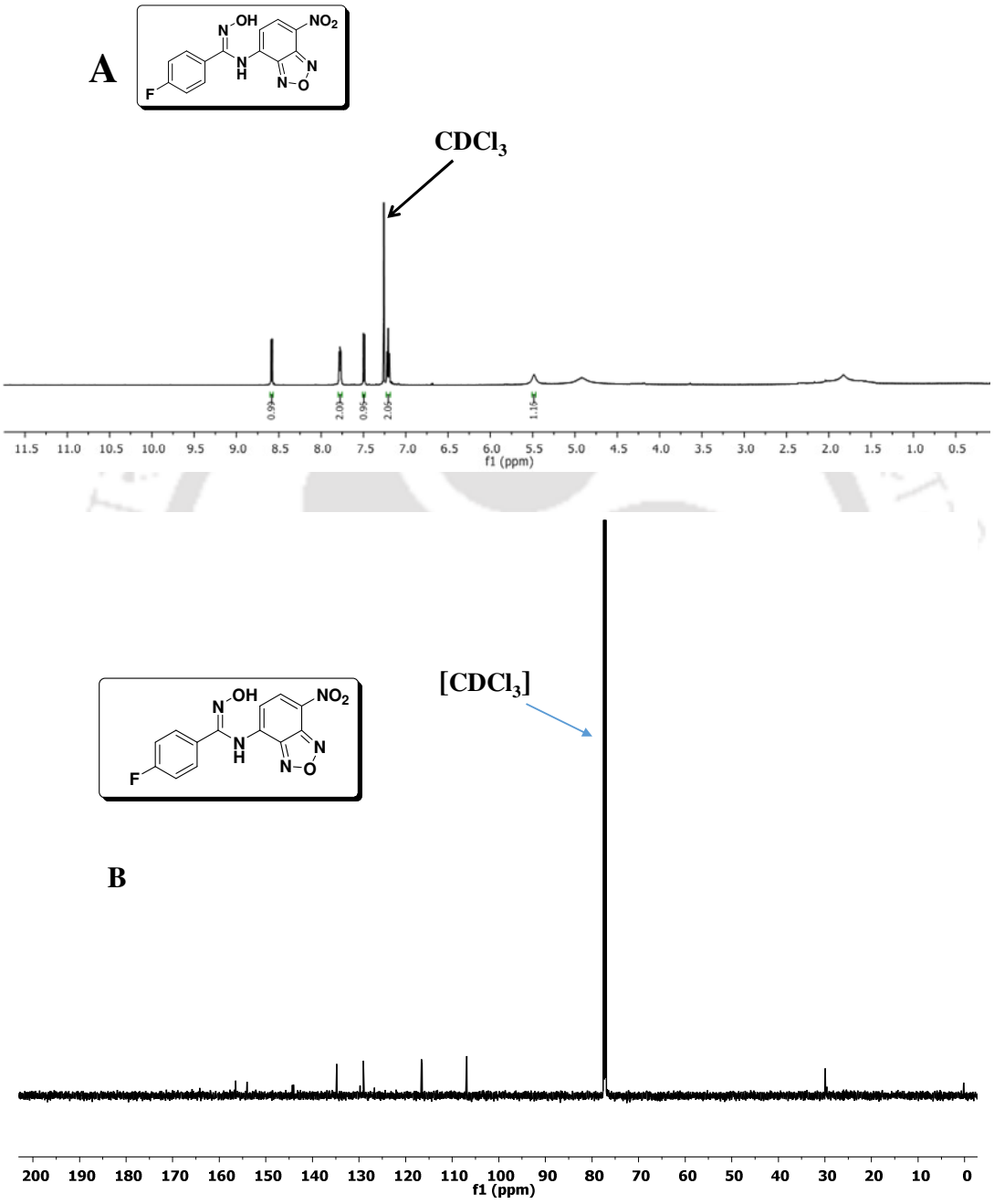

Figure 2.11.10. ^{1}H (**A**) NMR and ^{13}C (**B**) NMR of (Z)-4-fluoro-N'-hydroxy-N-(7-nitrobenzo[c][1,2,5]oxadiazol-4-yl)benzimidamide (**1j**).

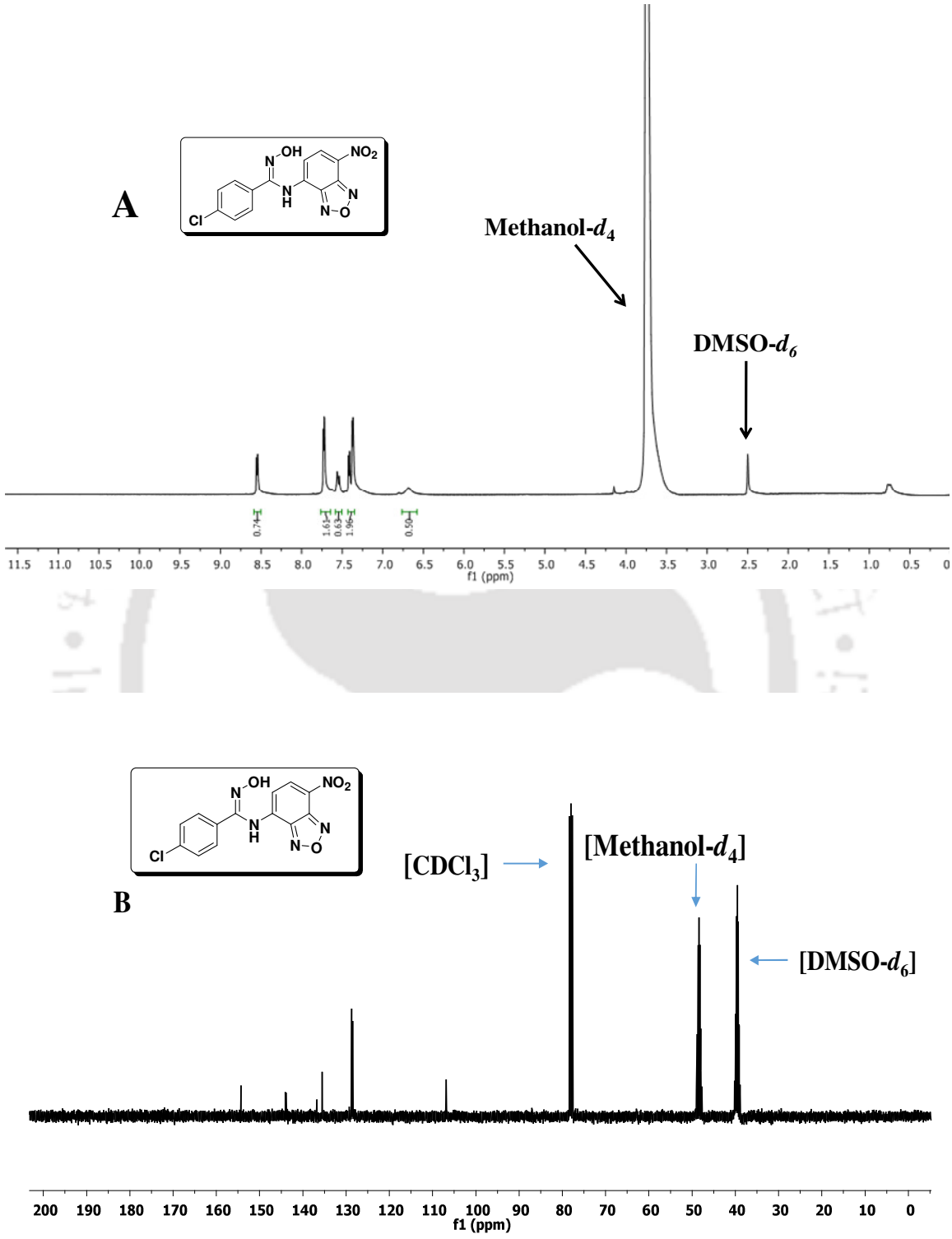

Figure 2.11.11. ^{1}H (**A**) NMR and ^{13}C (**B**) NMR of (Z)-4-chloro-N'-hydroxy-N-(7-nitrobenzo[c][1,2,5]oxadiazol-4-yl)benzimidamide (**1k**).

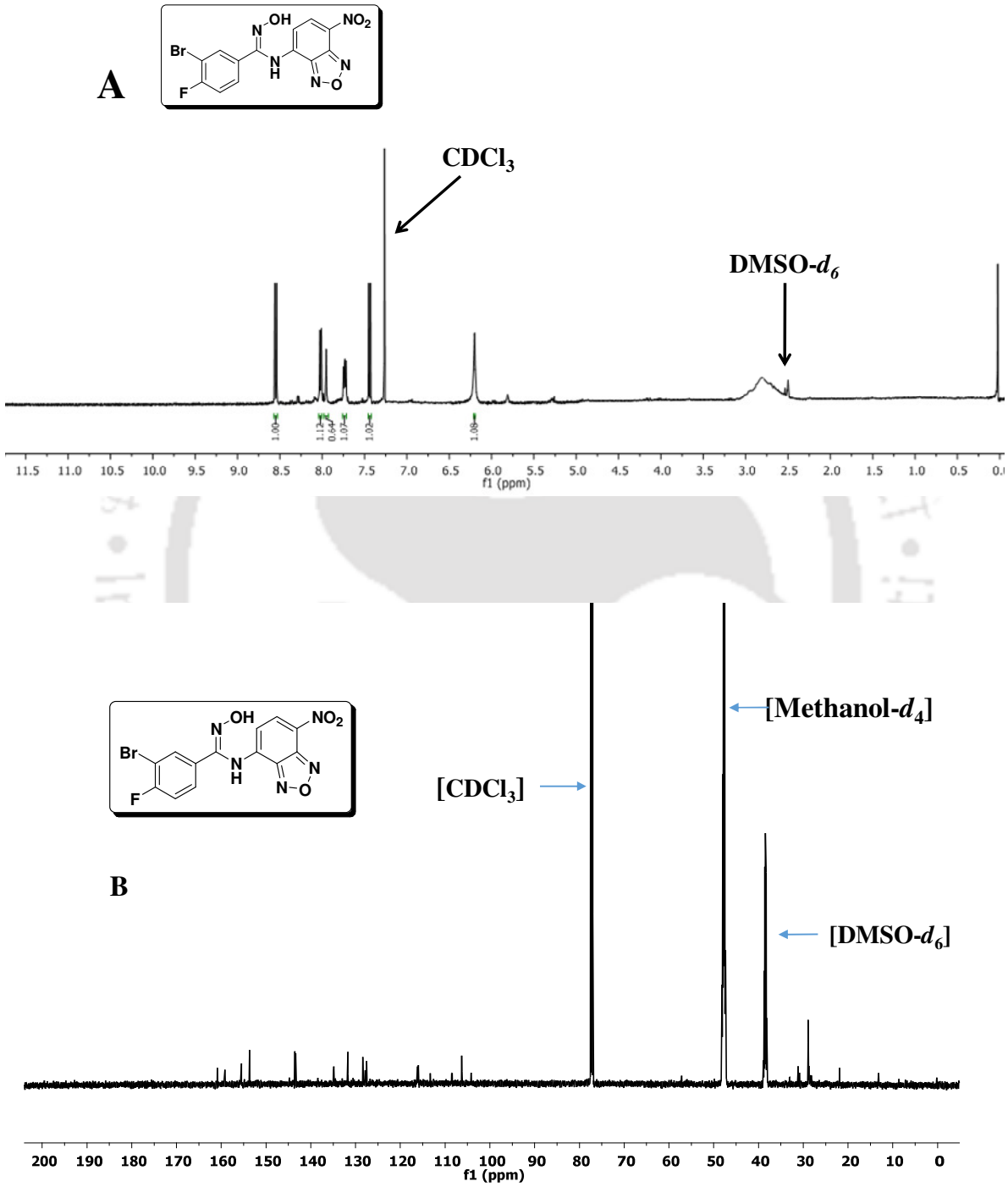

Figure 2.11.12. ^{1}H (**A**) NMR and ^{13}C (**B**) NMR of (Z)-3-bromo-4-fluoro-N'-hydroxy-N-(7-nitrobenzo[c][1,2,5]oxadiazol-4-yl)benzimidamide (**1n**)

CHAPTER 3

Development of 3-substituted Oxindoles as Mechanism-Based Inhibitors of Indoleamine 2,3-dioxygenase 1

IDO1 is considered as an important therapeutic target for the treatment of cancer, chronic infections and other diseases that are associated with immune suppression. Recent developments in understanding the catalytic mechanism of IDO1 enzyme revealed that conversion of *L*-Trp to *N*-formylkynurenine proceed through an epoxide intermediate state. In this chapter we have reported the synthesis of a series of 3-substituted oxindoles from *L*-Trp, tryptamine and isatin and study of their enzyme inhibitory properties both *in vivo* and *in vitro*.

Highlights

- Optimisation of C3-substition of the oxindole moiety directed to the identification of potent compounds showed IDO1 inhibition potencies in the low-micromolar range both in enzymatic as well as cellular assay.
- Compounds exhibited stronger selectivity for IDO1 enzyme over TDO enzyme.
- Ability of oxindole moiety of the substituted compounds to mimic the epoxide intermediate state of *L*-Trp.
- Structural simplicity and insignificant cytotoxicity of the potent compounds towards different model cancer cell lines makes them quite attractive for further investigation of IDO1 function and immunotherapeutic applications.

3.1. Background and focus of the present work

The heme-containing redox enzymes namely IDO1, catalyze the initial and rate-determining step for the transformation of *L*-Trp to *N*-formylkynurenine through kynurenine pathway.[1-3] Report suggests that the increased level of IDO1 expression is interrelated with reduced prognosis in different cancers, including pancreatic, ovarian and others along with various neurodegenerative disorder, age related cataract, HIV encephalitis and others.[1,4,5]

Cancer immunotherapy by targeting IDO1 enzyme is recognized as an exciting approach for drug development. IDO1 inhibition approach also showed augmented effect with chemotherapeutic and radio-therapeutic treatment of malignant tumors.[6,7] Currently, different inhibitors in combination with humanized antibodies are under clinical trials for the treatment of cancer and other diseases.[8,9] Tryptophan-based compound, *D*-1-MT is also under clinical trial as kynurenine pathway inhibitor, but its mechanism of action is uncertain. IDO1 is also a promising therapeutic target for the treatment of chronic viral infections and others that are related with the pathological immune suppression.[9,10]

There are several reported *L*-Trp or indole-based IDO1 inhibitors. *L*-1-MT is one of the commonly used IDO1 inhibitors but with moderate activity. Brassinin, tryptamine, carboline, keto-indoles, indol-2-yl ethanones, 1-methyl-tryptopha-ntirapazamine, isatin and other indole derivatives also showed poor to moderate IDO1 inhibitory activities.[11-17] Comprehensive mechanistic studies of IDO1 induced *L*-Trp catabolism revealed that the addition of ferrous heme-iron coordinated molecular oxygen to the C2-C3 double bond of the pyrrole ring is the prerequisite for the IDO1 supported oxidation of *L*-Trp. These studies also proposed the formation of epoxide intermediate state during the transformation of *L*-Trp to *N*-formylkynurenine by IDO1 enzyme.[18-20] Therefore, development of tryptophan or indole-based IDO1 inhibitors that can block this enzyme-dependent oxidative cleavage reaction of the pyrrole ring could construct mechanism-based effective IDO1 inhibitors (Figure 3.1).

In this chapter we have attempted to find effective IDO1 inhibitors, by synthesising 3-substituted oxindoles and exploring their enzyme inhibition potentials. Several of our tested oxindole-based compounds showed low-micromolar inhibitory activities against the purified IDO1 enzyme. Selected compounds also showed low-micromolar IDO enzyme inhibitory activity in MDA-MB-231 cells and almost no/negligible amount of cytoxicity. Additional studies showed that these potent compounds were more selective toward the IDO1 enzyme in comparison with the TDO

enzyme, making these oxindole derivatives of compelling value for further development as therapeutic agents targeting IDO1.

3.2. Origin of design

Earlier, *L*-Trp derivative 5-((1*H*-indol-3-yl)methyl)-3-methyl-2-thioxoimidazolidin-4-one, 1-methyltryptophantirapazamine and tryptamine derivatives were reported as moderate inhibitor of IDO1 enzyme.[4] However, no *L*-Trp analog showed low-micromolar activities, probably because of moderate affinity of *L*-Trp for IDO1 enzyme (K_d~ 300 μM).[4] Here we hypothesized that *L*-Trp derivative could mimic the transition/intermediate state of the enzymatic reaction thereby provide a better approach in developing potent IDO1 inhibitors. In this regard, we developed 3-substituted oxindoles derivatives of *L*-Trp and tryptamine. Recently, several oxindoles derivatives have been reported as potent inhibitors of TAK1 kinase and activators of AMP kinase.[21,22] Such type of derivatives also show antiglycation, antifungal, and other biological activities.[23,24] Oxindole based alkaloids from *Uncaria tomentosa* have been described to suppress *L*-Trp degradation.[25,26] Therefore, substituted oxindoles moiety can be considered as an useful tool in drug discovery.

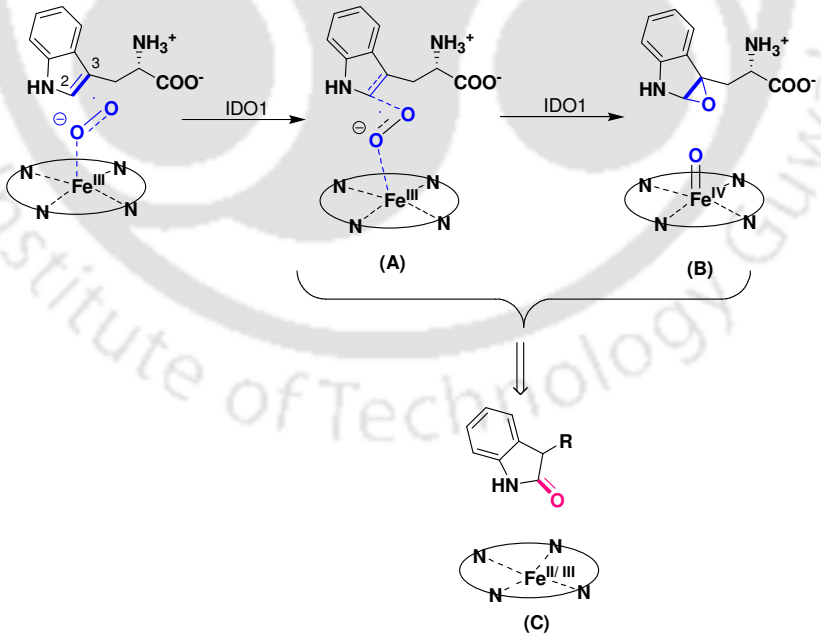

Figure 3.1. Proposed epoxide intermediate for the IDO1 induced metabolism of *L*-Trp (A, B) and its mimic (C).

A thorough understanding of the IDO1 assisted transformation of *L*-Trp to *N*-formylkynurenine recommend that the presence of carbonyl group at the C2-position of the pyrrole ring of *L*-Trp could perturb further radical addition of Fe(III)-superoxide intermediate (Figure 3.1).[18] Consequently, oxindole derivatives can hinder the IDO1 enzyme-dependent oxidative cleavage reaction of the pyrrole ring of *L*-Trp. Therefore, we hypothesized that oxindoles based derivatives can be used as potent inhibitor of IDO1 enzyme (Figure 3.1).

3.3. Synthesis

Initially, we synthesized oxindole derivatives **2** and **3** of *L*-Trp and tryptamine, respectively by treating with the oxidizing mixture of DMSO/HCl in AcOH solution.[27] To explore the role of hydrophobic substitution of the amine groups, oxindoles derivatives of *L*-Trp and tryptamine **4**, **5**, **6**, **7**, and **8** were synthesized from *N*-Cbz, *N*-Boc, *N*-benzoyl and *N*-acetyl protected *L*-Trp and tryptamine, respectively under the similar experimental conditions. To understand the importance of free acid group compounds, **9** and **10** were synthesized from only *C*-methyl and both *C*-benzyl and *N*-Cbz protected *L*-Trp (Scheme 3.1).[27] For the same purpose, 2-amino-3-(2-oxoindolin-3-yl) propanamide (**11**) was also synthesized from compound **4** according to the reported procedures.[28,29] To explore the role of C3-substitution of the oxindoles moiety at inhibiting the IDO1 enzyme activity, we also synthesized hydrazone (compound **12**-**17**), phenylimino (**18**-**20**) and alkene-2-indolinone (**21** and **22**) derivatives of isatin.

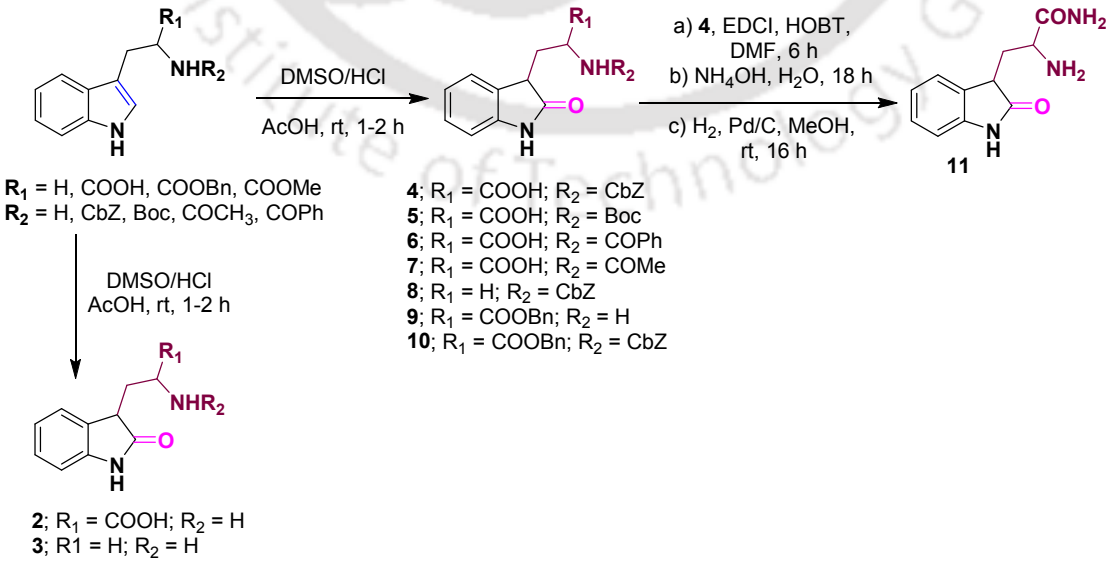

Scheme 3.1. Synthesis of oxindoles derivatives from *L*-Trp and tryptamine.

C3-substituted 3-hydroxy-3-alkyl derivatives of isatin and 5-chloroisatin were synthesized according to the reported procedure to explore the role substitution in the oxindole ring on IDO1 enzyme activity.[30] Condensation of substituted hydrazine or aniline with isatin in refluxing ethanol (in the presence of catalytic amount of AcOH) directly yielded hydrazones and phenylimino derivatives (Scheme 3.2).[30] The alkene-oxindole derivatives (**21** and **22**) were synthesized from isatin in the presence of either or piperidine acetate in water or piperidine in EtOH (Scheme 3.2).[31]

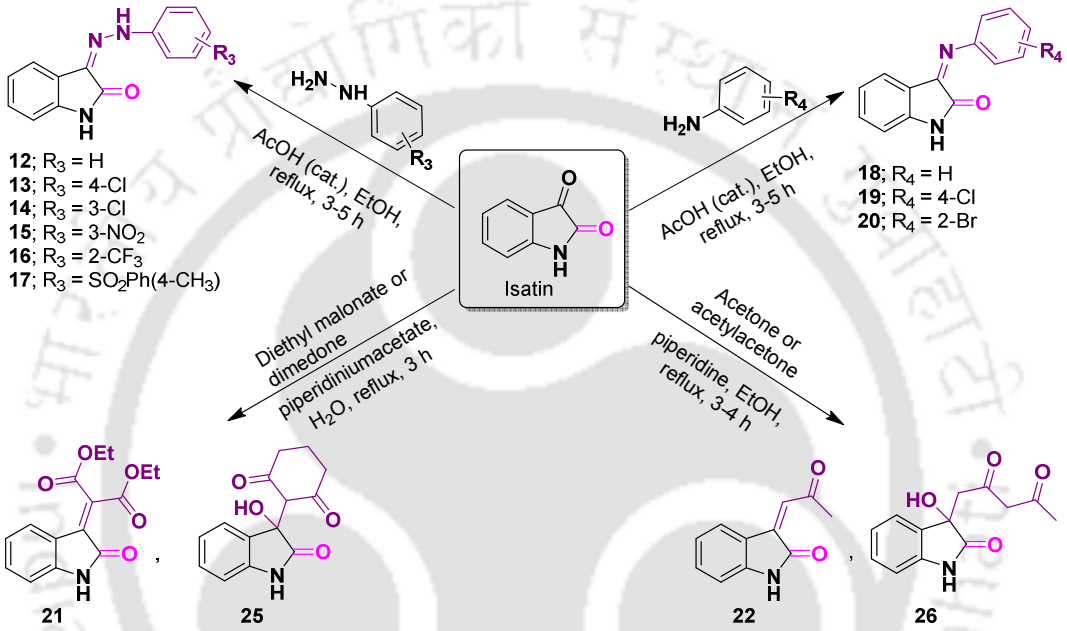

Scheme 3.2. Synthesis of hydrazone, phenylimino and alkene derivatives of isatin.

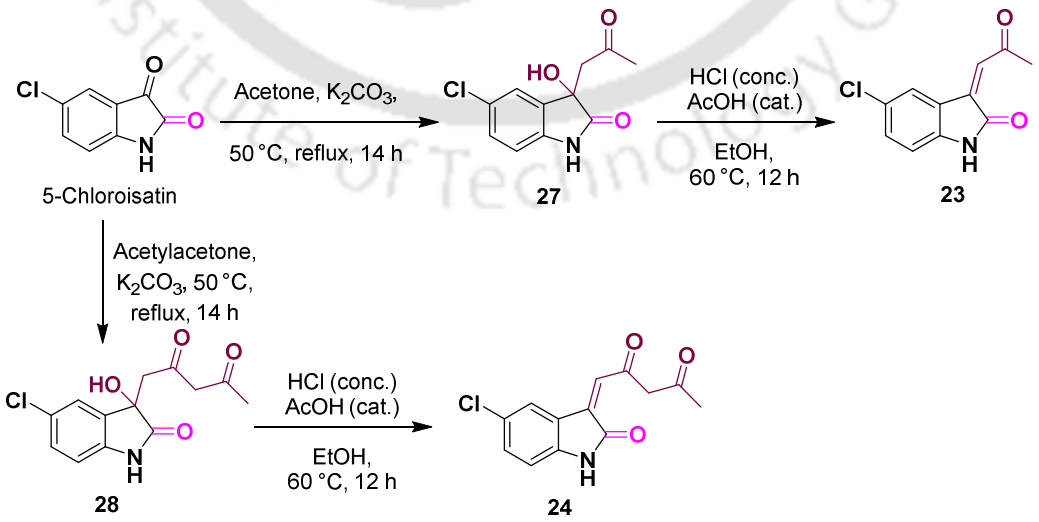

Scheme 3.3. Synthesis of alkene and 3-hydroxy-3-alkyl derivatives of 5-chloroisatin.

The 3-hydroxy-3-alkyl compounds (**25** and **26**) were synthesized from isatin in the presence of piperidine acetate in water and piperidine in EtOH, respectively (Scheme 3.2).[31] Condensation of 5-chloroisatin with acetone first yielded 3- hydroxy-3-alkyl compound **26** in the presence of K_2CO_3. Dehydration of compound **27** in the presence of concentrated HCl and catalytic amount of AcOH in ethanol yielded compound **23** (Scheme 3.3). Condensation of 5-chloroisatin with acetylacetone in the presence of K_2CO_3 yielded both alkene and 3-hydroxy-3-alkyl derivatives **24** and **28**, respectively (Scheme 3.3).[32] Hence, a range of substituted oxindole derivatives was synthesized from *L*-Trp, tryptamine, isatin and 5-chloroisatin.

3.4. Inhibitory activities of the oxindole derivatives against purified IDO1 enzyme

The inhibitory activity of the synthesized oxindole derivatives was first examined using standard spectrophotometric method monitoring the differences in absorbance values of the product generated from kynurenine and Ehrlich's reagent (at 480 nm) in the acidic medium.[1,8,33] Absorption spectra of the pure compounds (100 nM to 1 mM) showed no or little interference with this enzyme activity assay. The calculated K_m and k_{cat} values of the enzyme with *L*-Trp were 47.8 ± 2.5 μM and 3.7 ± 0.1 Sec^{-1}, respectively.[8] To improve the efficacy of the oxindole lead, we investigated two general modifications of the oxindole structure: (1) modification of the α-amino and/or α-carboxyl groups of *L*-Trp and tryptamine structure and (2) C3-substitution of the isatin.

3.4.1. Modification of the α-amino and/or α-carboxyl groups of *L*-Trp and tryptamine structure

We have explored the role of α-amino and/or α-carboxyl groups of oxindolealanine and 3-(2-aminoethyl) indolin-2-one on IDO1 enzyme activity (Table 3.1). The IC_{50} values of the compound **2**-**11** suggest that substitution at the free amino-group and the presence of free carboxyl-group (**4**-**7**) plays an important role in their IDO1 inhibitory activity. The IC_{50} values of compounds **7-10** further support these findings. The stronger IDO1 inhibitory activity of compound, **7** (IC_{50} = 0.62 μM) could be due the presence of free α-carboxyl group and substituted α-amino group with lesser bulkiness. The bulkiness of substituent at the α-amino group could also play a crucial role in proper fitting of the compounds within the active site of the IDO1 enzyme. Overall, oxindole moiety and its C3-substitutions play an important role in their IDO1 inhibitory activity activity. Under the experimental conditions, the IC_{50} value of *L*-1-MT was 385 μM, which is in

accordance with the reported values.[34,35] Interestingly, oxindolealanine (**2**) has been shown to be one of the oxidized products of *L*-Trp.[5] Whether feedback inhibition of IDO1 enzyme by compound **2** is physiologically relevant or it plays any important role in *L*-Trp metabolism remains to be investigated.

Table 3.1. Inhibitory activity of the *L*-Trp and tryptamine-based oxindole derivatives against purified human IDO1 enzyme.

Compound	IDO1 inhibition IC_{50} (μM)[a]	Compound	IDO1 inhibition IC_{50} (μM)[a]
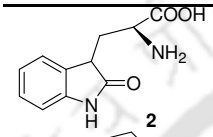 **2**	3.39 ± 0.29	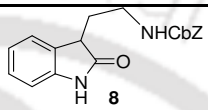 **8**	2.31 ± 0.21
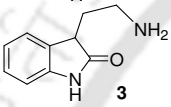 **3**	3.97 ± 0.39	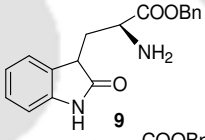 **9**	13.59 ± 0.19
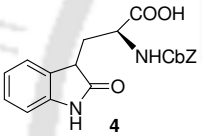 **4**	1.28 ± 0.28	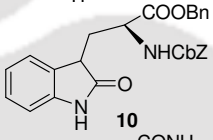 **10**	2.25 ± 0.23
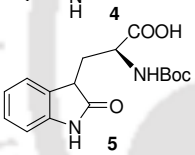 **5**	1.95 ± 0.32	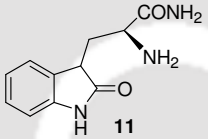 **11**	8.33 ± 0.21
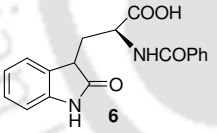 **6**	1.58 ± 0.27	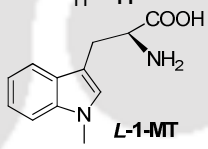 ***L*-1-MT**	385.41 ± 35.31
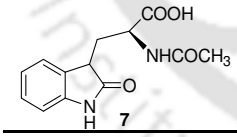 **7**	0.62 ± 0.11		

[a]IC_{50} values are the mean of five independent assays.

3.4.2. C3-substitution of the isatin

Our oxindolealanine and 3-(2-aminoethyl)indolin-2-one derivatives showed that 2-indolinone moiety is very important for their IDO1 inhibition activity. However, we presume that rotation at the C3-position could be one of the reasons for its moderate inhibitory activity. Therefore, for further optimization of its inhibition efficacy, we used a series of oxindole derivatives with restricted rotation at the C3-position. However, tested hydrazones, phenylindolinone and alkene derivatives of isatin showed moderate IDO1 inhibitory activities. In terms of structure-activity relationships with the hydrazones, it

appears that the presence of 4-chloro substitution (**13**) is favorable for the inhibitory activity with IC_{50} values of 0.63 μM (Table 3.2). Whereas, 2-bromo substituted phenylimino derivative of isatin **20** showed stronger IDO1 inhibitory activity (IC_{50} = 1.24 μM) among the tested phenylimino compounds (Table 3.2).

Table 3.2. Inhibitory activity of the isatin-based oxindole derivatives against purified human IDO1 enzyme.

Compound	IDO1 inhibition IC_{50} (μM)[a]	Compound	IDO1 inhibition IC_{50} (μM)[a]
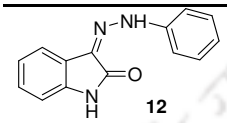 **12**	1.95 ± 0.29	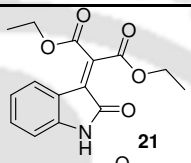 **21**	0.93 ± 0.06
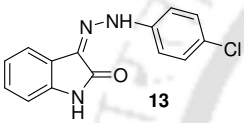 **13**	0.63 ± 0.15	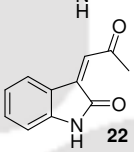 **22**	1.69 ± 0.13
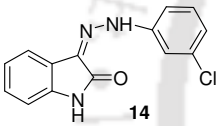 **14**	1.51 ± 0.15	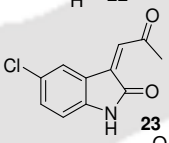 **23**	0.36 ± 0.08
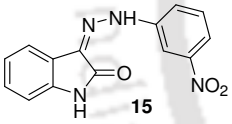 **15**	3.74 ± 0.32	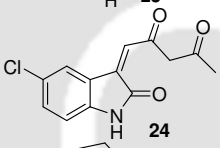 **24**	0.19 ± 0.07
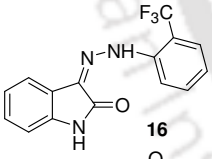 **16**	1.58 ± 0.12	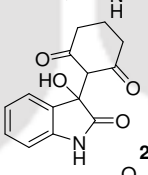 **25**	4.73 ± 0.61
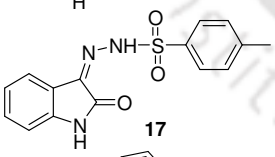 **17**	1.78 ± 0.39	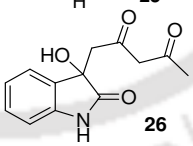 **26**	0.45 ± 0.09
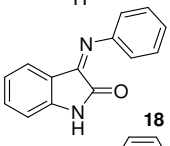 **18**	2.85 ± 0.42	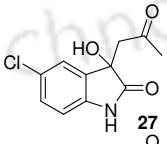 **27**	1.97 ± 0.41
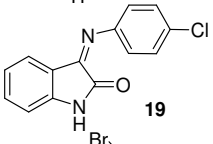 **19**	2.56 ± 0.22	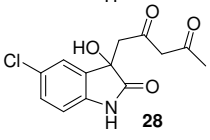 **28**	0.89 ± 0.07
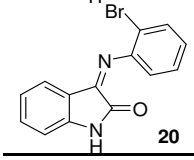 **20**	1.24 ± 0.38		

[a]IC_{50} values are the mean of five independent assays.

These results suggest that halogen substitution on the aryl ring of the hydrazone and phenylimino derivatives of oxindole also plays an important role on their IDO1 inhibition activity. The effect of halogen substitutions on the oxindole ring was also explored for probable interactions with the hydrophobic residues present within the pocket 'A' of IDO1 enzyme.

Several research groups had successfully taken advantage of these hydrophobic interactions in the optimization of the IDO1 inhibition efficacies.[4,8,9] The alkene oxindole derivatives of isatin and 5-chloroisatin showed moderate to strong inhibitory activity (IC_{50} values 0.19 to 1.69 μM). Compound **24** showed the considerably higher IDO1 enzyme inhibition potency (IC_{50} = 0.19 μM) among the tested compounds. We tested 3-hydroy-3-alkyled derivatives of isatin and 5-chloroisatin for further improvement of the efficacy of the oxindoles. Our activity assay showed that 3-hydroxy-3-alkyl-oxindole derivatives of isatin and 5-chloroisatin had moderate IDO1 inhibition activities (IC_{50} values 0.45 μM to 4.73 μM) among the tested oxindoles.

Therefore, both 5-chloro and suitable substitutions at the C3-position of the oxindole ring had considerable effect on IDO1 enzyme inhibition activity. However, 3-hydroxy-3-alkyl derivatives do not substantial effect of IDO1 inhibition efficacy. Recently 3-hydroxy-3-alkyl isatin derivatives were developed as comparable inhibitors for both IDO1 and TDO enzymes.[16] This also endorses the importance of C3-substituted oxindole moiety in designing inhibitors for these enzymes.

The inhibition efficacies of these oxindole derivatives were performed by spectrophotometric method. Therefore, additional IDO1 activity assay for selected compounds was performed by HPLC analysis according to the reported procedures.[8] The amount of *L*-Trp catabolism by IDO1 enzyme in the absence or presence of the potent inhibitors was monitored by HPLC analyses after quenching the reaction by acidification and hydrolyzing *N*-formylkynurenine to kynurenine (Table 3.3).

A standard curve was generated using pure kynurenine and then amount of kynurenine formation from *L*-Trp in the absence or presence of compounds under enzymatic reaction conditions was measured to investigate their inhibitory efficacies. The calculated concentrations of the tested compounds required to inhibit the kynurenine generation from *L*-Trp under similar experimental conditions were in the low-micromolar range and in accordance with the inhibition, activities calculated using *p*DMAB-method.[8] The differences in IC_{50} values of the compounds between the spectroscopic and HPLC-

based methods could be due to the methylene blue-ascorbate regeneration system, which preserves IDO1 in its active state (Fe^{2+}).

The IC_{50} values from HPLC-based assay also revealed that the presence of carbonyl group at the C2-position of the 5-member pyrrole ring is beneficial for the inhibitory activity of the tested compounds, whereas appropriate substitution at the C3-position of the oxindole ring assists the compounds to interact strongly with the IDO1 enzyme.

Table 3.3. HPLC based IDO1 inhibition assays of the selected compounds.

Compound	IDO1 inhibition (IC_{50} μM)[a]
***L*-1-MT**[b]	147.08 ± 13.67
2	3.86 ± 0.31
4	1.51 ± 0.19
7	0.71 ± 0.09
13	0.99 ± 0.17
14	1.88 ± 0.12
16	1.60 ± 0.26
17	2.28 ± 0.19
20	0.87 ± 0.17
21	0.69 ± 0.15
23	0.48 ± 0.10
24	0.30 ± 0.10
26	0.54 ± 0.09

[a]IC_{50} values calculated by HPLC method (are the mean of three independent assays).

[b]Reported compound.

LCMS chromatogram of the selected compounds under the experimental conditions of IDO1 inhibition assay and in different buffers revealed their stability. However, further oxidation of compound **2** into *N*-formylkynurenine under the enzymatic assay conditions cannot be confirmed because of direct formation of *N*-formylkynurenine (m/z = 236.0797) from substrate, *L*-Trp.

3.5. Spectroscopic based analysis of interaction of the selected oxindole derivatives with IDO1

The UV-absorption properties of the porphyrin-ring are highly sensitive to the changes in the polarity of the heme-surroundings and useful in understanding the ligand/substrate

binding ability to IDO1 enzyme [36-39] The UV-absorption spectra of ferric-IDO1 and deoxy-ferrous-IDO1 were recorded in the absence and presence of compounds, **4**, **7**, **23**, and **26** (Figure 3.2A and 3.2B). The absorption spectrum of only ferric-IDO1 showed a Soret peak at 404 nm, which is in accordance with the reported results.[9,37-40] In the presence of compounds, this Soret peak showed a slight blue shift with increase in intensity, under the similar experimental condition. Compound **26** showed a maximum blue shift of 9 nm, indicating its strong binding to the ferric-IDO1 enzyme, possibly through the carbonyl-oxygen of the oxindole-ring (Figure 3.2A). The blue shift of the Soret peak could be associated with the presence of an electron-withdrawing group close to the porphyrin-ring, which is also in accordance with their mode of interaction. Figure 3.2B showed that in the absence of any inhibitor the deoxy-ferrous-IDO1 enzyme exhibit Soret and Q-band at 421 nm and 558 nm.[9,37,38] However, in the presence of inhibitors the Soret band shifted to 419-425 nm and appearance of new Q bands around 527/558 nm (Figure 3.2B). This indicates their probable binding with the Fe^{2+}-IDO1 enzyme possibly via carbonyl-oxygen of the oxindole-ring.

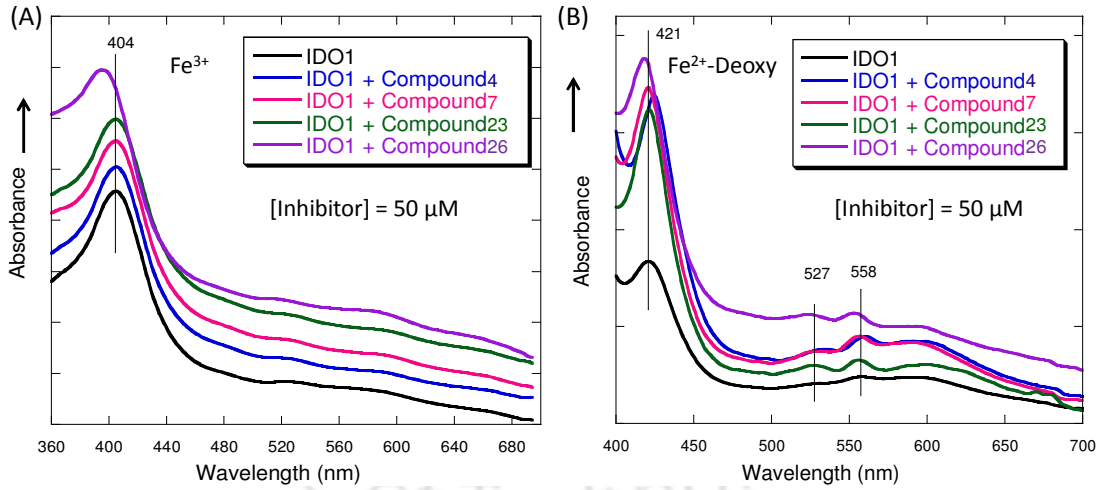

Figure 3.2. Absorption spectra of ferric-IDO1 (**A**) and deoxy-ferrous-IDO1 (**B**) enzyme in the absence and presence of the 50 µM compounds in 100 mM potassium phosphate buffer at pH 6.5. Y-axis is not same for both the spectra. IDO1 enzyme concentration = 5 µM. Ferrous-deoxy reaction environment was generated by adding $Na_2S_2O_4$ under N_2 atmosphere.

The absorption spectra of only compounds did not show any peak in this region (spectra not shown). Although further studies are required to prove the coordination of the oxindole derivatives to heme-group of IDO1, but the results strongly support the proposed mimic of the epoxide intermediate state for the *L*-Trp oxidation by these oxindoles.

3.6. Cellular IDO1 inhibitory activities of oxindoles

To explore the therapeutic potential of these oxindole derivatives, six of the most potent compounds were tested for the IDO1 cellular activity in MDA-MB-231 breast cancer cells. It is well documented that interferon gamma (IFN-γ) appreciably induce the expression of native human IDO1 enzyme from its mRNA in MDA-MB-231 cells.[8,41] The cellular inhibition activities of the compounds are in accordance with that of *in vitro* data against purified IDO1 enzyme. The calculated IC_{50} values of the compounds are within 0.33-1.26 μM range in MDA-MB-231 cells (Table 3.4). Control compound, *L*-1-MT showed IC_{50} values of 120 μM under the similar experimental conditions.[42] The differences in IC_{50} values of the compounds between the enzymatic assay against purified IDO1 and cellular assays could be due to the difficulty in controlling IDO1 redox activity, which maintains IDO1 in active state (Fe^{2+}) and/or environmental effect. Overall, a good correlation between these assays corroborates the IDO1 inhibition potencies of these oxindoles.

Table 3.4. IDO1 enzyme inhibitory activity of the selected compounds in MDA-MB-231 cells.

Compound	IDO1 inhibition in MDA-MB-231 cell[a] IC_{50} (μM)[b]
4	1.26 ± 0.17
7	0.48 ± 0.12
13	0.42 ± 0.14
23	0.46 ± 0.11
24	0.33 ± 0.09
26	0.49 ± 0.19
***L*-1-MT[c]**	119.66 ± 11.31

[a]IDO1 protein expression in MDA-MB-231cells was induced by human IFN-γ (20ng/mL).

[b]IC_{50} values are the mean of three independent assays.

[c]Reported compound.

MTT assay of the compounds in MDA-MB-231 (breast cancer), A549 (lung cancer), HeLa (cervical cancer) and J774A.1 (macrophage) cells (concentrations of IC_{50} and 2 × IC_{50} values from the enzymatic assay) also revealed no/negligible level of toxicity of the compounds under the tested conditions (Figure 3.3-3.5).

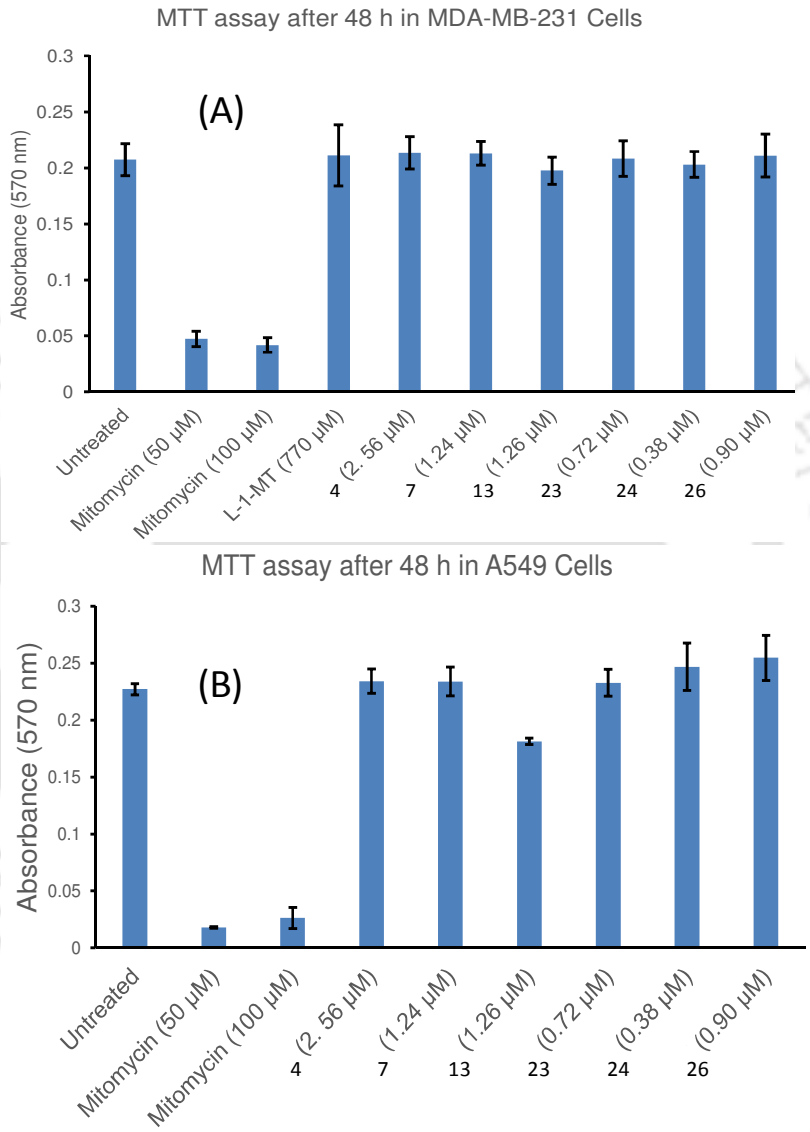

Figure 3.3. Effect of the selected oxindoles on the viability of MDA-MB-231 cells **(A)** and A549 cells **(B)** respectively. MDA-MB-231 and A549 cells were treated with the indicated concentrations of the compounds for 48 h. Absorbances of different amounts of formazan were plotted against the mentioned concentrations of the compounds. Data are averages with standard deviation (error bars) from three independent experiments. Mentioned concentrations of the oxindoles are the 2 × IC_{50} values of the compounds obtained from activity assay against purified enzyme.

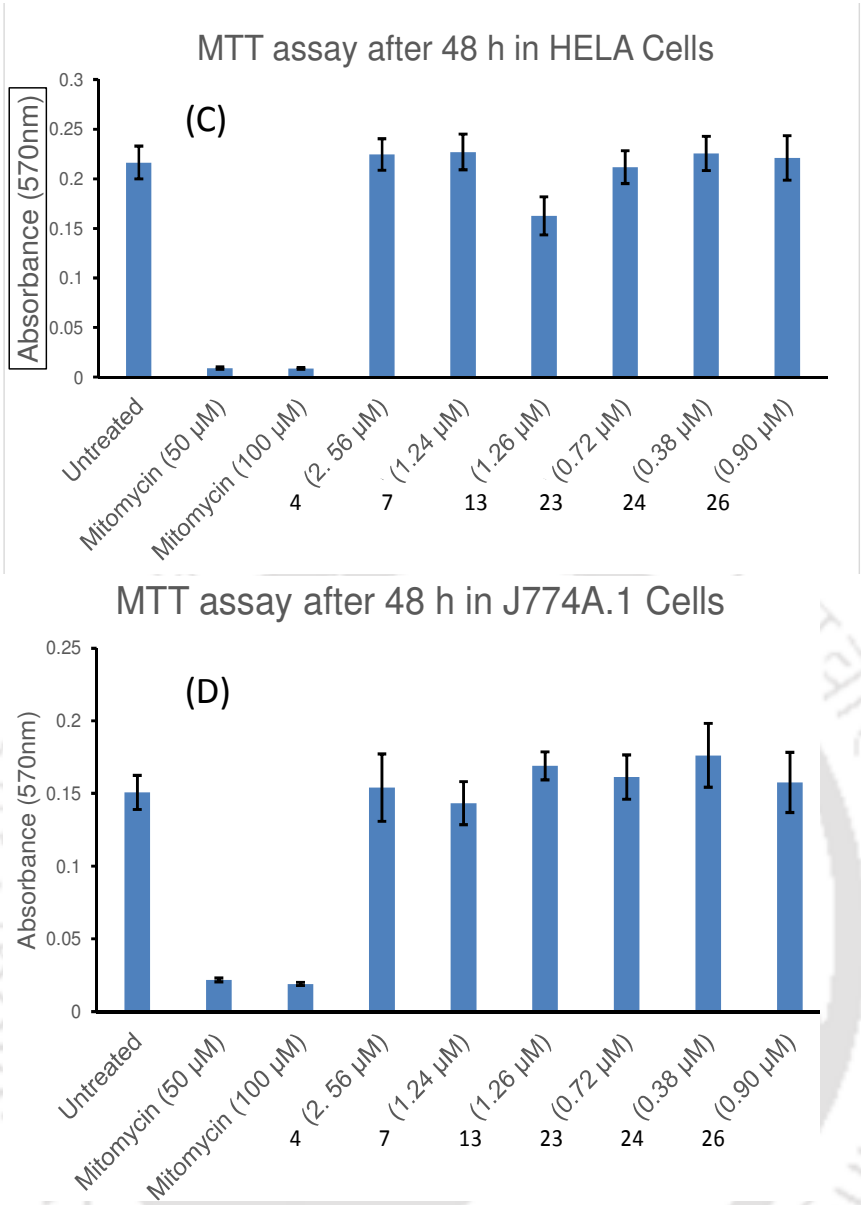

Figure 3.4. Effect of the selected oxindoles on the viability of Hela cells **(C)** and J774A1 cells **(D)** respectively. Hela cells and J774A1 cells were treated with the indicated concentrations of the compounds for 48 h. Absorbances of different amounts of formazan were plotted against the mentioned concentrations of the compounds. Data are averages with standard deviation (error bars) from three independent experiments. Mentioned concentrations of the oxindoles are the 2 × IC_{50} values of the compounds obtained from activity assay against purified enzyme.

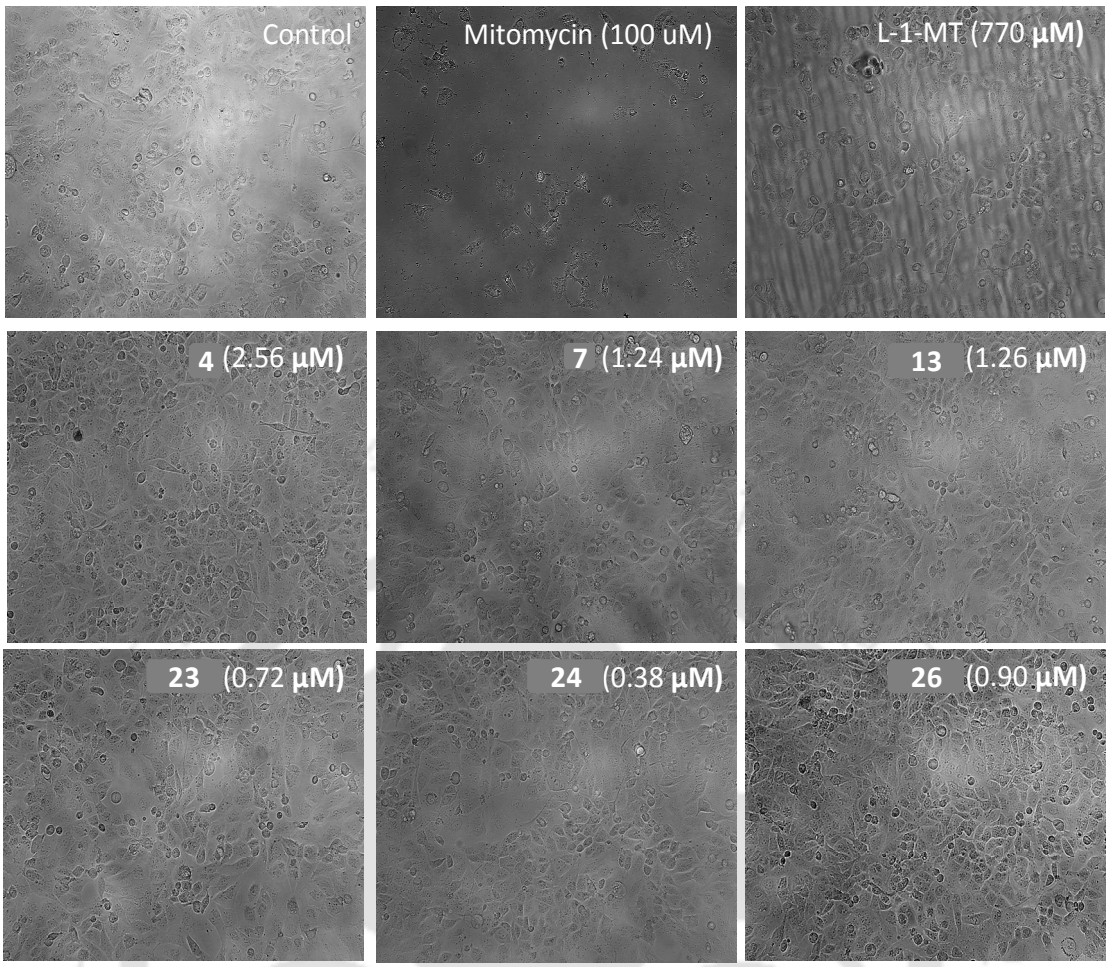

Figure 3.5. Effect of the selected oxindoles on the morphological changes of MDA-MB-231 cells. MDA-MB-231 cells were treated with the indicated concentrations of the compounds for 48 h and morphological changes were observed using Cytell Imaging System. Images were collected at 10x magnification. Images are representative of three independent experiments. Mentioned concentrations of the compounds are the 2 × IC_{50} values of the compounds obtained from activity assay against purified enzyme.

3.7. Mode of IDO1 enzyme inhibition by the potent oxindoles

To understand the mode of IDO1 inhibition by the compounds, we performed enzyme kinetics in the presence of eight potent compounds **4**, **7**, **13**, **20**, **23**, **24**, **26** and **28**. The plots of [S]/V against inhibitor concentrations ([I]) showed that **13** and **28** followed uncompetitive inhibition and **4**, **7**, **20**, **23**, **24** and **26** followed competitive inhibition modes (Figure 3.6 and 3.7). [S] and V represent the substrate concentration and initial rate of the reaction, respectively.

Detailed mechanistic studies for the IDO1 mediated transformation of *L*-Trp to *N*-formylkynurenine showed that formation of ferric superoxide intermediate due to binding of O_2 to the Fe(III) of the heme-group is the prerequisite for this oxidation reaction. Therefore, although these tested compounds follow competitive/uncompetitive mode of inhibition with respect to *L*-Trp but may not be competitive/uncompetitive with respect to O_2. For this reason, additional kinetics measurement with respect to O_2 is required to understand the comprehensive mode of IDO1 inhibition by these compounds.

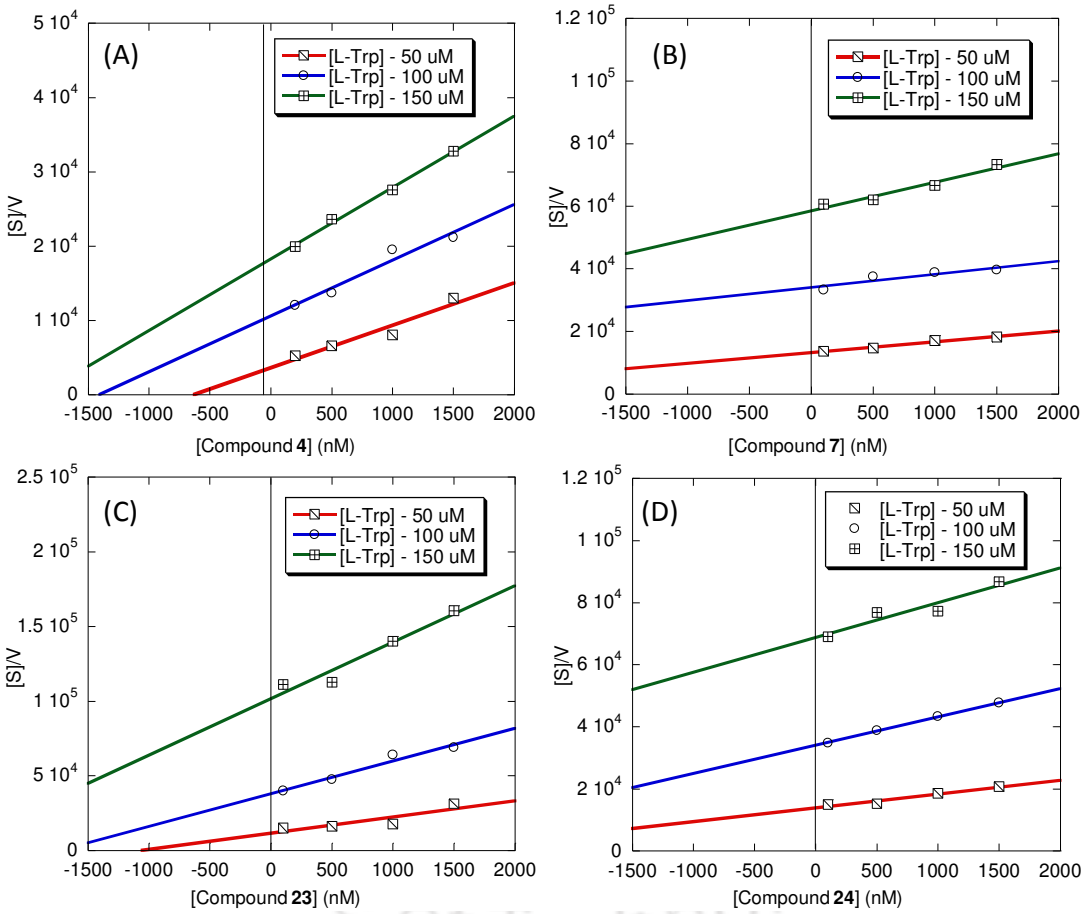

Figure 3.6. Determination of mode of inhibition of the potent compounds. Plot of [S]/V against concentrations of compounds **4** (A), **7** (B), **23** (C) and **24** (D). Concentration of *L*-Trp was varied from 50 µM to 150 µM. The concentrations of compounds were varied from 100 nM to 1500 nM. All the absorption measurements were performed in 50 mM phosphate buffer pH 6.5 at room temperature.

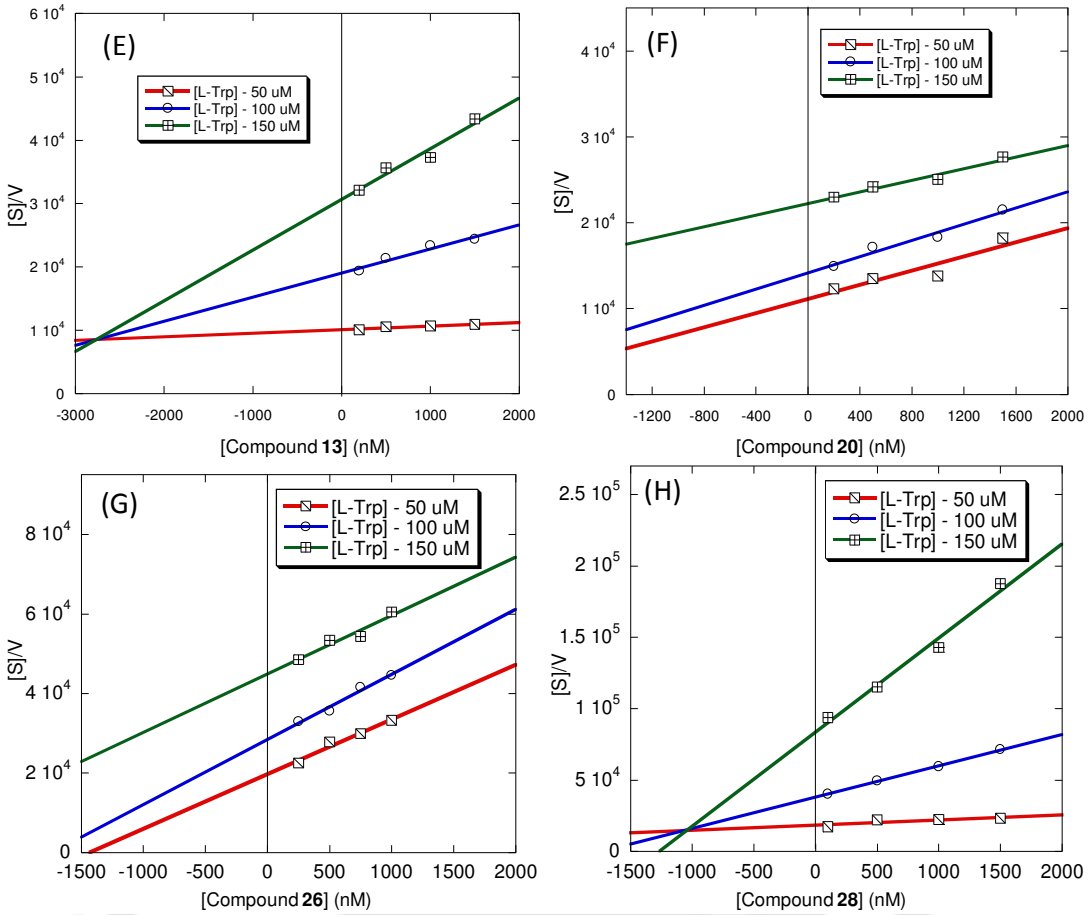

Figure 3.7. Determination of mode of inhibition of the potent compounds. Plot of [S]/V against concentration of compounds **13** (E), **20** (F), **26** (G) and **28** (H). Concentration of *L*-Trp was varied from 50 µM to 150 µM. The concentrations of compounds were varied from 100 nM to 1500 nM.

3.8. Probable mode of interaction of the potent oxindoles with IDO1 enzyme

With confirmation that potent oxindoles inhibit IDO1 enzyme activity, we performed molecular docking analyses of the three potent compounds to explore their probable mode of interaction with the IDO1 enzyme (PDB code: 2DOT).[43] Molecular docking analysis revealed that the potent compounds **7**, **24** and **26** presumably interact with the IDO1 enzyme in a similar pattern like *L*-Trp (Figure 3.8).[42] The oxindole moiety of the compounds is presumably placed in pocket-'A' and interacts with Ser167 residue through H-bonding. Hydrophobic amino acids like Phe163, Phe164, Tyr126 and others present in pocket-'A' could be involved in pi-stacking or halogen bonding and hydrophobic interactions with the oxindole moiety. Recently, it was reported that hydrophobic residues Phe163 and Phe164 are important for the activity of the IDO1 enzyme.[44]

Whereas, polar residues Ser167 and Tyr126 are crucial for the high *L*-Trp affinity of IDO1 enzyme.[45] Therefore, the mode of interactions clearly suggests that oxindole-moiety is mimicking the intermediate state for the *L*-Trp oxidation.

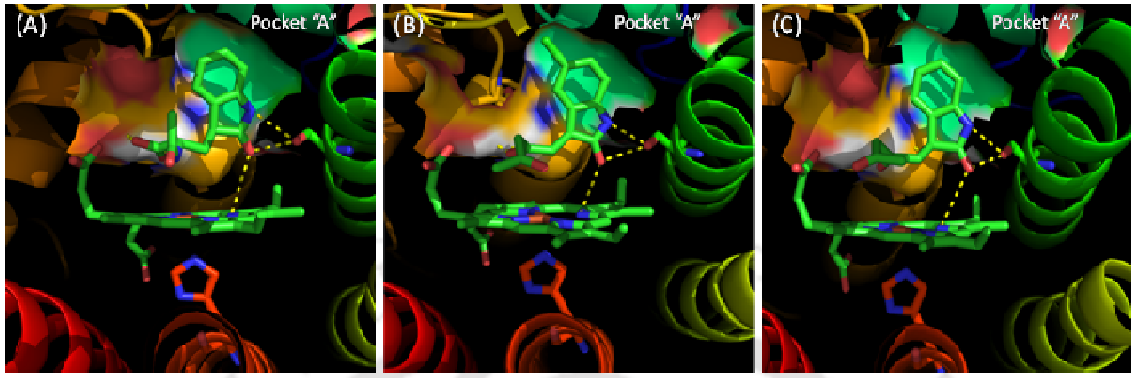

Figure 3.8. Probable mode of interaction of the compounds, **7** (A), **24** (B) and **26** (C) with the active site of the IDO1 enzyme (2DOT). The model structures were generated using MoleGro Virtual Docker, version 6.0. The oxygen and nitrogen atoms are shown in red and blue, respectively. Residues involved in interactions through hydrogen bond formation are shown using dashed lines (yellow). Images were generated using PyMol.

The model structures also predict that the carbonyl group of the oxindole ring is orientated towards the heme-group, which is in accordance with our predicted mode of the interaction of these mechanism-based inhibitors. The substituents at the C3-position may interact with IDO1 through different modes. The free α-carboxyl groups of compound **7** could be involved in H-bonding with Ser263 and Ala264 residues, whereas its acyl-protected α-amino group could be involved in interaction with heme-group. The carbonyl (from acetylacetone) of the alkene oxindole derivative **24** could be involved in H-bonding with the Ser263 and Ala264 residues. 5-Chloro substitution in the oxindole ring could assist compound **24** to interact with the residues in pocket-'A' through halogen bonding, pi-stacking and hydrophobic interactions. For compound **26** the carbonyl (from acetylacetone) and 3-hydroxyl group could be involved in interaction with Ser263 and Ala264 residues. Recently, 3-hydroxy-3-alkyl derivatives of isatins were developed as favorable inhibitors of TDO enzyme. This study also showed that 3-hydroxy group plays a crucial role in proper binding of the inhibitors within the active site of the TDO enzyme.[16] Therefore, H-bonding, hydrophobic and other interactions play important roles in stronger binding of the oxindole derivatives of *L*-Trp to the IDO1 active site. The

differences in IC_{50} values among these compounds suggest that the mode of interaction of these compounds with IDO1 could be different or volume/interaction pattern of C3-substituents could be crucial for their binding under the experimental conditions. Molecular docking analyses also support that suitable C3-substituted oxindoles may act as a mimic of the epoxide intermediate for the transformation of *L*-Trp to *N*-formylkynurenine by IDO1 enzyme.

3.9. Inhibitory activities of oxindoles against purified TDO enzyme

TDO is the other enzyme, which also catalyzes the initial, rate-limiting step of the kynurenine pathway. TDO also catabolizes more than 90% of the *L*-Trp in the liver to regulate its level. To investigate the efficacy of these oxindoles in selectively inhibiting IDO1 enzyme, TDO enzyme inhibition studies were also performed (Table 3.5).

Table 3.5. Inhibitory activity of the selected compounds against purified human IDO1 and TDO enzymes.

Compound	Mode of IDO1 inhibition	IDO1 inhibition (IC_{50} (μM))[a]	TDO inhibition (IC_{50} (μM))[a]	Selectivity ratio[b]
2	NM[c]	3.39 ± 0.29	60.22 ± 2.02	18
4	competitive	1.28 ± 0.28	27.20 ± 3.08	21
7	competitive	0.62 ± 0.11	83.47 ± 3.27	135
8	NM[c]	2.31 ± 0.21	58.33 ± 3.58	25
13	uncompetitive	0.63 ± 0.15	53.38 ± 0.51	85
14	NM[c]	1.51 ± 0.15	46.81 ± 4.21	31
16	NM[c]	1.58 ± 0.12	38.31 ± 4.56	24
17	NM[c]	1.78 ± 0.39	52.90 ± 3.31	30
18	competitive	1.24 ± 0.38	46.24 ± 6.06	37
21	NM[c]	0.93 ± 0.06	71.01 ± 5.09	76
23	competitive	0.36 ± 0.08	54.69 ± 2.59	152
24	competitive	0.19 ± 0.07	39.92 ± 1.03	210
26	competitive	0.45 ± 0.09	56.12 ± 6.14	124

[a]IC_{50} values are the mean of three independent assays against purified enzymes.

[b]Selectivity ratio is calculated as (IC_{50} value of TDO)/(IC_{50} value of IDO1).

NM[c] = not measured.

Screening against purified TDO enzyme revealed that these oxindoles were considerably inactive ($IC_{50} \geq 20$ μM) against TDO enzyme. Substitution at the 3-position of the oxindole ring also plays a significant role in inhibiting TDO enzyme activity.

Selected oxindole derivatives of *L*-Trp and tryptamine showed 18 to 135-fold stronger IDO1 inhibition in comparison with TDO enzyme under similar experimental conditions. Oxindole derivatives of isatins showed 20 to 200-fold stronger IDO1 inhibition in comparison with TDO enzyme. The most effective oxindole-based compound, **27** (based on the enzymatic and cellular assay) exhibited over 200-fold increase in inhibitory activity toward IDO1 enzyme when compared against TDO enzyme. Recently a series of 3-hydroxy substituted isatin derivatives were developed as the inhibitors for TDO enzyme. However, our studies suggest that suitable C3-subtituents is crucial in proper binding with the IDO1 over TDO enzyme.[16] HPLC-based TDO activity assay also showed that these potent compounds have preferential selectivity for IDO1 over TDO enzyme inhibitions (Table 3.6).

Table 3.6. HPLC based IDO1 and TDO inhibition assay of the selected compounds.

Compound	IDO1 inhibition (IC_{50} μM)[a]	TDO inhibition (IC_{50} μM)[a]
4	1.51 ± 0.19	20.93 ± 1.39
7	0.71 ± 0.09	51.38 ± 2.43
13	0.99 ± 0.17	46.27 ± 3.37
20	0.87 ± 0.17	31.48 ± 1.99
21	0.69 ± 0.15	36.79 ± 2.45
23	0.48 ± 0.10	25.16 ± 3.32
24	0.30 ± 0.10	20.93 ± 2.61
26	0.54 ± 0.09	21.63 ± 3.67

[a]IC_{50} values calculated by HPLC method (are the mean of three independent assays).

Overall in this study we have designed oxindole derivatives as mechanism-based inhibitors of IDO1 enzyme. Subsequent modification at the C3-position of the oxindole ring directed to the identification of potent inhibitors with low-micromolar IDO1 enzyme inhibitory activities under in vitro conditions. Low-micromolar IC_{50} values of the compounds and smaller differences in their inhibitory activities, suggest that the presence of oxindole-moiety could be the driving force for their moderate potencies. Overall, activity studies showed that *N*-acyl protected oxindolealanine (**7**) could considerably enhance the inhibition potency of the *L*-Trp derivatives. Suitable substitution and restricted rotation at the C3-position of the isatin/5-chloroisatin could also augment their inhibition potencies. UV-absorption properties of the heme-containing porphyrin-ring in the absence and presence of the compounds, clearly suggest that the oxindole derivatives

strongly interact with the IDO1 enzyme. Molecular model structures also proposed that additional hydrogen bond interaction of the oxindole ring with Ser167 residue along with the interaction with the residues present in "pocket-A" of the IDO1 enzyme could be the primary contributing factor for the stronger inhibitory properties. The potent compounds also exhibited a 15 to 210-fold stronger inhibition in IDO1 enzyme inhibition compared to TDO enzyme. Until now limited indole/tryptophan, based derivatives have been reported with such selective and stronger IDO1 enzyme inhibitors.[11-17] These results clearly suggest that designing compounds, which can perturb the electrophilic addition of O_2 of the oxygenated-heme group to the pyrrole ring of *L*-Trp, could be an efficient approach to improve the potency as well as the selectivity of IDO1 inhibitors.

3.10. Conclusion

In summary, in this chapter we have synthesized oxindole derivatives with moderate inhibitory activity against purified human IDO1 enzyme. Enzyme activity measurements showed that the oxindole ring plays an important role in their IDO1 inhibitory potencies. Halogen substitution and restricted rotation around C3-position of the oxindole ring were effective in improving their efficacies. Spectroscopic studies supported the interaction of potent compounds with the heme-group of IDO1 enzyme, indicating its preliminary role in mimicking the epoxide-intermediate for the IDO1 catalyzed transformation of *L*-Trp to *N*-formylkynurenine. IDO1 activity in the interferon gamma (IFN-γ) induced MDA-MB-231 cells showed that the tested compounds have minimal cytotoxicity and low-micromolar potencies. These oxindole derivatives also showed selectivity for IDO1 enzyme over TDO enzyme. Overall, these observations suggest that oxindole derivatives are potential inhibitor of IDO1 enzyme and could be of interest as drug target in cancer and other human diseases.

3.11. Experimental section

3.11.1. Instrumentation and Characterisation

As described in chapter 2 section 2.9.1.

3.11.2. General procedure for the synthesis of CbZ-protected *L*-Trp and tryptamine

L-Trp or tryptamine (29.4 mmol) was first dissolved in 1M NaOH (60 mL) and stirred at 0 °C for 30 min. Then benzylchloroformate (32.3 mmol) and 1M NaOH (30 mL) where

simultaneously added to the solution in drop-wise fashion.[32] The mixture was stirred for 12 h at room temperature. The solution was acidified with 6M HCl to pH 1-2 and extracted with EtOAc (3 × 200 mL). The combined organic layer was dried over anhydrous Na_2SO_4 and concentrated under reduced pressure. The product was used directly in the following reactions.

3.11.3. General procedure for the synthesis of benzyl-protected *L*-Trp

To a stirring solution of *L*-Trp (2.0 mmol) in toluene (50 mL) PTSA (4.8 mmol) was added. Then benzylalcohol (23.08 mmol) was added in dropwise fashion under stirring condition and the reaction mixture was refluxed for 24 h using dean stark apparatus. Excess toluene was removed under reduced pressure and the reaction mixture was diluted with water (50 mL). The compound was then extracted with EtOAc (3 × 100 mL). The combined organic layer was dried over anhydrous Na_2SO_4 and concentrated under reduced pressure. Column chromatography with silica gel and a gradient solvent system of MeOH to DCM (5-10%) yielded the target products (75%).

3.11.4. Synthesis of 2-acetylamino-3-(1*H*-indol-3-yl)propanoic acid

A solution of *L*-Trp (1.5 mmol) and acetic anhydride (3 mmol) in methanol (20 mL) was refluxed for overnight and then concentrated under reduced pressure.[46] The crude mixture was then diluted with water and extracted with EtOAc (3×30 mL). The combined organic layer was dried over anhydrous Na_2SO_4 followed by concentration under reduced pressure to obtain the *N*-acetylated product, which was directly used for next step without further purification.

3.11.5. Synthesis of 2-benzoylamino-3-(1*H*-indol-3-yl)propanoic acid

To a stirred solution of *L*-Trp (1.5 mmol) in 2 ml water was added 2 ml of 1M NaOH aqueous solution followed by the addition of benzoyl chloride (1.8 mmol) dissolved in 0.5M NaOH (8 mL) and chloroform (8 mL) drop wise at 0 °C under continuous stirring. Then the whole solution was allowed to stir at room temperature for 12 h.[47] After completion of the reaction (monitored by TLC), the residual solvent was removed under reduced pressure and the reaction mixture was further acidified with 0.5M HCl to pH 3-4. The aqueous layer was then extracted with EtOAc (3 × 30 mL) and the combined organic layer was dried over anhydrous Na_2SO_4 and concentrated under reduced pressure to obtain the desired solid product, which was directly used for the next step.

3.11.6. General procedure for the synthesis of oxindole derivatives of *L*-trp and tryptamine

The desired amount of substituted *L*-Trp or tryptamine (1.5 mmol) was first dissolved in acetic acid (1.5 mL) and then a mixture of DMSO and concentrated HCl (1:3 approx.) was slowly added under continuous stirring conditions.[27] The resulting solution was then stirred at room temperature for another 1-2 h. After completion of reaction (monitored by TLC), the reaction mixture was diluted with water (8 mL) and further extracted with EtOAc (3 × 30 mL). The combined organic layer was dried over anhydrous Na_2SO_4 and concentrated under reduced pressure. Column chromatography with silica gel and a gradient solvent system of methanol to dichloromethane (5-20%) yielded the target products.

3.11.7. Synthesis of 2-amino-3-(1*H*-indol-3-yl)propanamide(11)

To a stirring solution of compound **4** (1.5 mmol) in DMF (10 mL) was added 1-hydroxybenzotriazole (1.5 mmol) and EDCI (1.65 mmol). The whole mixture was then stirred for 2 h at room temperature under N_2 atmosphere.[29] Then aqueous ammonia solution (0.5 mL, 7.0 mmol) was added drop wise under continuous stirring condition and the resulting solution was allowed to stir for another 18 h at room temperature. Then water (20 mL) was added and washed with EtOAc (3 × 10 mL). The organic phase was again washed with 5% $NaHCO_3$ solution, dried over anhydrous Na_2SO_4, and concentrated under reduced pressure. The crude mixture was further hydrogenated (1 atmosphere pressure) in MeOH using Pd/C as catalytic amount (10 mol%) to obtain the crude product **11**. The pure compound was isolated using column chromatography with silica gel and a gradient solvent system of methanol to dichloromethane (10-35%).

3.11.8. General procedure for the synthesis of hydrazones and phenylimino derivatives of isatin

To a stirring solution of isatin (1 mmol) in ethanol was added appropriate amount of the aromatic hydrazine or primary amine (1 mmol) and a catalytic amount of acetic acid.[30] The whole solution was refluxed for 0.5-4 h under constant stirring. After the completion of the reaction, the solvent was evaporated under reduced pressure followed by washing the crude product with water (3 × 10 mL) and drying under reduced pressure. Column chromatography with silica gel and a gradient solvent system of ethyl acetate to hexane

(5-20%) yielded the target products. Recrystallization from ethanol also yielded desired pure product.

3.11.9. General procedure for the synthesis of oxindole derivatives, 22 and 26

To an ice cooled mixture of isatin (2.5 mmol) and acetone or acetyl acetone (2.5 mmol) was added 0.5 mL of piperidine under continuous stirring.[31] The whole mixture was stirred at 0 °C for 4 h and then cold ethanol was added. The resulted solid was filtered and dried under reduced pressure. Column chromatography with silica gel and a gradient solvent system of ethyl acetate to hexane (5-20%) yielded the target products.

3.11.10. General procedure for the synthesis of oxindole derivatives, 21 and 25

A solution of isatin (1 mmol) and diethyl malonate (1 mmol) or dimedone (1 mmol) in water was refluxed with a catalytic amount of piperidinium acetate for 3-4 h at 100 °C.[31] The solid thus obtained was filtered, washed properly with water and dried in oven. Further purification was performed with silica gel column chromatography using ethyl acetate: hexane gradient solvent system (5-20%) or recrystallized from ethanol to obtain the desired pure product.

3.11.11. General procedure for the synthesis of 5-chloroisatin derivatives

The compounds were synthesized according to reported procedure with slight modification.[32] The desired amount of 5-chloro isatin (1.1 mmol) was dissolved in acetone (10 mL) and then appropriate amount of K_2CO_3 (1.3 mmol) was added under stirring condition. The whole solution was then refluxed for 14 h at 50 °C. After completion of reaction (monitored by TLC), the reaction mixture of 3-hydroxy 5-chloroisatin was concentrated under reduced pressure and the residue obtained was triturated with diethyl ether resulting the alcohol intermediate as a white solid, which was directly used for the next step.

To a stirring solution of the 3-hydroxy 5-chloroisatin in ethanol (5 mL), was added concentrated HCl (approx. 1 ml) dropwise and a catalytic amount of acetic acid. Then the mixture was refluxed for 12 h at 60 °C under continuous stirring.[32] After the reaction was complete (monitored by TLC), the mixture was concentrated and washed with saturated $NaHCO_3$ solution. The aqueous layer was then extracted with EtOAc (3 × 30 mL) and the combined organic layer was further dried over anhydrous Na_2SO_4 and

concentrated under reduced pressure. Column chromatography with silica gel and a gradient solvent system of ethyl acetate to hexane (5-25%) yielded the target products.

3.11.12. Purification of the compounds by HPLC analysis

All synthesized compounds were further purified by analytical-HPLC analyses (with a purity level ≥ 94-95%) before performing *in vitro* enzyme activity, cellular activity, cell viability assays, and others. Waters 600 HPLC system with Ascentis® Express C18 2.7 µM analytical column (Sigma) at a flow rate of 0.5 mL/min was used for the purification of the compounds. All the compounds (~1 mg) were dissolved in MeOH (1 mL) for HPLC analyses. All the compounds have a strong absorption peak at 280 nm. Hence, HPLC analyses were performed using a UV-detector at 280 nm. During each injection 20 µL of the compound solution was used and fractions were collected. This step was repeated for more than 10-times to get sufficient amount of the pure compounds. A total run time was 10 min. All the collected fractions for each compound were dried under reduced pressure and verified by HRMS analyses. The mobile phase for HPLC measurements was 60% MeOH and 40% H_2O (isocratic mode).

3.11.13. IDO1 and TDO inhibition assay by spectrophotometric method

Both, IDO1 and TDO inhibition assays were performed according to the earlier reported procedures.[2,8,33,40] The solubility of the compounds in water was either moderate or poor. Hence, stock solution of the compounds were prepared by first dissolving in DMSO and then diluted with buffer. In the assay system the minimum and maximum amount of DMSO were 0.02% and 2%, respectively. The standard reaction mixture (500 µL) contained KPB (100 mM, pH 6.5 for IDO1 enzyme and 50 mM, pH 8.0 for TDO enzyme), sodium ascorbate (20 mM), methylene blue (10 µM), catalase (240 nM, from bovine liver), *L*-Trp (100 µM), purified enzyme (40 nM for IDO1 and 25 nM for TDO), DMSO (0.05%, v/v), triton-X 100 (0.01%, v/v) and inhibitors. First, the assay was performed using the inhibitors at different concentrations of 100 nM to 25 µM for both IDO1 and TDO and then repeated five times at a particular concentration. The reaction was quenched with 100 µL of 30% (w/v) trichloroacetic acid. The amount of kynurenine formation was quantified using 2% (w/v) *p*DMAB in acetic acid. The absorbance of the reaction mixture was recorded by at 480 nm. All these experiments were repeated for three times for each compound.

3.11.14. Spectroscopic measurements

The absorption spectra were recorded at room temperature using a Perkin Elmer Lambda-25 UV-Vis spectrophotometer. All the measurements were performed in 100 mM Tris buffer pH 7.4 with IDO1 enzyme concentration of 5 μM and compound concentration of 50 μM. The deoxy-reaction system was prepared by injecting sodium dithionite (~10-fold excess) into the samples pre-purged with N_2 gas.[9]

3.11.15. Determination of modes of enzyme inhibition by the compounds

The IDO1 enzyme inhibition mode of the selected compounds was measured according to the reported method.[8,48] The IDO1 enzyme kinetics was performed using 50 μM, 100 μM and 150 μM of *L*-Trp and 100 nM, 500 nM, 1000 nM and 1500 nM of inhibitor concentrations. The amount of generated *N*-formylkynurenine was monitored at different time interval for 5 min. However, initial slope was measured to calculate the initial rate of enzyme catalysis. The mode of inhibition was determined from the plot of [S]/V against inhibitor concentration [I]. Where, [S] and V represent *L*-Trp concentration and initial rate of enzyme catalysis, respectively.

3.11.16. Molecular docking analysis

As described in chapter 2 section 2.9.8.

3.11.17. IDO1 and TDO inhibition assay by HPLC analysis

The enzymatic reaction (100 μL) was performed in 100 mM potassium phosphate buffer at pH 6.5 using sodium-ascorbate (20 mM), catalase (240 nM), methylene blue (10 μM), purified enzyme (40 nM for IDO1 and 25 nM for TDO), *L*-Trp (150 μM), DMSO (0.05%, v/v) and triton-X 100 (0.01%, v/v). The assay was performed using the inhibitors concentrations of 0.5 μM to 1.5 μM for IDO1 and 10 μM to 25 μM for TDO. The reaction was performed at 37 °C for 1 h (reaction was completed in 20 min) and quenched by addition of 30% (w/v) trichloroacetic acid (20 μL). The reaction mixture was incubated at 50 °C for 30 min and then centrifuged at 10,000 rpm for 10 min. Then, 20 μL of supernatant from each reaction mixture was used for HPLC analyses. The mobile phase for HPLC measurements was 50% sodium citrate buffer (40 mM, pH 2.25) and 50% methanol with 400 μM SDS. The rate of flow through the Ascentis® Express C18, 2.7 μm HPLC column was 0.5 mL/min, and kynurenine was detected at a wavelength of 365

nm.[38] A similar HPLC analyses were performed using pure kynurenine and a standard curve was prepared. The IC_{50} values of the compounds were calculated from this standard curve. Similarly, TDO enzyme inhibition activity assay was performed for these selected compounds.

3.11.18. Cellular activity assay

For the *in vitro* cellular activity assay, MDA-MB-231 breast cancer cells were selected. The cells were treated with human Interferon gamma (IFN-γ) (5-1000 ng/mL) in complete media for 48 h to allow the over expression of IDO1 enzyme in the cells. After that, the compounds (20 nM to 1 mM) were incubated for a period of 4 h and 150 µM of *L*-Trp was incubated for further 5 h. Cells stimulated with IFN-γ alone served as negative control while cells stimulated with 150 µM *L*-Trp served as positive control. Then, the cells were washed with sterile cell-culture grade PBS and were trypsinized followed by centrifugation at 1000 rpm. The cell pellet was re-dissolved in sterile PBS and centrifuged at 1000 rpm. Then the pellet was lysed in 10 mM HEPES buffer by passing through a sterile syringe. The lysate was used for standard IDO1 assay as mentioned earlier and the IC_{50} values were determined for each compounds.[8,33,38,40,41]

3.11.19. Cell viability analysis

MDA-MB-231 breast cancer cells, A549 lung cancer cells and HeLa cervical cancer cells were cultured in DMEM/F12 media. J774A.1 macrophage cells were cultured in DMEM high glucose media. Both the media were supplemented with 10% Fetal Bovine Serum and 1% penicillin-streptomycin solution. Cells were maintained at 37 °C in a humidified 5% CO_2 incubator. 10,000 cells (of MDA-MB-231, A549, HeLa and J774A.1 cells) were seeded overnight in 96 well plates in total volume of 0.2 mL in their respective complete media. After 12 h cells were washed twice with cell culture grade phosphate buffer saline (PBS) and were incubated with the IDO1 inhibitors (at IC_{50} and 2 × IC_{50} values respectively) in 0.2 mL of DMEM/F12 serum free medium (incomplete medium) for 24 h and 48 h.[8,40,49] Cells were also treated with mitomycin-C at 50 µM and 100 µM concentrations prepared in serum free media, which served as positive control. Cells treated with incomplete medium alone were considered as 100% viable (served as negative control). The dye MTT (3-(4,5-dimethylthiazol-2-yl)-2,5-diphenyltetrazolium bromide) was used to measure cellular viability. After the treatment period, the cells were washed twice with PBS and taken for morphological analysis via cytell imaging system

(GE Healthcare). Images were collected at 10x magnification. After imaging, each well was incubated with 100 µL of MTT (0.5 mg/mL in PBS) for 4 h at 37 °C with 5% CO_2. Then, MTT solution was removed and the formazan crystals were dissolved in 100µL cell culture grade DMSO. The absorbance was determined using a spectrophotometer (Spectra Max M2) at 570 nm and 660 nm (to subtract scattering effects of crystals). MDA-MB-231 and J774A.1 cell lines were procured from national cell culture facility, Central Drug Research Institute, Lucknow, India. A549 and HeLa Cell lines were procured from National Center for Cell Science, Pune, India.

3.12. Spectroscopic characterization of the synthesized compounds

2-Amino-3-(2-oxoindolin-3-yl)propanoic acid (2): As pink solid (45% yield; rotamers, hygroscopic); ^{1}H NMR (600MHz, $CDCl_3$ + DMSO-d_6) δ_{ppm} 10.46 (s, 1H), 8.82 (br, s, 1H), 7.47-7.44 (m, 1H), 7.18 (d, 1H, J = 12 Hz), 7.13 (d, 1H, J = 6), 7.09-7.08 (m, 1H), 6.92-6.88 (m, 1H), 6.83-6.80 (m, 1H), 3.75-3.73 (m, 1H), 3.54-3.52 (m, 1H), 1.93-1.89 (m, 2H); ^{13}C NMR (100 MHz, $CDCl_3$ + DMSO-d_6) δ_{ppm} 179.8, (179.5), 169.8, 141.5, (141.4), 127.8, (127.7), 123.3, (123.2), 121.7, 109.8, (109.7), 51.3, (50.6), 43.5, (42.0), 30.2, (29.8); HRMS [ESI] calcd. for $C_{11}H_{12}N_2O_3$ $[M + H]^+$ 221.0921, found 221.0920

3-(2-Aminoethyl)indolin-2-one (3): As light brown solid (70% yield; rotamers, mp: 245-247 °C); ^{1}H NMR (400 MHz, $CDCl_3$ + DMSO-d_6) δ_{ppm} 10.41 (br s, 1H), 8.38 (br s, 2H), 7.24-7.16 (m, 2H), 7.00-6.96 (m, 1H), 6.90 (d, 1H, J = 8 Hz), 3.56-3.53 (m, 1H), 3.11-3.06 (m, 2H), 2.38-2.29 (m, 1H), 2.24-2.14 (m, 1H); ^{13}C NMR (151 MHz, $CDCl_3$ + DMSO-d_6) δ_{ppm} 178.3, (178.2), 141.6, (141.5), 127.5, (127.4), 127.2, 122.9, (121.1), 121.0, 109.2, (109.1), 43.0, (42.9), 36.4, 27.1, (27.0); HRMS [ESI] calcd. For $C_{10}H_{12}N_2O$ $[M + H]^+$ 177.1022, found 177.1026.

2-[((Benzyloxy)carbonyl)amino]-3-(2-oxoindolin-3-yl)propanoic acid (4): As light brown semi-solid (70% yield; rotamers); ^{1}H NMR (600 MHz, $CDCl_3$ + DMSO-d_6) δ_{ppm} 9.48 (br s, 1H), 7.33- 7.32 (m, 2H), 7.25-7.10 (m, 5H), 6.97-6.92 (m, 1H), 6.80 (d, 2H, J = 6 Hz), 5.04 (s, 2H), 4.59 (t, 1H), 3.48-3.34 (m, 1H), 2.36-2.31 (m, 2H); ^{13}C NMR (151 MHz, $CDCl_3$ + DMSO-d_6) δ_{ppm} 180.8, (180.6), 174.1, (174.0), 156.9, (156.5), 141.6, (141.5), 136.5, (136.3), 129.1, 128.5, (128.4), 128.3, 128.1, (128.0), 127.9, 124.7, 124.1,

122.8, (122.7), 110.2, 67.1, (66.9), 52.1, 40.3, 33.2, (32.0); HRMS [ESI] calcd. for $C_{19}H_{18}N_2O_5$ $[M + H]^+$ 355.128.8, found 355.1289.

2-((Tert-butoxycarbonyl)amino)-3-(2-oxoindolin-3-yl)propanoic acid (5): As brown semisolid (68% yield; rotamers); ^{1}H NMR (400 MHz, $CDCl_3$ + CD_3OD) δ_{ppm}7.61-7.59 (m, 1H), 7.13-7.09 (m, 1H), 6.51-6.45 (m, 2H), 4.28 (s, 1H), 3.61-3.43 (m, 1H), 2.92-2.91 (m, 2H), 1.27 (s, 9H); ^{13}C NMR (151 MHz,$CDCl_3$ + CD_3OD) δ_{ppm} 202.0, (201.9), 156.3, (156.3), 150.7, 134.8, 131.5, (131.4), 117.7, (117.5), 115.9, (115.8), 79.6, 52.2, 42.2, 29.7, 28.3; HRMS [ESI] calcd. for $C_{16}H_{20}N_2O_5$ $[M + H]^+$ 321.1445, found 321.1506.

2-Benzamido-3-(2-oxoindolin-3-yl)propanoic acid (isomeric mixture 6): As yellow semi-solid (60% yield; rotamers); ^{1}H NMR (400 MHz, $CDCl_3$ + DMSO-d_6) δ_{ppm} 10.15 (s, 1H), 10.07 (br s, 1H), 8.81-8.80 (m, 1H), 8.43 (br s, 1H), 7.91-7.84 (m, 2H), 7.47-7.33 (m, 3H), 7.20-7.09 (m, 1H), 6.97-6.91 (m, 1H), 6.84-6.80 (m, 1H), 4.96-4.90 (m, 1H), 4.82-4.78 (m, 1H), 2.61-2.51 (m, 1H), 2.40-2.24 (m, 1H); ^{13}C NMR (151 MHz, $CDCl_3$ + DMSO-d_6) δ_{ppm} 180.4, (179.8), 173.3, (173.2), 167.3, (166.8), 141.9, 133.6, (133.5), 131.3, (131.2), 128.0, 127.9, (127.7), 127.2, 124.2, (123.5), 122.0, (121.9), 109.8, (109.7), 51.2, 43.3, (43.1), 32.3, (31.3); HRMS [ESI] calcd. for $C_{18}H_{16}N_2O_4$ $[M + H]^+$ 325.1183, found 325.1155.

2-Acetamido-3-(2-oxoindolin-3-yl)propanoic acid (isomeric mixture, 7): As brown semi-solid (70% yield; rotamers); ^{1}H NMR (400 MHz, $CDCl_3$ + CD_3OD) δ_{ppm} 9.28 (br, s, 1H), 6.59-6.55 (m, 1H), 6.49-6.40 (m, 1H), 6.26-6.22 (m, 1H), 6.16-6.13 (m, 1H), 4.07-4.02 (m, 1H), 3.89-3.86 (m, 1H), 1.89 (s, 3H), 1.69-1.61 (m, 1H), 1.54-1.48 (m, 1H); ^{13}C NMR (151 MHz, $CDCl_3$ + CD_3OD) δ_{ppm} 180.3, (180.2), 172.2, (171.9), 141.7, (141.6), 128.3, (128.1), 124.2, 123.7, 110.1, (110.0), 50.3, (50.1), 39.8, 31.9, (31.1), 22.0, (21.9); HRMS (ESI) calcd. for $C_{13}H_{14}N_2O_4$ $[M + H]^+$ 263.1026, found 263.1012.

Benzyl [2-(2-oxoindolin-3-yl)ethyl]carbamate (8): As light brown solid (70% yield; rotamers, mp: 161-163 °C); ^{1}H NMR (400 MHz, $CDCl_3$ + DMSO-d_6) δ_{ppm} 9.65 (br s, 1H), 7.39-7.25 (m, 5H), 7.20-7.15 (m, 1H), 7.01-6.95 (m, 1H), 6.87-6.86 (m, 2H), 5.95 (br s, 1H), 5.07 (s, 2H), 3.43-3.38 (m, 1H), 2.74-2.65 (m, 2H), 2.12-2.09 (m, 2H); ^{13}C NMR (151 MHz, $CDCl_3$ + DMSO-d_6) δ_{ppm} 179.2, (179.1), 155.9, 141.6, 136.2, 128.7,

127.9, (127.4), 127.3, 123.5, (123.4), 121.4, 109.2, 65.8, 43.3, 37.8, 30.0; HRMS [ESI] calcd. for $C_{18}H_{18}N_2O_3$ $[M + H]^+$ 311.1390, found 311.1398.

Benzyl 2-amino-3-(2-oxoindolin-3-yl)propanoate (9): As yellow semi-solid (55% yield; rotamers); ^{1}H NMR (400 MHz, $CDCl_3$ + CD_3OD) δ_{ppm} 7.57 (d, 2H, J = 8 Hz), 7.37 (d, 1H, J = 8 Hz), 7.27-6.92 (m, 6H), 5.05 (s, 2H), 4.03 (t, 1H), 3.23-3.18 (m, 1H), 2.19 (s, 2H); ^{13}C NMR (151 MHz, $CDCl_3$ + CD_3OD) δ_{ppm} 174.6, (174.6), 170.6, 140.4, (141.3), 136.5, 128.7, 128.5, 128.3, 125.5, 124.4, 121.7, 119.1, 117.7, 111.5, (111.4), 67.7, 64.1, 53.5, 39.7; HRMS [ESI] calcd. for $C_{18}H_{18}N_2O_3$ $[M + H]^+$ 311.1390, found 311.1395.

Benzyl 2-(((benzyloxy)carbonyl)amino)-3-(2-oxoindolin-3-yl)propanoate (10): As light brown oil (55% yield; rotamers); ^{1}H NMR (600 MHz, $CDCl_3$ + DMSO-d_6) δ_{ppm} 9.18 (br s, 1H), 7.33-7.10 (m, 10H), 6.99-6.94 (m, 2H), 6.84 (d, 1H, J = 12 Hz), 6.40 (d, 1H, J = 12 Hz), 6.24 (d, 1H, J = 12 Hz), 5.06 (s, 4H), 4.66-4.64 (m, 1H), 3.53-3.51 (m, 1H), 2.38-2.31 (m, 1H); ^{13}C NMR (151 MHz, $CDCl_3$ + DMSO-d_6) δ_{ppm} 175.8, 174.8, (174.7), 156.7, (156.5), 141.3, 136.5, (136.3), 128.7, (128.6), 128.5, (128.4), 128.3, (128.2), 124.6, (124.3), 123.1, 110.6, (110.5), 67.3, (67.1), 53.2, (51.9), 43.5, (43.0), 40.3, (40.2), 32.8, (31.9); HRMS [ESI] calcd. for $C_{26}H_{24}N_2O_5$ $[M + H]^+$ 445.1758, found 445.1762.

2-Amino-3-(2-oxoindolin-3-yl)propanamide (11): As yellow semi-solid (45% yield; rotamers); ^{1}H NMR (400 MHz, $CDCl_3$ + DMSO-d_6) δ_{ppm} 7.91-7.86 (m, 1H), 7.81-7.73 (m, 1H), 7.66-7.60 (m, 1H), 7.49-7.36 (m, 1H), 3.67-3.63 (m, 1H), 3.01-2.97 (m, 1H), 2.27-2.23 (m, 1H), 2.13-2.09 (m, 1H); ^{13}C NMR (151 MHz, CD_3OD + DMSO-d_6) δ_{ppm} 181.2, 180.1, 144.4, 133.0, (132.9), 128.2, 123.7, 118.7, (118.4), 111.8, (111.3), 52.9, 43.1, 37.1; HRMS [ESI] calcd. for $C_{11}H_{13}N_3O_2$ $[M + NH_4]^+$ 237.1346, found 237.0859.

3-(2-Phenyl-hydrazono)indolin-2-one (12): As yellow solid (85% yield; mp: 208-210 °C (lit. mp 214-216 °C)[32]; ^{1}H NMR (600 MHz, $CDCl_3$ + DMSO-d_6) δ_{ppm} 12.69 (br s, 1H), 7.77 (br s, 1H), 7.64-7.63 (m, 1H), 7.38-7.34 (m, 4H), 7.23-7..20 (m, 1H), 7.10-7.08 (m, 1H), 7.06-7.04 (m, 1H), 6.90-6.88 (m, 1H); ^{13}C NMR (151 MHz, $CDCl_3$ + DMSO-d_6) δ_{ppm} 163.6, 142.7, 138.2, 129.6, 128.3, 126.9, 123.6, 122.9, 122.3, 119.4, 114.6, 110.4; HRMS [ESI] calcd. for $C_{14}H_{11}N_3O$ $[M + H]^+$ 238.0975, found 238.0977.

3-[2-(4-Chlorophenyl)hydrazono]indolin-2-one (13): As yellow solid (88% yield; mp: 262-264 °C (lit. mp 266-267 °C)[32]; ^{1}H NMR (600 MHz, $CDCl_3$ + DMSO-d_6) δ_{ppm} 10.59 (br s, 1H), 7.58-7.56 (m, 1H), 7.37-7.33 (m, 4H), 7.25-7.22 (m, 1H), 7.07-7.05 (m, 1H), 6.94-6.93 (m, 1H); ^{13}C NMR (151 MHz, $CDCl_3$ + DMSO-d_6) δ_{ppm} 163.6, 140.9, 139.3, 128.8, 127.9, 126.9, 121.5, 121.0, 118.5, 114.7, 110.2; HRMS [ESI] calcd. for $C_{14}H_{10}ClN_3O$ $[M + H]^+$ 272.0585, found 272.0584.

3-[2-(3-Chlorophenyl)-hydrazono]indolin-2-one (14): As yellow solid (80% yield; mp: 237-239 °C (lit. mp 233-234 °C)[32]; ^{1}H NMR (600 MHz, $CDCl_3$ + DMSO-d_6) δ_{ppm} 10.14 (br s, 1H), 7.44-7.43 (m, 1H), 7.11-7.04 (m, 3H), 6.98-6.97 (m, 1H), 6.90- 6.88 (m, 1H), 6.82-6.80 (m, 1H), 6.76-6.75 (m, 1H); ^{13}C NMR (151 MHz, $CDCl_3$ + DMSO-d_6) δ_{ppm} 163.9, 135.0, 130.3, 128.9, 128.9, 128.5, 122.3, 122.0, 121.3, 119.0, 113.7, 112.3, 110.6; HRMS [ESI] calcd. for $C_{14}H_{10}ClN_3O$ $[M + H]^+$ 272.0585, found 272.0587.

3-[2-(3-Nitrophenyl)-hydrazono]indolin-2-one (15): As yellow solid (70% yield; mp: 263-265 °C (lit. mp 267-269 °C)[35]; ^{1}H NMR (600 MHz, $CDCl_3$ + DMSO-d_6) δ_{ppm} 10.53 (br s, 1H), 8.20 (s, 1H), 7.83-7.82 (m, 1H), 7.64-7.60 (m, 1H), 7.52-7.49 (m, 2H), 7.24-7.23 (m, 1H), 7.08-7.06 (m, 1H), 6.94-6.93 (m, 1H); ^{13}C NMR (151 MHz, $CDCl_3$ + DMSO-d_6) δ_{ppm} 163.7, 149.0, 143.8, 140.1, 138.2, 130.1, 128.9, 122.0, 120.8, 119.4, 119.2, 116.4, 110.6, 108.1; HRMS [ESI] calcd. for $C_{14}H_{10}N_4O_3$ $[M + H]^+$ 283.0826, found 283.0833.

3-[2-(2-(Trifluoromethyl)phenyl)-hydrazono]indolin-2-one (16): As light yellow solid (65% yield; mp: 252-254 °C); ^{1}H NMR (600 MHz, $CDCl_3$ + DMSO-d_6) δ_{ppm} 8.04-8.02 (m,1H), 7.66-7.58 (m, 2H), 7.44-7.39 (m, 2H), 7.27-7.26 (m, 1H), 7.11-7.10 (m, 1H), 6.94-6.92 (m, 1H); ^{13}C NMR (151 MHz, $CDCl_3$ + DMSO-d_6) δ_{ppm} 163.1, 140.1, 140.0, 132.7, 130.4, 128.6, 125.5, 121.5, 120.5, 118.8, 114.4, 113.9, 110.2; HRMS [ESI] calcd. for $C_{15}H_{10}F_3N_3O$ $[M + H]^+$ 306.0849, found 306.0850.

4-Methyl-N'-(2-oxoindolin-3-ylidene)benzenesulfonohydrazide (17): As yellow solid (65% yield; mp: 196-198 °C (lit. mp 188 °C)[31]; ^{1}H NMR (600 MHz, $CDCl_3$ + DMSO-d_6) δ_{ppm} 8.10-8.09 (m, 2H), 8.01-7.99 (m, 2H), 7.58 (br s, 1H), 7.50-7.42 (m, 2H), 7.20-7.17

(m, 1H), 7.03-7.01 (m, 1H), 2.57 (s, 3H); ^{13}C NMR (151 MHz, $CDCl_3$ + DMSO-d_6) δ_{ppm} 148.1, 138.8, 135.0, 133.3, 133.1, 131.8, 131.2, 126.3, 125.8, 124.7, 123.2, 114.5, 24.9; HRMS [ESI] calcd. for $C_{15}H_{13}N_3O_3S$ $[M + H]^+$ 316.0750, found 316.0751.

3-(Phenylimino)indolin-2-one (18): As yellow solid (75% yield; mp: 230-232 °C); ^{1}H NMR (600 MHz, $CDCl_3$ + DMSO-d_6) δ_{ppm} 10.26 (br s, 1H), 7.36-7.34 (m, 1H), 7.30-7.29 (m, 1H), 7.20-7.16 (m, 2H), 7.93-7.92 (m, 2H), 6.82-6.80 (m, 1H), 6.61-6.60 (m, 1H), 6.48-6.47 (m, 1H); ^{13}C NMR (151 MHz, $CDCl_3$ + DMSO-d_6) δ_{ppm} 164.7, 155.2, 150.4, 146.8, 134.1, 129.3, 126.1, 125.1, 122.0, 117.7, 116.0, 111.6; HRMS [ESI] calcd. for $C_{14}H_{10}N_2O$ $[M + H]^+$ 223.0866, found 223.0870.

3-[(4-Chlorophenyl)-imino]indolin-2-one (19) : As yellow solid (70% yield; mp: 237-239 °C); ^{1}H NMR (600 MHz, $CDCl_3$ + DMSO-d_6) δ_{ppm} 10.32 (br s, 1H), 7.26-7.24 (m, 1H), 7.16-7.12 (m, 1H), 6.83-6.81 (m, 2H), 6.76-6.75 (m, 1H), 6.59-6.57 (m, 1H), 6.50-6.49 (m, 2H);^{13}C NMR (151 MHz, $CDCl_3$ + DMSO-d_6) δ_{ppm} 164.4, 155.7, 148.7, 147.1, 134.4, 129.4, 126.0, 122.0, 120.6, 119.4, 115.8, 111.8; HRMS [ESI] calcd. for $C_{14}H_9ClN_2O$ $[M + H]^+$ 257.0476, found 257.0476.

3-[(2-Bromophenyl)-imino]indolin-2-one (20): As yellow solid (45% yield; mp: 237-239 °C); ^{1}H NMR (600 MHz, $CDCl_3$ + DMSO-d_6) δ_{ppm} 10.51 (br s, 1H), 7.69-7.67 (m, 1H), 7.39-7.36 (m, 1H), 7.34-7.31 (m, 1H), 7.13-7.10 (m, 1H), 6.98-6.95 (m, 2H), 6.77-6.74 (m, 1H), 6.50-6.49 (m, 1H); ^{13}C NMR (151 MHz, $CDCl_3$ + DMSO-d_6) δ_{ppm} 165.3, 156.4, 148.9, 146.0, 135.2, 133.7, 128.7, 126.6, 123.3, 118.8, 116.5, 112.3; HRMS [ESI] calcd. for $C_{14}H_9BrN_2O$ [M + H]+ 300.9971, found 300.9974.

Diethyl 2-(2-oxoindolin-3-ylidene)malonate (21): As red semisolid (60% yield); ^{1}H NMR (600 MHz, $CDCl_3$ + DMSO-d_6) δ_{ppm} 8.81 (br s, 1H), 8.33 (d, 1H, J = 12 Hz), 7.30 (t, 1H), 6.70 (t, 1H), 6.82 (d, 1H, J = 6 Hz), 4.44-4.35 (m, 4H), 1.38-1.24 (m, 6H); ^{13}C NMR (151 MHz, $CDCl_3$ + DMSO-d_6) δ_{ppm} 168.0, 165.6, 163.1, 143.8, 135.0, 133.4, 129.7, 129.2, 123.0, 119.9, 110.5, 62.5, 14.1; HRMS [ESI] calcd. for $C_{15}H_{15}NO_5$ $[M + H]^+$ 290.1023, found 290.1025.

3-(2-Oxopropylidene)indole-2-one (22): As red solid (88% yield; mp: 172-174 °C); ^{1}H NMR (400 MHz, $CDCl_3$) δ_{ppm} 8.44 (d, 1H, J = 8 Hz), 7.27 (t, 1H), 7.20 (s, 1H), 6.97 (t, 1H), 6.79 (d, 1H, J = 8 Hz), 2.42 (s, 3H); ^{13}C NMR (100 MHz, $CDCl_3$) δ_{ppm} 198.7, 170.0, 143.6, 135.7, 133.3, 128.8, 128.0, 123.2, 120.9 110.3, 32.6; HRMS [ESI] calcd. for $C_{11}H_9NO_2$ $[M + H]^+$ 188.0706, found 188.0708.

5-Chloro-3-(2-oxopropylidene)indole-2-one (23): As red solid (75% yield; mp: 183-185 °C); ^{1}H NMR (400 MHz, $CDCl_3$) δ_{ppm} 8.59(d, 1H, J = 4 Hz), 7.40-7.38 (m, 1H), 6.89 (s, 1H), 6.87 (s, 1H), 2.60 (s, 3H); ^{13}C NMR (100 MHz, $CDCl_3$ + CD_3OD) δ_{ppm} 198.8, 169.8, 142.7, 135.3, 132.8, 128.9, 128.4, 121.9, 111.3, 32.4; HRMS [ESI] calcd. for $C_{11}H_8ClNO_2$ $[M + H]^+$ 222.0316, found 222.0322.

1-(5-Chloro-2-oxoindolin-3-ylidene)pentane-2,4-dione (24): As brown solid (60% yield; mp: 128-130 °C); ^{1}H NMR (400 MHz, $CDCl_3$ + DMSO-d_6) δ_{ppm} 9.45 (br, s, 1H), 7.23 (s, 1H), 7.12 (d, 1H, J = 8 Hz), 6.76-6.73 (m, 1H), 5.41 (s, 1H), 2.88 (s, 1H), 2.09 (s, 1H), 1.93 (s, 3H); ^{13}C NMR (100 MHz, $CDCl_3$ + DMSO-d_6) δ_{ppm} 191.8, 189.2, 178.6, 140.0, 132.1, 129.6, 127.8, 124.9, 111.6, 101.5, 74.9, 45.6, 24.1; HRMS [ESI] calcd. for $C_{13}H_{10}ClNO_3$ $[M + H]^+$ 282.0528, found 282.0398.

2-(3-Hydroxy-2-oxoindolin-3-yl)cyclohexane-1,3-dione (25): As light brown solid (55% yield; mp: 296-298 °C); ^{1}H NMR (600 MHz, $CDCl_3$ + DMSO-d_6) δ_{ppm} 10.44 (br s, 1H), 9.01 (s, 1H), 7.16-7.14 (m,1H), 6.93-6.88 (m, 2H), 6.85-6.84 (m, 1H), 3.48 (s, 1H), 2.39-2.10 (m, 4H), 1.98-1.96 (m, 2H); ^{13}C NMR (151 MHz, $CDCl_3$ + DMSO-d_6) δ_{ppm} 202.5, 170.2, 144.1, 121.7, 120.4, 112.8, 109.8, 100.2, 60.3, 46.7, 36.0, 20.1; HRMS [ESI] calcd. for $C_{14}H_{13}NO_4$ $[M + H]^+$ 260.0917, found 260.1440.

1-(3-Hydroxy-2-oxoindolin-3-yl)pentane-2,4-dione (26): As brown semi-solid (55% yield; rotamers); ^{1}H NMR (600 MHz, $CDCl_3$ + DMSO-d_6) δ_{ppm} 7.44-7.42 (m, 1H), 7.30-7.26 (m, 1H), 6.67-6.62 (m, 2H), 6.36 (br, s, 1H), 3.67 (s, 2H), 3.28-3.26 (m, 2H), 1.69-1.65 (m, 3H); ^{13}C NMR (151 MHz, $CDCl_3$ + DMSO-d_6) δ_{ppm} 194.5, 165.8, 151.7, 136.1, (136.0), 133.4, (133.2), 117.3, (117.2), 116.5, (116.3), 114.4, 47.3, (47.2), 42.2, (42.0),

26.3, 25.6, (24.5); HRMS [ESI] calcd. for $C_{13}H_{13}NO_4$ $[M + Na]^+$ 271.0769 found 271.0906.

5-Chloro-3-hydroxy-3-(2-oxopropyl)indolin-2-one (27): As white solid (75% yield; mp: 188-190); ^{1}H NMR (400 MHz, $CDCl_3$, DMSO-d_6) δ_{ppm} 9.58 (br, s, 1H), 7.32 (s, 1H), 7.23 (d, 1H, J = 8 Hz), 6.87-6.84 (m, 1H), 5.49 (s, 1H), 3.29-3.11 (m, 2H), 2.19 (s, 3H); ^{13}C NMR (100 MHz, $CDCl_3$ + CD_3OD) δ_{ppm} 205.8, 178.9, 140.4, 133.2, 129.7, 127.1, 124.0, 111.1, 73.0, 49.4, 29.1; HRMS [ESI] calcd. for $C_{11}H_{10}ClNO_3$ $[M + H]^+$ 240.0422, found 240.0420.

1-(5-Chloro-3-hydroxy-2-oxoindolin-3-yl)pentane-2,4-dione (28): As yellow semi-solid (40% yield; mp: 142-144 °C); ^{1}H NMR (600 MHz, $CDCl_3$) δ_{ppm} 7.41 (s, 1H), 7.25-7.24 (m, 1H), 6.65-6.62 (m, 1H), 6.36 (br, s, 1H), 3.69 (s, 2H), 3.28 (s, 2H), 1.69 (s, 3H); ^{13}C NMR (151 MHz, $CDCl_3$) δ_{ppm} 193.5, 165.1, 150.2, 136.2, 132.0, 120.8, 118.9, 115.1, 47.4, 42.4, 26.4, 24.6; HRMS [ESI] calcd. for $C_{13}H_{12}ClNO_4$ $[M + H]^+$ 282.0528 found 282.0398.

References

(1) Takikawa, O.; Yoshida, R.; Kido, R.; Hayaishi, O. Tryptophan Degradation in Mice Initiated by Indoleamine 2,3-Dioxygenase. *J. Biol. Chem.* **1986**, *261*, 3648-3653.

(2) Takikawa, O.; Kuroiwa, T.; Yamazaki, F.; Kido, R. Mechanism of Interferon-Gamma Action - Characterization of Indoleamine 2,3-Dioxygenase in Cultured Human-Cells Induced by Interferon-Gamma and Evaluation of the Enzyme-Mediated Tryptophan Degradation in Its Anticellular Activity. *J. Biol. Chem.* **1988**, *263*, 2041-2048.

(3) Croitoru-Lamoury, J.; Lamoury, F. M.; Caristo, M.; Suzuki, K.; Walker, D.; Takikawa, O.; Taylor, R.; Brew, B. J. Interferon-gamma regulates the proliferation and differentiation of mesenchymal stem cells via activation of indoleamine 2,3 dioxygenase (IDO). *PLoS One* **2011**, *6*, e14698.

(4) Rohrig, U. F.; Majjigapu, S. R.; Vogel, P.; Zoete, V.; Michielin, O. Challenges in the Discovery of Indoleamine 2,3-Dioxygenase 1 (IDO1) Inhibitors. *J. Med. Chem.* **2015**, *58*, 9421-9437.

(5) Vazquez, S.; Parker, N. R.; Sheil, M.; Truscott, R. J. Protein-bound kynurenine decreases with the progression of age-related nuclear cataract. *Invest. Ophthalmol. Vis. Sci.* **2004**, *45*, 879-883.

(6) Uyttenhove, C.; Pilotte, L.; Theate, I.; Stroobant, V.; Colau, D.; Parmentier, N.; Boon, T.; Van den Eynde, B. J. Evidence for a tumoral immune resistance mechanism based on tryptophan degradation by indoleamine 2,3-dioxygenase. *Nat. Med.* **2003**, *9*, 1269-1274.

(7) Okamoto, A.; Nikaido, T.; Ochiai, K.; Takakura, S.; Saito, M.; Aoki, Y.; Ishii, N.; Yanaihara, N.; Yamada, K.; Takikawa, O.; Kawaguchi, R.; Isonishi, S.; Tanaka, T.; Urashima, M. Indoleamine 2,3-dioxygenase serves as a marker of poor prognosis in gene expression profiles of serous ovarian cancer cells. *Clin. Cancer Res.* **2005**, *11*, 6030-6039.

(8) Paul, S.; Roy, A.; Deka, S.J.; Panda, S.; Trivedi, V.; Manna, D. Nitrobenzofurazan derivatives of N'-hydroxyamidines as potent inhibitors of indoleamine-2,3-dioxygenase 1. *Eur. J. Med. Chem.* **2016**, *121*, 364-375.

(9) Malachowski, W. P.; Winters, M.; DuHadaway, J. B.; Lewis-Ballester, A.; Badir, S.; Wai, J.; Rahman, M.; Sheikh, E.; LaLonde, J. M.; Yeh, S. R.; Prendergast, G. C.; Muller, A. J. O-alkylhydroxylamines as rationally-designed mechanism-based inhibitors of indoleamine 2,3-dioxygenase-1. *Eur. J. Med. Chem.* **2016**, *108*, 564-576.

(10) Dunn, G. P.; Old, L. J.; Schreiber, R. D. The immunobiology of cancer immunosurveillance and immunoediting. *Immunity* **2004**, *21*, 137-148.

(11) Peterson, A. C.; Migawa, M. T.; Martin, M. J.; Hamaker, L. K.; Czerwinski, K. M.; Zhang, W.; Arend, R. A.; Fisette, P. L.; Ozaki, Y.; Will, J. A.; Brown, R. R.; Cook, J.M. Evaluation of functionalized tryptophan derivatives and related compounds as competitive inhibitors of indoleamine 2,3-dioxygenase. *Med. Chem. Res.* **1994**, *3*, 531-544.

(12) Southan, M. D.; Truscott, R. J. W.; Jamie, J. F.; Pelosi, L.; Walker, M. J.; Maeda, H.; Iwamoto, Y.; Tone, S. Structural requirements of the competitive binding site of recombinant human indoleamine 2,3-dioxygenase. *Med. Chem. Res.* **1996**, *6*, 343-352.

(13) Dolusic, E.; Larrieu, P.; Blanc, S.; Sapunaric, F.; Norberg, B.; Moineaux, L.; Colette, D.; Stroobant, V.; Pilotte, L., Colau, D.; Ferain, T.; Fraser, G.; Galleni, M.; Frere, J. M.; Masereel, B.; Van den Eynde, B.; Wouters, J.; Frederick, R. Indol-2-yl ethanones as novel indoleamine 2,3-dioxygenase (IDO) inhibitors. *Bioorg. Med. Chem.* **2011**, *19*, 1550-1561.

(14) Dolusic, E.; Larrieu, P.; Blanc, S.; Sapunaric, F.; Pouyez, J.; Moineaux, L.; Colette, D.; Stroobant, V.; Pilotte, L.; Colau, D.; Ferain, T.; Fraser, G.; Galleni, M.; Frere, J. M.; Masereel, B.; Van den Eynde, B.; Wouters, J.; Frederick, R. Discovery and preliminary SARs of keto-indoles as novel indoleamine 2,3-dioxygenase (IDO) inhibitors. *Eur. J. Med. Chem.* **2011**, *46*, 3058-3065.

(15) Tanaka, M.; Li, X.; Hikawa, H.; Suzuki, T.; Tsutsumi, K.; Sato, M.; Takikawa, O.; Suzuki, H.; Yokoyama, Y. Synthesis and biological evaluation of novel tryptoline derivatives as indoleamine 2,3-dioxygenase (IDO) inhibitors. *Bioorg. Med. Chem.* **2013**, *21*, 1159-1165.

(16) Pantouris, G.; Loudon-Griffiths, J.; Mowat, C. G. Insights into the mechanism of inhibition of tryptophan 2,3-dioxygenase by isatin derivatives. *J. Enzyme Inhib. Med. Chem.* **2016**, *31*, 70-78.

(17) Lin, S. Y.; Yeh, T. K.; Kuo, C. C.; Song, J. S.; Cheng, M. F.; Liao, F. Y.; Chao, M. W.; Huang, H. L.; Chen, Y. L.; Yang, C. Y.; Wu, M. H.; Hsieh, C. L.; Hsiao, W.; Peng, Y. H.; Wu, J. S.; Lin, L. M.; Sun, M.; Chao, Y. S.; Shih, C.; Wu, S. Y.; Pan, S. L.; Hung, M. S.; Ueng, S.H. Phenyl Benzenesulfonylhydrazides Exhibit Selective Indoleamine 2,3-Dioxygenase Inhibition with Potent in Vivo Pharmacodynamic Activity and Antitumor Efficacy. *J. Med. Chem.* **2016**, *59*, 419-430.

(18) Chung, L. W.; Li, X.; Sugimoto, H.; Shiro, Y.; Morokuma, K. Density functional theory study on a missing piece in understanding of heme chemistry: the reaction mechanism for indoleamine 2,3-dioxygenase and tryptophan 2,3-dioxygenase. *J. Am. Chem. Soc.* **2008**, *130*, 12299-12309.

(19) Lewis-Ballester, A.; Batabyal, D.; Egawa, T.; Lu, C.; Lin, Y.; Marti, M. A.; Capece, L.; Estrin, D. A.; Yeh, S. R. Evidence for a ferryl intermediate in a heme-based dioxygenase. *Proc. Natl. Acad. Sci. U S A* **2009**, *106*, 17371-17376.

(20) Capece, L.; Lewis-Ballester, A.; Yeh, S. R.; Estrin, D. A.; Marti, M. A. Complete reaction mechanism of indoleamine 2,3-dioxygenase as revealed by QM/MM simulations. *J. Phys. Chem. B* **2012**, *116*, 1401-1413.

(21) Lockman, J. W.; Reeder, M. D.; Robinson, R.; Ormonde, P. A.; Cimbora, D. M.; Williams, B. L.; Willardsen, J. A. Oxindole derivatives as inhibitors of TAK1 kinase. *Bioorg. Med. Chem. Lett.* **2011**, *21*, 1724-1727.

(22) Yu, L. F.; Li, Y. Y.; Su, M. B.; Zhang, M.; Zhang, W.; Zhang, L. N.; Pang, T.; Zhang, R. T.; Liu, B.; Li, J. Y.; Li, J.; Nan, F.J. Development of Novel Alkene Oxindole Derivatives As Orally Efficacious AMP-Activated Protein Kinase Activators. *Acs. Med. Chem. Lett.* **2013**, *4*, 475-480.

(23) Fatima, I.; Ahmad, I.; Anis, I.; Malik, A.; Afza, N. Isatinones A and B, new antifungal oxindole alkaloids from *Isatis costata*. *Molecules* **2007**, *12*, 155-162.

(24) Khan, K. M.; Khan, M.; Ambreen, N.; Taha, M.; Rahim, F.; Rasheed, S.; Saied, S.; Shafi, H.; Perveen, S.; Choudhary, M. I. Oxindole Derivatives: Synthesis and Antiglycation Activity. *Med. Chem.* **2013**, *9*, 681-688.

(25) Winkler, C.; Wirleitner, B.; Schroecksnadel, K.; Schennach, H.; Mur, E.; Fuchs, D. In vitro effects of two extracts and two pure alkaloid preparations of Uncaria tomentosa on peripheral blood mononuclear cells. *Planta. Med.* **2004**, *70*, 205-210.

(26) Kuehnl, S.; Schroecksnadel, S.; Temml, V.; Gostner, J. M.; Schennach, H.; Schuster, D.; Schwaiger, S.; Rollinger, J. M.; Fuchs, D.; Stuppner, H. Lignans from Carthamus tinctorius suppress tryptophan breakdown via indoleamine 2,3-dioxygenase. *Phytomedicine* **2013**, *20*, 1190-1195.

(27) Kleijn, L. H. J.; Muskens, F. M.; Oppedijk, S. F.; de Bruin, G.; Martin, N. I. A concise preparation of the non-proteinogenic amino acid L-kynurenine. *Tetrahedron. Lett.* **2012**, *53*, 6430-6432.

(28) Doan, N. D.; Hopewell, R.; Lubell, W. D. N-aminoimidazolidin-2-one peptidomimetics. *Org. Lett.* **2014**, *16*, 2232-2235.

(29) Cobb, A. J. A.; Shaw, D. M.; Longbottom, D. A.; Gold, J. B.; Ley, S.V. Organocatalysis with proline derivatives: improved catalysts for the asymmetric Mannich, nitro-Michael and aldol reactions. *Org. Biomol. Chem.* **2005**, *3*, 84-96.

(30) Liang, C. Y.; Xia, J.; Lei, D.; Li, X.; Yao, Q. Z.; Gao, J. Synthesis, in vitro and in vivo antitumor activity of symmetrical bis-Schiff base derivatives of isatin. *Eur. J. Med. Chem.* **2014**, *74*, 742-750.

(31) Liu, H. X.; Wu, H. Y.; Luo, Z. L.; Shen, J.; Kang, G. W.; Liu, B. D.; Wan, Z. F.; Jiang, J. Regioselectivity-Reversed Asymmetric Aldol Reaction of 1,3-Dicarbonyl Compounds. *Chem. Eur. J.* **2012**, *18*, 11899-11903.

(32) Klock, C.; Jin, X.; Choi, K. H.; Khosla, C.; Madrid, P. B.; Spencer, A.; Raimundo, B. C.; Boardman, P.; Lanza, G.; Griffin, J. H. Acylideneoxoindoles: A new class of reversible inhibitors of human transglutaminase 2. *Bioorg. Med. Chem. Lett.* **2011**, *21*, 2692-2696.

(33) Austin, C. J. D.; Mizdrak, J.; Matin, A.; Sirijovski, N.; Kosim-Satyaputra, P.; Willows, R. D.; Roberts, T. H.; Truscott, R. J. W.; Polekhina, G.; Parker, M. W.; Jamie, J. F. Optimised expression and purification of recombinant human indoleamine 2,3-dioxygenase. *Protein Expr. Purif.* **2004**, *37*, 392-398.

(34) Huang, Q.; Zheng, M. F.; Yang, S. S.; Kuang, C. X.; Yu, C. J.; Yang, Q. Structure-activity relationship and enzyme kinetic studies on 4-aryl-1H-1,2, 3-triazoles as indoleamine 2,3-dioxygenase (IDO) inhibitors. *Eur. J. Med. Chem.* **2011**, *46*, 5680-5687.

(35) Cady, S. G.; Sono, M. 1-Methyl-Dl-Tryptophan, Beta-(3-Benzofuranyl)-Dl-Alanine (the Oxygen Analog of Tryptophan), and Beta-[3-Benzo(B)Thienyl]-Dl-Alanine (the Sulfur Analog of Tryptophan) Are Competitive Inhibitors for Indoleamine 2,3-Dioxygenase. *Arch. Biochem. Biophys.***1991**, *291*, 326-333.

(36) Dawson, J. H.; Andersson, L. A.; Sono, M. Spectroscopic investigations of ferric cytochrome P-450-CAM ligand complexes. Identification of the ligand trans to cysteinate in the native enzyme. *J. Biol. Chem.* **1982**, *257*, 3606-3617.

(37) Littlejohn, T. K.; Takikawa, O.; Skylas, D.; Jamie, J. F.; Walker, M. J.; Truscott, R. J. Expression and purification of recombinant human indoleamine 2, 3-dioxygenase. *Protein Expr. Purif.* **2000**, *19*, 22-29.

(38) Rohrig, U. F.; Majjigapu, S. R.; Grosdidier, A.; Bron, S.; Stroobant, V.; Pilotte, L.; Colau, D.; Vogel, P.; Van den Eynde, B. J.; Zoete, V.; Michielin, O. Rational design of 4-aryl-1,2,3-triazoles for indoleamine 2,3-dioxygenase 1 inhibition. *J. Med. Chem.* **2012**, *55*, 5270-5290.

(39) Schenkman, J. B.; Sligar, S. G.; Cinti, D.L. Substrate interaction with cytochrome P-450. *Pharmacol. Ther.* **1981**, *12*, 43-71.

(40) Panda, S.; Roy, A.; Deka, S. J.; Trivedi, V.; Manna, D. Fused Heterocyclic Compounds as Potent Indoleamine-2,3-dioxygenase 1 Inhibitors. *ACS Med. Chem. Lett.* **2016**, *7*, 1167–1172.

(41) Travers, M. T.; Gow, I. F.; Barber, M. C.; Thomson, J.; Shennan, D. B. Indoleamine 2,3-dioxygenase activity and L-tryptophan transport in human breast cancer cells. *Biochim. Biophys. Acta-Biomem.* **2004**, *1661*, 106-112.

(42) Rohrig, U. F.; Awad, L.; Grosdidier, A.; Larrieu, P.; Stroobant, V.; Colau, D.; Cerundolo, V.; Simpson, A. J. G.; Vogel, P.; Van den Eynde, B. J.; Zoete, V.; Michielin, O. Rational Design of Indoleamine 2,3-Dioxygenase Inhibitors. *J. Med. Chem.* **2010**, *53*, 1172-1189.

(43) Sugimoto, H.; Oda, S.; Otsuki, T.; Hino, T.; Yoshida, T.; Shiro, Y. Crystal structure of human indoleamine 2,3-dioxygenase: catalytic mechanism of O_2 incorporation by a heme-containing dioxygenase. *Proc. Natl. Acad. Sci. USA* **2006**, *103*, 2611-2616.

(44) Yuasa, H. J.; Mizuno, K.; Ball, H.J. Low efficiency IDO2 enzymes are conserved in lower vertebrates, whereas higher efficiency IDO1 enzymes are dispensable. *FEBS. J.* **2015**, *282*, 2735-2745.

(45) Yuasa, H. J. High l-Trp affinity of indoleamine 2,3-dioxygenase 1 is attributed to two residues located in the distal heme pocket. *FEBS J.* **2016**, *283*, 3651-3661.

(46) Wang, L.; Murai, Y.; Yoshida, T.; Okamoto, M.; Masuda, K.; Sakihama, Y.; Hashidoko, Y.; Hatanaka, Y.; Hashimoto, M. Hydrogen/deuterium exchange of cross-linkable alpha-amino acid derivatives in deuterated triflic acid. *Biosci. Biotech. Biochem.* **2014**, *78*, 1129-1134.

(47) Zhang, J. C.; Zhang, F. F.; Wang, L. W.; Du, J. L.; Wang, S. X.; Li, S.H. Synthesis, characterization, and cytotoxicity of complexes of platinum(II) with 2,2 '-bipyridine and *N*-benzoyl-L-amino acid dianion. *J. Coord. Chem.* **2012**, *65*, 2159-2169.

(48) Yang, S. S.; Li, X. S.; Hu, F. F.; Li, Y. L.; Yang, Y. Y.; Yan, J. K.; Kuang, C. X.; Yang, Q. Discovery of Tryptanthrin Derivatives as Potent Inhibitors of Indoleamine 2,3-Dioxygenase with Therapeutic Activity in Lewis Lung Cancer (LLC) Tumor-Bearing Mice. *J. Med. Chem.* **2013**, *56*, 8321-8331.

(49) Gorai, S.; Paul, S.; Sankaran, G.; Borah, R.; Santra, M. K.; Manna, D. Inhibition of phosphatidylinositol-3,4,5-trisphosphate binding to the AKT pleckstrin homology domain by 4-amino-1,2,5-oxadiazole derivatives. *Med. Chem. Comm.* **2015**, *6*, 1798-1808.

3.13. NMR Spectra of the Synthesized Compounds

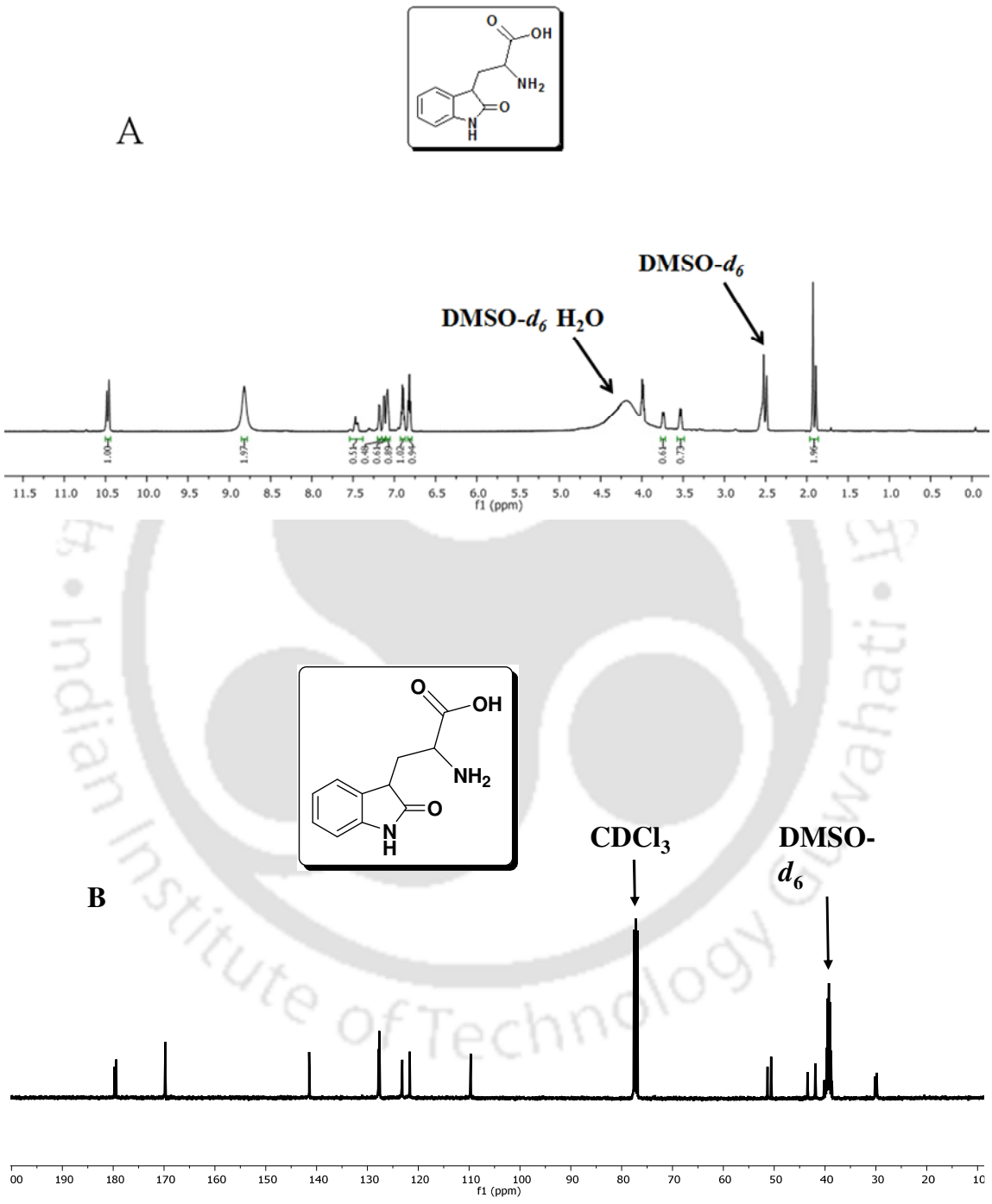

Figure 3.13.1. ^{1}H NMR **(A)** and ^{13}C NMR **(B)** spectra of 2-Amino-3-(2-oxoindolin-3-yl) propanoic acid (**2**)**.**

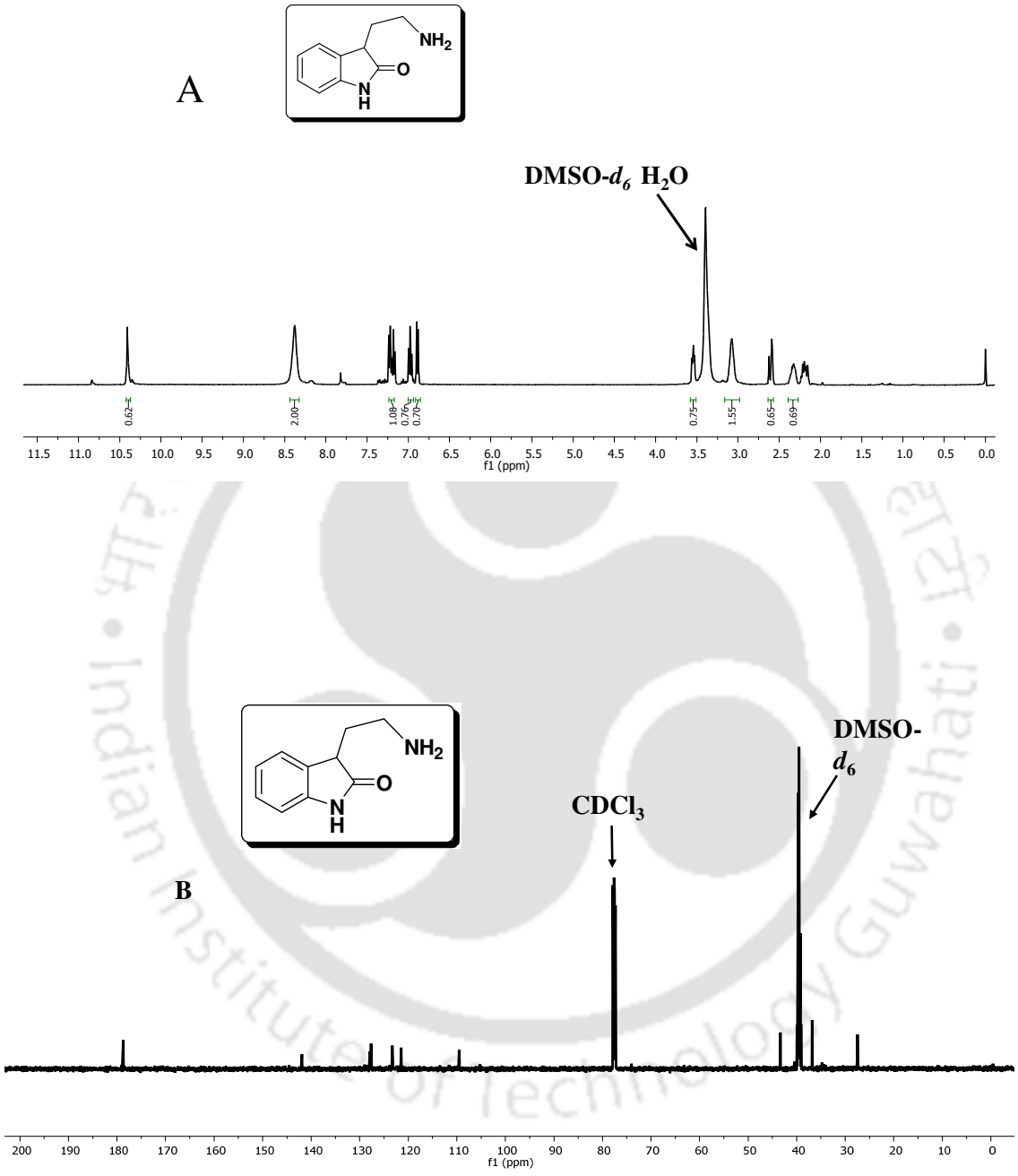

Figure 3.13.2. ^{1}H NMR **(A)** and ^{13}C NMR **(B)** spectra of 3-(2-aminoethyl)indolin-2-one **(3).**

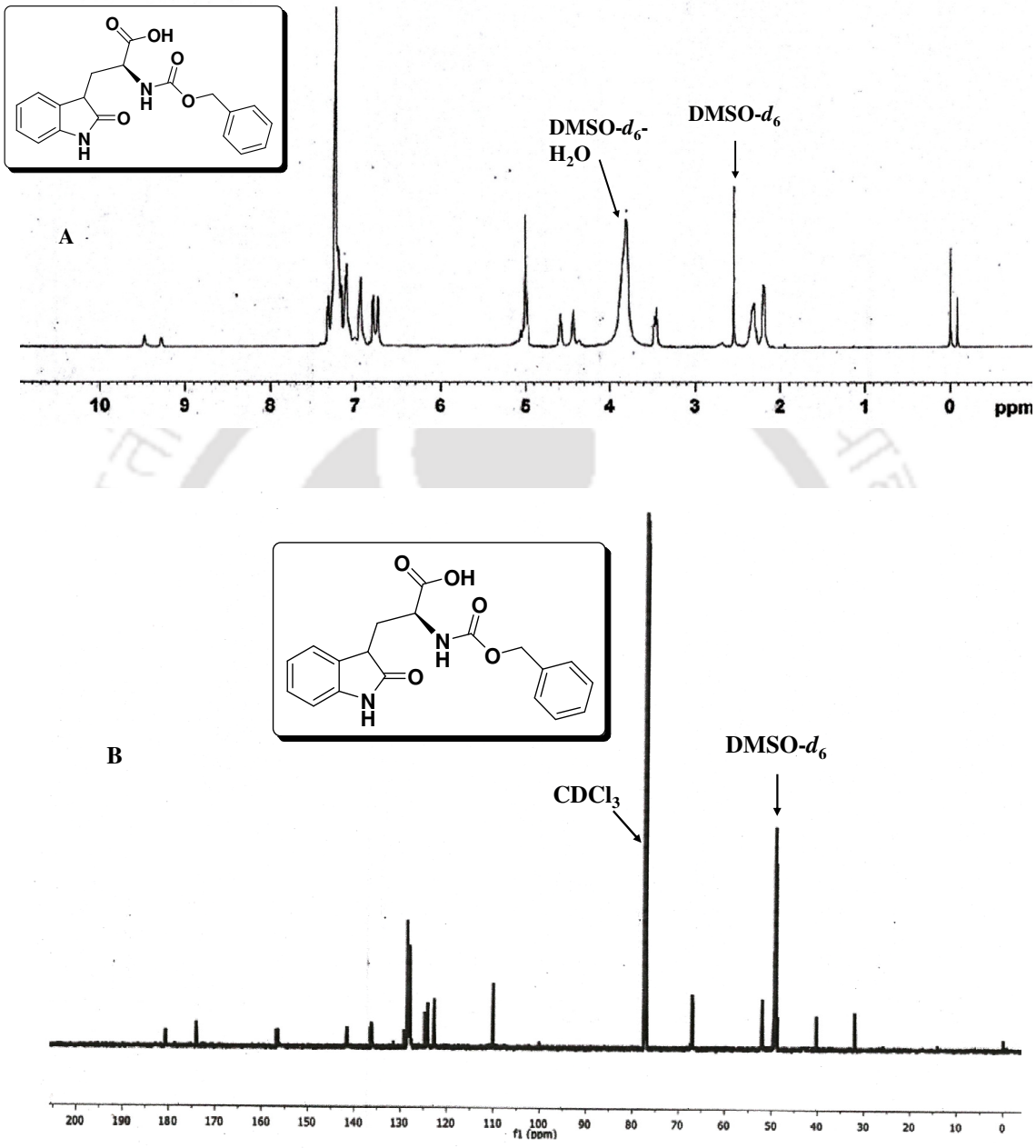

Figure 3.13.3. ^{1}H NMR **(A)** and ^{13}C NMR **(B)** spectra of 2-[((Benzyloxy)carbonyl)amino]-3-(2-oxoindolin-3-yl)propanoic acid **(4).**

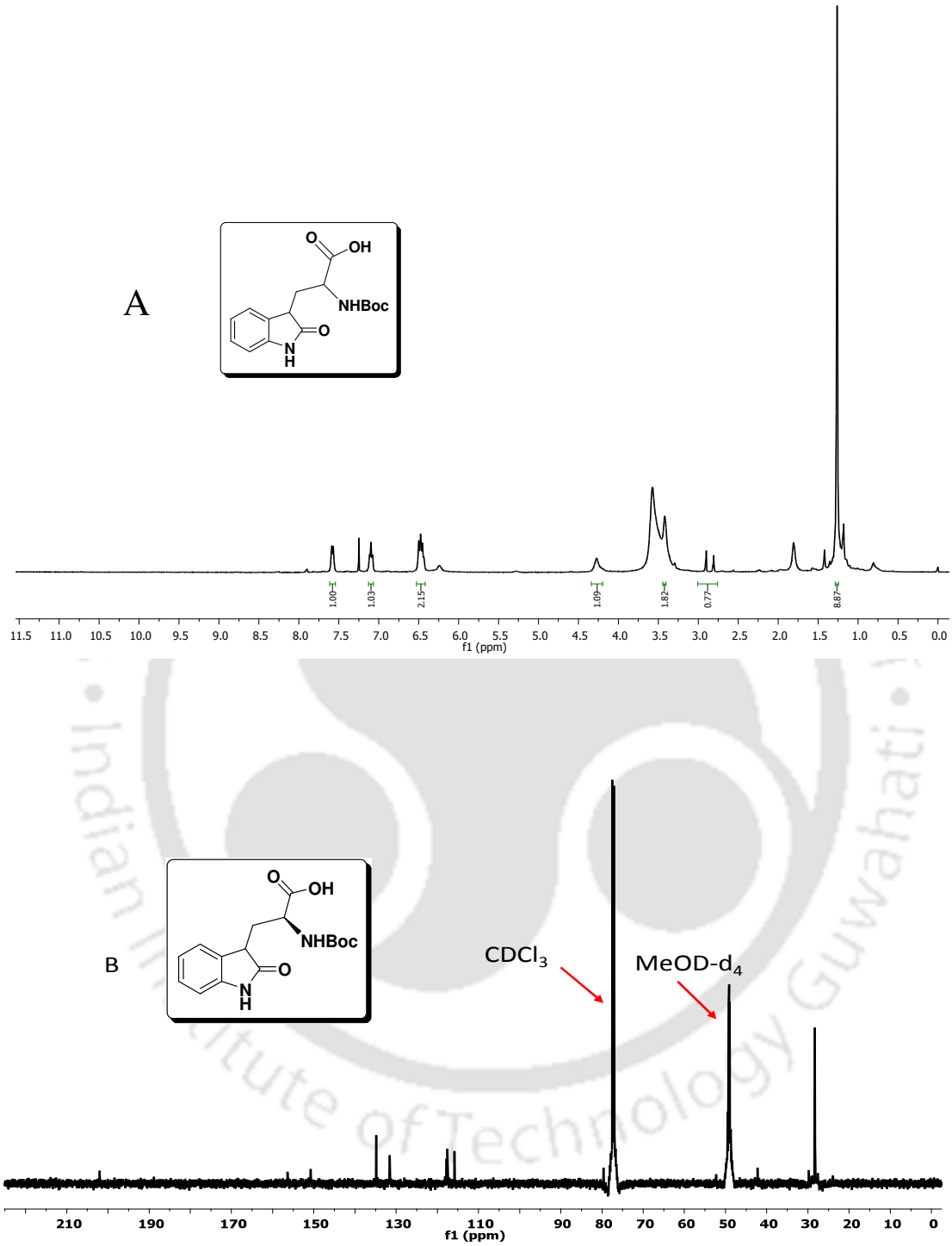

Figure 3.13.4. ^{1}H NMR **(A)** and ^{13}C NMR **(B)** spectra of 2-((Tert-butoxycarbonyl)amino)-3-(2-oxoindolin-3-yl)propanoic acid **(5).**

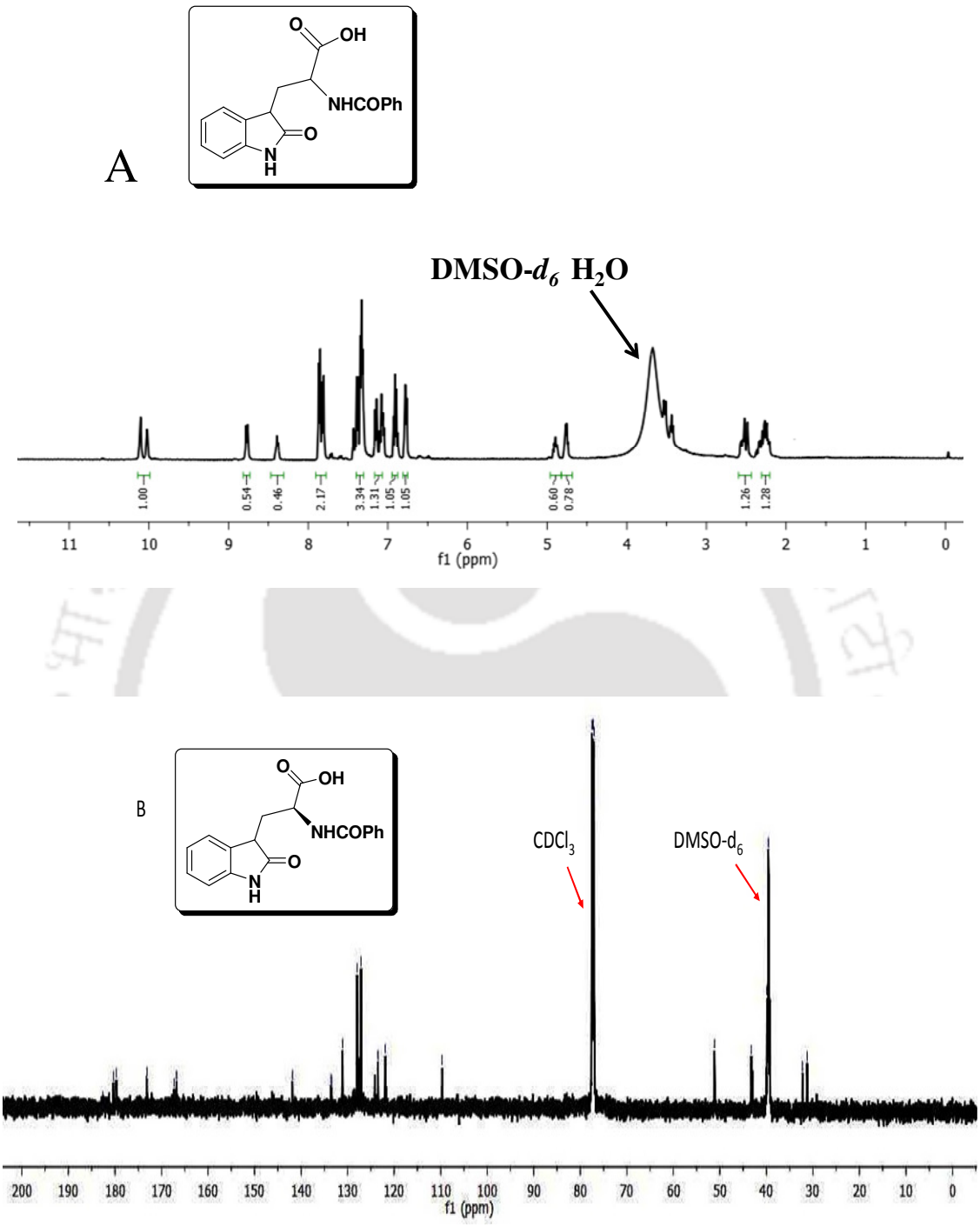

Figure 3.13.5. ^{1}H NMR **(A)** and ^{13}C NMR **(B)** spectra of 2-Benzamido-3-(2-oxoindolin-3-yl)propanoic acid (isomeric mixture of **6**).

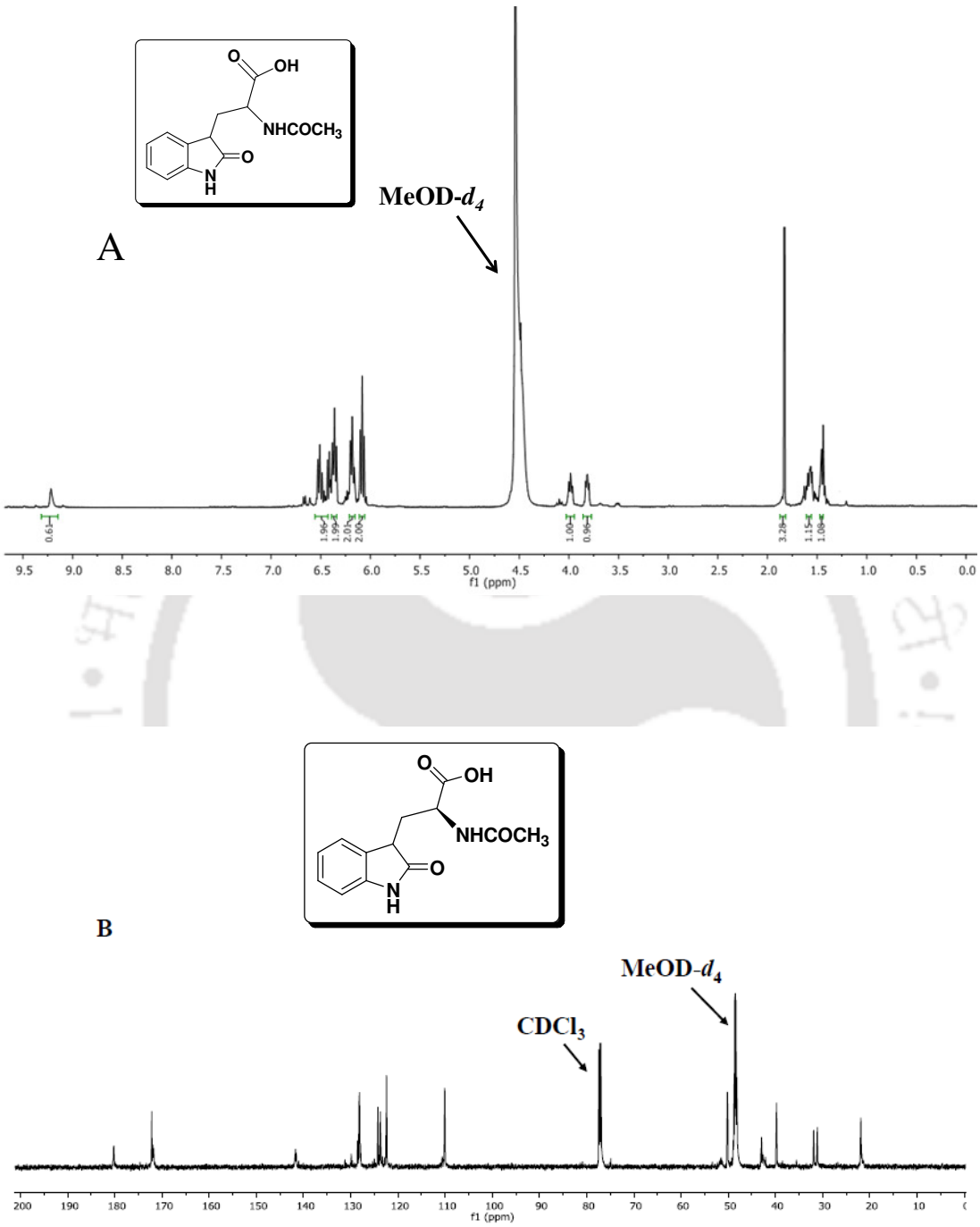

Figure 3.13.6. ^{1}H NMR **(A)** and ^{13}C NMR **(B)** spectra of 2-Acetamido-3-(2-oxoindolin-3-yl)propanoic acid (isomeric mixture of **7**).

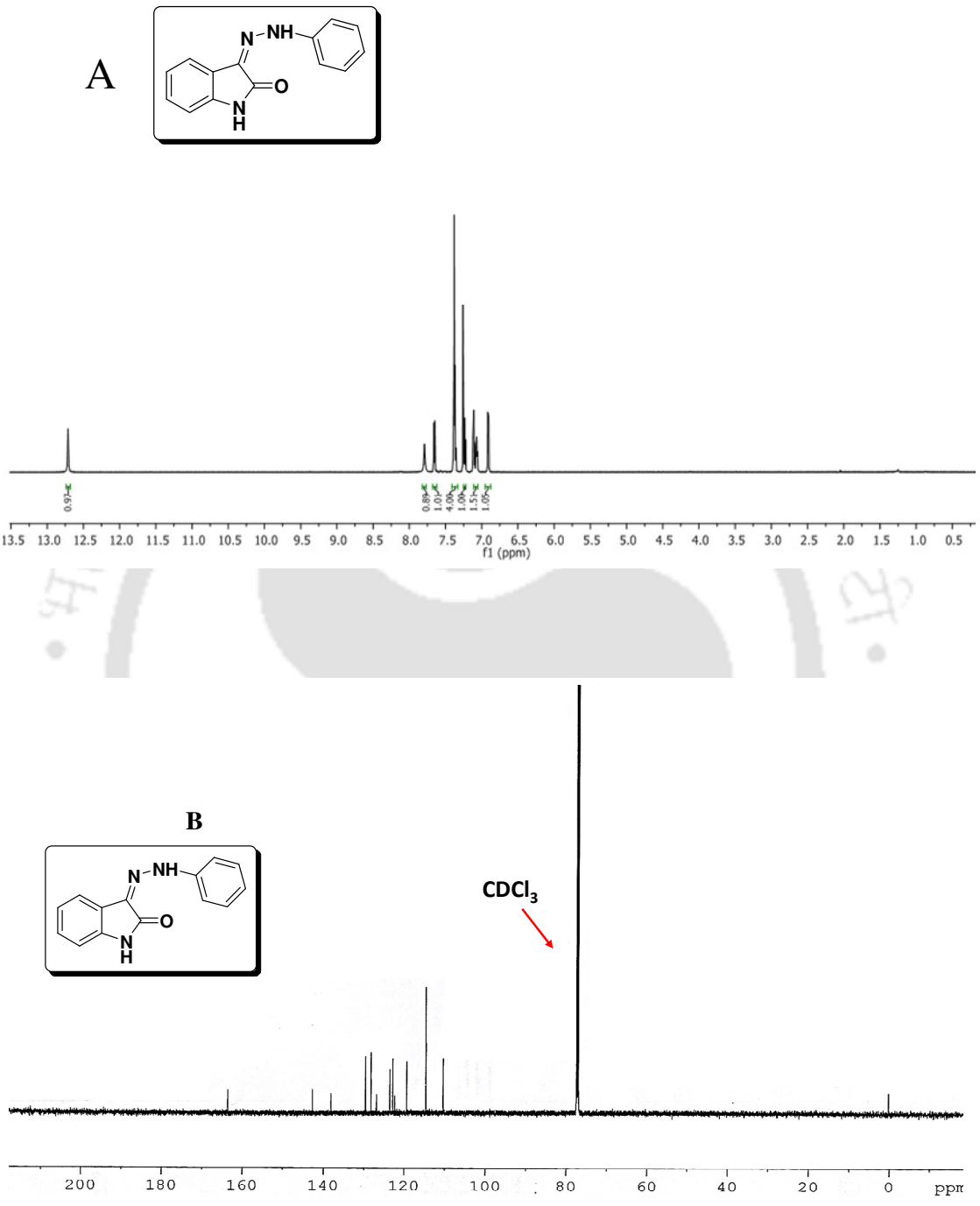

Figure 3.13.7. ^{1}H NMR **(A)** and ^{13}C NMR **(B)** spectra of 3-(2-Phenyl-hydrazono)indolin-2-one (**12**).

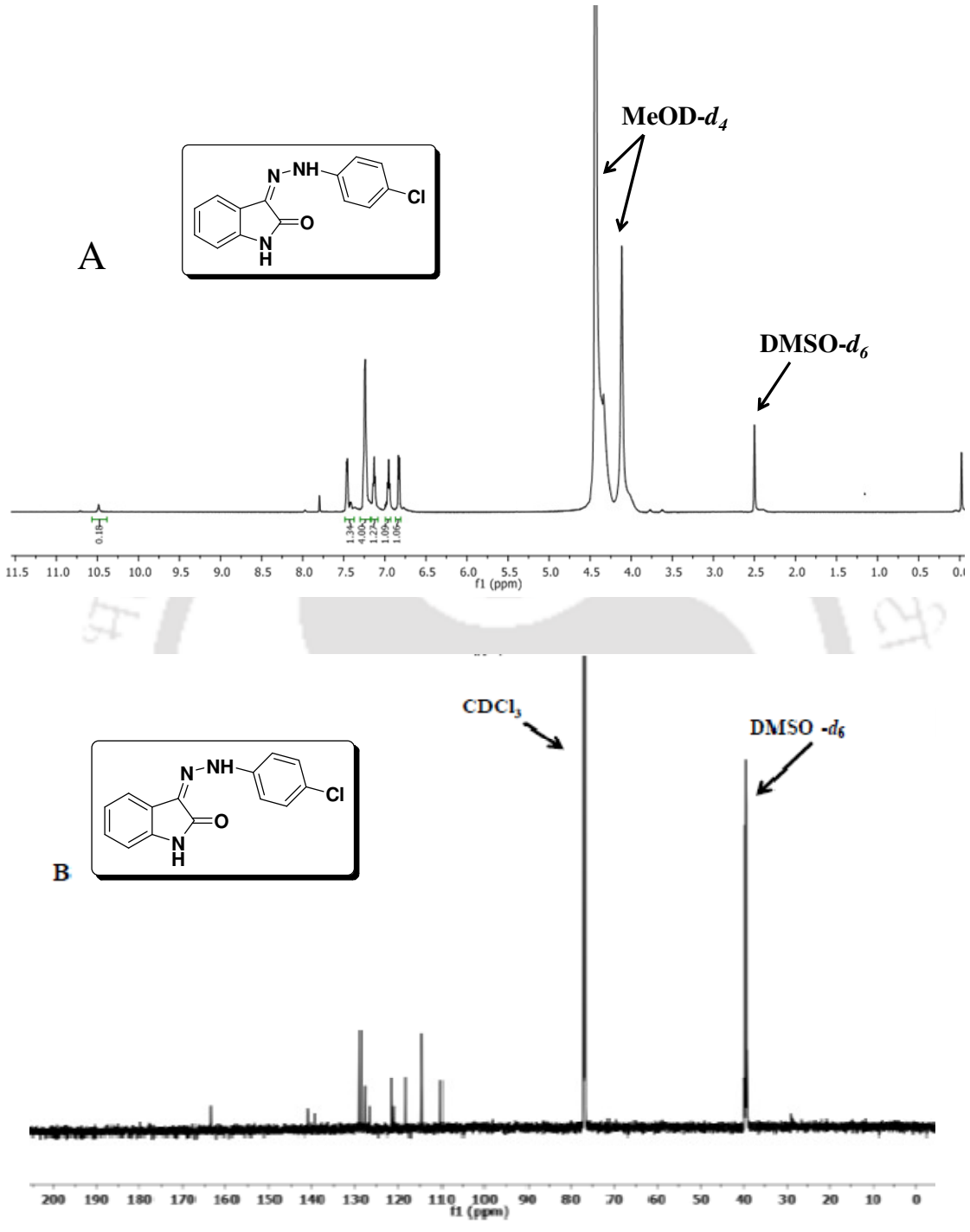

Figure 3.13.8. ^{1}H NMR **(A)** and ^{13}C NMR **(B)** spectra of 3-[2-(4-Chlorophenyl)hydrazono]indolin-2-one (**13**).

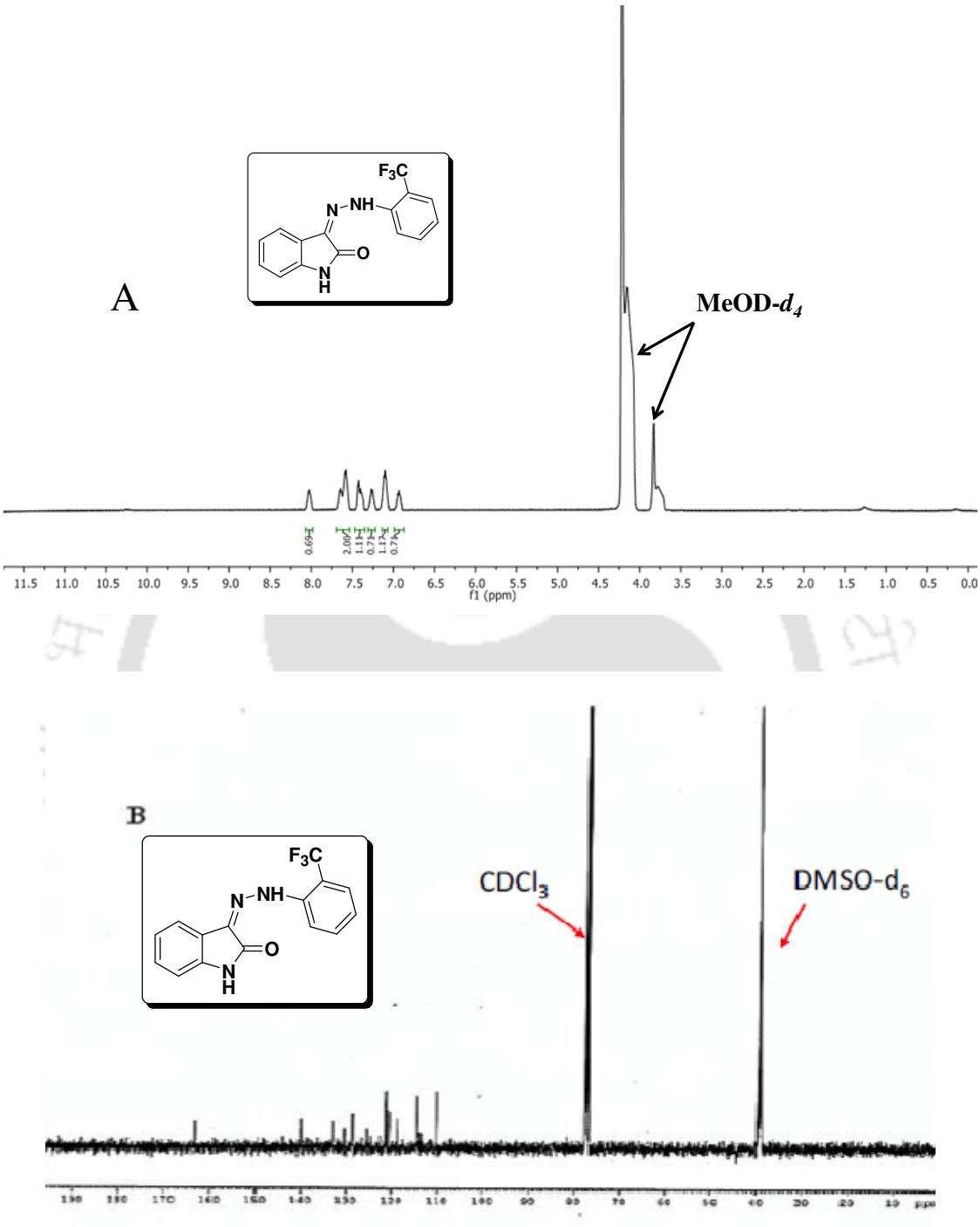

Figure 3.13.9. ^{1}H NMR **(A)** and ^{13}C NMR **(B)** spectra of 3-[2-(2-(Trifluoromethyl)phenyl)-hydrazono]indolin-2-one (**16**).

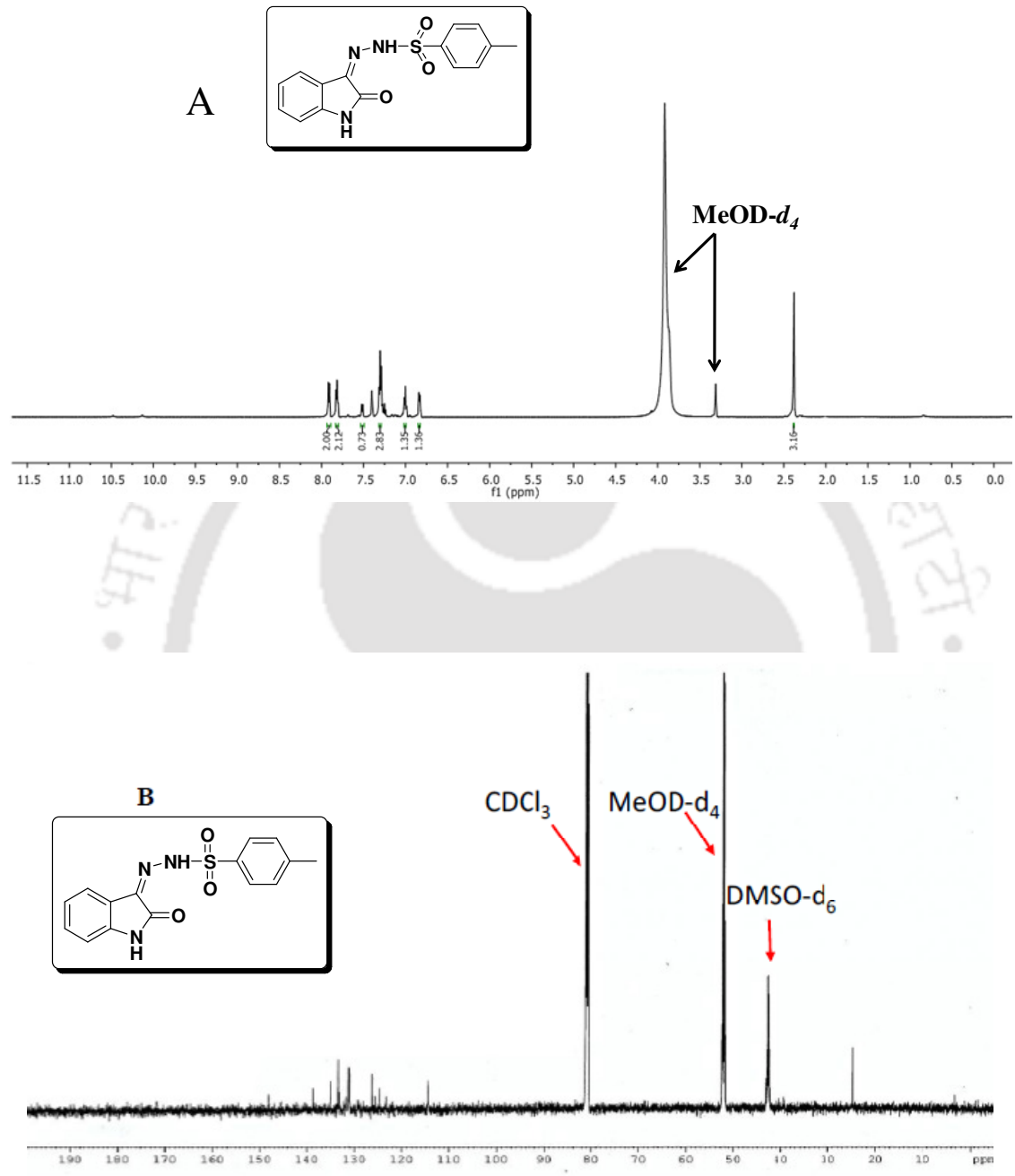

Figure 3.13.10. ^{1}H NMR **(A)** and ^{13}C NMR **(B)** spectra of 4-Methyl-N'-(2-oxoindolin-3-ylidene)benzenesulfonohydrazide (**17**)**.**

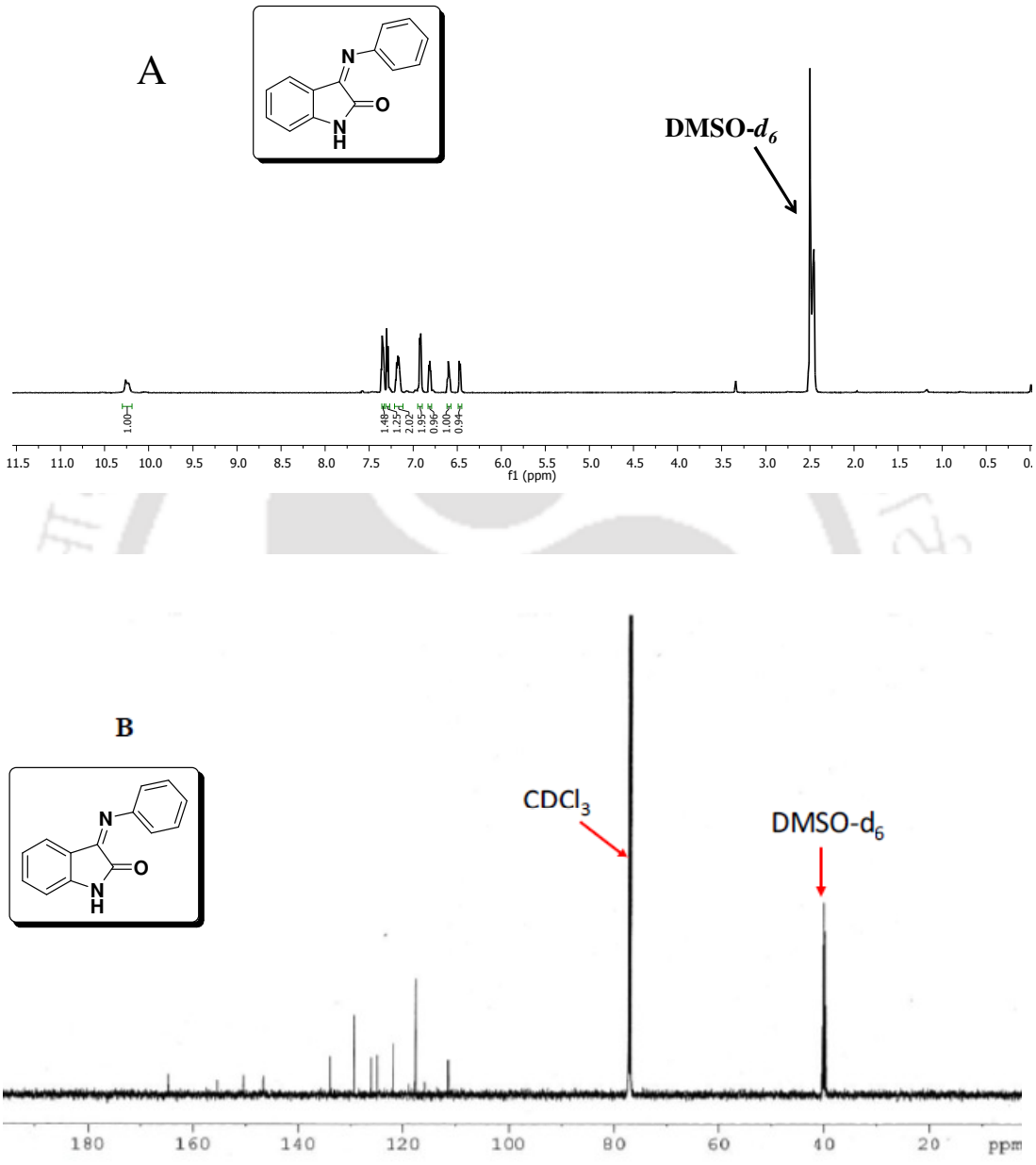

Figure 3.13.11. ^{1}H NMR **(A)** and ^{13}C NMR **(B)** spectra of 3-(Phenylimino)indolin-2-one (**18**).

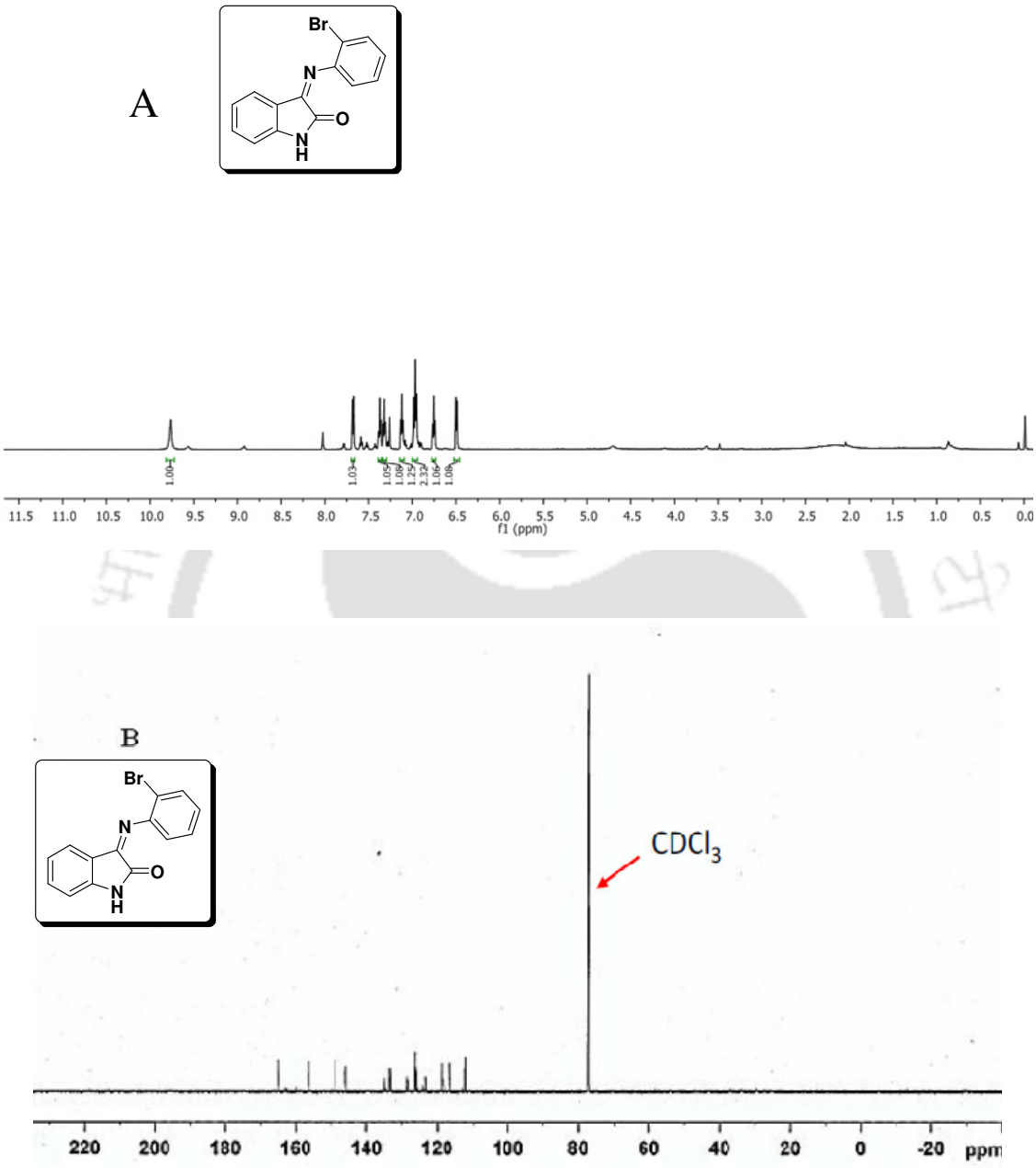

Figure 3.13.12. ^{1}H NMR **(A)** and ^{13}C NMR **(B)** spectra of 3-[(2-Bromophenyl)-imino]indolin-2-one (**20**)**.**

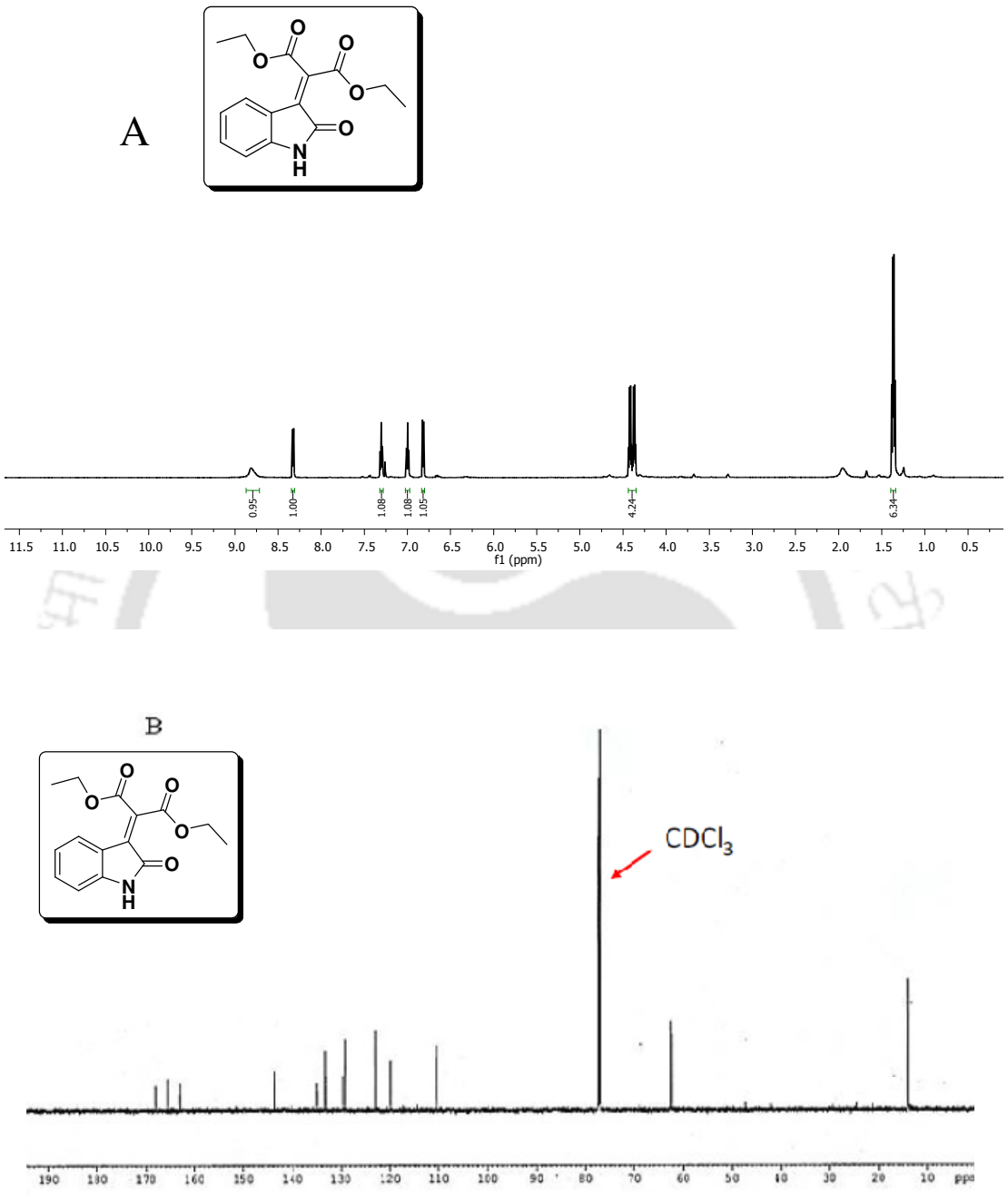

Figure 3.13.13. ^{1}H NMR **(A)** and ^{13}C NMR **(B)** spectra of Diethyl 2-(2-oxoindolin-3-ylidene)malonate (**21**).

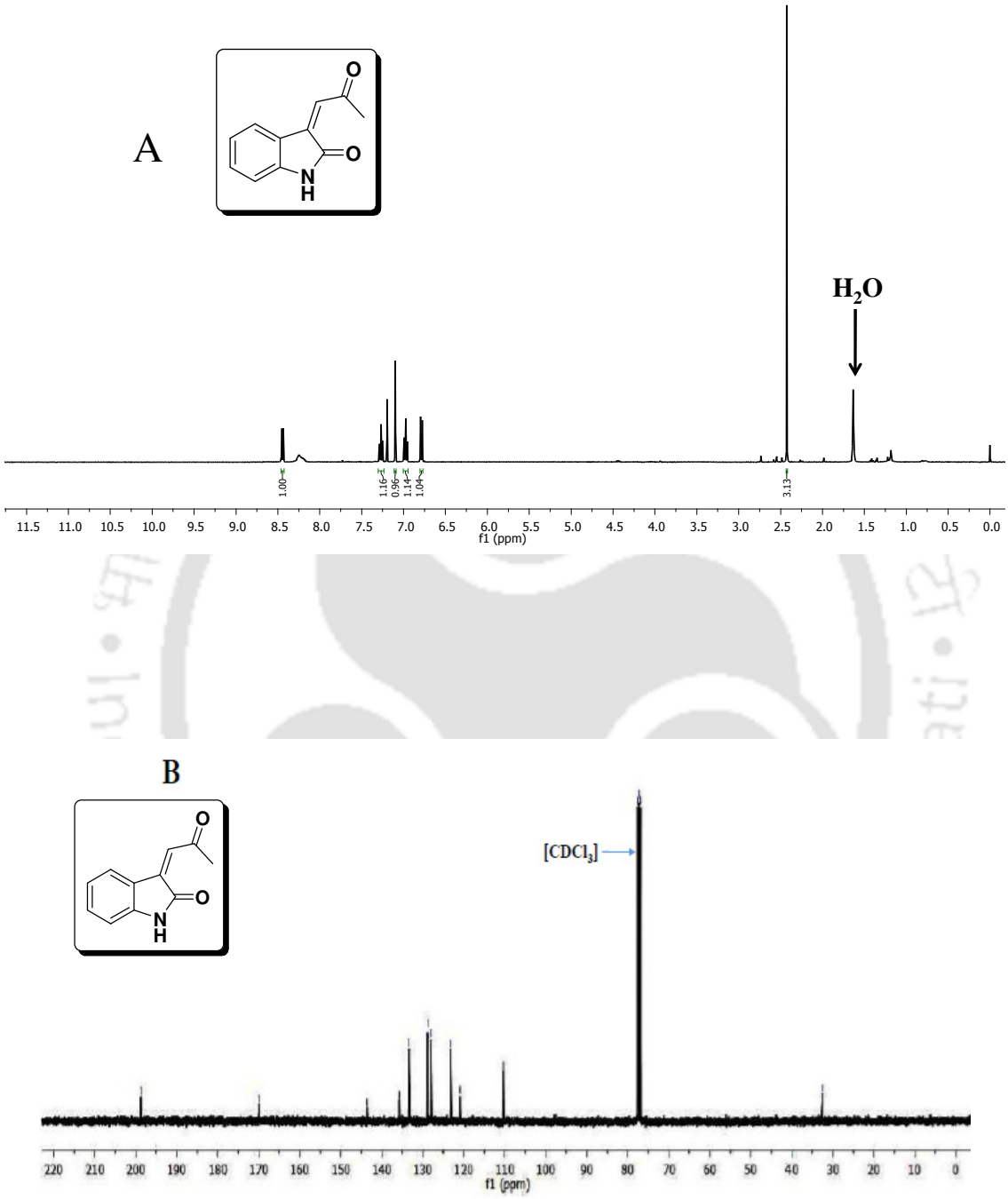

Figure 3.13.14. ^{1}H NMR **(A)** and ^{13}C NMR **(B)** spectra of 3-(2-Oxopropylidene)indole-2-one (**22**).

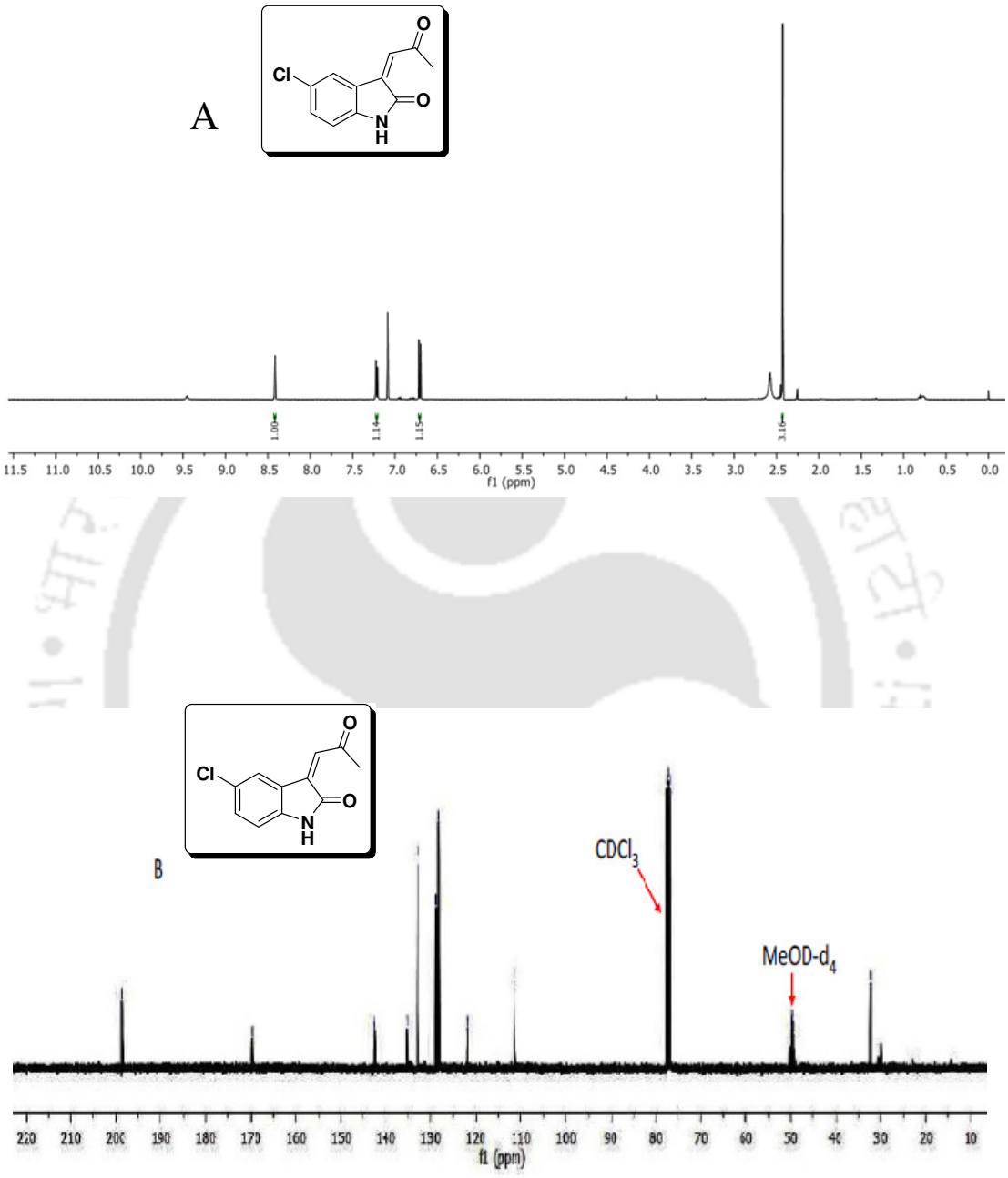

Figure 3.13.15. ^{1}H NMR **(A)** and ^{13}C NMR **(B)** spectra of 5-Chloro-3-(2-oxopropylidene)indole-2-one (**23**).

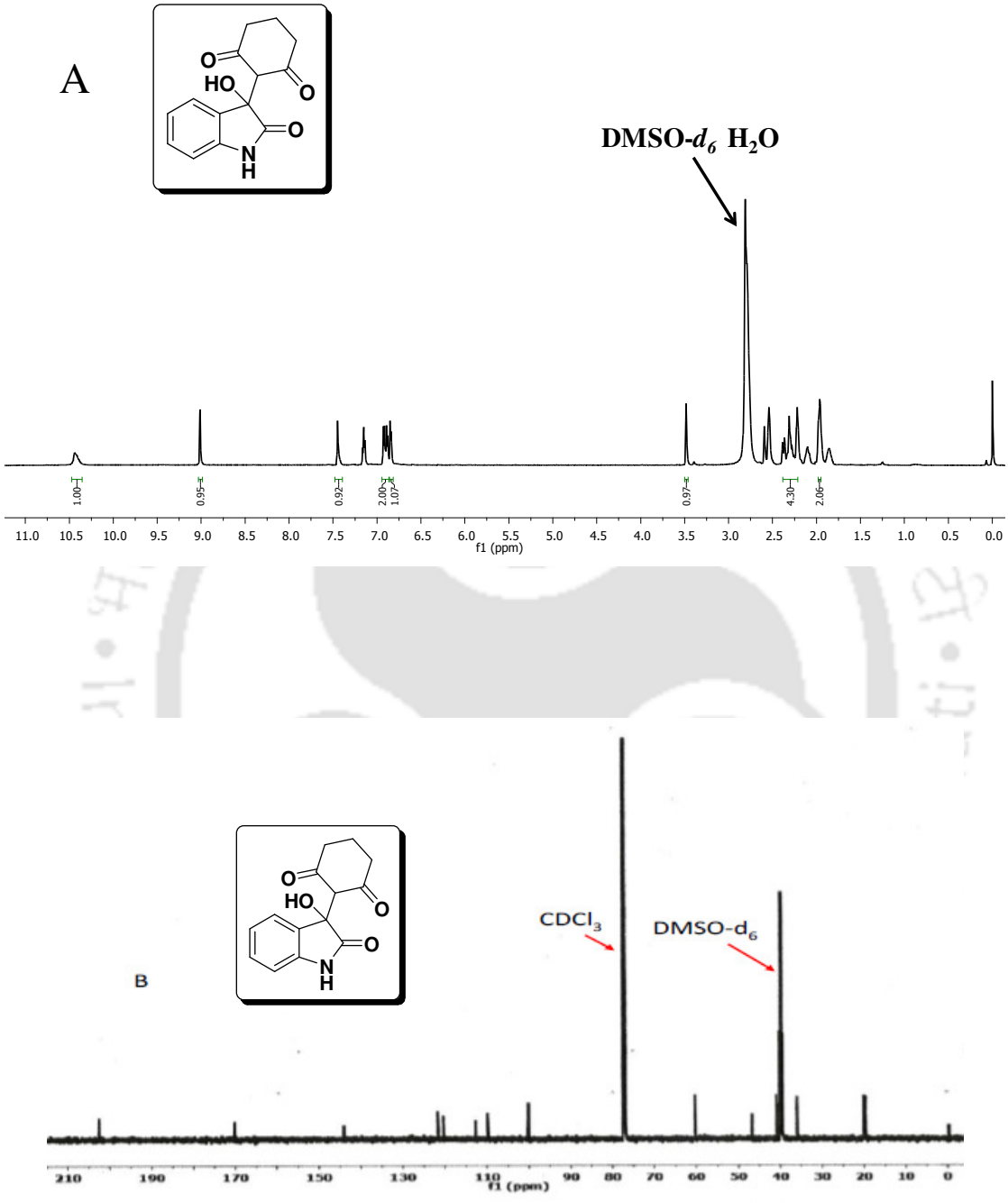

Figure 3.13.16. ^{1}H NMR **(A)** and ^{13}C NMR **(B)** spectra of 2-(3-Hydroxy-2-oxoindolin-3-yl)cyclohexane-1,3-dione (**25**)**.**

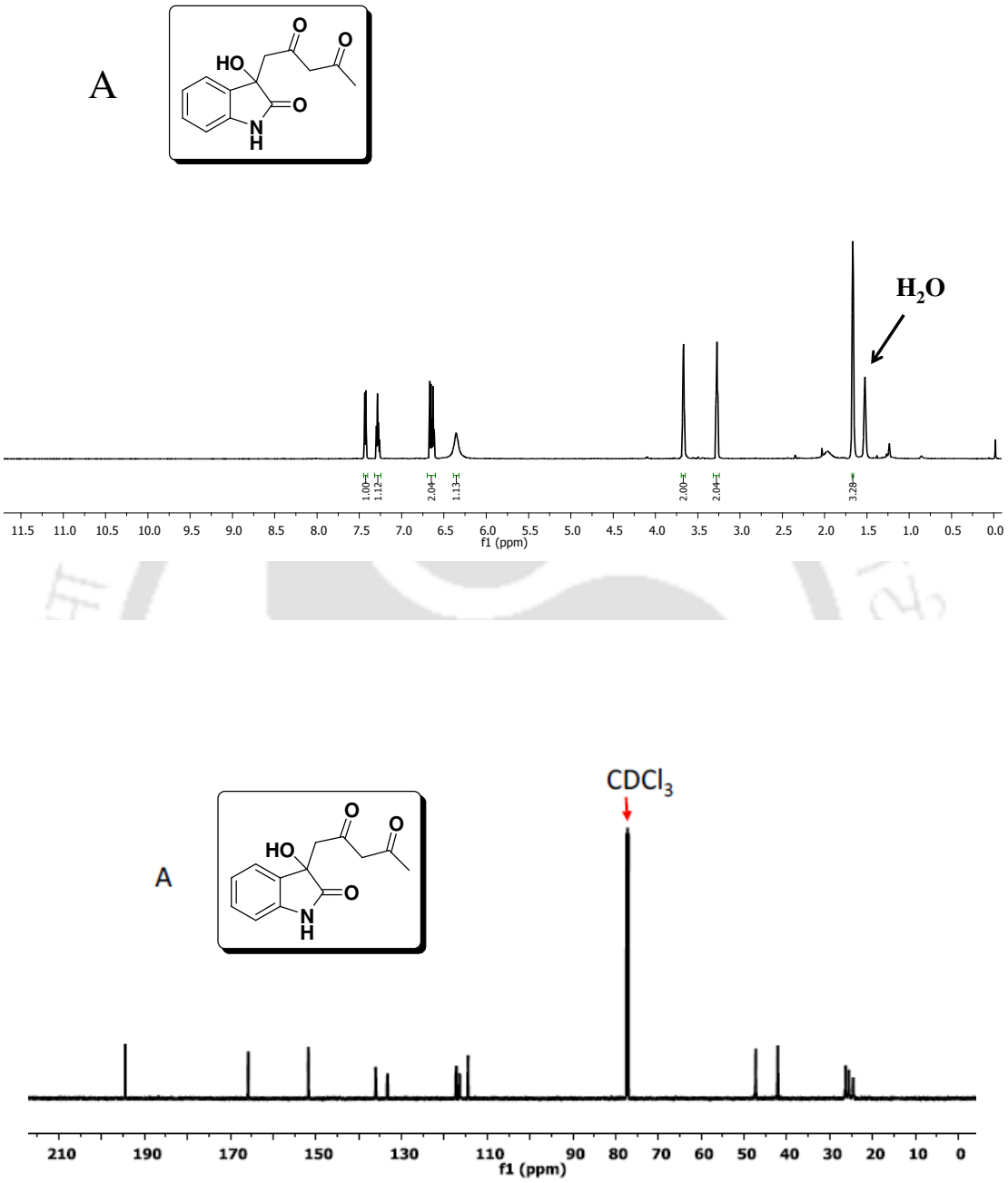

Figure 3.13.17. ^{1}H NMR **(A)** and ^{13}C NMR **(B)** spectra of 1-(3-Hydroxy-2-oxoindolin-3-yl)pentane-2,4-dione (**26**)**.**

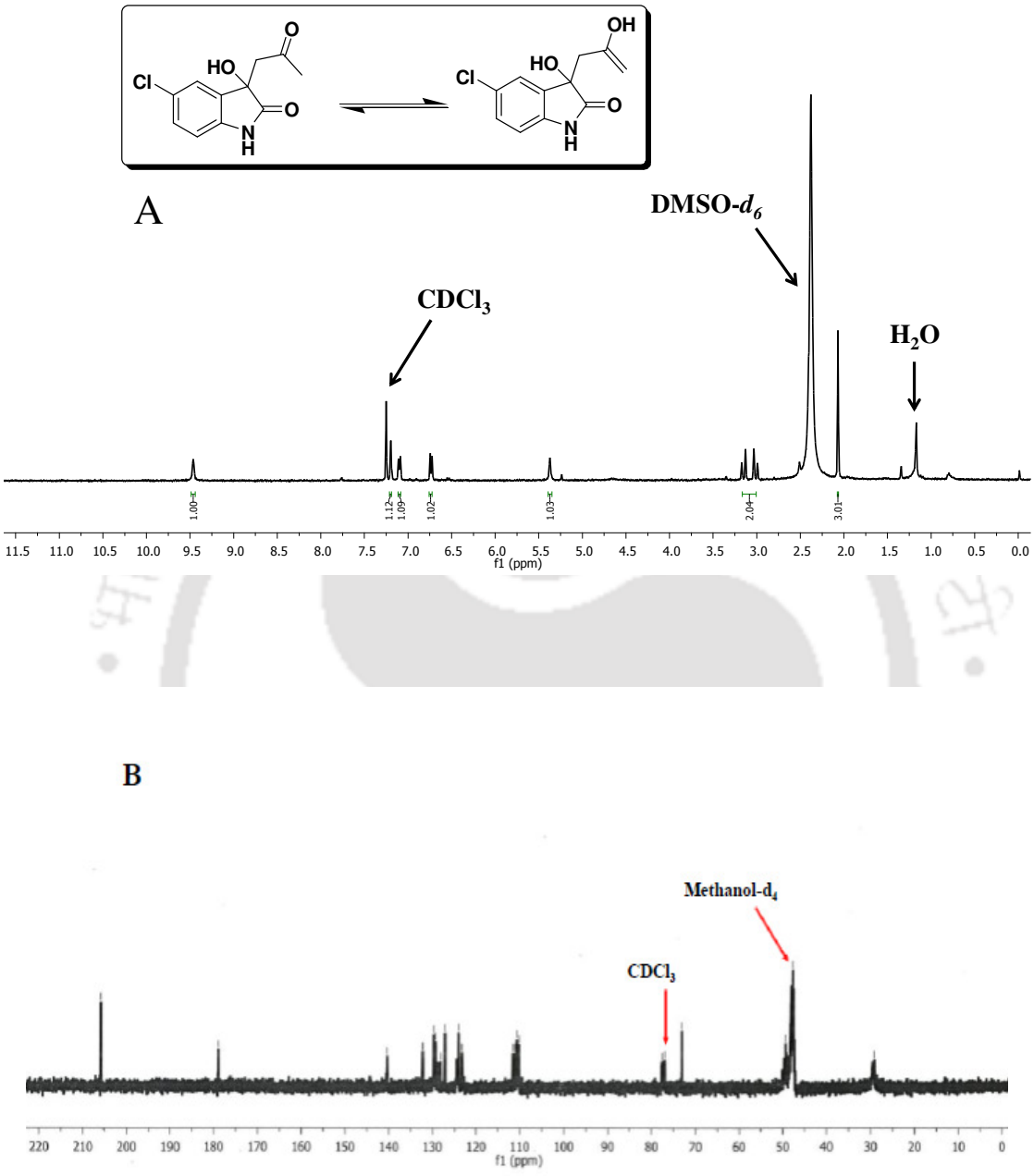

Figure 3.13.18. ^{1}H NMR **(A)** and ^{13}C NMR **(B)** spectra of 5-Chloro-3-hydroxy-3-(2-oxopropyl)indolin-2-one (**27**)**.**

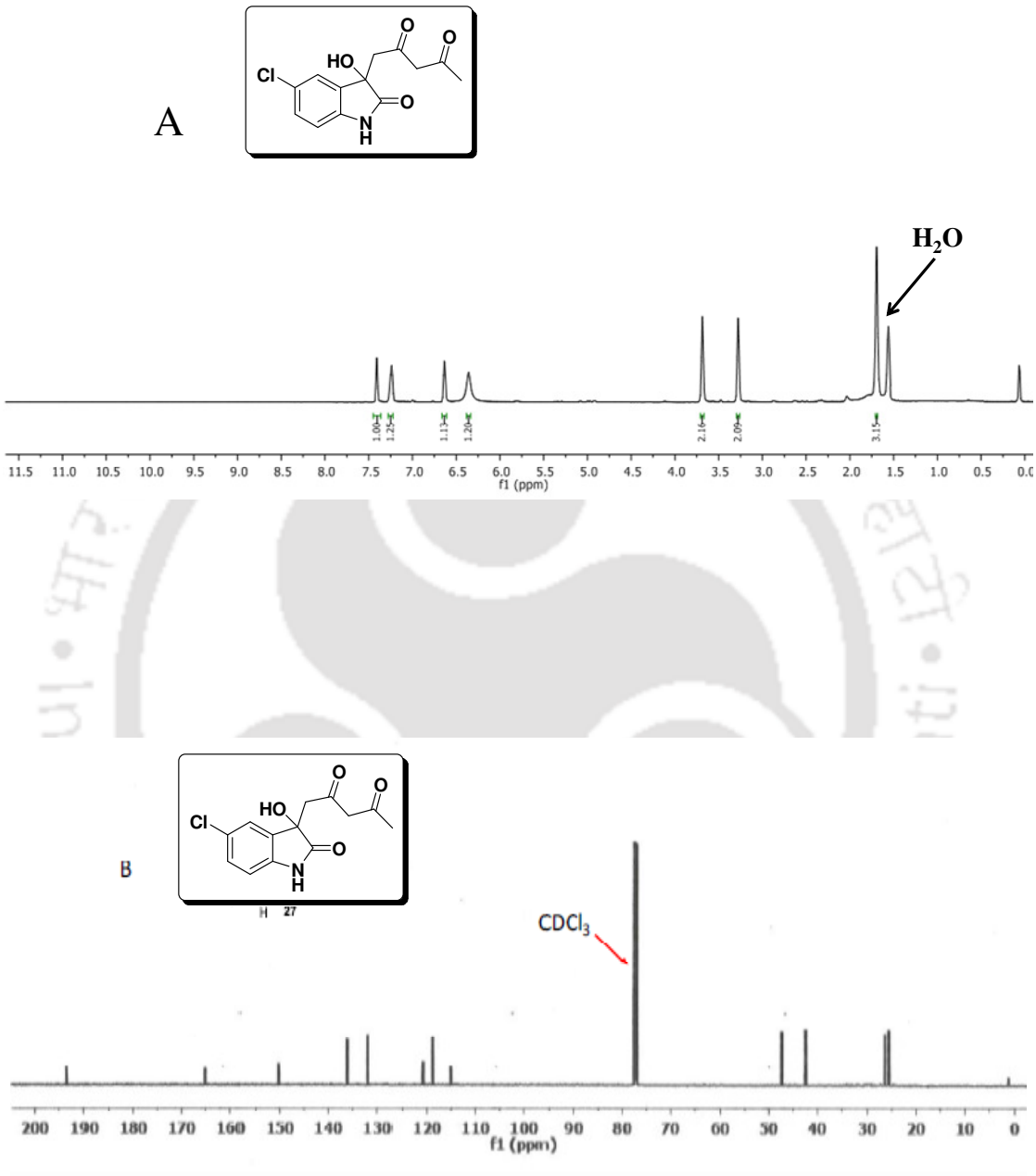

Figure 3.13.19. ^{1}H NMR **(A)** and ^{13}C NMR **(B)** spectra of 1-(5-Chloro-3-hydroxy-2-oxoindolin-3-yl)pentane-2,4-dione (**28**)**.**

CHAPTER 4

Substituted 1*H*-Indazoles as Potent Inhibitors for Immunosuppressive Enzyme Indoleamine 2,3-Dioxygenase 1

It is well established that the over-expression of the immunosuppressive enzyme, IDO1 is associated with poor prognosis of patients for a wide range of malignancies and it is a validated target for the treatment of diseases that are associated with immune suppression, including cancer. In this chapter, we described the synthesis of a series of C3-substituted 1*H*-indazoles along with their inhibitory activities studies against human IDO1 enzyme that were tested using *in-vitro* and cellular enzyme activity assay.

Highlights

- Synthesis of structurally unique C3-substituted 1*H*-indazoles targeting the immunosuppressive enzyme indoleamine 2,3-dioxygenase 1.
- Identification of 3-carbohydrazide derivatives of 1*H*-indazoles based on activity studies that showed inhibitory potencies at nanomolar range with negligible cytotoxicity.
- Suitable substitution at the C3-position in the indazole ring enhancing the possibility of interrupting further radical reaction with Fe (III)-superoxide intermediate thereby providing a better insight towards the designing of mechanism-based IDO1 inhibitors.
- Moderate selectivity of these potent compounds for IDO1 enzyme over tryptophan 2,3-dioxygenase enzyme that suggest the potential future prospect of these heterocyclic compounds as an attractive molecules for immunotherapeutic applications.

4.1. Background and focus of the present work

L-Trp metabolism through kynurenine pathway is not only associated with the neurological disorders but also plays an important role in immunosuppression. Hindering this tumor induced immunosuppressive mechanism and thereby restoring the defense mechanism of the immune system is considered as a promising approach in immunotherapy towards the treatment of cancer and other diseases.[1-6] Several clinical studies suggests that the up-regulation of IDO1 induced by cytokines like interferon γ has been detected in several cancers including colorectal, pancreatic, non-small cell lung and glioblastoma.[4,5] Over-expressed IDO1 defends cancer cells from the attack by the T-cells[6] and its induction assist the growth, survival, invasion, and metastasis of malignant cells (MC) expressing TAAs by shielding them from identification and attack by the T-cells.[2,6,7] Such anomaly in the immune system is regarded as one of the crucial parameter in growth and progression of the tumors, which also results in poor clinical outcome.[4, 5] *In vivo* studies with IDO1 animal models demonstrated that selective inhibition of IDO1 enzyme resulted in impaired growth of tumor, slow metastases development, and prolonged survival[8,9] thereby promoting it to be a potential therapeutic target for the cancer immunotherapy.

Several classes of potent IDO1 inhibitors containing the natural products, scaffolds of indole, quinone/iminoquinone, imidazoles, triazoles, hydroxyamidines and others have been developed through high throughput-screening, structure-based design and natural product screening.[7,10,11] Most of the reported IDO1 inhibitors showed low potency or failed *in vivo* assay. Currently, three IDO1 inhibitors indoximod, epacadostat and GDC-0919 are under clinical studies for the treatment of cancer and other diseases as a monotherapy or in combination with traditional cancer chemotherapies or newly developed immune checkpoint inhibitors. The *in vivo* studies revealed that indoximod, epacadostat and GDC-0919 reduced the kynurenine concentration in plasma and tissue by around 50% and decrease tumor size.[12,13] All these results are in consistent with the proposed mechanism of action of the potent IDO1 inhibitors as immune modulator. Hence, developments of specific IDO1 inhibitions are highly demanding.

In this chapter we have investigated IDO1 enzyme inhibitory activity by a series of 3-and 5-substituted 1*H*-indazoles derivatives. Several of the resulting compounds exhibited good to moderate inhibition capability towards the IDO1 enzyme with inhibitory potency in the micromolar range under *in vitro* conditions. Selected compounds also showed IDO1 enzyme inhibitory activity in MDA-MB-231 cells and almost

no/negligible amount of toxicity at the cellular level. Additional counter screening against TDO enzyme showed their selectivity for IDO1 enzyme.

4.2. Origin of design

In our quest of discovering new heterocyclic drug, we are focused on finding structurally simple but potent inhibitors of IDO1 enzyme for cancer immunotherapy.[10,13-15] Recently, molecular docking analyses and pharmacophore models identified 1*H*-indazole scaffold as a novel class of IDO1 inhibitor.[16] However, no indazole derivatives displayed low-micromolar activities. In-depth structural investigation, molecular docking analyses and reported experimental evidences revealed that these 4- and 6-substituted 1*H*-indazole may not be suitable for proper binding to the active site of IDO1 enzyme.[16] In an attempt to find potent IDO1 inhibitors, we synthesized 3-and 5-substituted 1*H*-indazoles and examined their enzyme inhibition potential. Several of our tested indazole-based compounds showed IDO1 enzyme inhibitory activities in the 0.72-10 micromolar ranges under the *in vitro* conditions with no/negligible cytotoxicity. Additional studies revealed that compounds **31a** and **31d** were 17- to 25-fold more selective toward the IDO1 enzyme in comparison with the TDO enzyme, making 1*H*-indazole derivatives of potent value for additional development as therapeutic agents.

4.3. Synthesis

A series of 3(*N*′-aryl)carboxamide derivatives of 1*H*-indazoles were synthesized from 1*H*-indazole-3-carboxylic acid. Coupling of 1*H*-indazole-3-carboxylic acid with substituted arylamine in the presence of HOBt and EDC.HCl in DMF solvent yielded the target compounds **29(a-f)** and **30** (Scheme 4.1).[17] Similarly, compound **30** was synthesized using 2-aminopyrimidine under the similar reaction conditions.

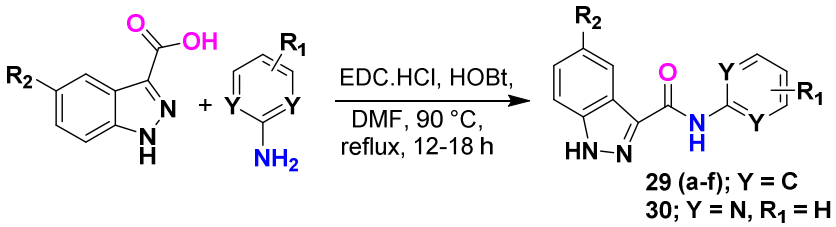

Scheme 4.1. Synthesis of 3(*N*′-aryl)carboxamide derivatives of 1*H*-indazoles from 1*H*-indazole-3-carboxylic acid.

N´-aryl-1*H*-indazole-3-carbohydrazide derivatives **31(a-e)** were also synthesized under the similar experimental conditions using 1*H*-indazole-3-carboxylic acid and arylhydrazines (Scheme 4.2).[17] This single step synthesis of 1*H*-indazole derivatives is advantageous for large-scale production and structural modification. The IDO1 inhibitory activities of the synthesized 1*H*-indazoles were initially evaluated by spectrophotometric method as described earlier.[7,10,13,18]

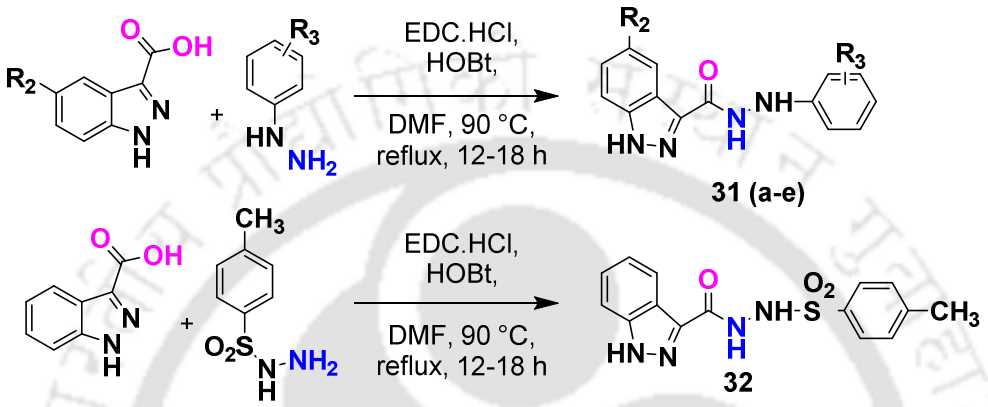

Scheme 4.2. Synthesis of 3-carbohydrazide derivatives of 1*H*-indazoles from 1*H*-indazole-3-carboxylic acid.

The spectral properties of the compounds (0.1 μM to 200 μM) showed no or little interference with this activity assay. The measured K_m and k_{cat} values of the purified IDO1 enzyme with the *L*-Trp as substrate were 24.86 ± 3.9 μM and 5.23 ± 0.32 s^{-1}, respectively. Recently, 1*H*-indazole moiety was identified as an important lead compound in designing IDO1 inhibitor.[16] In an effort to further optimize the potency of 1*H*-indazole scaffold, we explored two general structural modifications of the 1*H*-indazole structures, firstly the modification of 3(*N´*-aryl)carboxamide moiety and secondly the modification of 3-carbohydrazide derivatives.

4.4. Inhibitory activity study against purified human IDO1 enzyme

To identify the IDO1 inhibitory efficiencies of the 1*H*-indazoles, we examined the 3(*N´*-aryl)carboxamide derivatives of 1*H*-indazoles. We postulated that the presence of substituted 3(*N´*-aryl)carboxamide moiety in the compound's core structural unit could play a vital role in their IDO1 inhibitory efficiencies. Structural modifications including installation of -OMe, -OAc, -OH and -NO_2 groups in the *N´*-aryl ring or incorporation of

Br- group in the indazole moiety of the compounds were investigated. However, these substitutional effects also lead to a moderate change in inhibitor potency (Table 4.1). Among the tested compounds **29c** showed moderate IDO1 inhibition potency with IC_{50} value of 8.5 μM (Table 4.1). Compound **29c** showed 25% and 60% IDO1 inhibition 1 μM and 10 μM concentrations, respectively.

Table 4.1. Inhibitory activity of the 3(*N'*-aryl)carboxamide derivatives of 1*H*-indazoles against purified human IDO1 enzyme.

Compound	IDO1 inhibition IC_{50} (μM)[a]
29a; $R_1 = R_2 = H$	14.52 ± 0.97
29b; R_1 = 4-OMe, $R_2 = H$	11.23 ± 0.89
29c; R_1 = 4-OAc, $R_2 = H$	8.54 ± 0.73
29d; R_1 = 4-OH, $R_2 = H$	16.52 ± 1.35
29e; R_1 = 4-NO_2, $R_2 = H$	20.04 ± 1.48
29f; $R_1 = H$, R_2 = Br	13.56 ± 1.16
30 $R_1 = R_2 = H$	14.82 ± 1.36

[a]IC_{50} values are the mean of five independent assays.

In addition, we also investigated IDO1 inhibitory efficacies of 3-carbohydrazide derivatives of 1*H*-indazoles **31(a-e)**. The presence of substituted 3(*N´*-aryl)carbohydrazide moieties in the compound's core structural unit could allow them to have the suitable conformation for binding to the IDO1 enzyme. Interestingly, couple of compounds displayed strong IDO1 inhibitory activities with IC_{50} vales of 720-770 nM (Table 4.2).

Table 4.2. inhibitory activity of the 3-carbohydrazide derivatives of 1*H*-indazoles against purified human IDO1 enzyme.

Compound	IDO1 inhibition IC_{50} (μM)[a]
31a; $R_2 = R_3 = H$	0.72 ± 0.09
31b; $R_2 = H$, R_3 = 4-Cl	8.35 ± 0.39
31c; $R_2 = H$, R_3 = 3-NO_2	6.53 ± 0.23
31d; R_2 = Br, $R_3 = H$	0.77 ± 0.17
31e; R_2 = Br, R_3 = 4-Cl	2.25 ± 0.32
32	16.95 ± 2.13

[a]IC_{50} values are the mean of five independent assays.

Compounds **31a** and **31d** exhibited stronger IDO1 inhibitory activities with the inhibitory ratios of 98% and 88% at 10 μM concentrations, respectively. However, further structural modifications including installation of 4-Cl or 3-NO_2 groups in the *N´*-aryl ring or incorporation of bromo group in the indazole scaffold were ineffective against IDO1 activity.

The IDO1 enzyme activities in the presence of selected 1*H*-indazoles were also investigated by HPLC-analyses for additional validation of their inhibition efficiencies.[10,12,13] The calculated IC_{50} values revealed that the inhibitory efficiencies of the selected compounds are within 0.47-17.9 μM range and follows a similar pattern as that measured by using the spectrophotometric method (Table 4.3). The differences in IC_{50} values between the spectrophotometric and HPLC-based assays could depend on the precision of the methylene blue-ascorbate redox system to keep IDO1 in its active form (Fe^{2+}).[19]

Table 4.3. HPLC based IDO1 inhibition assays of the selected compounds.

Compound	IDO1 inhibition (IC_{50} μM)[a]
29a	10.33 ± 2.17
29b	15.32 ± 3.12
30	14.58 ± 2.29
31a	0.74 ± 0.39
31c	10.52 ± 1.27
31d	0.46 ± 0.12
31e	6.61 ± 1.15

[a]IC_{50} values calculated by HPLC method (are the mean of three independent assays).

The HPLC-based assay also revealed that 3(*N´*-aryl)carbohydrazide derivatives of 1*H*-indazole **31a** and **31d** displayed stronger (IC_{50} = 460-740 nM) and compound **31e** showed moderate (IC_{50} = 6.61 μM) inhibitory activities among all the tested compounds (Table 4.3). Overall, the inhibitory efficacy of the 1*H*-indazoles is sensitive to the C3-substitution, possibly due to the restricted space in pocket-A of the IDO1 enzyme. Stronger inhibitory activities of the 3(*N´*-aryl)carbohydrazide derivatives of 1*H*-indazole, **31a** and **31d** could be due to both interaction of *N´*-phenyl-carbohydrazide moiety with the residues present within the IDO1 binding pocket-A and interaction of 1*H*-indazole moiety with the heme-group. Any substitution in the *N´*-phenyl ring showed significantly reduced inhibitory effect on IDO1 activity. Presence of 5-Br group in the 1*H*-indazole

moiety also showed slender difference in their inhibitory potencies. All these results support the proposed binding mode for compound **31a** and **31d** with IDO1. This could explain why 3(*N´*-aryl)carbohydrazide derivatives **31a** and **31d** showed lower IC_{50} values.

4.5. Spectroscopic based analysis of interaction of 1*H*-indazole derivatives with IDO1

The ligand-binding propensity to the IDO1 enzyme was examined by UV-Vis spectral analysis. The optical properties of heme-group are highly sensitive to the local environment.[10,12,13,19,20] The IC_{50} values of the 1*H*-indazoles reveal their capability in inhibiting IDO1 enzyme activity, but failed to provide any direct evidence of ligand binding to the active site of the IDO1 enzyme. In this regard, we measured the UV-Vis spectra of ferric-IDO1 and deoxy-ferrous-IDO1 in the absence and presence of the selected compounds (Figure 4.1). For ferric-IDO1 enzyme, the Soret band (404 nm) got red-shifted by 2-5 nm in the presence of compounds (**31a**, **31d** and **31e**). However, for deoxy-ferrous-IDO1 enzyme there was no substantial shift in Soret (421 nm) and Q-band (556 nm).

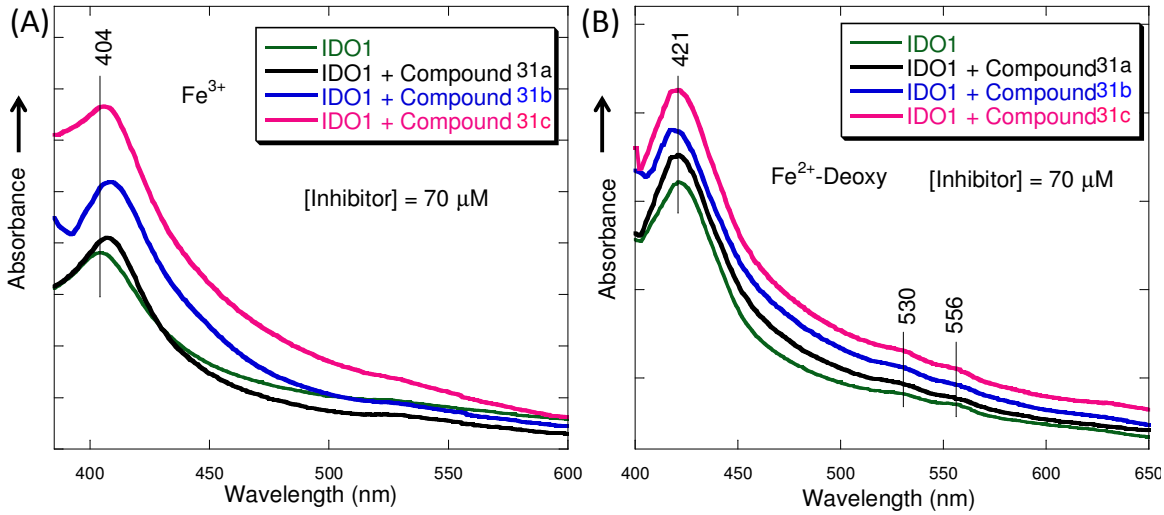

Figure 4.1. Absorption spectra of ferric-IDO1 (**A**) and deoxy-ferrous-IDO1 (**B**) enzyme in the absence and presence of the compounds (70 µM) in 50 mM Tris-HCl buffer at pH 8.0. [IDO1] = 5 µM. Ferrous-deoxy reaction environment was generated by adding $Na_2S_2O_4$ to the solution under N_2 atmosphere (**B**).

These spectral properties suggest direct binding of the compounds (**31a**, **31d** and **31e**) to the ferric-IDO1 enzyme. The UV-Vis spectra of compounds in Tris-HCl buffer did not show any peak in this region. Additional studies are required in confirming the direct binding of these 1*H*-indazoles to the IDO1 enzyme. However, the UV-Vis spectral analyses certainly indicate the binding of compounds to the ferric-IDO1 enzyme. The HPLC-based assay and UV-Vis spectral analysis of enzyme-compound solution suggests that binding of these potent compounds to the IDO1 enzyme is not off-target.

4.6. Cellular IDO1 inhibitory activities of 1*H*-indazole derivatives

To understand the therapeutic prospective of these selected compounds, cellular IDO1 inhibitory activities were measured in MDA-MB-231 (breast tumor) cells. It is well documented that in MDA-MB-231 cells interferon (IFN)-γ considerably induce the expression of native IDO1 enzyme from its mRNA.[10,12,13,21] Inhibitory activities (EC_{50}) of the compounds under the cellular environments follow similar pattern as that of against purified IDO1 enzyme (Table 4.4). Control compound, 4-amino-*N*-(3-chloro-4-fluorophenyl)-*N*'-hydroxy-1,2,5-oxadiazole-3-carboximidamide[11] showed EC_{50} values of 59 nM, under the similar experimental conditions, which is in accordance with the earlier reported values.[10,12,13,20,21] However, smaller differences in the compound's EC_{50} and IC_{50} values could be because of the difficulties in regulating the IDO1 redox activity and/or local environmental effect. Overall, a good correlation between these assays substantiates the IDO1 inhibition efficacies of these 1*H*-indazoles. MTT assay of the compounds in MDA-MB-231 cells also revealed low level of toxicity of the compounds under the experimental conditions (Figure 4.2 and 4.3).

Table 4.4. IDO1 enzyme inhibitory activity of the selected compounds in MDA-MB-231 cells.

Compound	IDO1 inhibition in MDA-MB-231 cells[a] EC_{50} (μM)[b]
29c	284 ± 10
31a	381 ± 12
31d	281 ± 10
31e	355 ± 12

[a]IDO1 protein expression in MDA-MB-231cells was induced by human IFN-γ (20ng/mL).

[b]EC_{50} values are the mean of three independent assays.

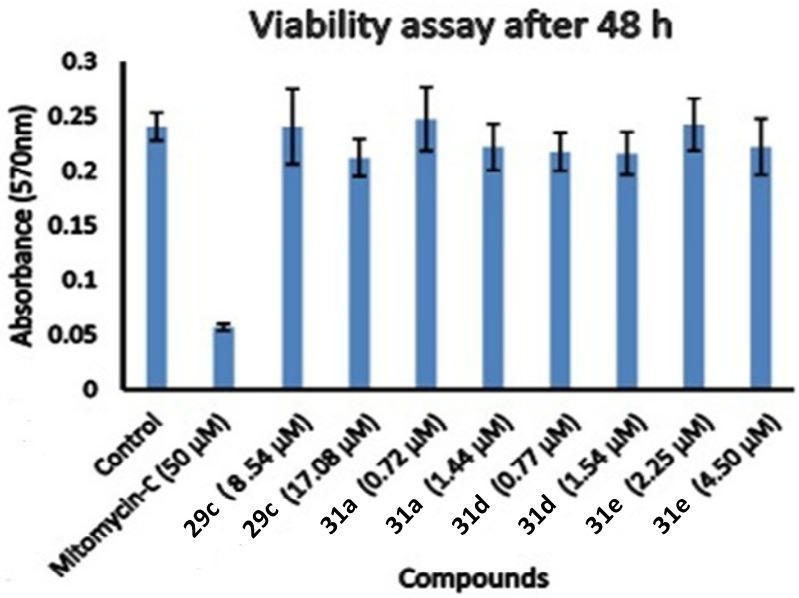

Figure 4.2. Effect of the selected 1*H*-indazole derivatives on the viability of MDA-MB-231 cells. MDA-MB-231 cells were treated with the indicated concentrations of the compounds for 48 h. Cell viability was determined by the MTT assay. Absorbance of different amounts of formazan was plotted against the mentioned concentrations of the compounds. Data are averages with standard deviation (error bars) from three independent experiments. Mentioned concentrations of the 1*H*-indazole derivatives are the IC_{50} and 2 × IC_{50} values of the compounds obtained from activity assay against purified enzyme.

4.7. Mode of IDO1 enzyme inhibition by the potent 1*H*-indazole derivatives

The enzyme inhibition studies revealed that selected 1*H*-indazoles strongly inhibit the catalytic activity of the IDO1 enzyme. Therefore, we performed enzyme kinetics measurements in the absence and presence of these compounds to investigate their mode of IDO1 inhibition. The modes of IDO1 inhibition by the compounds were examined using the Lineweaver-Burk plot.[10,13,22,23] The plots of 1/V against 1/[S] revealed that compounds **29a**, **29b**, **30**, and **31c** followed uncompetitive inhibition, **31a**, **31d** and **31e** followed mixed inhibition modes (Figure 4.4). V and [S] represent the initial reaction rate and the substrate concentration, respectively.

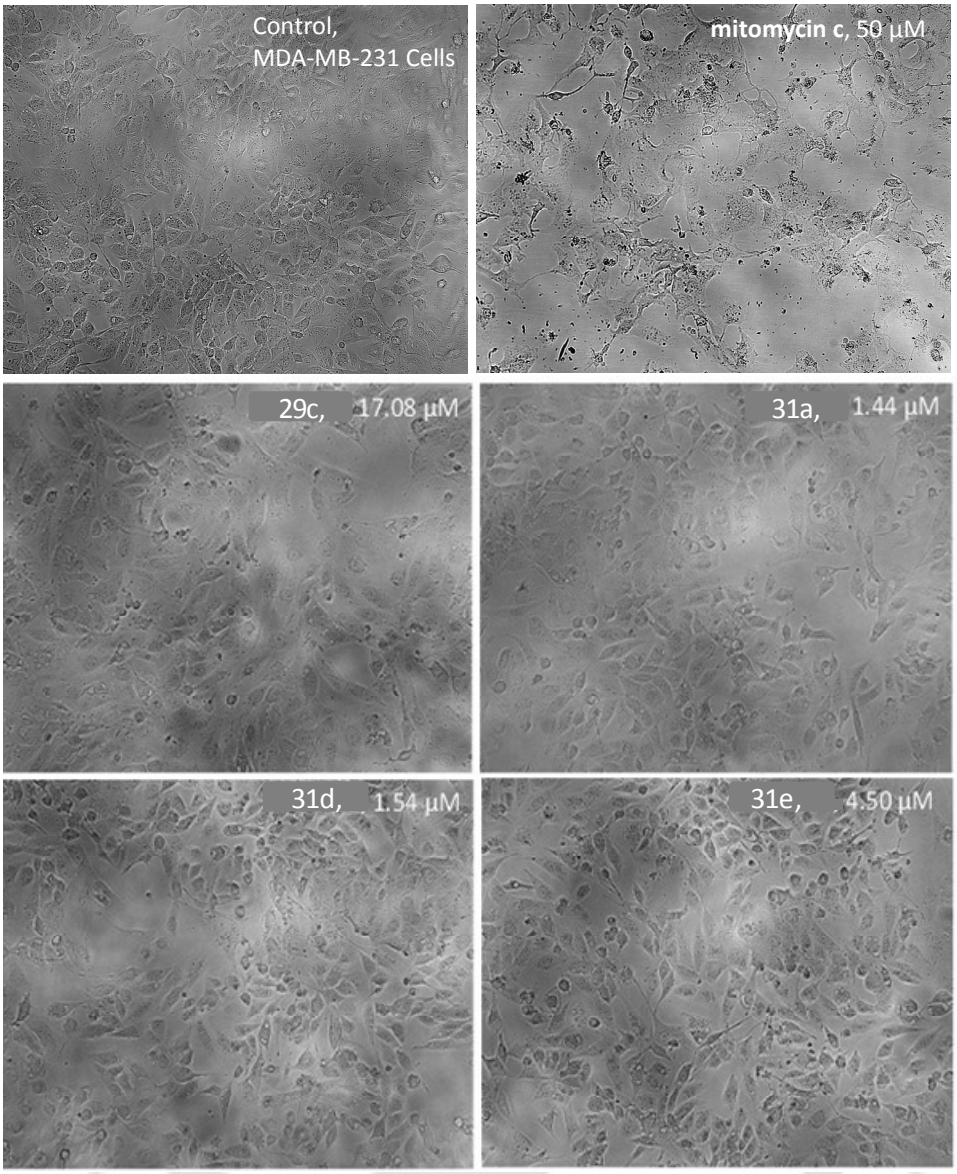

Figure 4.3. Effect of the selected 1*H*-indazole derivatives on the morphological changes of MDA-MB-231 cells. MDA-MB-231 cells were treated with the indicated concentrations of the compounds for 48 h and morphological changes were observed using cytell imaging system. Images were collected at 10x magnification. Images are representative of three independent experiments. Mentioned concentrations of the compounds are the 2 × IC_{50} values of the compounds obtained from activity assay against purified enzyme. Mitomycin-C was used as positive control.

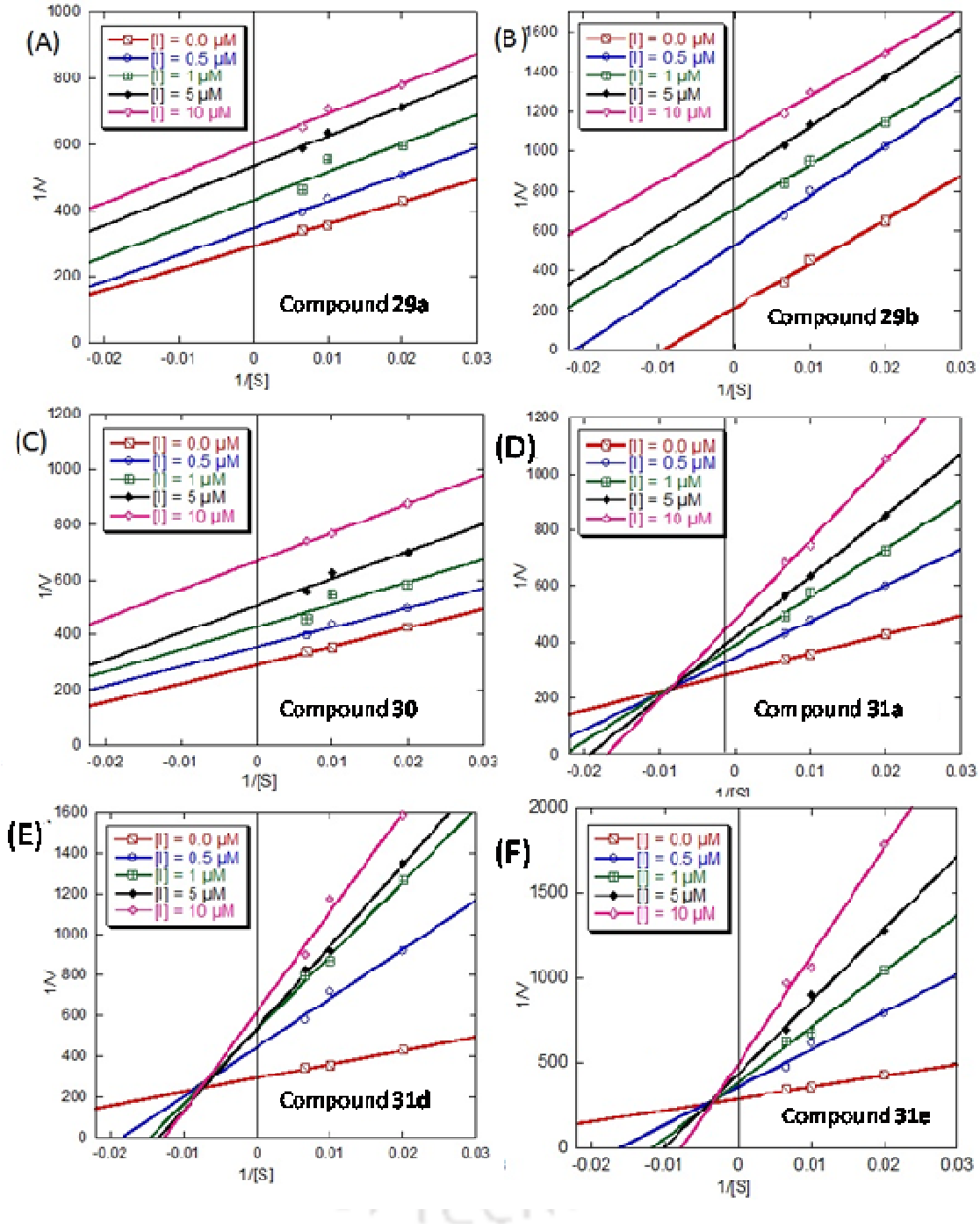

Figure 4.4. Determination of mode of inhibition of the selected compounds. Plot of 1/V against 1/[S] at different concentration of the compounds **29a** (A), **29b** (B), **30** (C), **31a** (D), **31d** (E) and **31e** (F). Concentration of *L*-Trp was varied from 50 µM to 150 µM. The concentrations of compounds were varied from 0.5 µM to 10 µM. All the absorption measurements were performed in 50 mM phosphate buffer pH 6.5 at room temperature.

However, these calculated modes of IDO1 inhibition may not authenticate their actual mode of enzyme inhibition. There are several reports of uncompetitive and noncompetitive inhibitors, which strongly bind IDO1 enzyme and inhibit its catalytic activity.[12,24] Meanwhile, the detailed mechanistic studies of IDO1 promoted catabolism of *L*-Trp demonstrate that the formation of ferric-superoxide intermediate is the primary requirement for this oxidation process. Therefore, supplementary kinetic studies with respect to O_2 are needed to investigate the definite mode of IDO1 enzyme inhibition by these compounds, which beyond the scope of this investigation.[7,10,12,13]

4.8. Probable mode of interaction of the potent 1*H*-indazole derivatives with IDO1 enzyme

The inhibitory activity and binding studies revealed that the potent compounds interact with the IDO1 enzyme through its heme-containing active site. To further understand their probable mode of interactions we performed molecular docking analyses of the potent compounds with the IDO1 enzyme (PDB code: 4PK5).[25] The docking score and scoring functions are shown in Table 4.5.

The interaction energy of compound **31a**, **31d** and **31e** is -119.46 kJ/mol, -143.09 kJ/mol, -145.58 kJ/mol, -158.97 kJ/mol respectively. The model structures and their interaction energies suggest that the 3-carbohydrazide derivatives of 1*H*-indazoles (**31a** and **31d**) preferably interact with IDO1 enzyme through its "pocket-A" (comprises of Y126, F163 and S167 residues) and the porphyrin ring.[7,18,26] The 1*H*-indazole ring and *N*´-phenyl ring of the 3-carbohydrazide moiety could be involved in interaction with Y126, F163, F164 residues and others present in "pocket-A" through pi-stacking and hydrophobic interactions (Figure 4.6). The 1*H*-indazole ring could be involved in hydrogen bonding interaction with the S167 residue and heme group. An additional hydrogen bonding between the 3-carbohydrazide moiety of the compounds with S167 residue was observed for both the compounds. However, the model structure suggests that compound **31e** interact differently with IDO1 enzyme. The 5-bromo-1*H*-indazole moiety could interact through "pocket-A" whereas, 4-Cl substituted 3(*N*´-aryl)carbohydrazide moiety could interact with "pocket-B" of the IDO1 enzyme. The 1*H*-indazole ring of compound **31e** could be involved in hydrogen bonding with the heme group. The 3-carbohydrazide moiety of the compounds could interact with the backbone of A264 residue. The interaction energies are in accordance with the spectroscopic based binding studies.

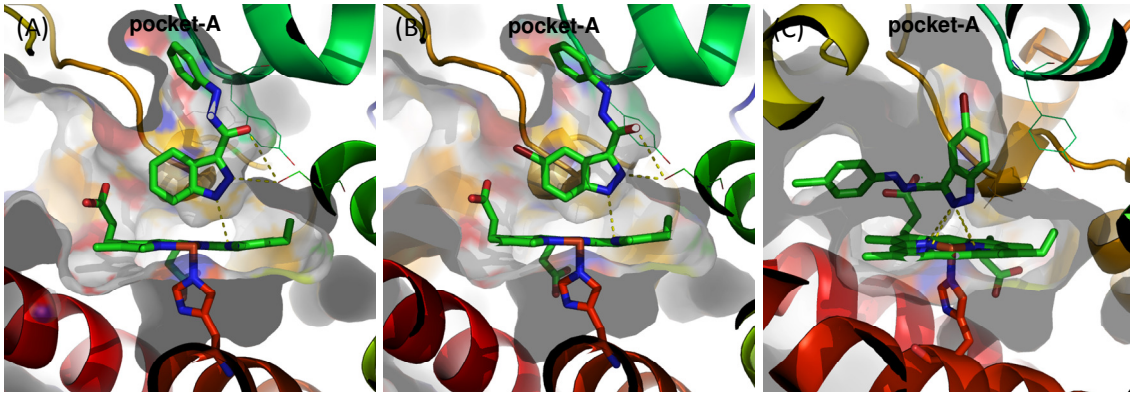

Figure 4.6. Probable mode of interaction of the compounds **31a** (A), **31d** (B), and **31e** (C) with the IDO1 enzyme (4PK5). The model structures were generated using MoleGro Virtual Docker, version 6.0. Residues involved in interactions through hydrogen bond formation are shown using dashed lines (yellow). Images were generated using PyMol.

Table 4.5. Docking score of 1*H*-indazole-3-carbohydrazide derivatives.

Compound	Rerank score (kJ/mol)[a]	Interaction (kJ/mol)[b]	Internal (kJ/mol)[c]	H-Bond (kJ/mol)[d]	LE1[e]	LE3[f]
31a	-98.9685	-143.092	5.1982	-4.61021	-6.89469	-4.94842
31d	-100.788	-145.58	5.69299	-4.74755	-6.99434	-5.03941
31e	-88.2928	-158.971	14.7389	-2.49776	-6.86819	-4.20442

[a]There rank score is a linear combination of E-inter (steric, Van der Waals, hydrogen bonding, electrostatic) between the ligand and the protein, and E-intra. (torsion, sp2-sp2, hydrogen bonding, Van der Waals, electrostatic) of the ligand weighted by pre-defined coefficients(kJ/mol).

[b]The total interaction energy between the pose and the protein (kJ/mol).

[c]The internal energy of the pose (kJ/mol).

[d]Hydrogen bonding energy (kJ/mol).

[e]Ligand efficiency 1: MolDock score divided by heavy atoms count.

[f]Ligand efficiency 3: Rerank score divided by heavy atoms count.

Model structures also suggest that the presence of additional 4-chloro substitution in the *N*′-aryl ring (for compound **31e**) plays an important role in interaction with the IDO1 enzyme. However, the presence of 5-bromo substitution in the 1*H*-indazole ring (for compound **31d** and **31e**) might not have any substantial role for their interaction with the IDO1, which is in accordance with its effectiveness for IDO1 inhibitory activity (Table 4.3). Docking scores/ interaction energies of 1*H*-indazole-3-carbohydrazide derivatives **31a**, **31d** and **31e** are in accordance with the IC_{50} values of the compounds.

The differences in the mode of interaction among compounds **31a**, **31d** and **31e** could be due to their effectiveness in proper fitting into the binding pocket, which is considered as rigid-body during docking analysis. In solution the IDO1 binding pocket may have different conformation(s), which may possibly explain the reason for their very similar IC_{50}/EC_{50} values. Therefore, hydrogen bonding, hydrophobic interactions and pi-stacking play important roles in stronger binding of these compounds.[12,18,27] The alterations in IC_{50} values among the selected compounds under the experimental conditions propose that their mode of interaction with the IDO1 enzyme could be dissimilar than the predicted one by molecular docking analysis. Strength of interaction and molecular volume of the compounds could also be important for their preferential binding under the experimental conditions.

4.9. Inhibitory activities of 1*H*-indazole derivatives against purified TDO enzyme

In addition, we performed TDO enzyme activities in the absences and presences of the potent compounds. TDO also catalyzes the rate determining step of the kynurenine pathway in liver and regulate the cellular level of *L*-Trp. Hence, to determine the selectivity of these compounds at inhibiting IDO1 activity, TDO activity was also measured in UV-Vis spectroscopic and HPLC method. TDO activity studies showed that these 1*H*-indazoles have variable enzyme inhibition potencies. Compounds **31a** and **31d** showed preferential inhibitory activity for IDO1 (>17-fold) over TDO enzyme under the similar experimental conditions (Table 4.6).

Table 4.6. Inhibitory activity of the selected compounds against purified human IDO1 and TDO enzymes.

Compound	Mode of inhibition	IDO1 inhibition ($IC_{50}\mu M$)[a]	TDO inhibition ($IC_{50}\mu M$)[a]	Selectivity ratio[b]
29a	uncompetitive	14.52 ± 0.97	92.3 ± 3.58	6
29b	uncompetitive	11.23 ± 0.89	92.4 ± 4.54	8
30	uncompetitive	14.82 ± 1.36	81.9 ± 6.23	5
31a	mixed	0.72 ± 0.09	12.3 ± 1.51	17
31c	uncompetitive	6.53 ± 0.23	17.9 ± 1.32	3
31d	mixed	0.77 ± 0.17	19.1 ± 1.36	25
31e	mixed	2.25 ± 0.32	10.5 ± 1.02	5

[a]IC_{50} values are the mean of three independent assays against purified enzymes.

[b]Selectivity ratio is calculated as (IC_{50} value of TDO)/(IC_{50} value of IDO1).

Table 4.7. HPLC based IDO1 and TDO inhibition assay of the selected compounds.

Compound	IDO1 inhibition (IC_{50} μM)[a]	TDO inhibition (IC_{50} μM)[a]
29a	10.33 ± 2.17	136.89 ± 8.37
29b	15.32 ± 3.12	174.42 ± 8.37
30	14.58 ± 2.29	85.72 ± 2.31
31a	0.74 ± 0.39	8.12 ± 1.17
31c	10.52 ± 1.27	44.91 ± 1.71
31d	0.46 ± 0.12	8.87 ± 2.95
31e	6.61 ± 1.15	29.26 ± 2.39

[a]IC_{50} values are the mean of three independent assays against purified enzymes.

4.10. Conclusion

Thus in conclusion, in this chapter we have synthesized a series of 3-substituted 1*H*-indazoles and investigated their IDO1 enzyme inhibition efficiencies. Structural modifications including substitution on the 3-aryl ring and installation of 3(*N*′-aryl)carboxamide moiety and 3-carbohydrazide moiety were explored for stronger IDO1 inhibition activity. Couple of 3-carbohydrazide derivatives exhibited low-micromolar level inhibitory activity against purified human IDO1 enzyme. The presence of 1*H*-indazole ring and suitably substituted carbohydrazide moiety at the C3 position of the parent scaffold plays a key role for their strong in vitro inhibitory activities. Spectroscopic-based binding studies indicate that the 3-carbohydrazide derivatives of 1*H*-indazoles (**31a** and **31d**) preferably interact with the ferric-IDO1 enzyme. Lower toxicity and moderate activity for IDO1 enzyme support the requirement of further development of 1*H*-indazole derivatives as potent inhibitor of IDO1 enzyme. Overall, suitable C3-substitution in the indazole ring might interrupt further radical reaction with Fe (III)-superoxide intermediate leading to a better approach in designing mechanism-based IDO1 inhibitors.

4.11. Experimental section

4.11.1. Instrumentation and Characterisation

As described in chapter 2 section 2.9.1.

4.11.2. General procedure for the synthesis of 3(*N′*-aryl)carboxamide and *N′*-aryl-1*H*-indazole-3-carbohydrazide derivatives of 1*H*-indazoles from indazole 3-carboxylic acid[17]

To a stirring solution of indazole 3-carboxylic acid (1.0 mmol), HOBt (1.2 mmol) and EDC.HCl (1.2 mmol) in DMF, was added. After stirring for 10 minutes substituted aniline/ arylhydrazine/ benzenesulfonohydrazide (1.1 mmol) was added dropwise. Then the whole solution was refluxed at 90 °C for 12-18 h under N_2 atmosphere. After completion of reaction (monitored by TLC), the solvent was removed under reduced pressure and washed with water and brine solution (3 × 20 mL) and further extracted with ethyl acetate (3 × 30 mL). The combined organic layer was dried over anhydrous Na_2SO_4 and the solvent was evaporated under reduced pressure. Column chromatography with silica gel and a gradient solvent system of methanol to dichloromethane (5-20%) yielded the corresponding target products in moderate to good yields.[17]

4.11.3. Synthetic scheme for the preparation of *N*-(4-hydroxyphenyl)-1*H*-indazole-3-carboxamide from indazole 3-carboxylic acid

4.11.3.1. Synthesis of 4-nitrophenyl acetate[28]

To an ice cold solution of 4-nitrophenol (3 mmol) and triethylamine (6 mmol) in dichloromethane (30 mL), was added acetyl chloride (4.5 mmol) dropwise at 0 °C under continuous stirring condition. The whole solution was then allowed to stir at 0-5 °C for 3 h and then at room temperature for another 3 h. After consumption of the starting material (monitored by TLC), the reaction mixture was diluted with water and extracted with CH_2Cl_2 (3 × 30 mL). The combined organic layer was dried over anhydrous Na_2SO_4 and the organic solvent was removed under reduced pressure to obtain 4-nitrophenyl acetate (98% yield) as white solid, which was directly used for the next step without further purification.[28]

4.11.3.2. Synthesis of 4-aminophenyl acetate[22]

To a stirring solution of 4-nitrophenyl acetate (1000 mg, 5.52 mmol) in ethyl acetate (20 mL) was added catalytic amount of 5% Pd/charcoal (20 mg). The solution was then stirred at room temperature for 4 h under hydrogen gas at 3 atmospheric pressure. After completion of reaction (monitored by TLC), the solution was filtered over a celite pad

and the filtrate was concentrated under reduced pressure resulting the 4-aminophenyl acetate (99% yield) as a brown solid.

4.11.3.3. Synthesis of 4-(1*H*-indazole-3-carboxamido)phenyl acetate[17]

To a stirring solution of indazole 3-carboxylic acid (1.0 mmol), HOBt (1.2 mmol) and EDC.HCl (1.2 mmol) in DMF, was added. After stirring for 10 min 4-aminophenyl acetate (1.1 mmol) was added dropwise. Then the whole solution was refluxed at 90 °C for 12-18 h under N_2 atmosphere. After completion of reaction (monitored by TLC), the solvent was removed under reduced pressure and washed with water and brine solution (3 × 20 mL) and further extracted with ethyl acetate (3 × 30 mL). The combined organic layer was dried over anhydrous Na_2SO_4 and the solvent was evaporated under reduced pressure. The crude product was purified by column chromatography with silica gel using a gradient solvent system of methanol to dichloromethane (5-20%) to obtain the 4-(1*H*-indazole-3-carboxamido)phenyl acetate as a white solid (64% yield).[17]

4.11.3.4. Synthesis of *N*-(4-hydroxyphenyl)-1*H*-indazole-3-carboxamide.[29]

The desired amount of 4-(1*H*-indazole-3-carboxamido)phenyl acetate (1.7 mmol) was first dissolved in MeOH (20 mL) and then 1M aqueous sodium hydroxide solution (2 mL approx.) was added under stirring condition. The resultant solution was stirred at room temperature for 3 h and then acidified with 1M HCl solution.[29] Then, it was concentrated under reduced pressure and the aqueous layer was further extracted with ethyl acetate (3 × 30 mL). The combined organic layer was dried over anhydrous Na_2SO_4 and the solvent was removed under reduced pressure. The crude product was further purified using column chromatography with silica gel and a gradient solvent system of ethyl acetate to hexane (30-45%) to yield *N*-(4-hydroxyphenyl)-1*H*-indazole-3-carboxamide (60% yield).

4.11.4. Purification of the compounds by HPLC analysis

Before performing *in vitro* enzyme activity, cellular activity, cell viability assays all the synthesized compounds were purified by analytical-HPLC analysis by using Waters 600E HPLC system with an Ascentis® express C18, 2.7 µm HPLC column at a flow rate of 0.5 mL/minute. A solution of 60% methanol and 40% water (isocratic mode) was used as the mobile phase. All the compounds (~1 mg) were dissolved in 1 mL of 60% methanol and 40% water solvent system (total run time was 10 min). The purity levels of the compounds were ≥ 93-98 %. Analyses were performed by injecting 20 µL of the

compound solutions using a UV-detector at 300 nm and the fractions were collected. It was repeated for more than 10-times.[10,13,32] The entire collected fractions for a particular compound were dried under reduced pressure and finally the compounds were verified by HRMS analysis.

4.11.5. IDO1 and TDO inhibition assay by spectrometric method

Both, IDO1 and TDO inhibition assays were performed according to the earlier reported procedures.[7,10,12,13,33,34] The solubility of the compounds in water was either moderate or poor. Hence, stock solution of the compounds were prepared by first dissolving in DMSO and then diluted with buffer. In the assay system the minimum and maximum amount of DMSO were 0.02% and 2%, respectively. The standard reaction mixture (500 µL) contained KPB (100 mM, pH 6.5 for IDO1 enzyme and 50 mM, pH 8 for TDO enzyme), sodium ascorbate (20 mM), methylene blue (10 µM), catalase (240 nM, from bovine liver), *L*-Trp (150 µM), purified enzyme (40 nM for IDO1 and 25 nM for TDO), DMSO (0.05%, v/v), triton-X 100 (0.01%, v/v) and inhibitors (0.1 µM to 200 µM for IDO1 and 1 µM to 100 µM for TDO). The reaction was quenched using 100 µL of 30% (w/v) trichloroacetic acid. The amount of kynurenine formation was quantified using 2% (w/v) *p*DMAB in acetic acid. The absorbance of the reaction mixture was recorded by at 480 nm. All these experiments were repeated for three times for each compound.

4.11.6. IDO1 and TDO inhibition assay by HPLC analysis

HPLC based enzymatic assay for IDO1 and TDO were performed according to the reported procedures.[10,13,18] The reaction mixture (250 µL) contained KPB (100 mM, pH 6.5 for IDO1 and 50 mM, pH 8 for TDO), sodium ascorbate (20 mM), methylene blue (10 µM), catalase (240 nM, from brovin liver, Sigma), *L*-Trp (150 µM), purified enzyme (40 nM for IDO1 and 25 nM for TDO), DMSO (0.05 %, v/v), triton-X 100 (0.01 %, v/v) and inhibitors. The concentrations of the compounds were varied from 0.5 µM to 10 µM for IDO1 and 10 µM to 100 µM for TDO. The reaction mixture was incubated at 37 ℃ for 1 h in the absence and presence of the synthesized compounds. The reaction was then quenched using 50 µL of 30 % (w/v) trichloroacetic acid and incubated at 65 ℃ for additional 15 min to allow complete hydrolysis of *N*-formylkynurenine to kynurenine. Then the reaction mixture was centrifuged at 10,000 rpm for 10 minutes and 100 µL of the clear reaction mixture was transferred to another tube for HPLC analysis. Then, 20 µL of the solution was injected through Ascentis® express C18, 2.7 µm HPLC column with

a flow rate of 0.5 mL/min and mobile phase, containing 50 % sodium citrate buffer (40 mM, pH 2.25) and 50% methanol (v/v) with 400 µM SDS. The area under the curve at 365 nm correspond to the kynurenine formation in the absence, presence of inhibitors were recorded, and the IC_{50} values were calculated using a standard curve prepared with pure kynurenine (from Sigma) under similar experimental conditions.[10,13,18]

4.11.7. Spectroscopic measurement

The efficacy of the compound's direct binding to the enzyme active site was measured by UV-Vis spectroscopic analysis.[10,12,13] The spectra were recorded at room temperature using a Perkin Elmer Lambda-25 UV-Vis spectrophotometer. All the measurement was performed using 50 mM Tris-HCl buffer (pH 8.0), IDO1 enzyme (5 µM) and selected compounds (70 µM). The deoxy-reaction system was generated by injecting sodium diothionite (~ 10-fold excess) into the solution pre-purged with N_2 gas.

4.11.8. Cellular activity assay

For the *in vitro* cellular activity assay, MDA-MB-231 breast cancer cells were selected. The cells were treated with human Interferon gamma (IFN-γ) (20 ng/mL) in DMEM/F12 complete media for 48 h to allow the over expression of IDO1 enzyme in the cells. After that, the compounds (0.5 µM to 50 µM) were incubated for a period of 4 h and 150 µM of *L*-Trp was incubated for further 5 h. Cells stimulated with IFN-γ alone served as negative control while cells stimulated with 150 µM *L*-Trp served as positive control. Then, the cells were washed with sterile cell-culture grade PBS and were trypsinized followed by centrifugation at 1000 rpm. The cell pellet was re-dissolved in sterile PBS and centrifuged at 1000 rpm. Then the pellet was lysed in 10 mM HEPES buffer by passing through a sterile syringe. The lysate was used for standard IDO1 assay as mentioned earlier and the IC_{50} values were determined for each compounds.[10,13,21]

4.11.9. Cell viability analysis

The dye MTT (3-(4,5-dimethylthiazol-2-yl)-2,5-diphenyltetrazolium bromide) was used to measure cell viability analysis. For this experiment 10,000 cells were seeded in 0.2 mL DMEM/F12 complete medium in 96 well plates and cell culture grade PBS was used to wash the cells after 12 h incubation. After that, the compounds, at a concentration of IC_{50} and $2\times IC_{50}$, respectively were incubated into the incomplete medium for 48 h. Cells were also treated with mitomycin-C at 50 µM and 100 µM concentrations prepared in serum

free media, which served as positive control. Only the cells treated with incomplete medium were considered as 100% viable (served as negative control). Then the cells were washed with PBS and taken for morphological analysis using cytell imaging system (GE Healthcare). After imaging, 100 µL of MTT (0.5 mg/mL in PBS) was added into the each well and incubated for 4 h at 37 ºC with 5% CO_2. Then the MTT solution was removed and the formazan crystal were dissolved in 100 µL cell culture grade DMSO. The absorbance was determined using spectrophotomter (Spectromax M2) at 570 nm and 600 nm.[10,13,35]

4.11.10. Determination of mode of enzyme inhibition

IDO1 enzyme inhibition mode of the selected compounds was measured according to the reported procedure using spectrophotometric method.[10,13] The assay was performed by varying *L*-Trp concentration from 50 µM to 150 µM and compound concentrations from 0.5 µM to 10 µM. The formation of *N*-formylkynurenine was recorded at different time interval. The mode of enzyme inhibition was determined from the plot of 1/V against 1/[S], where V is the initial rate of the enzymatic reaction and [S] is the *L*-Trp concentration.

4.11.11. Molecular docking analysis

MoleGro Virtual Docker version 6.0 (MoleGro Aps, Aarhus, Denmark) was used for molecular docking analysis of the compounds with IDO1 enzyme (PDB code: 4PK5).[10,13,25,36,37] The apo-protein was generated and processed by energy minimization. The most stable three-dimensional structure of the ligands was prepared by using the Aotomated Topology Builder (ATB) and Repository server (http://atb.uq.edu.au/). The occupied position of the ligand (in the crystal structure) was used as the center of docking site (radius: 12 Å; and center: x = 61, y = 51, z = 19) and the other parameters were set default during docking analysis. Two hundred docked structure were generated in each docking run for an individual ligand and energetically favoured docked conformations were evaluated based on the moledock and re-rank scores (docking score-based on energy function such as a force field with repulsive and attractive van-der Waals terms and electrostatic term). After that, the docking poses were analyzed with PyMOL software (The PyMOL Molecular Graphics System, Version 1.0r1, Schrödinger, LLC).

4.12. Spectroscopic Characterization of the Synthesized Compounds

1*H*-indazole-3-carboxylic acid phenylamide (29a)[30]: As brown solid (77%), mp: 204-206 °C; ^{1}H NMR (600 MHz, $CDCl_3$ + MeOD-d_4) δ_{ppm} 8.28 (d, 1H, J = 12 Hz), 7.66 (d, 2H, J = 12 Hz), 7.49 (d, 1H, J = 12 Hz), 7.36-7.29 (m, 3H), 7.22-7.20 (m, 1H), 7.08-7.05 (m, 1H); ^{13}C NMR (151 MHz, $CDCl_3$ + MeOD-d_4) δ_{ppm} 161.5, 141.7, 138.4, 137.7, 128.9, 127.0, 124.2, 122.7, 121.9, 120.0, 110.4; HRMS [31] calcd for $C_{14}H_{11}N_3O$ $[M + H]^+$ 238.0975, found 238.0973.

1*H*-indazole-3-carboxylic acid (4-methoxy-phenyl)-amide (29b)[31]: As white solid (74%), mp: 201-203 °C; ^{1}H NMR (600 MHz, $CDCl_3$ + MeOD-d_4) δ_{ppm} 8.88 (br, s, 1H), 8.35 (d, 1H, J = 12 Hz), 7.58 (d, 2H, J = 12 Hz), 7.45 (d, 1H, J = 6 Hz), 7.36-7.34 (m, 1H), 7.24-7.21 (m, 1H), 6.86-6.84 (m, 2H), 3.74 (s, 3H); ^{13}C NMR (151 MHz, $CDCl_3$ + MeOD-d_4) δ_{ppm} 161.0, 156.5, 141.7, 139.2, 131.2, 127.4, 123.0, 122.6, 122.2, 121.8, 121.7, 114.4, 110.3, 55.7; HRMS [31] calcd for $C_{15}H_{13}N_3O_2$ $[M + H]^+$ 268.1081, found 268.1081.

4-(1*H*-indazole-3-carboxamido)phenyl acetate (29c): As white solid (71%), mp: 217-219 °C; ^{1}H NMR (600 MHz, $CDCl_3$ + MeOD-d_4) δ_{ppm} 9.08 (br, s, 1H), 8.33-8.31 (m, 1H), 7.70-7.68 (m, 2H), 7.47 (d, 1H, J = 12 Hz), 7.37-7.34 (m, 1H), 7.25-7.22 (m, 1H), 7.04-7.02 (m, 2H), 2.24 (s, 3H); ^{13}C NMR (151 MHz, $CDCl_3$ + MeOD-d_4) δ_{ppm} 170.2, 161.2, 146.8, 141.7, 138.7, 135.9, 127.4, 123.1, 122.4, 122.2, 120.9, 120.8, 110.5, 21.2; HRMS [ESI] calcd for $C_{16}H_{13}N_3O_3$ $[M + H]^+$ 296.1030, found 296.1064.

1*H*-indazole-3-carboxylic acid (4-hydroxy-phenyl)-amide (29d): As white solid (57%), mp: 222-224 °C; ^{1}H NMR (600MHz, $CDCl_3$ + DMSO-d_6) δ_{ppm} 12.60 (br, s, 1H), 8.79 (br, s, 1H), 8.43-8.42 (m, 1H), 8.34 (d, 1H, J = 12 Hz), 7.49-7.48 (d, 2H, J = 6 Hz), 7.35-7.26 (m, 1H), 7.22-7.19 (m, 1H), 6.81 (d, 2H, J = 12 Hz); ^{13}C NMR (151 MHz, $CDCl_3$ + MeOD-d_4) δ_{ppm} 161.3, 153.8, 141.7, 138.6, 129.8, 127.1, 122.7, 122.2, 122.0, 115.6, 110.4; HRMS [ESI] calcd for $C_{14}H_{11}N_3O_2$ $[M + H]^+$ 254.0924, found 254.0959.

1*H*-indazole-3-carboxylic acid (4-nitro-phenyl)-amide (29e): As yellow solid (64%), mp: 192-194 °C; ^{1}H NMR (600 MHz, $CDCl_3$ + MeOD-d_4) δ_{ppm} 7.94-7.91 (m, 1H), 7.76-7.73 (m, 1H), 7.66-7.63 (m, 1H), 7.46-7.43 (m, 1H), 7.40-7.31 (m, 3H), 7.17-7.13 (m,

1H); ^{13}C NMR (151 MHz, $CDCl_3$ + MeOD-d_4) δ_{ppm} 165.2, 140.7, 139.4, 128.4, 127.1, 126.9, 126.3, 122.8, 122.2, 121.6, 117.4, 110.9, 110.3; HRMS [ESI] calcd for $C_{14}H_{10}N_4O_3$ $[M + H]^+$ 286.0826, found 286.0831

5-Bromo-1*H*-indazole-3-carboxylic acid phenylamide (29f): As white solid (61%), mp: 189-191 °C; ^{1}H NMR (600 MHz, $CDCl_3$ + DMSO-d_6) δ_{ppm} 12.30 (br, s, 1H), 7.40-7.38 (m, 2H), 6.84-6.82 (m, 2H), 6.68-6.64 (m, 2H), 6.52-6.48 (m, 2H); ^{13}C NMR (151 MHz, $CDCl_3$ + DMSO-d_6) δ_{ppm}; 160.0, 139.8, 137.5, 137.2, 129.1, 128.3, 123.8, 123.3, 122.9, 119.3, 115.1, 111.8; HRMS [ESI] calcd for $C_{12}H_9N_5O$ $[M + H]^+$ 240.0880, found 240.0868.

1*H*-indazole-3-carboxylic acid pyrimidin-2-ylamide (30): As yellow solid (54%), mp: 241-243 °C; ^{1}H NMR (600 MHz, $CDCl_3$ + DMSO-d_6) δ_{ppm} 9.28 (br, s, 1H), 8.45 (s, 1H), 7.72-7.71 (d, 2H, J = 6 Hz), 7.44-7.40 (m, 2H), 7.31-7.28 (m, 2H), 7.07-7.04 (m, 1H); ^{13}C NMR (151 MHz, $CDCl_3$ + DMSO-d_6) δ_{ppm} 164.3, 140.2, 139.0, 126.1, 122.8, 121.5, 121.3, 109.9; HRMS [ESI] calcd for $C_{14}H_{10}BrN_3O$ $[M + H]^+$ 316.0080, found 316.0078.

1*H*-indazole-3-carboxylic acid *N*-phenyl-hydrazide (31a): As brown solid (78%), mp: 226-228 °C; ^{1}H NMR (600 MHz, $CDCl_3$ + MeOD-d_4) δ_{ppm} 8.18-8.15 (m, 1H), 7.50-7.47 (m, 1H), 7.35-7.31 (m, 1H), 7.19-7.12 (m, 3H), 6.89-6.86 (m, 2H), 6.81-6.77 (m, 1H); ^{13}C NMR (151 MHz, $CDCl_3$+ MeOD-d_4) δ_{ppm} 163.7, 148.1, 141.3, 136.8, 129.0, 127.0, 122.7, 122.1, 121.6, 120.8, 113.3, 110.4; HRMS [ESI] calcd for $C_{14}H_{12}N_4O$ $[M + H]^+$ 253.1084, found 253.1085.

1*H*-indazole-3-carboxylic acid *N*-(4-chloro-phenyl)-hydrazide (31b): As yellow solid (61%), mp: 235-237 °C; ^{1}H NMR (600 MHz, MeOD-d_4 + DMSO-d_6) δ_{ppm} 7.35-7.34 (d, 1H, J = 6 Hz), 6.83-6.82 (d, 1H, J = 6 Hz), 6.63-6.60 (m, 1H), 6.45-6.42 (m, 1H), 6.36-6.35 (d, 2H, J = 6 Hz), 6.05-6.04 (d, 2H, J = 6 Hz); ^{13}C NMR (151 MHz, MeOD-d_4 + DMSO-d_6) δ_{ppm} 163.7, 149.2, 141.8, 137.7, 129.3, 127.4, 123.5, 123.0, 122.7, 122.0, 114.7, 111.3; HRMS [ESI] calcd for $C_{14}H_{11}ClN_4O$ $[M + H]^+$ 287.0694, found 287.0693.

1*H*-indazole-3-carboxylic acid *N*-(3-chloro-phenyl)-hydrazide (31c): As yellow solid (55%), mp: 108-110 °C; ^{1}H NMR (400 MHz, $CDCl_3$ + MeOD-d_4) δ_{ppm} 7.75-7.71 (m, 2H),

7.68-7.64 (m, 2H), 7.44-7.37 (m, 4H); ^{13}C NMR (151 MHz, $CDCl_3$ + DMSO-d_6 + MeOD-d_4) δ_{ppm} 162.9, 149.9, 148.4, 140.8, 136.0, 129.0, 127.5, 126.3, 125.0, 121.8, 118.0, 116.9, 113.0, 109.5; HRMS [ESI] calcd for $C_{14}H_{11}N_5O_3$ $[M + H]^+$ 298.0935, found 298.0938.

5-Bromo-1*H*-indazole-3-carboxylic acid *N*-phenylhydrazide (31d): As orange solid (58%), mp: 256-258 °C; ^{1}H NMR (600 MHz, $CDCl_3$ + DMSO-d_6) δ_{ppm} 9.30 (br, s, 1H), 8.36-8.32 (m, 1H), 7.40-7.35 (m, 2H), 7.14-7.09 (m, 2H), 6.88-6.75 (m, 3H); ^{13}C NMR (151 MHz, $CDCl_3$ + DMSO-d_6) δ_{ppm} 162.3, 148.3, 139.6, 136.1, 129.4, 128.7, 124.0, 123.3, 120.1, 115.4, 113.0, 112.0; HRMS [ESI] calcd for $C_{14}H_{11}BrN_4O$ $[M + H]^+$ 331.0189, found 331.0188.

5-Bromo-1*H*-indazole-3-carboxylic acid *N*-(4-chloro-phenyl)-hydrazide (31e): As brown semi-solid (40%); ^{1}H NMR (600 MHz, $CDCl_3$ + DMSO-d_6) δ_{ppm} 9.86 (br, s, 1H), 8.23 (d, 1H, J = 12 Hz), 7.53-7.51 (m, 2H), 7.21-7.14 (m, 3H), 7.04-7.01 (m, 1H); ^{13}C NMR (151 MHz, $CDCl_3$ + DMSO-d_6) δ_{ppm} 161.5, 158.8, 138.4, 136.1, 128.7, 128.3, 128.0, 123.8, 120.3, 118.7, 116.1, 113.5; HRMS [ESI] calcd for $C_{14}H_{10}BrClN_4O$ $[M + H]^+$ 364.9799, found 364.9797.

1*H*-indazole-3-carboxylic acid *N*-(p-tosyl)-hydrazide (32): As white solid (77%), mp: 198-200 °C; ^{1}H NMR (600 MHz, $CDCl_3$ + MeOD-d_4) δ_{ppm} 7.92-7.89 (m, 1H), 7.74-7.65 (m, 2H), 7.46-7.29 (m, 3H), 7.16-7.13 (m, 2H), 2.28 (s, 3H); ^{13}C NMR (151 MHz, $CDCl_3$ + MeOD-d_4) δ_{ppm} 161.5, 144.6, 141.2, 136.0, 134.0, 129.6, 128.4, 126.8, 126.3, 122.9, 121.4, 117.2, 110.5, 21.5; HRMS [ESI] calcd for $C_{15}H_{14}N_4O_3S$ $[M + H]^+$ 331.0859, found 331.0858.

References

(1) Dunn, G. P.; Old, L. J.; Schreiber, R. D. The immunobiology of cancer immunosurveillance and immunoediting. *Immunity* **2004**, *21*, 137-148.

(2) Kershaw, M. H.; Westwood, J. A.; Slaney, C. Y.; Darcy, P. K. Clinical application of genetically modified T cells in cancer therapy. *Clin Transl. Immunol.* **2014**, *3*, e16.

(3) Munn, D. H.; Mellor, A. L. Indoleamine 2,3-dioxygenase and tumor-induced tolerance. *J. Clin. Invest.* **2007**, *117*, 1147-1154.

(4) Okamoto, A.; Nikaido, T.; Ochiai, K.; Takakura, S.; Saito, M.; Aoki, Y.; Ishii, N.; Yanaihara, N.; Yamada, K.; Takikawa, O.; Kawaguchi, R.; Isonishi, S.; Tanaka, T.; Urashima, M. Indoleamine 2,3-Dioxygenase Serves as a Marker of Poor Prognosis in Gene Expression Profiles of Serous Ovarian Cancer Cells. *Clin. Cancer Res.* **2005**, *11*, 6030-6039.

(5) Uyttenhove, C.; Pilotte, L.; Theate, I.; Stroobant, V.; Colau, D.; Parmentier, N.; Boon, T.; Van den Eynde, B. J. Evidence for a tumoral immune resistance mechanism based on tryptophan degradation by indoleamine 2,3-dioxygenase. *Nat. Med.* **2003**, *9*, 1269-1274.

(6) Zou, W. P. Immunosuppressive networks in the tumour environment and their therapeutic relevance. *Nat. Rev. Cancer* **2005**, *5*, 263-274.

(7) Rohrig, U. F.; Majjigapu, S. R.; Vogel, P.; Zoete, V.; Michielin, O. Challenges in the Discovery of Indoleamine 2,3-Dioxygenase 1 (IDO1) Inhibitors. *J. Med. Chem.* **2015**, *58*, 9421-9437.

(8) Hou, D. Y.; Muller, A. J.; Sharma, M. D.; DuHadaway, J.; Banerjee, T.; Johnson, M.; Mellor, A. L.; Prendergasts, G. C.; Munn, D. H. Inhibition of indoleamine 2,3-dioxygenase in dendritic cells by stereoisomers of 1-methyl-tryptophan correlates with antitumor responses. *Cancer Res.* **2007**, *67*, 792-801.

(9) Muller, A. J.; DuHadaway, J. B.; Donover, P. S.; Sutanto-Ward, E.; Prendergast, G. C. Inhibition of indoleamine 2,3-dioxygenase, an immunoregulatory target of the cancer suppression gene Bin1, potentiates cancer chemotherapy. *Nat. Med.* **2005**, *11*, 312-319.

(10) Panda, S.; Roy, A.; Deka, S. J.; Trivedi, V.; Manna, D. Fused Heterocyclic Compounds as Potent Indoleamine-2,3-dioxygenase 1 Inhibitors. *Acs Med. Chem. Lett.* **2016**, *7*, 1167-1172.

(11) Yue, E. W.; Douty, B.; Wayland, B.; Bower, M.; Liu, X. D.; Leffet, L.; Wang, Q.; Bowman, K. J.; Hansbury, M. J.; Liu, C. N.; Wei, M.; Li, Y. L.; Wynn, R.; Burn, T. C.; Koblish, H. K.; Fridman, J. S.; Metcalf, B.; Scherle, P. A.; Combs, A. P. Discovery of Potent Competitive Inhibitors of Indoleamine 2,3-Dioxygenase with *in Vivo*

Pharmacodynamic Activity and Efficacy in a Mouse Melanoma Model. *J. Med. Chem.* **2009**, *52*, 7364-7367.

(12) Malachowski, W. P.; Winters, M.; DuHadaway, J. B.; Lewis-Ballester, A.; Badir, S.; Wai, J.; Rahman, M.; Sheikh, E.; LaLonde, J. M.; Yeh, S. R.; Prendergast, G. C.; Muller, A. J. O-alkylhydroxylamines as rationally-designed mechanism-based inhibitors of indoleamine 2,3-dioxygenase 1. *Eur. J. Med. Chem.* **2016**, *108*, 564-576.

(13) Paul, S.; Roy, A.; Deka, S. J.; Panda, S.; Trivedi, V.; Manna, D. Nitrobenzofurazan derivatives of N'-hydroxyamidines as potent inhibitors of indoleamine-2,3-dioxygenase 1. *Eur. J. Med. Chem*. **2016**, *121*, 364-375.

(14) Panda, S.; Maity, P.; Manna, D. Transition Metal, Azide, and Oxidant-Free Homo- and Heterocoupling of Ambiphilic Tosylhydrazones to the Regioselective Triazoles and Pyrazoles. *Org. Lett.* **2017**, *19*, 1534-1537.

(15) Paul, S.; Panda, S.; Manna, D. Mild method for the synthesis of 1*H*-indazoles through oxime-phosphonium ion intermediate. *Tett. Lett.* **2014**, *55*, 2480-2483.

(16) Qian, S.; He, T.; Wang, W.; He, Y. Y.; Zhang, M.; Yang, L. L.; Li, G. B.; Wang, Z. Y. Discovery and preliminary structure–activity relationship of 1*H*-indazoles with promising indoleamine-2,3-dioxygenase 1 (IDO1) inhibition properties. *Bioorg. Med. Chem.* **2016**, 24, 6194-6205.

(17) Pasquini, S.; Botta, L.; Scincraro, T.; Mugnaini, C.; Ligresti, A.; Palazzo, E.; Maione, S.; Di Marzo, V.; Corelli, F. Investigations on the 4-Quinolone-3-carboxylic Acid Motif. 2. Synthesis and Structure−Activity Relationship of Potent and Selective Cannabinoid-2 Receptor Agonists Endowed with Analgesic Activity in Vivo. *J. Med. Chem.* **2008,** *51*, 5075-5084.

(18) Rohrig, U. F.; Majjigapu, S. R.; Grosdidier, A.; Bron, S.; Stroobant, V.; Pilotte, L.; Colau, D.; Vogel, P.; Van den Eynde, B. J.; Zoete, V.; Michielin, O. Rational Design of 4-Aryl-1,2,3-Triazoles for Indoleamine 2,3-Dioxygenase 1 Inhibition. *J. Med. Chem.* **2012**, *55*, 5270-5290.

(19) Lewis-Ballester, A.; Batabyal, D.; Egawa, T.; Lu, C.; Lin, Y.; Marti, M. A.; Capece, L.; Estrin, D. A.; Yeh, S. R. Evidence for a ferryl intermediate in a heme-based dioxygenase. *Proc. Natl. Acad. Sci. U S A* **2009**, *106*, 17371-17376.

(20) Huang, Q.; Zheng, M. F.; Yang, S. S.; Kuang, C. X.; Yu, C. J.; Yang, Q. Structure–activity relationship and enzyme kinetic studies on 4-aryl-1*H*-1,2,3-triazoles as indoleamine 2,3-dioxygenase (IDO) inhibitors. *Eur. J. Med. Chem.* **2011,** *46*, 5680-5687.

(21) Travers, M. T.; Gow, I. F.; Barber, M. C.; Thomson, J.; Shennan, D. B. Indoleamine 2,3-dioxygenase activity and L-tryptophan transport in human breast cancer cells. *Biochim. Biophys. Acta-Biomem.* **2004**, *1661*, 106-112.

(22) Elhalem, E.; Bailey, B. N.; Docampo, R.; Ujvary, I.; Szajnman, S. H.; Rodriguez, J. B. Design, Synthesis, and Biological Evaluation of Aryloxyethyl Thiocyanate Derivatives against Trypanosoma cruzi. *J. Med. Chem.* **2002**, *45*, 3984-3999.

(23) Yang, S. S.; Li, X. S.; Hu, F. F.; Li, Y. L.; Yang, Y. Y.; Yan, J. K.; Kuang, C. X.; Yang, Q. Discovery of Tryptanthrin Derivatives as Potent Inhibitors of Indoleamine 2,3-Dioxygenase with Therapeutic Activity in Lewis Lung Cancer (LLC) Tumor-Bearing Mice. *J. Med. Chem.* **2013**, *56*, 8321-8331.

(24) Kumar, S.; Malachowski, W. P.; DuHadaway, J. B.; LaLonde, J. M.; Carroll, P. J.; Jaller, D.; Metz, R.; Prendergast, G. C.; Muller, A. J. Indoleamine 2,3-Dioxygenase Is the Anticancer Target for a Novel Series of Potent Naphthoquinone-Based Inhibitors. *J. Med. Chem.* **2008**, *51*, 1706-1718.

(25) Tojo, S.; Kohno, T.; Tanaka, T.; Kamioka, S.; Ota, Y.; Ishii, T.; Kamimoto, K.; Asano, S.; Isobe, Y. Crystal Structures and Structure-Activity Relationships of Imidazothiazole Derivatives as IDO1 Inhibitors. *ACS Med. Chem. Lett.* **2014**, *5*, 1119-1123.

(26) Rohrig, U. F.; Awad, L.; Grosdidier, A.; Larrieu, P.; Stroobant, V.; Colau, D.; Cerundolo, V.; Simpson, A. J. G.; Vogel, P.; Van den Eynde, B. J.; Zoete, V.; Michielin, O. Rational Design of Indoleamine 2,3-Dioxygenase Inhibitors. *J. Med. Chem.* **2010**, *53*, 1172-1189.

(27) Matsuno, K.; Takai, K.; Isaka, Y.; Unno, Y.; Sato, M.; Takikawa, O.; Asai, A. *S*-Benzylisothiourea derivatives as small-molecule inhibitors of indoleamine-2,3-dioxygenase. *Bioorg. Med. Chem. Lett.* **2010**, *20*, 5126-5129.

(28) Bano, M.; Barot, K. P.; Jain, S. V.; Ghate, M. D. Identification of 3-hydroxy-4[3,4-dihydro-3-oxo-2*H*-1,4-benzoxazin-4-yl]-2,2-dimethyldihydro-2*H*-benzopyran derivatives as potassium channel activators and anti-inflammatory agents. *Med. Chem. Res.* **2015**, *24*, 3008-3020.

(29) Conte, I.; Giuliano, C.; Ercolani, C.; Narjes, F.; Koch, U.; Rowley, M.; Altamura, S.; De Francesco, R.; Neddermann, P.; Migliaccio, G.; Stansfield, I. Synthesis and SAR of piperazinyl-*N*-phenylbenzamides as inhibitors of hepatitis C virus RNA replication in cell culture. *Bioorg. Med. Chem. Lett.* **2009**, *19*, 1779-1183.

(30) Shi, J. J.; Ji, F. H.; He, P. L.; Yang, Y. X.; Tang, W.; Zuo, J. P.; Li, Y. C. Synthesis and Hepatitis C Antiviral Activity of 1-Aminobenzyl-1*H*-indazole-3-carboxamide Analogues. *Chem. Med. Chem.* **2013**, *8*, 722-725.

(31) Nakano, H.; Hasegawa, T.; Imamura, R.; Saito, N.; Kojima, H.; Okabe, T.; Nagano, T. Development of a potent and selective FLT3 kinase inhibitor by systematic expansion of a non-selective fragment-screening hit. *Bioorg. Med. Chem. Lett.* **2016**, *26*, 2370-2374.

(32) Heyes, M. P.; Saito, K.; Crowley, J. S.; Davis, L. E.; Demitrack, M. A.; Der, M.; Dilling, L. A.; Elia, J.; Kruesi, M. J.; Lackner, A. et al. Quinolinic acid and kynurenine pathway metabolism in inflammatory and non-inflammatory neurological disease. *Brain* **1992**, *115*, 1249-1273.

(33) Austin, C. J. D.; Mizdrak, J.; Matin, A.; Sirijovski, N.; Kosim-Satyaputra, P.; Willows, R. D.; Roberts, T. H.; Truscott, R. J. W.; Polekhina, G.; Parker, M. W.; Jamie, J. F. Optimised expression and purification of recombinant human indoleamine 2,3-dioxygenase. *Protein Expr. Purif.* **2004**, *37*, 392-398.

(34) Takikawa, O.; Kuroiwa, T.; Yamazaki, F.; Kido, R. Mechanism of interferon-gamma action. Characterization of indoleamine 2,3-dioxygenase in cultured human cells induced by interferon-gamma and evaluation of the enzyme-mediated tryptophan degradation in its anticellular activity. *J. Biol. Chem.* **1988**, *263*, 2041-2048.

(35) Gorai, S.; Paul, S.; Sankaran, G.; Borah, R.; Santra, M. K.; Manna, D. Inhibition of phosphatidylinositol-3,4,5-trisphosphate binding to the AKT pleckstrin homology domain by 4-amino-1,2,5-oxadiazole derivatives. *Med. Chem. Comm.* **2015**, *6*, 1798-1808.

(36) Mamidi, N.; Borah, R.; Sinha, N.; Jana, C.; Manna, D. Effects of Ortho Substituent Groups of Protocatechualdehyde Derivatives on Binding to the C1 Domain of Novel Protein Kinase C. *J. Phys. Chem. B* **2012**, *116*, 10684-10692.

(37) Mamidi, N.; Gorai, S.; Mukherjee, R.; Manna, D. Development of diacyltetrol lipids as activators for the C1 domain of protein kinase C. *Mol. Biosyst*. **2012**, *8,* 1275-1285.

4.13. NMR Spectra of the Synthesized Compounds

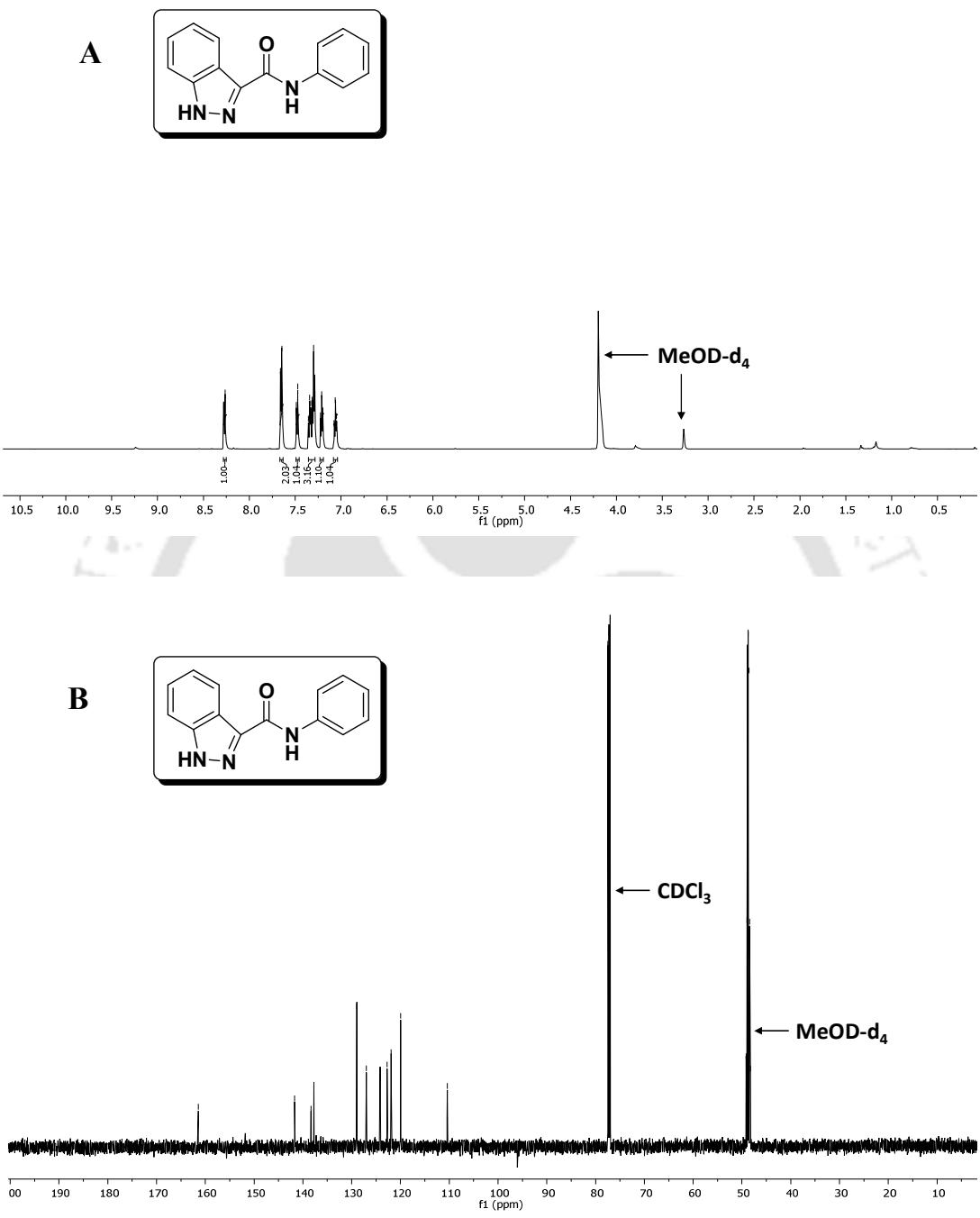

Figure 4.13.1. ^{1}H NMR **(A)** and ^{13}C NMR **(B)** spectra of 1*H*-indazole-3-carboxylic acid phenylamide (**29a**).

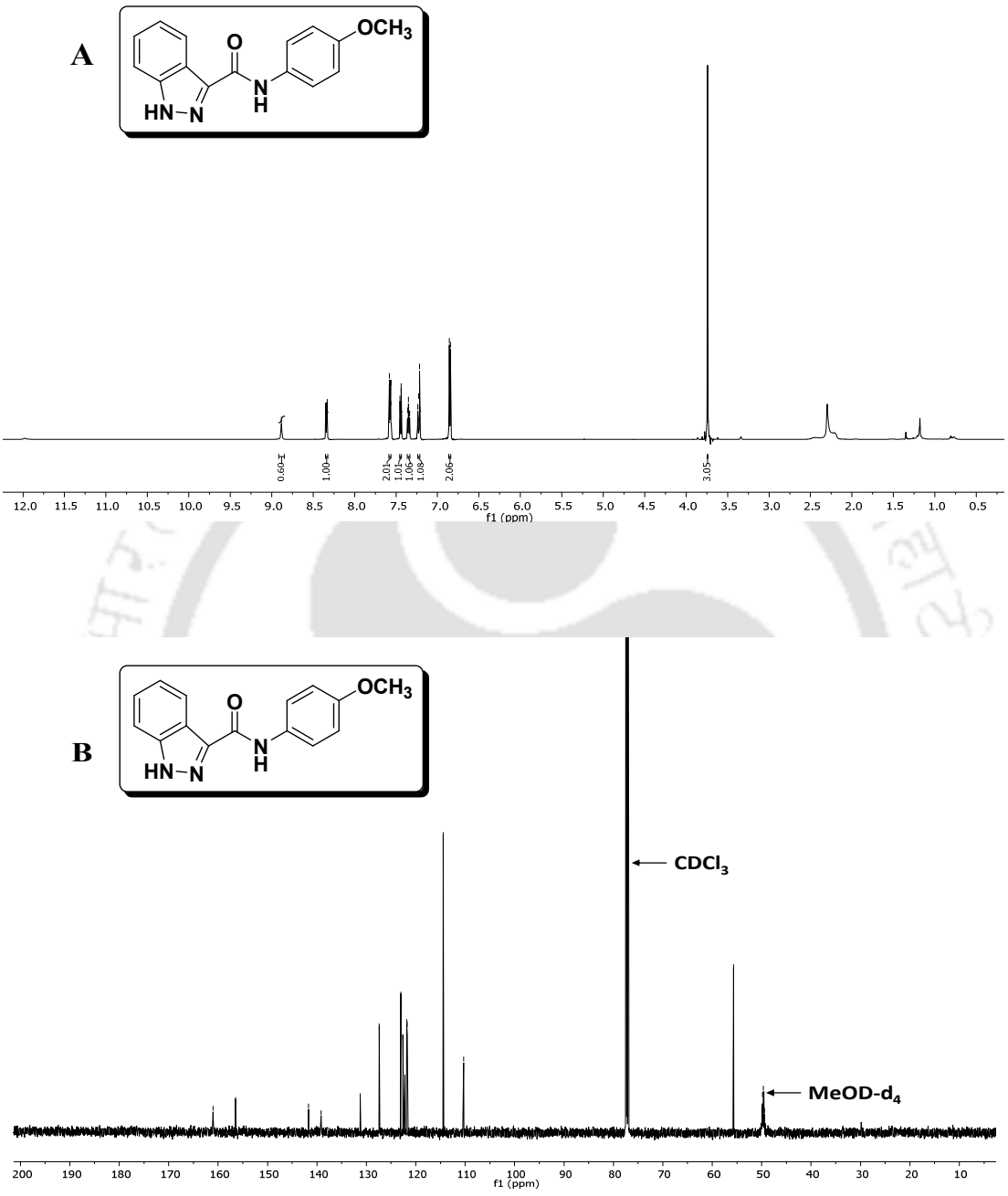

Figure 4.13.2. ^{1}H NMR **(A)** and ^{13}C NMR **(B)** spectra of 1*H*-indazole-3-carboxylic acid (4-methoxy-phenyl)-amide (**29b**).

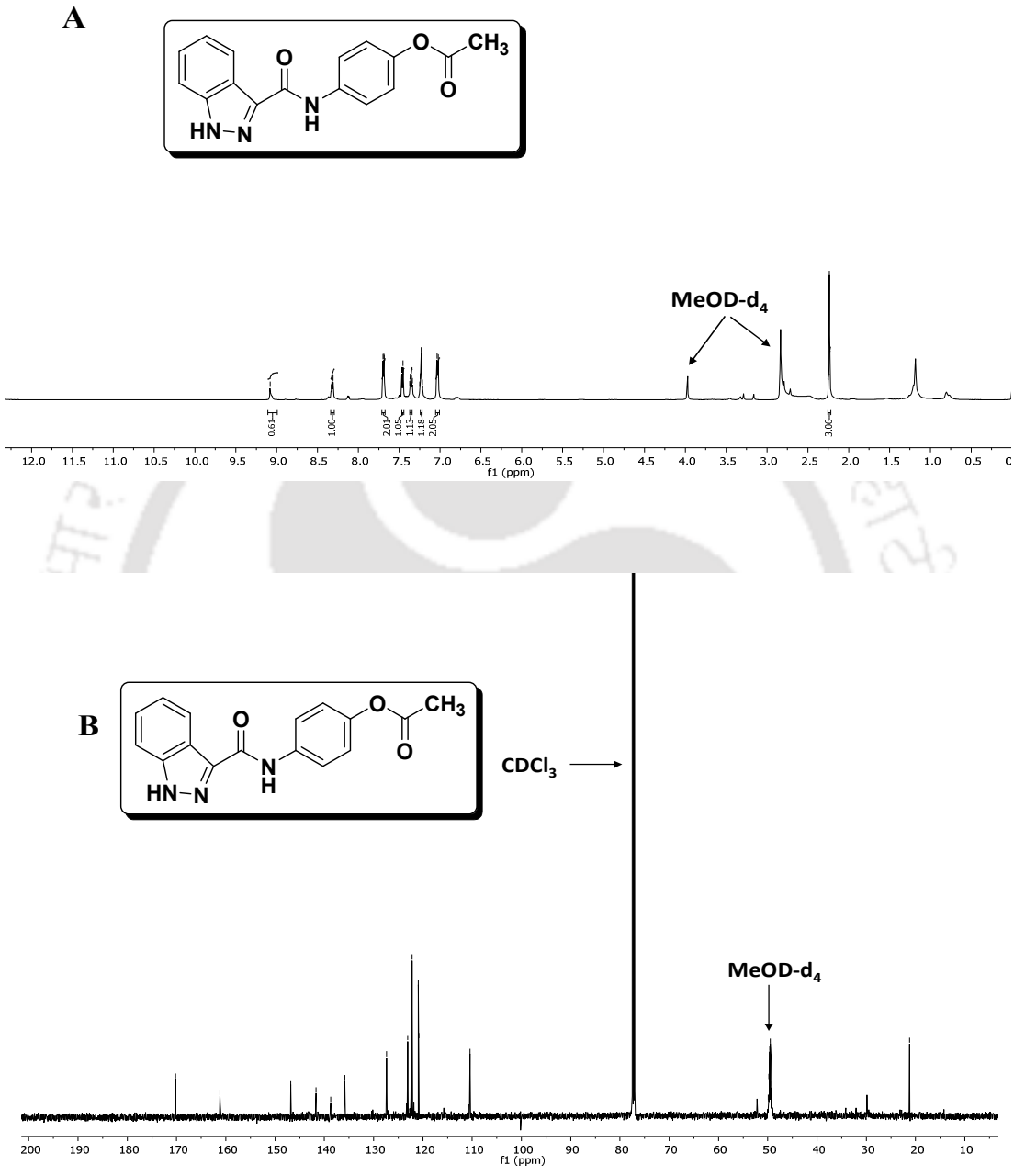

Figure 4.13.3. ^{1}H NMR **(A)** and ^{13}C NMR **(B)** spectra of 4-(1*H*-indazole-3-carboxamido)phenyl acetate (**29c**).

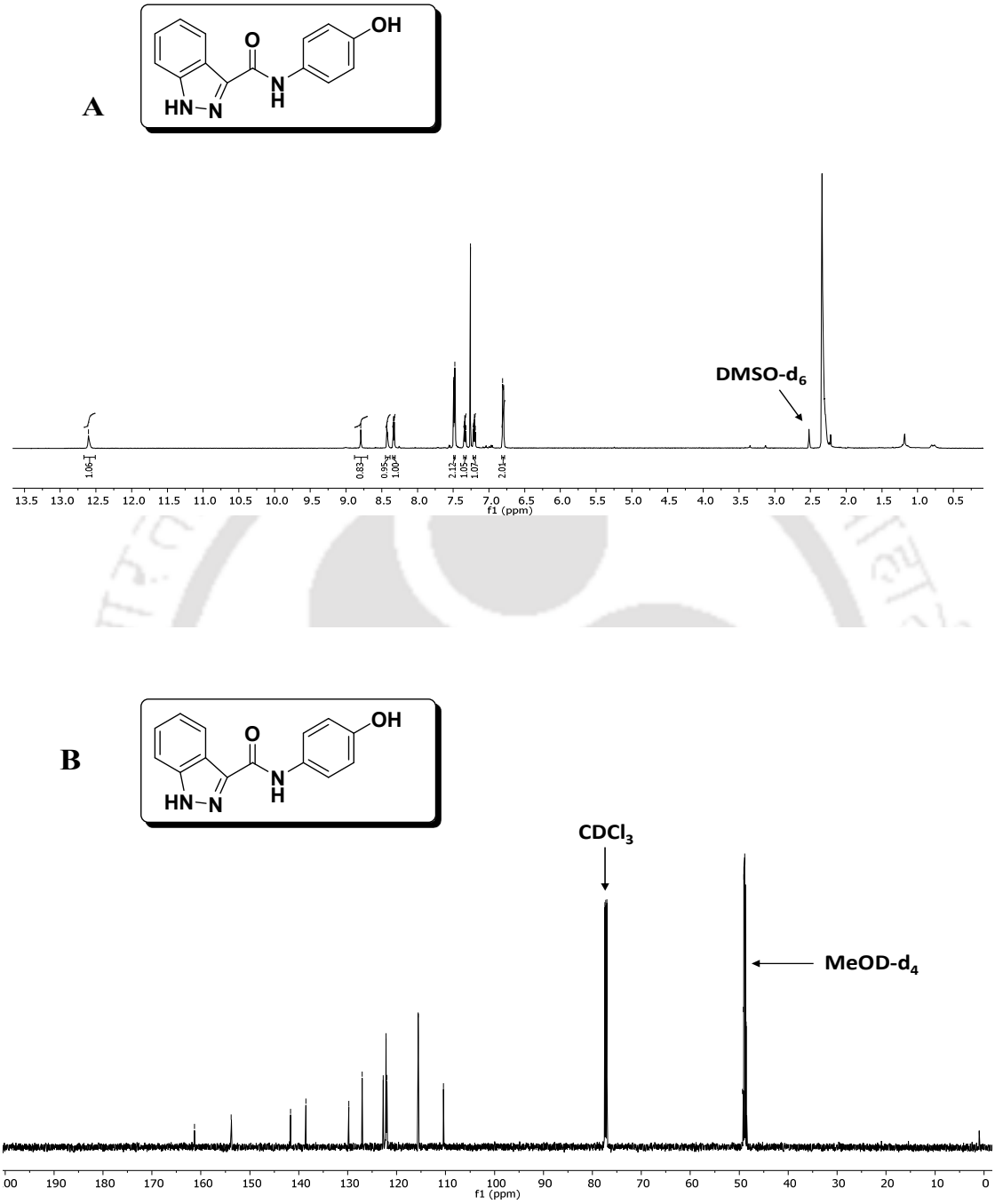

Figure 4.13.4. ^{1}H NMR **(A)** and ^{13}C NMR **(B)** spectra of 1*H*-indazole-3-carboxylic acid (4-hydroxy-phenyl)-amide (**29d**).

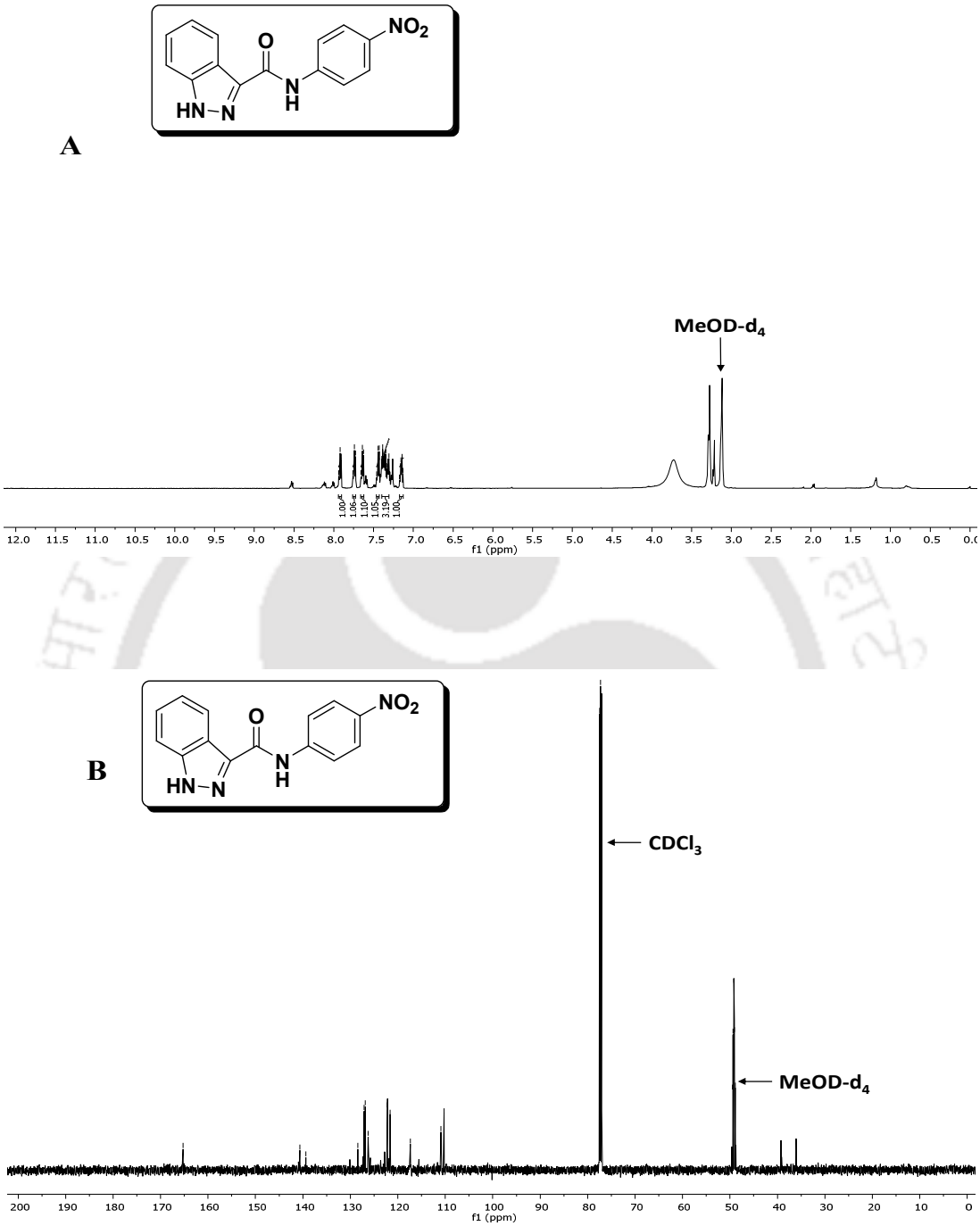

Figure 4.13.5. ^{1}H NMR **(A)** and ^{13}C NMR **(B)** spectra of 1*H*-indazole-3-carboxylic acid (4-nitro-phenyl)-amide (**29e**).

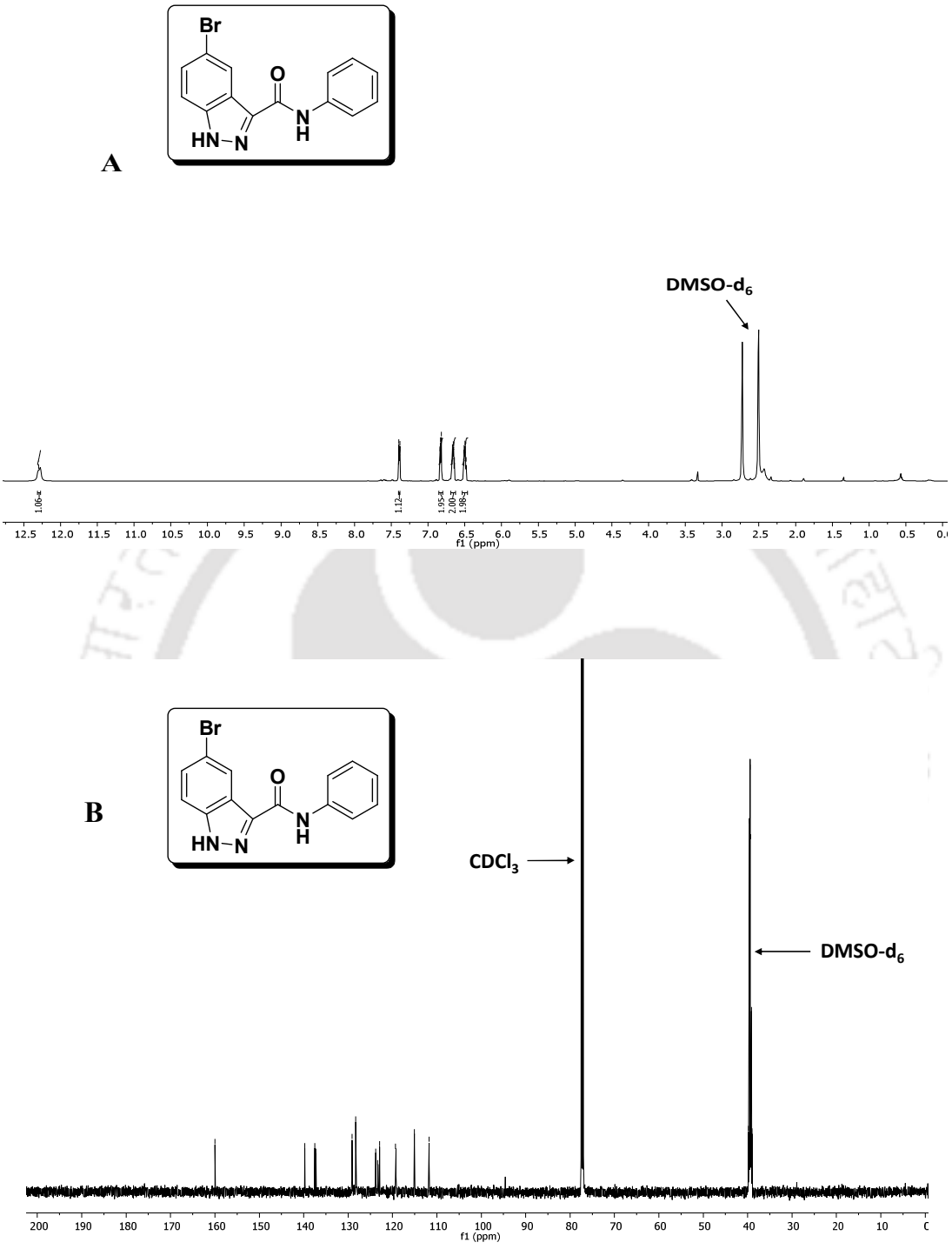

Figure 4.13.6. ^{1}H NMR **(A)** and ^{13}C NMR **(B)** spectra of 5-Bromo-1*H*-indazole-3-carboxylic acid phenylamide (**29f**).

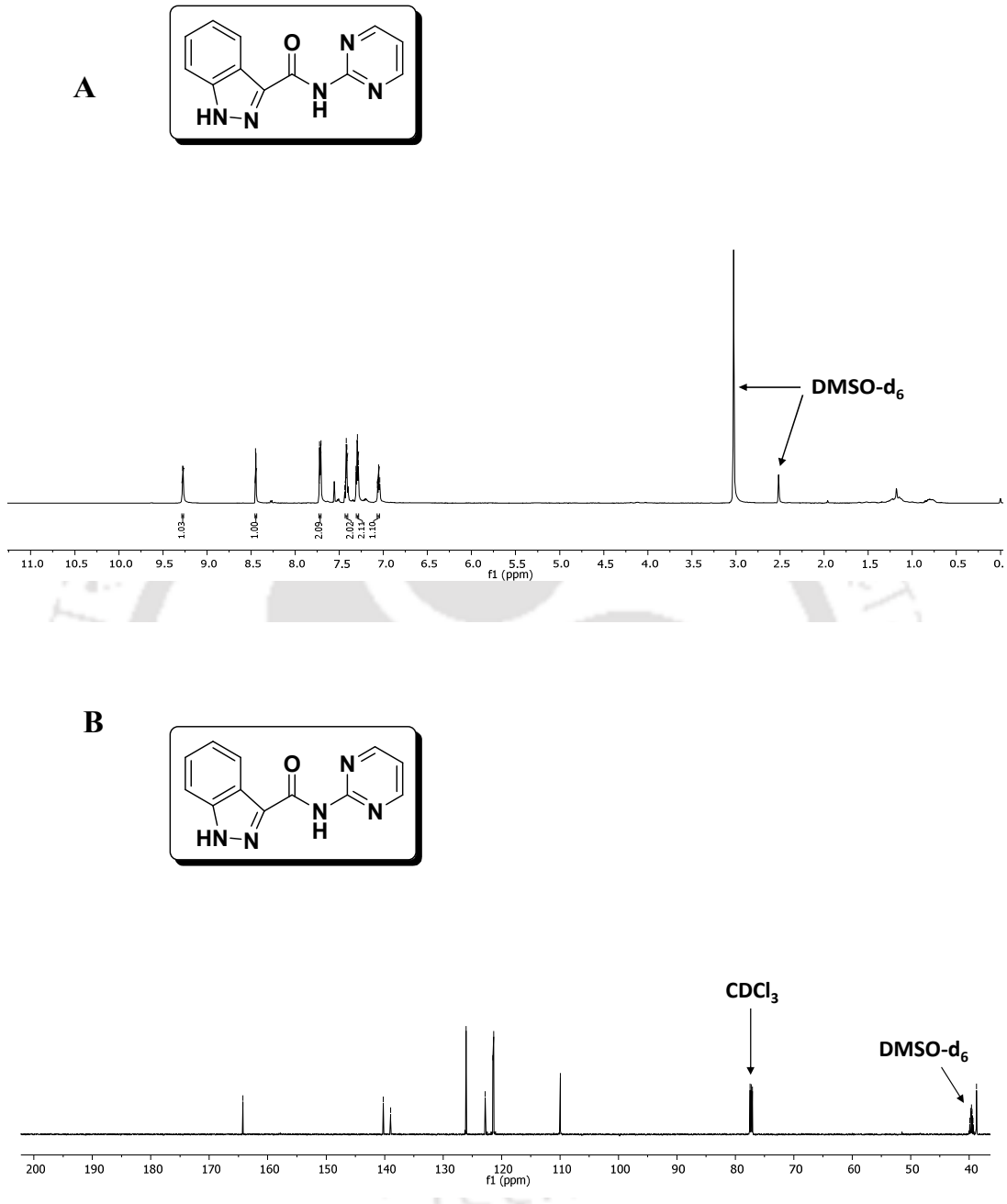

Figure 4.13.7. ^{1}H NMR **(A)** and ^{13}C NMR **(B)** spectra of 1*H*-indazole-3-carboxylic acid pyrimidin-2-ylamide (**30**).

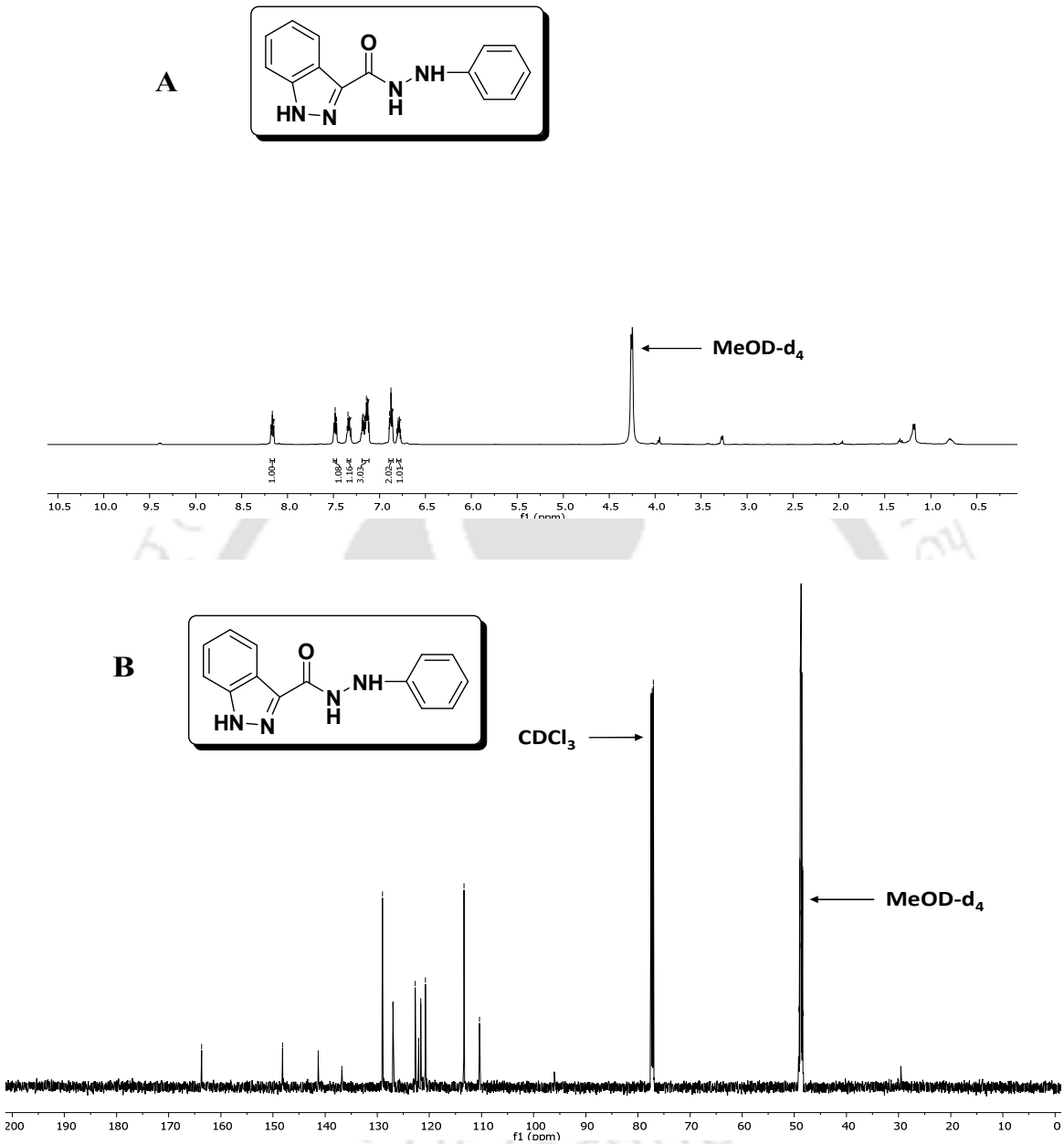

Figure 4.13.8. ^{1}H NMR **(A)** and ^{13}C NMR **(B)** spectra of 1*H*-indazole-3-carboxylic acid *N*-phenyl-hydrazide (**31a**).

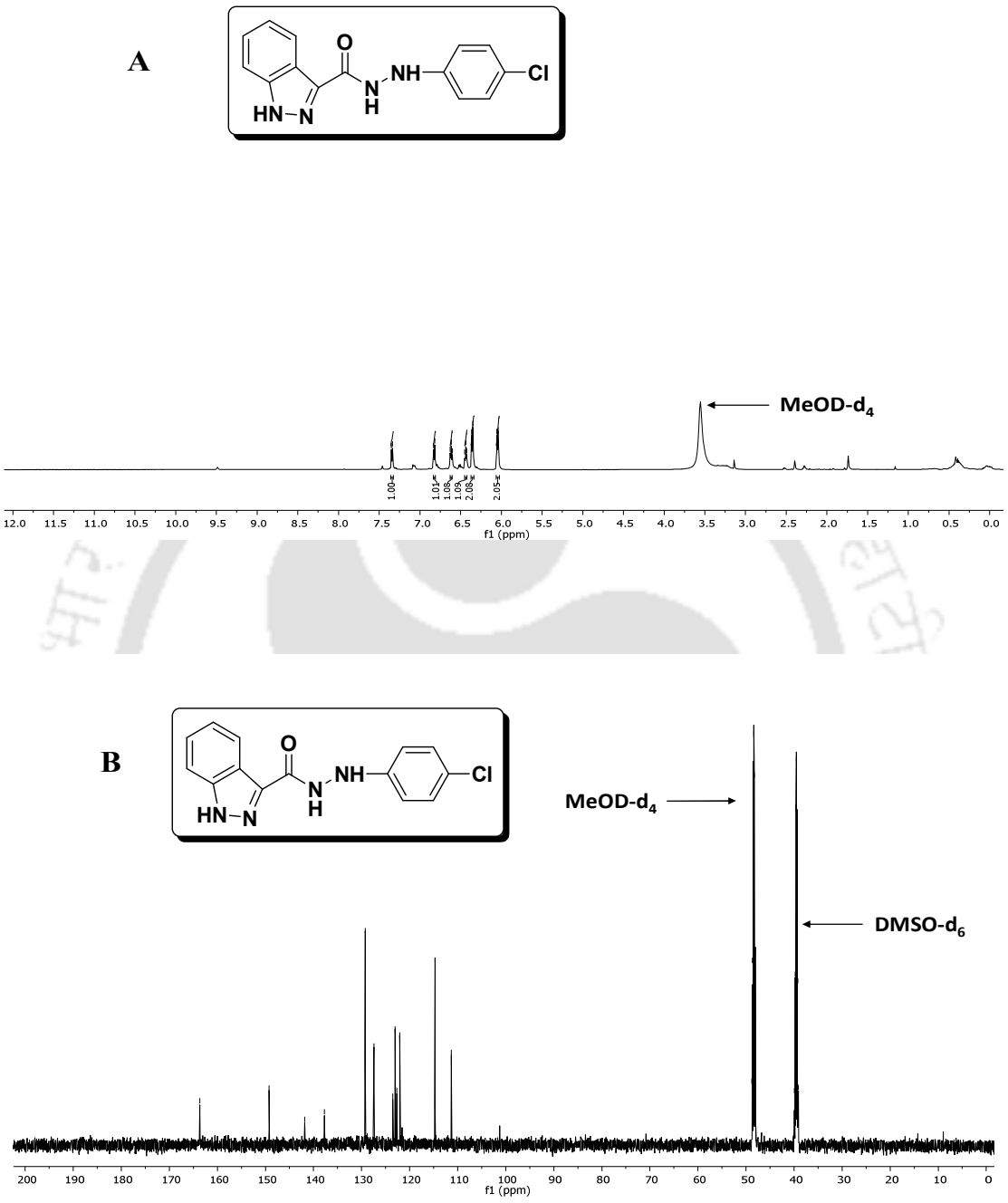

Figure 4.13.9. ^{1}H NMR **(A)** and ^{13}C NMR **(B)** spectra of 1*H*-indazole-3-carboxylic acid *N*-(4-chloro-phenyl)-hydrazide (**31b**).

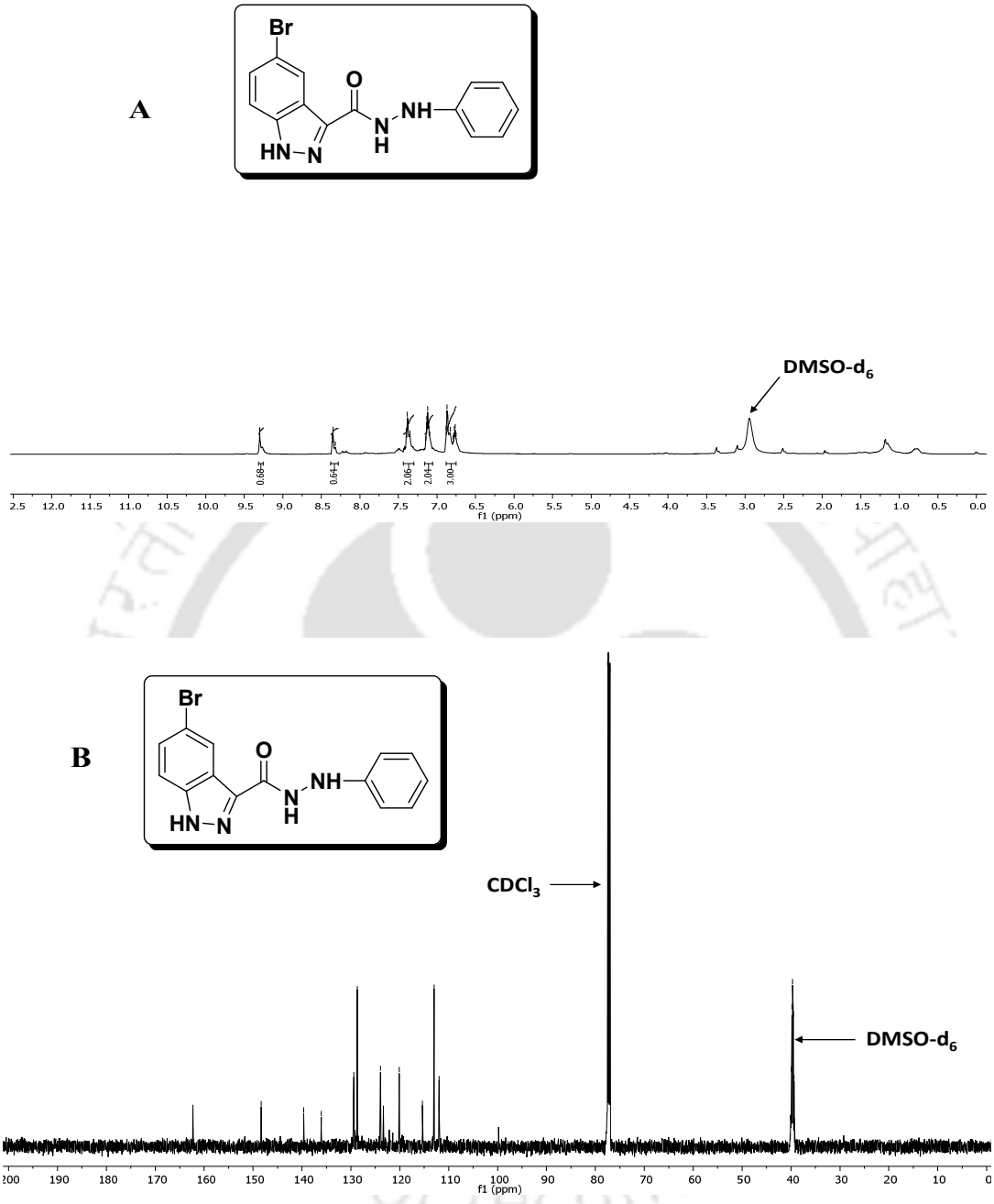

Figure 4.13.10. ^{1}H NMR **(A)** and ^{13}C NMR **(B)** spectra of 5-Bromo-1*H*-indazole-3-carboxylic acid *N*-phenylhydrazide (**31d**).

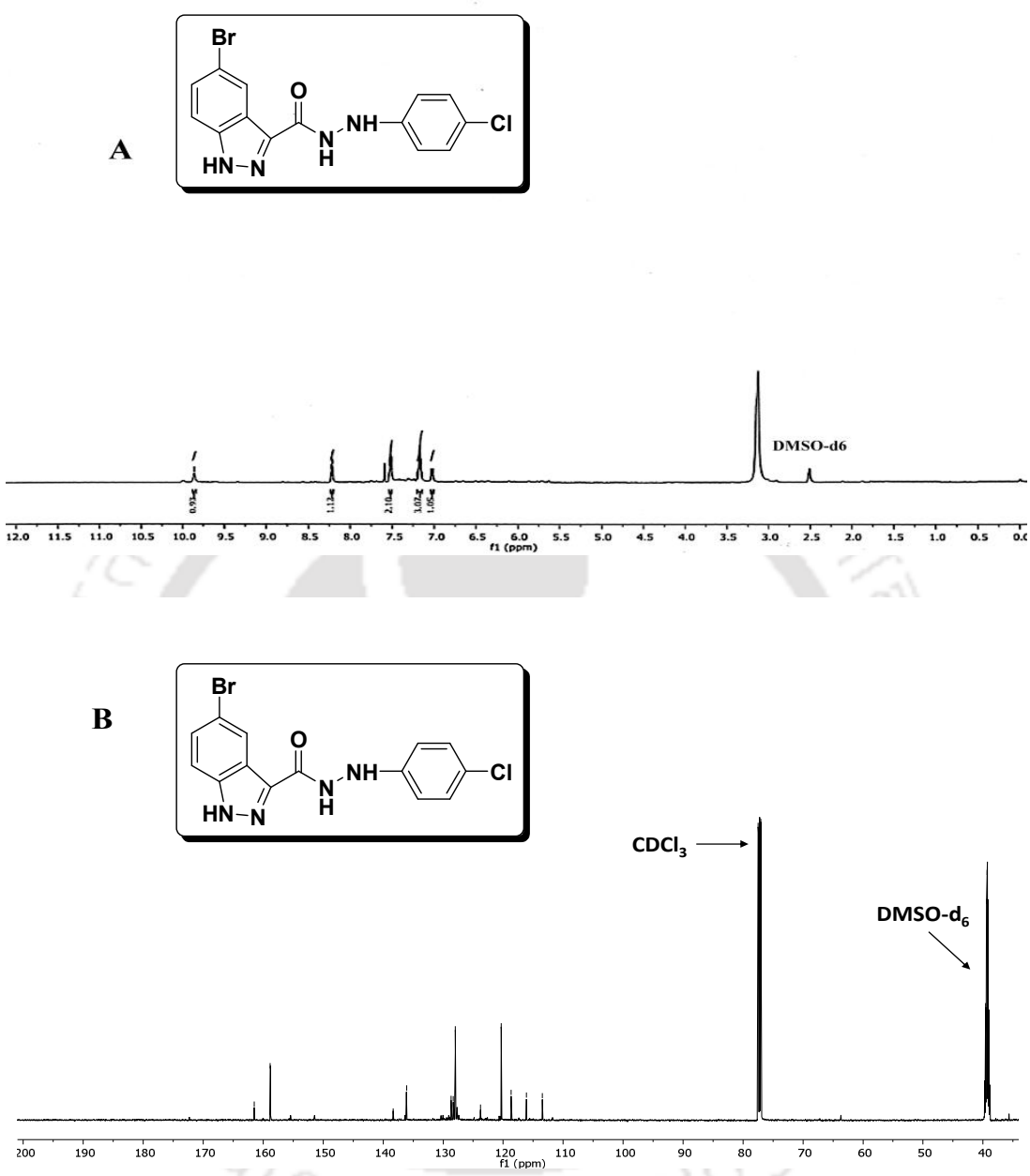

Figure 4.13.11. ^{1}H NMR **(A)** and ^{13}C NMR **(B)** spectra of 5-Bromo-1*H*-indazole-3-carboxylic acid *N*-(4-chloro-phenyl)-hydrazide (**31e**).

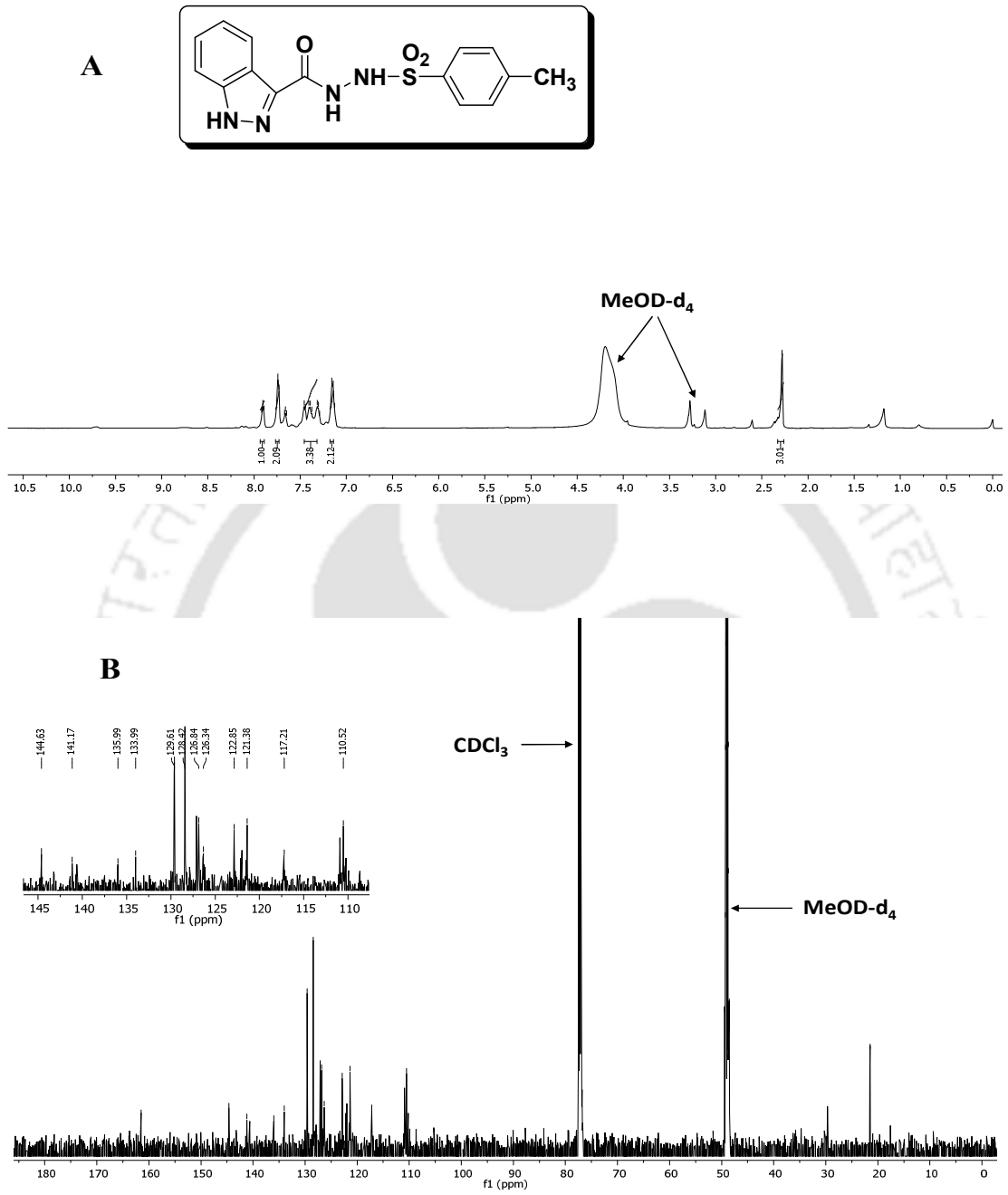

Figure 4.13.12. ^{1}H NMR **(A)** and ^{13}C NMR **(B)** spectra of 1*H*-indazole-3-carboxylic acid *N*-(p-tosyl)-hydrazide (**32**).

Conclusion and Future Perspective

Overall this report describes the successful design and synthesis of small molecules targeting the inhibition of IDO1 enzyme. Although, a variety of chemical series of IDO1 inhibitors have been reported until date but most of the scaffolds have never been further used after their initial studies. Inconsistent results or unconfirmed activity and /or specificity in the subsequent studies are one of the major factors for such cases. Hence, there is a demand for the design and synthesis of novel molecules, which can actively, inhibits the IDO1 with higher potency and selectivity as compared to that of the other heme-containing enzymes and low cytotoxicity.

Most of our tested compounds exhibited enzyme inhibition activity ranging from nanomolar to lower-micromolar range. So far, very limited studies have been carried out to explore the modification of the hydroxyamidine moiety as an IDO1 inhibitor, despite of its several biological activities as well as its potential drug candidate ability. Our results obtained from the compounds containing hydroxyamidine scaffold moiety as reported in the chapter 2, suggested that the presence of both benzimidamide as well as, the heterocyclic nitrobenzofurazan moiety plays a significant role in achieving better inhibitory capabilities. IDO1 inhibition assay in the interferon gamma (IFN-γ) induced MDA-MB-231 cells showed that the nitrobenzofurazan derivatives of hydroxyamidines have minimal toxicity and stronger potencies. These hydroxyamidine derivatives also exhibited stronger selectivity for IDO1 enzyme over TDO enzyme. These compounds also could be considered as good molecular probes on the basis of their ligand efficiency values. Moreover the structure activity relationship obtained by systematically substituting the *N*′-hydroxybenzimidamide moiety with halogen and methyl group also provided an insight regarding the role of hydrophobic interaction with the active site of the enzyme. It was observed that there was a significant contribution of the halogen substitution (preferably chloro- and fluoro-derivatives) towards the enhancement of the overall inhibitory potencies as compared to that of the lead compound.

It is evident from the already reported crystal structure of IDO1, that pocket A of the active site consists of variety of hydrophobic residues. These residues can participate in different interactions primarily hydrophobic (as observed mostly in case of the halogen substituted phenyl-ring derivatives of the several tested compounds) as well as can be involved in pi-stacking with the aromatic-ring of the inhibitor molecules oriented towards the pocket A. Thus another scope for the development of inhibitors targeting the

inhibition of IDO1 is to develop new molecules with polynuclear aromatic hydrocarbon thereby exploiting the possible pi-stacking interaction with the residues of the active pocket A. Thus, by systematically substituting the phenyl-ring with suitable functionality, the overall effect of both hydrophobic and π-stacking can be further explored. Although, the larger size of the aromatic-ring in the polynuclear aromatic derivatives might contribute towards the steric hindrance which could negatively interfere with the proper fitting within the cavity of pocket A. Similarly the role of the benzofurazan moiety can also be explored by properly introducing different functional groups in the aromatic-ring as well as modification of the nitro group as well. Overall, our findings suggest that these nitrobenzofurazan derivatives of the *N*′-hydroxyamidines can be a useful structural class of compounds for cancer and other human diseases.

The chapter 3 describes the investigation of structure activity relationship of the oxindole moiety and IDO1 inhibitory potencies. The activity measurements established the significant role played by the oxindole-ring in the overall IDO1 inhibitory potencies. Herein, we have also systematically synthesized different derivative to evaluate the role of free acid/amino group, the effect of free rotation in the C3-position of the oxindole-ring as well as the role of –OH group in the C3-position of the indole-ring. Halogen substitution and restricted rotation around C3-position of the oxindole-ring were effective in improving their efficacies. Spectroscopic studies further supported the interaction of potent compounds with the heme-group of IDO1 enzyme, indicating its preliminary role in mimicking the epoxide-intermediate for the IDO1 catalysed transformation of *L*-Trp to *N*-formylkynurenine. These oxindole derivatives also showed minimal cytotoxicity and low-micromolar potencies along with selectivity for IDO1 over TDO enzyme.

The results obtained from our study contributed towards the better understanding of these modifications in regard to its IDO1 inhibitory capability. The results indicates that designing compounds, which can perturb the electrophilic addition of O_2 of the oxygenated-heme group to the pyrrole-ring of *L*-Trp, could be an efficient approach to improve the potency as well as the selectivity of IDO1 inhibitors. Another scope of modification is to study the effect of heteroatom in the indole-ring by substituting the –NH group with other heteroatom such as oxygen, sulphur etc. Here also, we observed the better inhibitory ability of the halogen substituted derivatives in both *in vivo* and *in vitro* studies, as compared to that of the other tested compounds. These can be further attributed to the enhance ability of the halogen derivative to participate in the hydrophobic interaction within the pocket A residues. Similarly, in the chapter 4 the

indole derivatives, also demonstrated significant inhibitory potencies under similar *in vivo* and *in vitro* experimental conditions.

Therefore, this thesis demonstrated the development of heterocyclic small molecules as potent inhibitors of IDO1 enzyme. Suitable substitution to these hydroxyamidine, oxindole and indazole scaffolds contributed to the proper orientation, suitable fitting within the binding site and interaction with the heme-containing active site of the IDO1 enzyme. It is noteworthy that synthesis of small molecules under mild conditions provided several potent compounds with inhibitory activity in the nanomolar range with no/negligible cytotoxic effect. The development of IDO1 enzyme inhibitor is not only important for development of IDO1 inhibitor, but also helps to understand their role as anti-cancer agents without having moderate to high cytotoxicity. In addition IDO1 inhibitors found application in several diseases that are associated with kynurenine metabolism pathway including Alzheimer, age-related cataract, HIV-encephalitis and others. The hydroxyamidine, oxindole and indazole moieties are also found to have a wide range of applications as bioactive molecules exhibiting antiviral, antibacterial, anticancer properties.

Since the synthesized compounds are based on theoretical approaches and *in vitro* activity values, hence it is difficult to validate these predictions and *in vitro* results under *in vivo* conditions. Additional experimental studies are required for further establishment ofthe effect of these aforementioned modifications of these hydroxyamidine, oxindole and indazole scaffolds. Further studies are going on in our laboratory to develop more effective and potent inhibitors and to gain a better insight regarding the designing of new inhibitors based on the structure activity relationship study. Hence, structural simplicity and low-micromolar/nanomolar inhibition potencies, of the synthesized compounds not only establish them as a potential inhibitor of IDO1 enzyme but also makes them quite attractive and potential drug target for further investigation of IDO1 function and immunotherapeutic applications.

List of publications

(1) Pradhan, N.; **Paul, S.**; Deka, S. J.; Roy, A.; Trivedi, V.; Manna, D. Identification of Substituted 1*H*-Indazoles as Potent Inhibitors for Immunosuppressive enzyme Indoleamine 2,3-dioxygenase 1. *Chem. Select* **2017**, *2*, 5511-5517.

(2) **Paul, S.**; Roy, A.; Deka, S. J.; Panda, S.; Srivastava, G. N.; Trivedi, V.; Manna, D. Synthesis and evaluation of oxindoles as promising inhibitors of the immunosuppressive enzyme indoleamine 2,3-dioxygenase 1. *Med. Chem. Comm.* **2017**, *8*, 1640-1654.

(3) **Paul, S.**; Roy, A.; Deka, S. J.; Panda, S.; Trivedi, V.; Manna, D. Nitrobenzofurazan derivatives of *N*′-hydroxyamidines as potent inhibitors of Indoleamine-2,3-dioxygenase 1. *Eur. J. Med. Chem.* **2016**, *121*, 364-375.

(4) Saha, A.; Panda, S.; **Paul, S.**; Manna. D. Phospahate bioisotere containing amphiphiles: a novel class of squaramide based lipids. *Chem. Commun.* **2016**, *52*, 9438-9441.

(5) Das. M. C.; **Paul, S.**; Gupta, P.; Tribedi, P.; Sarkar, S.; Manna, D.; Bhattacharjee, S. 3-Amino-4-Aminoximidofurazan derivatives: small molecules possessing antimicrobial and antibiofilm activity against Staphylococcus aureus and Pseudomonas aeruginosa. *J. Appl. Microbiol.* **2016**, *120*, 842-859.

(6) Gorai, S.; **Paul, S.**; Sankaran, G.; Borah, R.; Santra, M.; Manna, D. Inhibition of Phosphatidylinoisotol-3,4,5-triphosphate Binding to AKT Plekstrin Homology Domain by 4-Amino-1,2,5-oxadiazole Derivatives. *Med. Chem. Comm*. **2015**, *6*, 1798-1808.

(7) **Paul. S.**; Panda, S.; Manna, D. Mild method for the synthesis of 1H-indazoles through oxime-phosphonium ion intermediate. *Tett. Lett*. **2014**, *55*, 2480-2483.